

INVESTIGATION OF DECOUPLING TECHNIQUES FOR LINEAR AND  
NONLINEAR SYSTEMS

A THESIS SUBMITTED TO  
THE GRADUATE SCHOOL OF NATURAL AND APPLIED SCIENCES  
OF  
MIDDLE EAST TECHNICAL UNIVERSITY

BY

TANER KALAYCIOĞLU

IN PARTIAL FULLFILLMENT OF THE REQUIREMENTS  
FOR  
THE DEGREE OF DOCTOR OF PHILOSOPHY  
IN  
MECHANICAL ENGINEERING

MARCH 2018



Approval of the thesis:

**INVESTIGATION OF DECOUPLING TECHNIQUES FOR LINEAR AND  
NONLINEAR SYSTEMS**

submitted by **TANER KALAYCIOĞLU** in partial fulfillment of the requirements for  
the degree of **Doctor of Philosophy in Mechanical Engineering Department,**  
**Middle East Technical University** by,

Prof. Dr. Halil Kalıpçılar  
Dean, Graduate School of **Natural and Applied Sciences**

\_\_\_\_\_

Prof. Dr. M. A. Sahir Arıkan  
Head of Department, **Mechanical Engineering**

\_\_\_\_\_

Prof. Dr. H. Nevzat Özgüven  
Supervisor, **Mechanical Engineering Dept., METU**

\_\_\_\_\_

**Examining Committee Members:**

Assoc. Prof. Dr. Ender Ciğeroğlu  
Mechanical Engineering Dept., METU

\_\_\_\_\_

Prof. Dr. H. Nevzat Özgüven  
Mechanical Engineering Dept., METU

\_\_\_\_\_

Assoc. Prof. Dr. Melin Şahin  
Aerospace Engineering Dept., METU

\_\_\_\_\_

Prof. Dr. S. Kemal İder  
Mechanical Engineering Dept., Çankaya University

\_\_\_\_\_

Prof. Dr. Erhan Budak  
Manufacturing Engineering Dept., Sabancı University

\_\_\_\_\_

**Date:** 30/03/2018

**I hereby declare that all information in this document has been obtained and presented in accordance with academic rules and ethical conduct. I also declare that, as required by these rules and conduct, I have fully cited and referenced all material and results that are not original to this work.**

Name, Last Name : Taner KALAYCIOĞLU

Signature :

## **ABSTRACT**

### **INVESTIGATION OF DECOUPLING TECHNIQUES FOR LINEAR AND NONLINEAR SYSTEMS**

Kalaycıoğlu, Taner

Ph.D., Department of Mechanical Engineering

Supervisor: Prof. Dr. H. Nevzat Özgüven

March 2018, 189 Pages

Structural coupling methods are widely used in predicting dynamics of coupled systems. In this study, the reverse problem, i.e. predicting the dynamic behavior of a particular subsystem from the knowledge of the dynamics of the overall system and of all the other subsystems, is studied. This problem arises when a substructure cannot be measured separately, but only when coupled to neighboring substructures. The dynamic decoupling problem of coupled linear structures is well investigated in literature. However, decoupling of coupled structures that include a nonlinear element such as clearance, friction and nonlinear stiffness still remains untouched.

In this thesis, firstly, decoupling techniques for coupled linear structures are investigated. Two new methods for decoupling of coupled linear systems are introduced and their performances were compared to those of the best decoupling methods known in literature. Then, the dynamic decoupling problem of coupled nonlinear structures is considered for the first time. A method is developed for calculating FRFs of a substructure decoupled from a coupled nonlinear structure

involving any type of nonlinearity that can be modelled as a single nonlinear element. Depending on where the nonlinear element is, i.e., either in the known or unknown substructure, or at the connection, the formulation differs. Firstly, applications of the method are demonstrated on nonlinear lumped parameter systems using simulated experimental data. Then, real-life applicability of the proposed method is shown through two nonlinear experimental test structures. Finally, the method is applied on a real-life engineering problem in order to demonstrate its performance.

**Keywords:** Nonlinear decoupling, Nonlinear uncoupling, Nonlinear subsystem identification, Nonlinear substructure decoupling

## ÖZ

# DOĞRUSAL VE DOĞRUSAL OLMAYAN SİSTEMLER İÇİN AYRIŞTIRMA TEKNİKLERİNİN İNCELENMESİ

Kalaycıođlu, Taner

Doktora, Makine Mühendisliđi Bölümü

Tez Yöneticisi: Prof. Dr. H. Nevzat Özgüven

Mart 2018, 189 Sayfa

Yapısal birleřtirme yöntemleri, birleřmiř sistemlerin dinamiđinin kestirilmesinde yaygın olarak kullanılmaktadır. Bu alıřmada ters problem, yani bir alt yapının dinamik davranıřının birleřmiř yapının ve tüm diđer alt yapıların dinamik davranıř bilgileri kullanılarak hesaplanması incelenmiřtir. Bu problem, bir alt yapının ayrı olarak ölçülemediđi fakat komřuluđundaki bir alt yapıya birleřtirildiđi takdirde ölçülebildiđi durumlarda ortaya çıkmaktadır. Birleřmiř dođrusal yapıların dinamik olarak ayrıřtırılması problemi literatürde oldukça fazla incelenmiřtir. Fakat boşluk, sürtünme ve dođrusal olmayan direngenlik gibi dođrusal olmayan eleman içeren birleřmiř yapıların ayrıřtırılması problemi hala özölememiřtir.

Bu tezde, ilk olarak, birleřmiř dođrusal yapılar için ayrıřtırma teknikleri incelenmiřtir. Birleřmiř dođrusal sistemlerin ayrıřtırılması amacıyla iki yeni yöntem önerilmiř ve bunların performansları literatürde bilinen en iyi ayrıřtırma yöntemlerinin performansları ile kıyaslanmıřtır. Daha sonra, birleřmiř dođrusal olmayan yapıların dinamik olarak ayrıřtırılması problemi ilk defa ele alınmıřtır. Herhangi bir türde

doğrusalsızlık içeren ve içerdığı doğrusalsızlık tek bir doğrusal olmayan eleman ile modellenebilen birleşmiş doğrusal olmayan bir yapıdan ayrıştırılan alt yapının frekans tepki fonksiyonlarını hesaplamak için yeni bir yöntem geliştirilmiştir. Doğrusal olmayan elemanın nerede bulunduğuna, yani bilinen alt yapıda ya da bilinmeyen alt yapıda veya bu iki alt yapının bağlantısında olup olmadığına bağlı olarak formülasyon değişiklik göstermektedir. İlk olarak, yöntemin uygulamaları doğrusal olmayan toplu parametrelili sistemler üzerinde teorik olarak hesaplanmış veriler kullanılarak gösterilmiştir. Sonra, önerilen yöntemin gerçek hayatta uygulanabilirliği doğrusal olmayan dinamik davranışa sahip iki farklı deneysel test düzeneği üzerinde gösterilmiştir. Son olarak, yöntemin performansı gerçek bir mühendislik problemine uygulanarak sergilenmiştir.

**Anahtar Kelimeler:** Doğrusal olmayan ayrıştırma, Doğrusal olmayan alt sistem tanılama, Doğrusal olmayan alt yapı ayrıştırma



To Azra Güneş...

## ACKNOWLEDGEMENTS

I would like to express my sincere appreciation to my supervisor, Prof. Dr. H. Nevzat Özgüven for his boundless help, excellent supervision and leading guidance from beginning to end of thesis work.

The author also would like to thank Assoc. Prof. Dr. Melin Şahin and Assoc. Prof. Dr. Ender Cığeroğlu for their guidance as members of thesis progress committee.

I am especially thankful to my dear wife Esra Uludağ Kalaycıoğlu for her infallible love, support, patience and encouragement to complete this study.

I dedicate this thesis to my daughter Azra Güneş Kalaycıoğlu, whose birth has brought wonderful fun, great motivation and bright inspiration into my life.

I would like to offer my most profound gratitude to my deceased grandparents Yusuf and Naile Kalaycıoğlu who always encouraged me to pursue my education. I hope you will be proud of your grandson.

I am grateful to my father İdris Kalaycıoğlu, my mother Süheyla Kalaycıoğlu, my brother Kerem Kalaycıoğlu and his family for their endless love and vulnerable support throughout my life.

I would like to express my special thanks to my colleague, Dr. Güvenç Canbaloğlu for his discussion and continuous moral support throughout this work. I would also like to thank all my other colleagues at ASELSAN Inc., especially Dr. Arif Cem Gözükara, Özge Mencek, Kamil Alper Yalçınkaya and Onur Sert, for their technical support and helpful advice.

I would like to thank my superior Dr. Ali Mürteza Çolakođlu and my managers Dr. İhsan Özsoy and Sabri Çetin for giving me the opportunity to use the computational and testing capabilities in ASELSAN Inc.

The scholarship provided by the Scientific and Technological Research Council of Turkey (TÜBİTAK) is thankfully acknowledged.

## TABLE OF CONTENTS

ABSTRACT .....	v
ÖZ.....	vii
ACKNOWLEDGEMENTS .....	x
TABLE OF CONTENTS .....	xii
LIST OF TABLES .....	xv
LIST OF FIGURES.....	xvi
LIST OF SYMBOLS .....	xxiii
LIST OF ABBREVIATIONS .....	xxv
CHAPTERS	
1. INTRODUCTION .....	1
1.1. Structural Decoupling .....	1
1.2. Motivation.....	4
1.3. Literature Survey .....	8
1.4. Scope of the Thesis .....	12
2. ON DECOUPLING OF LINEAR SYSTEMS.....	15
2.1. Proposed Linear Decoupling Formulations .....	15
2.1.1. Theory of the Coupling Force Method .....	15
2.1.2. Derivation of First Decoupling Formulation Proposed (Formulation 1).....	19
2.1.3. Derivation of Second Decoupling Formulation Proposed (Formulation 2).....	20
2.2. Applications and Performances of Decoupling Formulations Proposed	22
2.2.1. A Case Study – Decoupling of a Linear Lumped Parameter System .....	22
2.2.2. Comparison of Proposed Approaches with well-known Existing Methods .....	26

3. DECOUPLING OF NONLINEAR SYSTEMS - THEORY .....	35
3.1. Harmonic Response Analysis in Nonlinear Systems .....	35
3.1.1. Dynamic Modeling of Systems with Nonlinear Elements .....	35
3.1.2. Calculation of Nonlinear Response by Using DFM.....	37
3.2. Measurement of FRFs in Nonlinear Structures .....	42
3.2.1. Controlled Force Amplitude Test.....	43
3.2.2. Controlled Displacement Amplitude Test.....	44
3.3. Theory of Parametric Identification Approach using Modal Model for Nonlinear Systems .....	45
3.4. Theory of FDM-NS .....	46
3.4.1. Nonlinearity in the Unknown Subsystem.....	47
3.4.2. Nonlinearity in the Known Subsystem.....	49
3.4.3. Nonlinearity at the Connection of Two Subsystems .....	50
4. APPLICATIONS OF FDM-NS TO NONLINEAR LUMPED PARAMETER MDOF SYSTEMS .....	53
4.1. Case Study 1 - Nonlinearity in the Unknown Subsystem .....	53
4.2. Case Study 2 - Nonlinearity in the Known Subsystem .....	59
4.3. Case Study 3 - Nonlinearity at the Connection of Subsystems .....	63
5. EXPERIMENTAL VERIFICATION OF FDM-NS.....	75
5.1. Application of FDM-NS to a Nonlinear T-Beam.....	75
5.1.1. Experimental Setup .....	76
5.1.2. Preliminary Analyses .....	78
5.1.3. Experimental Work and Application of FDM-NS .....	81
5.2. Application of FDM-NS to a Coupled Cantilever Beam System with a Nonlinear Element.....	87
5.2.1. Experimental Setup .....	87
5.2.2. Preliminary Analyses .....	89
5.2.3. Experimental Work and Application of FDM-NS .....	92
5.2.4. Verification of FDM-NS Results .....	99
6. APPLICATION OF FDM-NS ON A REAL ENGINEERING SYSTEM ....	105

6.1. Coupled Nonlinear System, its Subsystems and the Test Setup.....	105
6.2. Preliminary FEA and Test on the Coupled System .....	111
6.3. Application of FDM-NS .....	114
6.3.1. Experimental Measurements on the Coupled System .....	115
6.3.2. Harmonic Analyses on the Known Linear Subsystem .....	116
6.3.3. Implementation of FRF Decoupling.....	119
6.3.3.1. FRF Decoupling using Standard Interface .....	119
6.3.3.2. FRF Decoupling using Extended Interface.....	120
6.4. Verification of FDM-NS Results .....	122
7. SUMMARY AND CONCLUSIONS .....	127
REFERENCES.....	133
APPENDICES.....	145
A. PUBLISHED PAPERS DURING PHD .....	145
CURRICULUM VITAE .....	187

## LIST OF TABLES

### TABLES

<b>Table 1.</b> Physical parameters of the lumped parameter system.....	23
<b>Table 2.</b> List of most recent linear decoupling methods .....	27
<b>Table 3.</b> Mean and Standard Deviation (SD) of FRAC values for each method wrt varying pollution level .....	31
<b>Table 4.</b> Physical parameters of the coupled system.....	53
<b>Table 5.</b> Physical parameters of the known SDOF subsystem.....	71
<b>Table 6.</b> Mass of the accelerometer and force transducer .....	79
<b>Table 7.</b> Identified parameters for the nonlinear element.....	85
<b>Table 8.</b> Equipment used in the modal testing .....	89

## LIST OF FIGURES

### FIGURES

<b>Figure 1.</b> Common concept of decoupling technique.....	2
<b>Figure 2.</b> Sample applications of decoupling [2] .....	3
<b>Figure 3.</b> Wing stores carried by fighter/attack aircraft. ....	4
<b>Figure 4.</b> A F-16 jet fighter full of stores mounted under its wings via pylons .....	5
<b>Figure 5.</b> System model and pylon nonlinearity [13].....	6
<b>Figure 6.</b> Integration of ASELPOD to a fighter aircraft.....	7
<b>Figure 7.</b> Integration of LGK (Laser Guidance Kit) to a fighter aircraft .....	7
<b>Figure 8.</b> Notation used for the coupled system, its subsystems and their coordinate sets.....	16
<b>Figure 9.</b> Freebody diagram of each subsystem itself .....	17
<b>Figure 10.</b> Decoupling of a linear lumped parameter system.....	22
<b>Figure 11.</b> Point FRFs at the 2nd DOF of the coupled system: exact (—, black), polluted (*, blue) and FRF curve fitted (- -, red).....	24
<b>Figure 12.</b> Point FRFs at the 2nd DOF of the unknown subsystem: exact (—, black), predicted using Formulation 1 (*, magenta) .....	25
<b>Figure 13.</b> Point FRFs at the 2nd DOF of the unknown subsystem: exact (—, black), predicted using Formulation 2 (*, blue) .....	25
<b>Figure 14.</b> Point FRFs at the 2nd DOF of the unknown subsystem: exact (—, black), predicted via proposed formulations using data polluted with SD of 15e-5: Formulation 2 (*, blue), Formulation 1 (*, magenta) and via formulations given in literature: Eq. (28) (*, cyan), Eq. (30) (*, green), Eq. (34) (*, red) .....	30
<b>Figure 15.</b> Maximum mean FRAC values obtained with the associated linear decoupling method for a given pollution level – measured internal known subsystem DOFs combination (Cell color indicates the method which gives the maximum FRAC value).....	33



<b>Figure 16.</b> Mean FRAC values obtained via Eq. (34) and Formulation 2 for a given pollution level – measured internal known subsystem DOFs combination – greater FRAC value is always given on top of other at each grid (Cell color indicates the method which gives higher FRAC value).....	34
<b>Figure 17.</b> Force-displacement characteristic of cubic stiffness type of nonlinear element.....	41
<b>Figure 18.</b> Force-displacement characteristic of piecewise linear stiffness type of nonlinear element.....	42
<b>Figure 19.</b> Measured FRFs of a nonlinear structure under constant harmonic excitation of different magnitudes .....	44
<b>Figure 20.</b> Measured FRFs of a nonlinear structure for different response levels of the nonlinear element involved.....	45
<b>Figure 21.</b> Inclusion of the connecting nonlinear element, a) in the unknown subsystem, b) in the known subsystem .....	51
<b>Figure 22.</b> Decoupling of a nonlinear coupled system – nonlinearity is at the coupling DOF of the unknown subsystem.....	54
<b>Figure 23.</b> Point FRFs of the unknown subsystem at $m_2$ (colored points) and fitted FRF curves (black lines) .....	55
<b>Figure 24.</b> Modal parameter variations for the 1st mode wrt response amplitude of the nonlinear element (*, identified parameters & —, fitted curves) .....	56
<b>Figure 25.</b> Modal parameter variations for the 2nd mode wrt response amplitude of the nonlinear element (*, identified parameters & —, fitted curves).....	57
<b>Figure 26.</b> Forward frequency sweep response of the unknown subsystem at $m_2$ ....	58
<b>Figure 27.</b> Backward frequency sweep response of the unknown subsystem at $m_2$ .	58
<b>Figure 28.</b> Decoupling of a nonlinear coupled system – nonlinearity is in the known subsystem.....	59
<b>Figure 29.</b> Polluted and curve fitted point receptances of the coupled system and the known subsystem at $m_4$ .....	61
<b>Figure 30.</b> Frequency responses of the coupled system and the known subsystem at $m_4$ under constant amplitude harmonic excitation .....	61

<b>Figure 31.</b> Exact and decoupled point receptances of the unknown subsystem at $m_2$ .....	62
<b>Figure 32.</b> Decoupling of a nonlinear coupled system – nonlinearity is at the connection of subsystems.....	63
<b>Figure 33.</b> Force-displacement characteristic of gap nonlinearity .....	64
<b>Figure 34.</b> Point FRFs of the coupled system at $m_3$ (colored points) and fitted FRF curves (black lines).....	66
<b>Figure 35.</b> Point FRFs of the known subsystem at $m_3$ .....	66
<b>Figure 36.</b> Point FRFs of the unknown subsystem at $m_0$ (above) along with its transfer FRFs between $m_0$ and $m_2$ (below) .....	67
<b>Figure 37.</b> Modal parameter variations for the 1st mode of the transfer FRFs of the unknown subsystem between $m_0$ and $m_2$ wrt response amplitude of the nonlinear element (*, identified parameters & —, fitted curves).....	68
<b>Figure 38.</b> Modal parameter variations for the 2nd mode of the transfer FRFs of the unknown subsystem between $m_0$ and $m_2$ wrt response amplitude of the nonlinear element (*, identified parameters & —, fitted curves).....	69
<b>Figure 39.</b> Modal parameter variations for the 3rd mode of the transfer FRFs of the unknown subsystem between $m_0$ and $m_2$ wrt response amplitude of the nonlinear element (*, identified parameters & —, fitted curves).....	69
<b>Figure 40.</b> Modal parameter variations for the 1st mode of the point FRFs of the unknown subsystem at $m_0$ wrt response amplitude of the nonlinear element (*, identified parameters & —, fitted curves).....	70
<b>Figure 41.</b> Modal parameter variations for the 2nd mode of the point FRFs of the unknown subsystem at $m_0$ wrt response amplitude of the nonlinear element (*, identified parameters & —, fitted curves).....	70
<b>Figure 42.</b> Modal parameter variations for the 3rd mode of the point FRFs of the unknown subsystem at $m_0$ wrt response amplitude of the nonlinear element (*, identified parameters & —, fitted curves).....	71
<b>Figure 43.</b> Construction of a new nonlinear coupled system - nonlinearity at the connection of two subsystems again .....	72

<b>Figure 44.</b> Predicted and directly calculated responses of the new coupled system at $m_5$ obtained via forward frequency sweeping .....	73
<b>Figure 45.</b> Predicted and directly calculated responses of the new coupled system at $m_5$ obtained via backward frequency sweeping .....	73
<b>Figure 46.</b> Physical dimensions of the test setup .....	76
<b>Figure 47.</b> Picture of the test setup used in the experiment.....	77
<b>Figure 48.</b> View of the equipment used in the experiment .....	78
<b>Figure 49.</b> FEM of the test structure .....	79
<b>Figure 50.</b> Modal analysis results of the T-beam assembly – its fundamental resonance .....	80
<b>Figure 51.</b> Modal analysis results of the cantilever beam by itself – its fundamental resonance.....	81
<b>Figure 52.</b> Point FRFs of the T-beam assembly at the connection point j under transverse loading for constant harmonic displacement amplitude of 1 mm.....	82
<b>Figure 53.</b> Model of the test rig.....	83
<b>Figure 54.</b> Point FRFs of the T-beam assembly at the connection point j under harmonic loading of constant magnitudes 0.25 N and 0.5 N in transverse direction	84
<b>Figure 55.</b> DF values obtained via DDF Method [82,83] for stiffness (left) and damping (right) nonlinearities.....	85
<b>Figure 56.</b> Point FRFs of the cantilever beam alone at its tip point j in transverse direction.....	86
<b>Figure 57.</b> Setup used in the experiment.....	88
<b>Figure 58.</b> Dimensions and technical details of the test system.....	88
<b>Figure 59.</b> FEM of the test structure .....	90
<b>Figure 60.</b> Fundamental mode of the coupled cantilever beams assembly.....	91
<b>Figure 61.</b> Fundamental mode of the long cantilever beam alone .....	92
<b>Figure 62.</b> Experimental procedure followed during controlled displacement amplitude test .....	93

<b>Figure 63.</b> Measured transfer FRFs (symbols) and fitted FRF curves (lines) of the coupled system between internal point (i) and connection point (j) in transverse direction for various response levels of the nonlinear element .....	94
<b>Figure 64.</b> Measured point FRFs (symbols) and fitted FRF curves (lines) of the coupled system at connection point (j) in transverse direction for various response levels of the nonlinear element.....	94
<b>Figure 65.</b> Measured point FRFs of the known subsystem alone at its coupling DOF (j) in transverse direction.....	95
<b>Figure 66.</b> Calculated point (above) and transfer (below) FRFs of unknown subsystem (lines) and those measured for coupled system (dots) in transverse direction when excited from connection point (j) .....	96
<b>Figure 67.</b> Variation of the modal parameters of the first mode of the unknown nonlinear subsystem for $\mathbf{H}_{ji}^U$ wrt relative response amplitude, $ \mathbf{X}_j - \mathbf{X}_i $ (*, identified parameters & —, fitted curves) .....	98
<b>Figure 68.</b> Variation of the modal parameters of the first mode of the unknown nonlinear subsystem for $\mathbf{H}_{ji}^U$ wrt relative response amplitude, $ \mathbf{X}_j - \mathbf{X}_i $ (*, identified parameters & —, fitted curves) .....	99
<b>Figure 69.</b> Dimensions and technical details of the modified test system .....	100
<b>Figure 70.</b> Measured point FRFs of the modified known subsystem by itself at its coupling DOF (j) in transverse direction.....	101
<b>Figure 71.</b> Measured and calculated responses of the modified test system at its coupling DOF (j) for harmonic excitation of amplitude 0.4 N in transverse direction .....	102
<b>Figure 72.</b> Measured and calculated responses of the modified test system at its coupling DOF (j) for harmonic excitation of amplitude 0.4 N in transverse direction – zoomed around resonance .....	103
<b>Figure 73.</b> Coupled engineering structure – passive isolated IMU system.....	106
<b>Figure 74.</b> Known linear subsystem – IMU and its mechanical interface plate.....	107

<b>Figure 75.</b> Unknown nonlinear subsystem – tray grounded with elastomer isolators .....	108
<b>Figure 76.</b> View of the fixed connection between two subsystems .....	109
<b>Figure 77.</b> Coupled nonlinear system under testing.....	110
<b>Figure 78.</b> Linear FEM of the coupled system.....	112
<b>Figure 79.</b> Comparison of harmonic responses at point j and q of the linear FEM of the coupled system .....	113
<b>Figure 80.</b> Measured point FRFs of the coupled system at point j via controlled force amplitude test .....	114
<b>Figure 81.</b> Measured point FRFs and the fitted FRF curve of the coupled nonlinear system at point j for 0.05 mm displacement amplitude of elastomer isolators .....	115
<b>Figure 82.</b> Measured transfer FRFs and the fitted FRF curve of the coupled nonlinear system between point i and j for 0.05 mm displacement amplitude of elastomer isolators .....	116
<b>Figure 83.</b> Point FRFs of the known linear subsystem at point j calculated via FEA and measured via hammer test .....	117
<b>Figure 84.</b> Point and transfer FRFs of the known linear subsystem at and between point i and j calculated via FEA.....	118
<b>Figure 85.</b> Predicted point FRFs of the unknown subsystem at point j by using standard interface for 0.05 mm displacement amplitude of elastomer isolators.....	120
<b>Figure 86.</b> FRFs of the coupled nonlinear system at and between point i and j for 0.05 mm displacement amplitude of elastomer isolators .....	121
<b>Figure 87.</b> Predicted point FRFs of the unknown subsystem at point j by using extended interface for 0.05 mm displacement amplitude of elastomer isolators.....	122
<b>Figure 88.</b> Variation of resonance frequency wrt load carried by an elastomer isolator (825-GS-55) [87].....	123
<b>Figure 89.</b> Unknown nonlinear subsystem under testing .....	124
<b>Figure 90.</b> Measured point FRFs, fitted FRF curve and FRF curve obtained after mass cancellation of the unknown nonlinear subsystem at point j for 0.05 mm displacement amplitude of elastomer isolators .....	125

**Figure 91.** Predicted (using standard and extended interfaces) and measured point FRFs of the unknown nonlinear subsystem at point j by for 0.05 mm displacement amplitude of elastomer isolators ..... 126

## LIST OF SYMBOLS

$A$	Modal constants
$\mathbf{A}$	Accelerance matrix
$\mathbf{B}$	Boolean matrix
$c$	Viscous damping
$\mathbf{C}$	Viscous damping matrix
$\mathbf{D}$	Structural damping matrix
$\mathbf{f}$	Generalized harmonic forcing vector
$\mathbf{F}$	Amplitude vector of generalized harmonic
$i$	Unit imaginary number
$\mathbf{I}$	Identity matrix
$\mathbf{H}$	Receptance matrix
$k$	Stiffness
$k_c$	Cubic stiffness coefficient
$\mathbf{K}$	Stiffness matrix
$m$	Mass
$\mathbf{M}$	Mass matrix
$n$	Internal nonlinear restoring force
$\mathbf{N}$	Internal nonlinear restoring force vector
$t$	Time
$x$	Generalized displacement
$\mathbf{x}$	Generalized displacement vector
$\dot{x}$	Generalized velocity vector
$\dot{\mathbf{x}}$	Generalized velocity vector
$\ddot{\mathbf{x}}$	Generalized acceleration vector
$X$	Amplitude of complex steady state harmonic displacements
$\mathbf{X}$	Amplitude vector of complex steady state harmonic displacements

$\mathbf{Z}$	Dynamic stiffness matrix
$\Delta$	Nonlinearity matrix
$\delta$	Elongation
$\eta$	Loss factor
$\lambda$	Relaxation coefficient
$\nu$	Describing function representation of the nonlinearity
$\theta$	Generic angle
$\omega$	Frequency
$\psi$	Phase angle



## LIST OF ABBREVIATIONS

B&K	Brüel&Kjaer
BWD	Backward
DDF	Direct Nonlinearity by Describing Functions
DF	Describing Function
DFM	Describing Function Method
DOF	Degree of Freedom
FDM-NS	FRF Decoupling Method for Nonlinear Systems
FE	Finite Element
FEA	Finite Element Analysis
FEM	Finite Element Method
FRAC	Frequency Assurance Criteria
FRF	Frequency Response Function
FWD	Forward
IMU	Inertial Measurement Unit
LGK	Laser Guidance Kit
MDOF	Multi Degree of Freedom
SD	Standard Deviation
SDOF	Single Degree of Freedom



## CHAPTER 1

### INTRODUCTION

#### 1.1. Structural Decoupling

Most mechanical systems are appeared as an assembly of components and the modal analysis is widely being used to analyze the dynamics of such systems or their components [1]. Considerable effort has been devoted to structural coupling methods that predict the total dynamic behavior of a complex machine from those of its components.

Conversely, the dynamics of a whole system may be known, but that of its component cannot be measured separately. If measurement can be made only when it is coupled to neighboring substructures, then a decoupling problem arises. It can be briefly defined as the identification of the dynamics of a structural subsystem that is part of a larger system. In other words, decoupling studies focus on predicting the response of an unknown subsystem from the known responses of the complete system and the remaining subsystem (Figure 1).

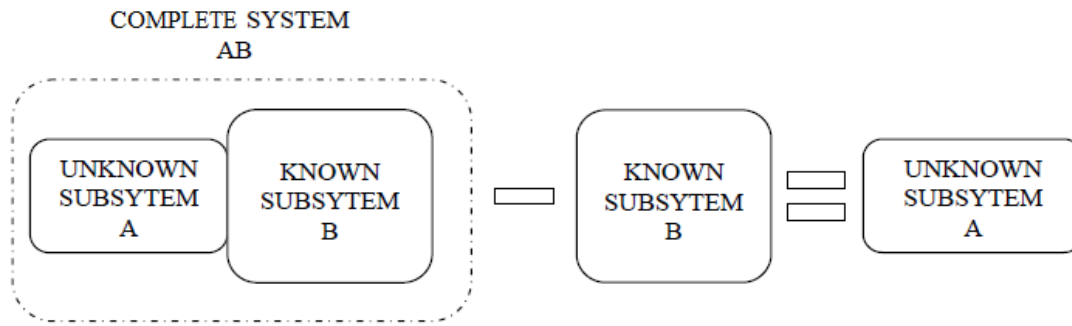


**Figure 1.** Common concept of decoupling technique

For example, it is not possible to measure the dynamics of the tire alone easily in a tire-suspension of an automobile (Figure 2). Therefore, the tire should be supported by the wheel, suspension and so on, which brings additional dynamics on the measurement.

Another example can be given using the same figure (Figure 2). Here, it is aimed to obtain pure bearing dynamics in order to use it in design simulations of rotating machinery. However, a special fixture has to be used in order to excite the bearing in practice that results in the implicit measurement of the bearing dynamics. So, the result of this measurement with the fixture will also involve the dynamics of the fixture in addition to that of the bearing, which may have resonances, mass-additive effect and so on.

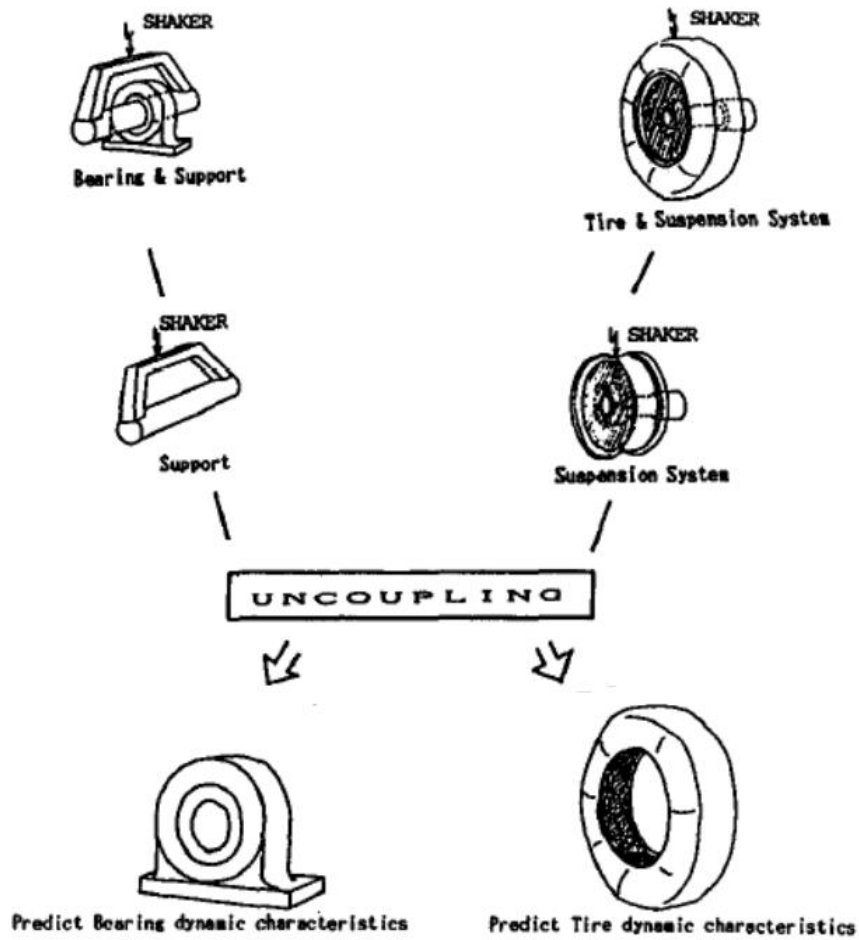


**Figure 2.** Sample applications of decoupling [2]

Another area of application can be encountered in the train industry for car-bogie assemblies [3]. Structure-borne vibrations due to the contact between rail and wheel flange are transmitted into the car body through the wheel suspending bogie system. So, an adequate mathematical model of the bogie is essential to analyze this phenomenon. Since the stand-alone testing of bogie system does not represent its operating conditions, it should be tested as a sub-component of the fully assembled coach.

Decoupling techniques are also used in design improvement of subsystems to identify their individual contribution to the total system. Another common application of decoupling is mass cancellation to eliminate mass loading effect of accelerometers in FRF measurements [1,4]. Other practices of structural decoupling include subsystem identification in damage detection, identification of joints and structural health monitoring [5-8]. Despite such promising applications, decoupling problem is still one of the most challenging subjects in structural dynamics.

## 1.2. Motivation

Decoupling techniques can also be used in the solution of several problems encountered in defense industry. The motivation of this thesis work is a problem encountered in fighter aircrafts. Fighter aircrafts are required to carry a large variety of external stores mounted at various locations on their wings (Figure 3).



**Figure 3.** Wing stores carried by fighter/attack aircraft.

Pylons are the suspension devices used to mount those external stores on an aircraft (Figure 4).



**Figure 4.** A F-16 jet fighter full of stores mounted under its wings via pylons

In some cases, the dynamics of an aircraft may be needed when a different store or a different combination of stores are mounted on it. This requires performing ground vibration tests for each different store or store combination on an aircraft. This can also be achieved by coupling each store to the aircraft theoretically if an adequate mathematical model of the aircraft-pylon structure including pylon connection dynamics is available. In order to construct this mathematical model, aircraft-pylon structure should be tested while the pylon is preloaded with a large load corresponding to the weight of the store. Then, a subsystem identification method would provide a solution to decouple the aircraft-pylon structure including pylon connection dynamics from the aircraft-pylon-store assembly. Furthermore, it is a well-known fact that store/pylon connection exhibits friction and hardening nonlinearities [9-12]. A pylon model and a typical pylon nonlinearity are given in Figure 5. Thus, the decoupling

method, which is going to be used to identify the aircraft-pylon structure dynamics, should have the capability to handle nonlinear connections between pylon and store.

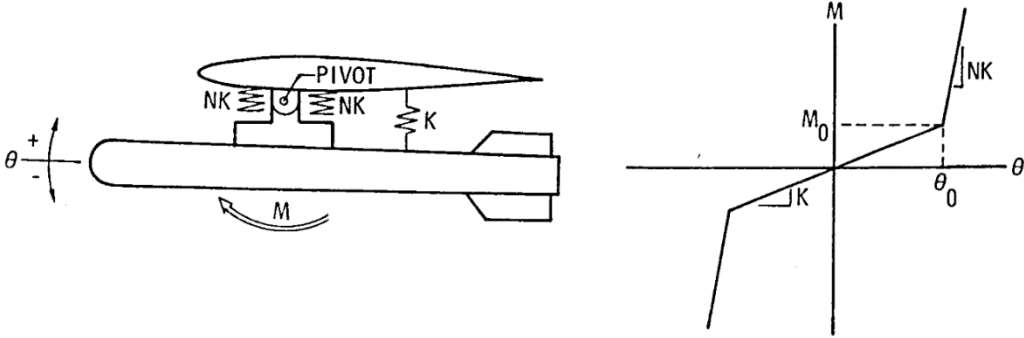


**Figure 5.** System model and pylon nonlinearity [13]

As one of Turkey's leading defense industry company, ASELSAN Inc. designs, develops and manufactures targeting systems (Figure 6), guided bombs (Figure 7), and integrates these systems to different aircraft platforms. Integration of such subsystems is very crucial since it can drastically change the dynamic characteristics of the target platform, misestimation of which prior to integration may result in catastrophic failures.





**Figure 6.** Integration of ASSELPOD to a fighter aircraft



**Figure 7.** Integration of LGK (Laser Guidance Kit) to a fighter aircraft

The initial objective of this thesis was to examine all available decoupling techniques in detail and to develop alternative techniques that can be used for decoupling of linear

coupled structures. It was also aimed to extend the linear decoupling methods for decoupling of nonlinear structures. Several attempts are made to develop a new decoupling theory one of which results in two different linear decoupling formulations. However, studies on these proposed formulations are terminated due to their performance concerns. Then, it is totally focused on developing a method that can decouple nonlinear structures which is the ultimate purpose of this thesis. To the best of author's knowledge, this work presents the first applicable method to uncouple nonlinear structures.

### **1.3. Literature Survey**

Since engineering structures are generally designed as an assembly of several components, it is computationally expensive and time consuming to constitute a FEM each time particularly when various design alternatives are going to be evaluated. Therefore, several structural coupling methods have been developed in order to reduce the effort necessary for dynamic reanalysis of such systems [14-32].

Even though several different coupling methods are available in literature based on the linearity assumption, most of the engineering structures are intrinsically nonlinear. During the past three decades, structural coupling of nonlinear subsystems has been investigated and led to several coupling methods considering the nonlinear effect [33-41].

Several studies have also been carried on structural decoupling of linear systems, which becomes an important problem when the dynamic behavior of a system is known, but it is not easy to measure the dynamic characteristics of one of its components due to geometric limitations (i.e., due to difficulty in measuring and/or exciting a subsystem separately).

Investigation on decoupling problem dates back to three decades ago, when the first attempt to extract objective component's dynamics in an assembly was performed by

Okubo and Miyazaki [2]. They have proposed an uncoupling method and applied it in order to extract the dynamics of a bearing. Since it is not practical to excite a bearing without a special fixture, dynamics of the fixture should be extracted to obtain the pure bearing dynamics.

Gray and Starkey [42] proposed a method for substructure uncoupling use of which is especially suggested for the cases where modeling the connection elements between substructures is challenging. The method is shown to work on lumped parameter structures and it is further applied to a Ford Ranger light truck.

Gontier and Bensaibi [43] presented a theoretical method in time domain for in situ identification of the mechanical parameters of a joint via modal analysis of the known greater structure. In this study, the interface compatibility and equilibrium equations are formulated in terms of the polynomial coefficients of the discrete time transfer functions. They verified the technique by applying it to lumped parameter systems, as well as to a real beam structure supported by an elastic device of unknown characteristics.

Silva et al. [44] presented a decoupling methodology as a means of modeling the dynamic behavior of structural elements, more specifically, for the dynamic characterization of joints. They regenerate FRFs from a mathematical model using the modal parameters identified from the experimental data as to avoid the direct use of data with experimental errors during decoupling calculations involving three matrix inversions. They also emphasized the difficulties during experimental measurement of the FRFs relating all the connection coordinates. Maia et al. [45] proposed a different uncoupling technique for joint identification. In this technique, they used coupling formulation of Jetmundsen et al. [18] and obtained a better formulation in terms of the number of matrix inversions. In this formulation, only internal DOFs of the known substructure are used to obtain joint's frequency response.

Kalling et al. [46] also studied the decoupling problem by performing state-space

model identification including a sensitivity analysis showing possible ill conditioning due to inertia ratios at the interface.

Zhen et al. [47] proposed an inverse substructuring formulation that differs from the classical approach in that the FRFs of individual substructures and dynamic characteristics of the coupling elements were predicted directly from the coupled system FRFs. Although this technique is advantageous since no substructure level spectra response is needed, it requires whole coupled system spectra response and it is sensitive to measurement errors and/or inconsistencies. The proposed technique was applied to study the dynamics of motor vehicle and product transport system [48,49], showing its applicability in industry. Then, it was further developed for multi-coordinate coupled multi-substructure product transport system [50,51].

D'Ambrogio and Fregolent [52] proposed two FRF based decoupling techniques; namely, impedance and mobility based decoupling approaches, which show ill-conditioning troubles due to the internal resonances of the known subsystem with fixed interface. As to circumvent ill-conditioning, they used FRFs at some internal DOFs of the known subsystem.

Cloutier and Avitabile [53] proposed the Constraint Force-based decoupling approach which is proved to be promising with a single connection but not as efficient for multiple connections. They compared their approach with impedance and mobility-based approaches [52] and concluded that the impedance and mobility-based approaches can produce more accurate results when appropriate internal DOFs are used.

Sjövall and Abrahamsson [3] presented a subsystem identification method based on reconstruction of the interface forces acting between the unknown subsystem and its neighbor. It is shown in this study that the subsystem identification is sensitive to the existence of general anti-resonances in the frequency domain of interest due to ill-

conditioned matrix inversion. In order to overcome this ill-conditioning problem, they suggested the use of proper non-interface response DOFs from the test of the coupled system, but this requires extensive pretest analyses.

A general framework for dynamic substructuring is presented in [28] and [29] in which the so-called dual domain decomposition technique that allows retaining the full set of global DOFs by enforcing equilibrium at the connection of substructures is introduced. The substructuring problem using the dual domain decomposition can be directly formulated from [29], whereas a similar formulation for the decoupling problem is derived and discussed in [54] for collocated approach where DOFs used to ensure equilibrium are the same as DOFs used to enforce compatibility, and in [55] and [56] for non-collocated approach where DOFs used to ensure equilibrium are not the same as DOFs used to enforce compatibility.

Batista and Maia [57] suggested three different formulations based on the classical decoupling procedure of Jetmundsen et al. [18] taking the effects of including different sets of DOFs into account on the coupled system: (i) exclusion of connection DOFs, (ii) inclusion of connection DOFs only and (iii) inclusion of connection DOFs and internal DOFs of the known subsystem. They concluded that the formulation that performs best requires measurements at the connection points of the substructures.

D'Ambrogio and Fregolent [58] proposed the so-called hybrid assembly approach. They compared dual [54] and hybrid assembly approaches by applying them to an experimental test bed and end up with similar results in terms of predicted FRFs of the unknown subsystem. In subsequent applications, the dual assembly approach [54] was successfully used to estimate the subsystem dynamics in machine tools [59,60], wind turbines [61] and flexible space payloads [62].

Dynamic decoupling of linear structures is well investigated in literature despite some accuracy problems. Even so, the dynamic decoupling problem of nonlinear structures

still remains intact. Additional challenge in nonlinear decoupling problem is that the presence of a nonlinearity in a coupled system results in different system FRFs depending on the level of excitation. Thus, application of linear decoupling approaches will also end up with different FRFs of an unknown substructure at each time. In order to overcome this challenge, firstly the nonlinear system identification techniques are investigated. Detailed reviews of these work are given by Kerschen et al. [9] and Noël et al. [63].

#### **1.4. Scope of the Thesis**

The scope of the thesis is given as follows:

In Chapter 2, the theories of the two new methods for decoupling of linear systems are given in detail both of which are based on the inverse application of a structural coupling method developed in a previous work. Applications of the proposed linear decoupling approaches are given in order to show their applicability and accuracy. Then, the same case study is studied by using some well-known linear decoupling methods available in literature. Finally, an assessment of the proposed approaches in comparison to those recently given in the literature is made in terms of correlation between the predicted FRFs and the true FRFs of the unknown subsystem.

In Chapter 3, first, the theory of response calculation for nonlinear systems, which is frequently used in the succeeding chapter, is given here for the sake of completeness. Then, the theory of the parametric modal identification technique for nonlinear systems and that of the linear decoupling technique adopted in this thesis are summarized. Finally, the theory of the proposed FRF Decoupling Method for Nonlinear Systems (FDM-NS) is given in detail.

In Chapter 4, applications of FDM-NS are demonstrated on nonlinear lumped parameter systems through numerical case studies which vary in terms of the location of the nonlinear element. While a cubic stiffness type of nonlinear element exists in the unknown subsystem in the first case, it is located in the known subsystem in the second case. In the third and the last case, a piecewise stiffness type of nonlinear element is used which connects both subsystems to each other.

In Chapter 5, FDM-NS is applied to experimental test systems in order to verify the method on real nonlinear systems. In the first experiment, decoupling of a nonlinear T-beam assembly is examined where the subsystem with a nonlinear element is taken as the known substructure. In the second experiment, decoupling of a nonlinear test structure composed of two cantilever beams connected at their tips with an unknown nonlinear element is studied. This problem is handled by including the unknown nonlinear connection element in the unknown subsystem.

In Chapter 6, application of FDM-NS to a real engineering problem is illustrated. The engineering system is composed of an Inertial Measurement Unit (IMU) and its mechanical interface plate which are placed on a tray grounded with rubber isolators. The rubber isolators introduce nonlinearity to the overall system due to their displacement dependent stiffness characteristics. In this application, point FRFs of the tray grounded with rubber isolators at its connection interface are predicted by decoupling IMU and its mechanical interface plate from the whole nonlinear system via FDM-NS. Then, the results obtained are compared with those measured experimentally.

In Chapter 7, a brief summary and conclusions are given.





## CHAPTER 2

### ON DECOUPLING OF LINEAR SYSTEMS

In this chapter, two new decoupling formulations are proposed after a detailed investigation of existing methods for decoupling of linear systems. Then, their performances are evaluated and compared with the best of those given in literature using a case study with a lumped parameter system. By using simulated test data, the effects of using limited number of measurement coordinates in the known subsystem on predicted FRFs of the unknown subsystem are examined in detail.

#### **2.1. Proposed Linear Decoupling Formulations**

In this section, the theories of two new methods proposed for decoupling of linear systems are given in detail. These approaches are based on the inverse application of a structural modification method suggested by Tahtalı and Özgüven [64] such that resulting equations of this the so called “Coupling Force Method” are reorganized to be used for substructure decoupling for linear systems. Here, the derivation of both formulations proposed is presented after introducing a brief theory of the “Coupling Force Method”.

##### **2.1.1. Theory of the Coupling Force Method**

In this section, the underlying theory of the Coupling Force Method is given for completeness. It should be noted that the notation used here and hereafter for all systems/subsystems and the coordinate sets are given in Figure 8.

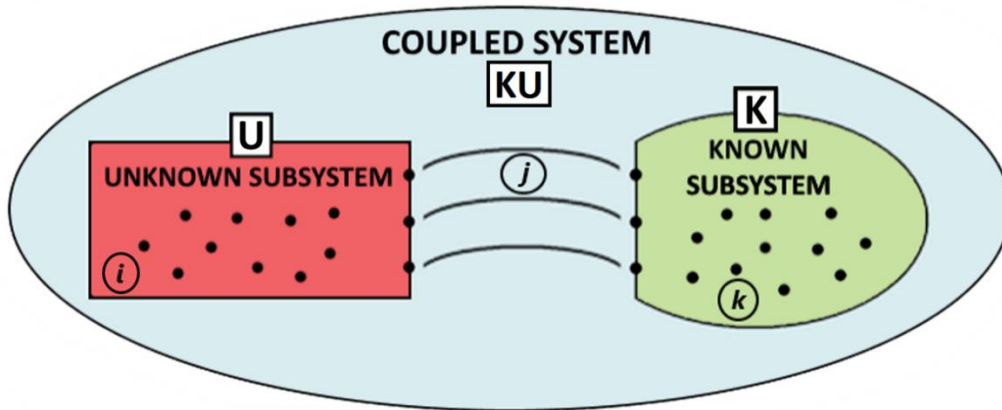


**Figure 8.** Notation used for the coupled system, its subsystems and their coordinate sets

As can be seen from Figure 8, superscripts U and K refer to the unknown and known subsystems, respectively, whereas superscript KU represents the coupled system. Subscript i denotes the coordinates that belong to the unknown subsystem only, subscript j refers to the connection coordinates (connection may be rigid or elastic) between the unknown and known subsystems, and finally subscript k represents the coordinates that belong to the known subsystem only.

Considering the free body diagram of each subsystem as shown in Figure 9, the following equations can be written for the unknown and the known subsystems, respectively:

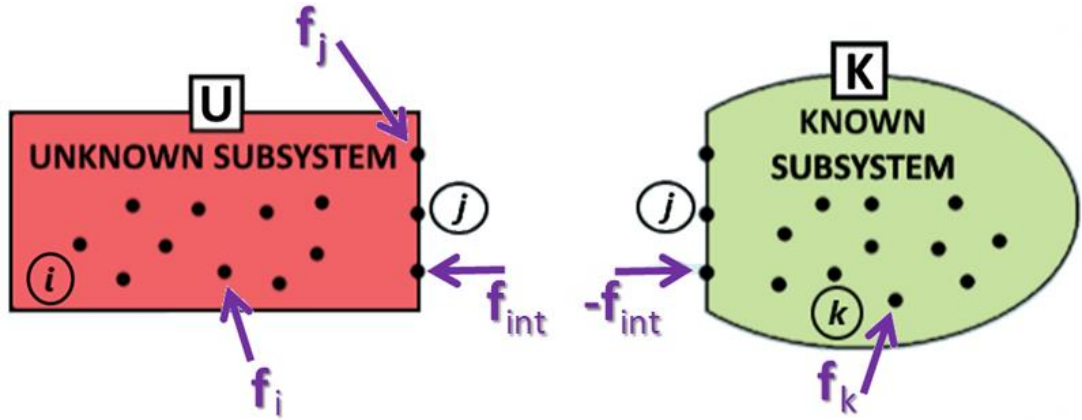


**Figure 9.** Freebody diagram of each subsystem itself

$$\begin{Bmatrix} \mathbf{X}_i^U \\ \mathbf{X}_j^U \end{Bmatrix} = \begin{pmatrix} \mathbf{H}_{ii}^U & \mathbf{H}_{ij}^U \\ \mathbf{H}_{ji}^U & \mathbf{H}_{jj}^U \end{pmatrix} \begin{Bmatrix} \mathbf{F}_i \\ \mathbf{F}_j + \mathbf{F}_{int} \end{Bmatrix} \quad (1)$$

$$\begin{Bmatrix} \mathbf{X}_j^K \\ \mathbf{X}_k^K \end{Bmatrix} = \begin{pmatrix} \mathbf{H}_{jj}^K & \mathbf{H}_{jk}^K \\ \mathbf{H}_{kj}^K & \mathbf{H}_{kk}^K \end{pmatrix} \begin{Bmatrix} -\mathbf{F}_{int} \\ \mathbf{F}_k \end{Bmatrix} \quad (2)$$

Here,  $\mathbf{H}$  represents receptance matrix whereas  $\mathbf{X}$ ,  $\mathbf{F}_{int}$  and  $\mathbf{F}$  correspond to amplitude vectors of generalized displacement, coupling reaction force and external force, respectively. Expansion of Eq. (1) and Eq. (2) yields the following relations:

$$\mathbf{X}_i^U = \mathbf{H}_{ii}^U \mathbf{F}_i + \mathbf{H}_{ij}^U (\mathbf{F}_j + \mathbf{F}_{int}) \quad (3)$$

$$\mathbf{X}_j^U = \mathbf{H}_{ji}^U \mathbf{F}_i + \mathbf{H}_{jj}^U (\mathbf{F}_j + \mathbf{F}_{int}) \quad (4)$$

$$\mathbf{X}_j^K = -\mathbf{H}_{jj}^K \mathbf{F}_{int} + \mathbf{H}_{jk}^K \mathbf{F}_k \quad (5)$$

$$\mathbf{X}_k^K = -\mathbf{H}_{kj}^K \mathbf{f} + \mathbf{H}_{kk}^K \mathbf{F}_k \quad (6)$$

When two subsystems are rigidly coupled, one can equate the displacement vectors of both subsystems at the coupling coordinates to each other, i.e.  $\mathbf{X}_j^U = \mathbf{X}_j^K$ . Thus, coupling reaction force can be obtained as given below by equating the right hand sides of Eq. (4) and Eq. (5):

$$\mathbf{F}_{\text{int}} = \left[ \mathbf{H}_{jj}^U + \mathbf{H}_{jj}^K \right]^{-1} \left[ \mathbf{H}_{jk}^K \mathbf{F}_k - \mathbf{H}_{ji}^U \mathbf{F}_i - \mathbf{H}_{jj}^U \mathbf{F}_j \right] \quad (7)$$

So, the response of the coupled system can be rewritten by substituting Eq. (7) into Eqs. (3), (5) and (6) as follows:

$$\mathbf{X}_i^{KU} = \mathbf{H}_{ii}^U \mathbf{F}_i + \mathbf{H}_{ij}^U \left( \mathbf{F}_j + \left[ \mathbf{H}_{jj}^U + \mathbf{H}_{jj}^K \right]^{-1} \left[ \mathbf{H}_{jk}^K \mathbf{F}_k - \mathbf{H}_{ji}^U \mathbf{F}_i - \mathbf{H}_{jj}^U \mathbf{F}_j \right] \right) \quad (8)$$

$$\mathbf{X}_j^{KU} = -\mathbf{H}_{jj}^K \left[ \mathbf{H}_{jj}^U + \mathbf{H}_{jj}^K \right]^{-1} \left[ \mathbf{H}_{jk}^K \mathbf{F}_k - \mathbf{H}_{ji}^U \mathbf{F}_i - \mathbf{H}_{jj}^U \mathbf{F}_j \right] + \mathbf{H}_{jk}^K \mathbf{F}_k \quad (9)$$

$$\mathbf{X}_k^{KU} = -\mathbf{H}_{kj}^K \left[ \mathbf{H}_{jj}^U + \mathbf{H}_{jj}^K \right]^{-1} \left[ \mathbf{H}_{jk}^K \mathbf{F}_k - \mathbf{H}_{ji}^U \mathbf{F}_i - \mathbf{H}_{jj}^U \mathbf{F}_j \right] + \mathbf{H}_{kk}^K \mathbf{F}_k \quad (10)$$

Furthermore, the response of the coupled system can also be expressed as the multiplication of the FRF matrix and the external forcing vector:

$$\begin{pmatrix} \mathbf{X}_i^{KU} \\ \mathbf{X}_j^{KU} \\ \mathbf{X}_k^{KU} \end{pmatrix} = \begin{pmatrix} \mathbf{H}_{ii}^{KU} & \mathbf{H}_{ij}^{KU} & \mathbf{H}_{ik}^{KU} \\ \mathbf{H}_{ji}^{KU} & \mathbf{H}_{jj}^{KU} & \mathbf{H}_{jk}^{KU} \\ \mathbf{H}_{ki}^{KU} & \mathbf{H}_{kj}^{KU} & \mathbf{H}_{kk}^{KU} \end{pmatrix} \begin{pmatrix} \mathbf{F}_i \\ \mathbf{F}_j \\ \mathbf{F}_k \end{pmatrix} \quad (11)$$

Equations (8), (9), (10) and (11) are the resulting formulations of the Coupling Force Method proposed by Tahtalı and Özgüven [64].

In the following sections, derivation of the proposed linear decoupling formulations using Equations (9), (10) and (11) will be presented.

### 2.1.2. Derivation of First Decoupling Formulation Proposed (Formulation 1)

Here, derivation of the first Decoupling Formulation Proposed, which is abbreviated as Formulation 1 for simplicity, is explained in detail.

Let us consider Eq. (9) and assume that only the  $k^{\text{th}}$  coordinates of the coupled system are harmonically excited, whereas the rest of external force vector is equal to zero, such that;

$$\begin{pmatrix} \mathbf{F}_i \\ \mathbf{F}_j \\ \mathbf{F}_k \end{pmatrix} = \begin{pmatrix} \mathbf{0}_{i \times I} \\ \mathbf{0}_{j \times I} \\ \mathbf{F}_{k \times I} \end{pmatrix} \quad (12)$$

By using Eq. (11) and Eq. (12), Eq. (9) can be rewritten as

$$\mathbf{H}_{jk}^{KU} \mathbf{F}_{k \times I} = -\mathbf{H}_{jj}^K (\mathbf{H}_{jj}^U + \mathbf{H}_{jj}^K)^{-1} \mathbf{H}_{jk}^K \mathbf{F}_{k \times I} + \mathbf{H}_{jk}^K \mathbf{F}_{k \times I} \quad (13)$$

Multiplying both sides of Eq. (13) by  $(\mathbf{F}_{k \times I})^{-1}$  from right hand side, one can obtain

$$\mathbf{H}_{jk}^K - \mathbf{H}_{jk}^{KU} = \mathbf{H}_{jj}^K (\mathbf{H}_{jj}^U + \mathbf{H}_{jj}^K)^{-1} \mathbf{H}_{jk}^K \quad (14)$$

Pre and post multiplication of both sides of Eq. (14) by  $(\mathbf{H}_{jj}^K)^{-1}$  and  $(\mathbf{H}_{jk}^K)^{-1}$ , respectively, results in

$$(\mathbf{H}_{jj}^K)^{-1} (\mathbf{H}_{jk}^K - \mathbf{H}_{jk}^{KU}) (\mathbf{H}_{jk}^K)^{-1} = (\mathbf{H}_{jj}^U + \mathbf{H}_{jj}^K)^{-1} \quad (15)$$

Taking reciprocal of both sides of Eq. (15), one can come up with the following expression:

$$\mathbf{H}_{jk}^K \left( \mathbf{H}_{jk}^K - \mathbf{H}_{jk}^{KU} \right)^{-1} \mathbf{H}_{jj}^K = \mathbf{H}_{jj}^U + \mathbf{H}_{jj}^K \quad (16)$$

Rearrangement of Eq. (16) provides the Formulation 1 which gives the connection point FRFs of an unknown subsystem in terms of those of the coupled system and known subsystem:

$$\mathbf{H}_{jj}^U = \mathbf{H}_{jk}^K \left( \mathbf{H}_{jk}^K - \mathbf{H}_{jk}^{KU} \right)^{-1} \mathbf{H}_{jj}^K - \mathbf{H}_{jj}^K \quad (17)$$

Remarkably, if it is assumed that only the  $j^{\text{th}}$  coordinates of the coupled system are harmonically excited while the rest of the external force vector is zero, that is,

$$\begin{pmatrix} \mathbf{F}_i \\ \mathbf{F}_j \\ \mathbf{F}_k \end{pmatrix} = \begin{pmatrix} \mathbf{0}_{i \times I} \\ \mathbf{F}_{j \times I} \\ \mathbf{0}_{k \times I} \end{pmatrix} \quad (18)$$

Eq. (9) can be reduced into the decoupling formulation previously proposed by Batista and Maia [57]:

$$\mathbf{H}_{jj}^U = \mathbf{H}_{jj}^K \left( \left( \mathbf{H}_{jj}^{KU} \right)^{-1} \mathbf{H}_{jj}^K - \mathbf{I}_{j \times j} \right)^{-1} \quad (19)$$

### 2.1.3. Derivation of Second Decoupling Formulation Proposed (Formulation 2)

Here, derivation of the second Decoupling Formulation Proposed, which is abbreviated as Formulation 2 for simplicity, is explained in detail.

Let us consider Eq. (10) this time and assume that only the  $j^{\text{th}}$  coordinates of the coupled system are harmonically excited and the rest of the external force vector is zero as given in Eq. (18). Then by using Eq. (11) and Eq. (18), one can rewrite Eq. (10) as follows:

$$\mathbf{H}_{kj}^{\text{KU}} \mathbf{F}_{j \times l} = \mathbf{H}_{kj}^{\text{K}} \left( \mathbf{H}_{jj}^{\text{U}} + \mathbf{H}_{jj}^{\text{K}} \right)^{-1} \mathbf{H}_{jj}^{\text{U}} \mathbf{F}_{j \times l} \quad (20)$$

Multiplying both sides of Eq. (20) by  $\left( \mathbf{F}_{j \times l} \right)^{-1}$  from right hand side, one can obtain:

$$\mathbf{H}_{kj}^{\text{KU}} = \mathbf{H}_{kj}^{\text{K}} \left( \mathbf{H}_{jj}^{\text{U}} + \mathbf{H}_{jj}^{\text{K}} \right)^{-1} \mathbf{H}_{jj}^{\text{U}} \quad (21)$$

Pre and post multiplication of both sides of Eq. (21) by  $\left( \mathbf{H}_{kj}^{\text{K}} \right)^{-1}$  and  $\left( \mathbf{H}_{jj}^{\text{U}} \right)^{-1}$ , respectively, results in

$$\left( \mathbf{H}_{kj}^{\text{K}} \right)^{-1} \mathbf{H}_{kj}^{\text{KU}} \left( \mathbf{H}_{jj}^{\text{U}} \right)^{-1} = \left( \mathbf{H}_{jj}^{\text{U}} + \mathbf{H}_{jj}^{\text{K}} \right)^{-1} \quad (22)$$

Taking reciprocal of both sides of Eq. (22), one can come up with the following expression:

$$\mathbf{H}_{jj}^{\text{U}} \left( \mathbf{H}_{kj}^{\text{KU}} \right)^{-1} \mathbf{H}_{kj}^{\text{K}} = \mathbf{H}_{jj}^{\text{U}} + \mathbf{H}_{jj}^{\text{K}} \quad (23)$$

Rearrangement of Eq. (23) provides the Formulation 2 which gives the connection point FRFs of an unknown subsystem in terms of those of the coupled system and known subsystem:

$$\mathbf{H}_{jj}^{\text{U}} = \mathbf{H}_{jj}^{\text{K}} \left( \left( \mathbf{H}_{kj}^{\text{KU}} \right)^{-1} \mathbf{H}_{kj}^{\text{K}} - \mathbf{I}_{j \times j} \right)^{-1} \quad (24)$$

Again, it just so happens that if only the  $k^{\text{th}}$  coordinates of the coupled system are harmonically excited as shown in Eq. (12), Eq. (10) can likewise be reduced to the formulation previously proposed by Maia et al. [45]:

$$\mathbf{H}_{jj}^U = \mathbf{H}_{jk}^K \left( \mathbf{H}_{kk}^K - \mathbf{H}_{kk}^{KU} \right)^{-1} \mathbf{H}_{kj}^K - \mathbf{H}_{jj}^K \quad (25)$$

## 2.2. Applications and Performances of Decoupling Formulations Proposed

In this section, applications of the proposed decoupling formulations to a lumped parameter system are presented and their performances are compared with those of some well-known techniques using a case study. Finally, the linear decoupling method to be used in the upcoming decoupling studies for nonlinear systems is decided.

### 2.2.1. A Case Study – Decoupling of a Linear Lumped Parameter System

The coupled system to be decoupled in this application is composed of rigidly connected two linear lumped parameter subsystems as shown in Figure 22.

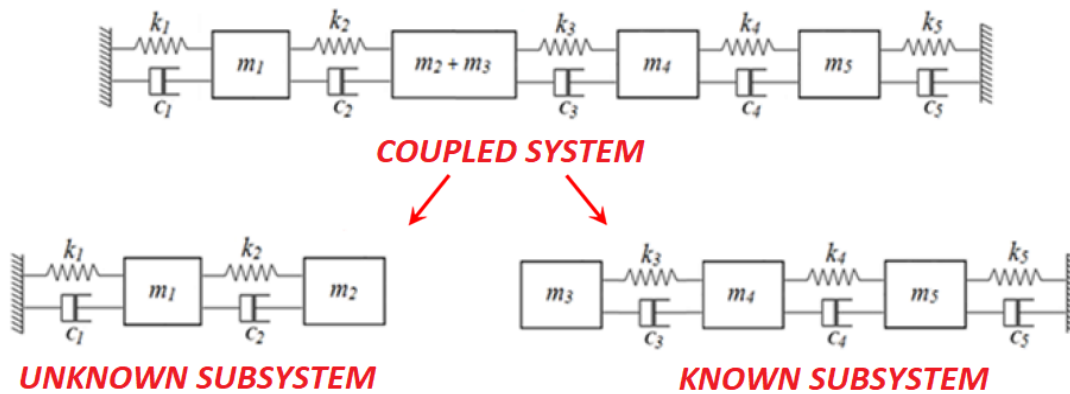


**Figure 10.** Decoupling of a linear lumped parameter system



Note that  $k$ ,  $m$  and  $c$  represent stiffness, mass and viscous damping parameters, respectively. Physical parameters of the known and the unknown subsystems are given in Table 1.

**Table 1.** Physical parameters of the lumped parameter system

Element Number ( $i$ )	$m_i$ [kg]	$k_i$ [N/m]	$c_i$ [Ns/m]
1	2.5	1500	0.15
2	3	2000	0.20
3	2	2100	0.21
4	3	1900	0.19
5	2.5	2200	0.22

Here, it is assumed that FRFs of the coupled system at the known subsystem coordinates are experimentally measured and the physical model of the known subsystem is available. The aim is to obtain FRFs of the unknown subsystem at its connection DOF. In order to simulate the measured FRFs of the coupled system, exact FRFs of the coupled system ( $\hat{\mathbf{H}}$ ) are initially calculated by using the physical parameters given in Table 1 and then polluted by simply adding complex random variables as shown below:

$$\mathbf{H}_{ab}^{KU}(\omega_k) = \hat{\mathbf{H}}_{ab}^{KU}(\omega_k) + m_{ab,k} + i n_{ab,k} \quad (26)$$

Here,  $m_{ab,k}$  and  $n_{ab,k}$  are independent random variables with Gaussian distribution, zero mean and a standard deviation of  $5e-5$  m/N which bring a noticeable pollution on calculated FRFs. The effect of such a pollution on the point FRFs at the 2<sup>nd</sup> DOF (the

coupling DOF) of the coupled system is illustrated in Figure 11 together with the FRF obtained after curve fitting.

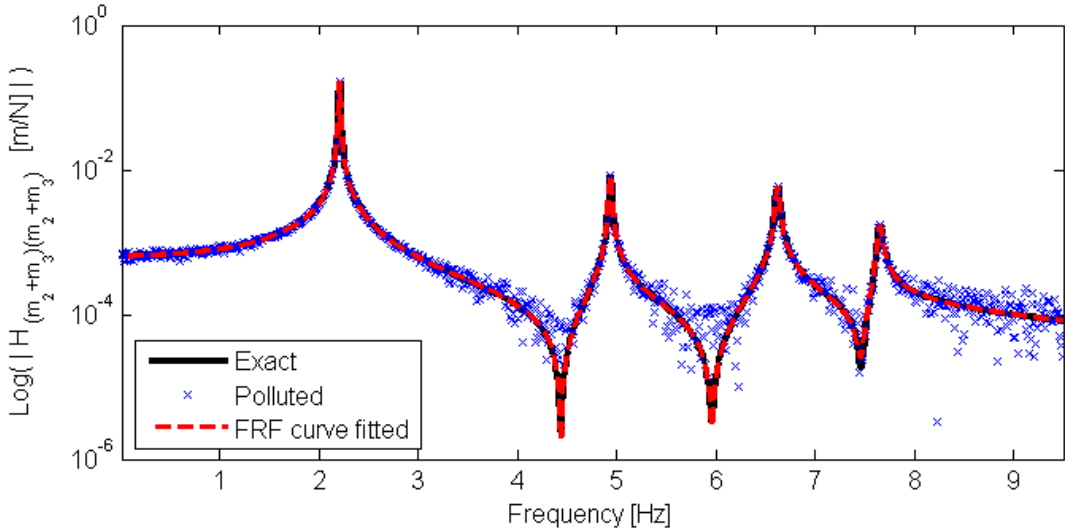


**Figure 11.** Point FRFs at the 2nd DOF of the coupled system: exact (—, black), polluted (\*, blue) and FRF curve fitted (- -, red)

Then, point FRFs at the coupling DOF of the unknown subsystem is calculated by using the proposed formulations employing the FRF curves fitted to the polluted FRFs of the coupled structure. Predicted FRFs using Formulation 1 and Formulation 2 are given in Figure 12 and Figure 13, respectively, along with the exact ones.

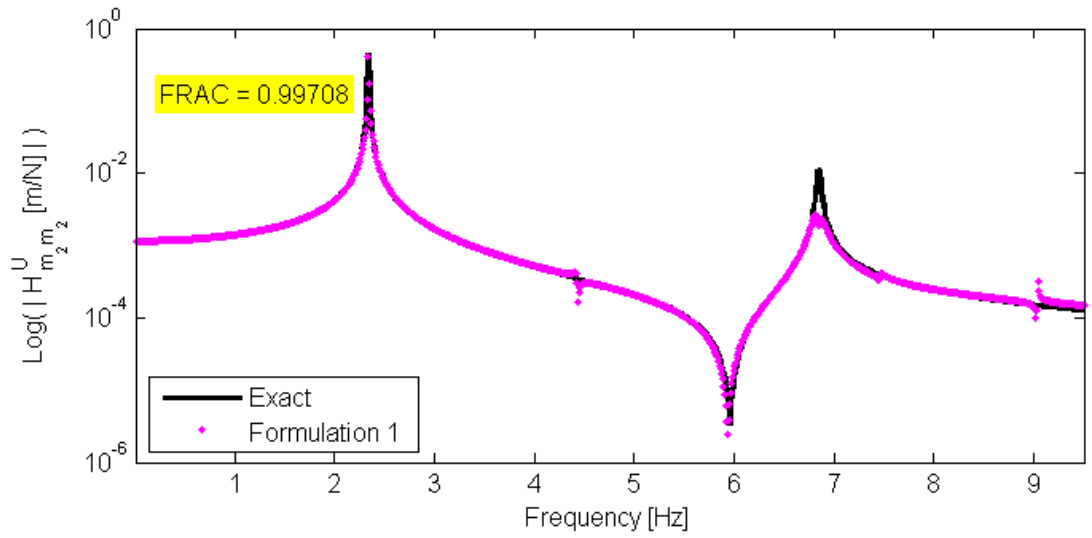


**Figure 12.** Point FRFs at the 2nd DOF of the unknown subsystem: exact (—, black), predicted using Formulation 1 (\*, magenta)

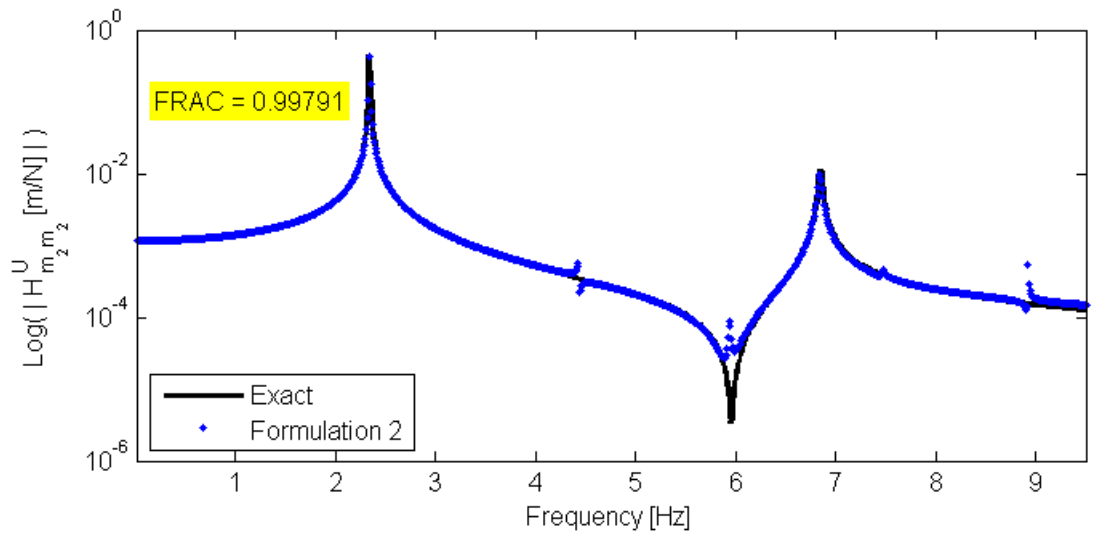


**Figure 13.** Point FRFs at the 2nd DOF of the unknown subsystem: exact (—, black), predicted using Formulation 2 (\*, blue)

Figure 12 and Figure 13 show that both approaches predict the unknown subsystem FRFs satisfactorily. However, predicted FRFs via Formulation 2 seem to fit better to the exact FRFs by visual inspection, especially around 2<sup>nd</sup> resonance.

In order to make a sound comparison, rather than visual inspection, the Frequency Response Assurance Criterion (FRAC) [65] is used. FRAC identifies the degree of similarity between a measured and analytical FRF, so that its low values indicate little correlation whereas high values indicate better correlation. FRAC values for the predicted FRFs by using Formulation 1 and Formulation 2 are calculated as 0.99708 and 0.99791, respectively. This result, once again shows that both equations can successfully be used for decoupling at least for the case study given here and Formulation 2 gives slightly better results compared to Formulation 1.

### **2.2.2. Comparison of Proposed Approaches with well-known Existing Methods**

In this section, performances of the proposed formulations are compared with those of well-known recent decoupling methods. The final equations for these methods and the input data required for each of them are summarized in Table 2.

**Table 2.** List of most recent linear decoupling methods

Ref.	Decoupling Formulation	Requires which elements of $\mathbf{H}^K$	Requires which elements of $\mathbf{H}^{KU}$	Eq.
[57]	$\mathbf{H}_{jj}^U = \mathbf{H}_{jk}^K \mathbf{H}_{kj}^K \left( \mathbf{H}_{jk}^K \left( \mathbf{H}_{kk}^K - \mathbf{H}_{kk}^{KU} \right) \mathbf{H}_{kj}^K \right)^{-1} \mathbf{H}_{jk}^K \mathbf{H}_{kj}^K - \mathbf{H}_{jj}^K$	$\begin{pmatrix} \mathbf{H}_{jj}^K & \mathbf{H}_{jk}^K \\ \mathbf{H}_{kj}^K & \mathbf{H}_{kk}^K \end{pmatrix}$	$\mathbf{H}_{kk}^{KU}$	(27)
[57]	$\mathbf{H}_{jj}^U = \left( \mathbf{H}_{jj}^K \left( \mathbf{H}_{jj}^K - \mathbf{H}_{jj}^{KU} \right) - \mathbf{I}_{jj} \right) \mathbf{H}_{jj}^K$	$\mathbf{H}_{jj}^K$	$\mathbf{H}_{jj}^{KU}$	(28)
[57]	$\mathbf{H}_{jj}^U = \mathbf{H}_{jj}^K \mathbf{H}_{jj}^K \left( \mathbf{H}_{jk}^K \left( \mathbf{H}_{kj}^K - \mathbf{H}_{kj}^{KU} \right) \mathbf{H}_{jj}^K \right)^{-1} \mathbf{H}_{jk}^K \mathbf{H}_{kj}^K - \mathbf{H}_{jj}^K$	$\begin{pmatrix} \mathbf{H}_{jj}^K & \mathbf{H}_{jk}^K \\ \mathbf{H}_{kj}^K & \mathbf{H}_{kk}^K \end{pmatrix}$	$\mathbf{H}_{kj}^{KU}$	(29)
[45]	$\mathbf{H}_{jj}^U = \mathbf{H}_{jk}^K \left( \mathbf{H}_{kk}^K - \mathbf{H}_{kk}^{KU} \right)^{-1} \mathbf{H}_{kj}^K - \mathbf{H}_{jj}^K$	$\begin{pmatrix} \mathbf{H}_{jj}^K & \mathbf{H}_{jk}^K \\ \mathbf{H}_{kj}^K & \mathbf{H}_{kk}^K \end{pmatrix}$	$\mathbf{H}_{kk}^{KU}$	(30)
[2]	$\mathbf{H}_{jj}^U = \left( \mathbf{I} - \mathbf{H}_{jj}^{KU} \left[ \mathbf{H}_{jj}^K \right]^{-1} \right)^{-1} \mathbf{H}_{jj}^{KU}$	$\mathbf{H}_{jj}^K$	$\mathbf{H}_{jj}^{KU}$	(31)

[52]	$\mathbf{H}_{jj}^U = \begin{pmatrix} \mathbf{I} - \mathbf{H}_{jj}^{KU} \mathbf{Z}_{jj}^K - \mathbf{H}_{jk}^{KU} \mathbf{Z}_{kj}^K \\ -\mathbf{H}_{kj}^{KU} \mathbf{Z}_{jj}^K - \mathbf{H}_{kk}^{KU} \mathbf{Z}_{kj}^K \end{pmatrix}^+ \begin{pmatrix} \mathbf{H}_{jj}^{KU} \\ \mathbf{H}_{kj}^{KU} \end{pmatrix}$	$\begin{pmatrix} \mathbf{Z}_{jj}^K & - \\ \mathbf{Z}_{kj}^K & - \end{pmatrix}$	$\begin{pmatrix} \mathbf{H}_{jj}^{KU} & \mathbf{H}_{jk}^{KU} \\ \mathbf{H}_{kj}^{KU} & \mathbf{H}_{kk}^{KU} \end{pmatrix}$	(32)
[52]	$\mathbf{H}_{jj}^U = \begin{pmatrix} \mathbf{H}_{jj}^{KU} \\ \mathbf{H}_{jk}^{KU} \end{pmatrix}^T \left( \begin{pmatrix} \mathbf{I}_{jj} & \mathbf{0}_{jk} \end{pmatrix} - \begin{pmatrix} \mathbf{H}_{jj}^K \\ \mathbf{H}_{kj}^K \end{pmatrix}^+ \begin{pmatrix} \mathbf{H}_{jj}^{KU} & \mathbf{H}_{jk}^{KU} - \mathbf{H}_{jk}^K \\ \mathbf{H}_{kj}^{KU} & \mathbf{H}_{kk}^{KU} - \mathbf{H}_{kk}^K \end{pmatrix} \right)^+$	$\begin{pmatrix} \mathbf{H}_{jj}^K & \mathbf{H}_{jk}^K \\ \mathbf{H}_{kj}^K & \mathbf{H}_{kk}^K \end{pmatrix}$	$\begin{pmatrix} \mathbf{H}_{jj}^{KU} & \mathbf{H}_{jk}^{KU} \\ \mathbf{H}_{kj}^{KU} & \mathbf{H}_{kk}^{KU} \end{pmatrix}$	(33)
[54]	$\mathbf{H}^U = \begin{pmatrix} \mathbf{H}^{KU} & \mathbf{0} \\ \mathbf{0} & -\mathbf{H}^K \end{pmatrix} - \begin{pmatrix} \mathbf{H}^{KU} & \mathbf{0} \\ \mathbf{0} & -\mathbf{H}^K \end{pmatrix} \begin{pmatrix} (\mathbf{B}^{KU})^T \\ (\mathbf{B}^K)^T \end{pmatrix} \dots$ $\left( \begin{pmatrix} \mathbf{B}^{KU} & \mathbf{B}^K \end{pmatrix} \begin{pmatrix} \mathbf{H}^{KU} & \mathbf{0} \\ \mathbf{0} & -\mathbf{H}^K \end{pmatrix} \begin{pmatrix} (\mathbf{B}^{KU})^T \\ (\mathbf{B}^K)^T \end{pmatrix} \right)^{-1} \begin{pmatrix} \mathbf{B}^{KU} & \mathbf{B}^K \end{pmatrix} \begin{pmatrix} \mathbf{H}^{KU} & \mathbf{0} \\ \mathbf{0} & -\mathbf{H}^K \end{pmatrix}$	$\begin{pmatrix} \mathbf{H}_{jj}^K & \mathbf{H}_{jk}^K \\ \mathbf{H}_{kj}^K & \mathbf{H}_{kk}^K \end{pmatrix}$ <p style="text-align: center;">or at least</p> $\mathbf{H}_{jj}^K$	$\begin{pmatrix} \mathbf{H}_{jj}^{KU} & \mathbf{H}_{jk}^{KU} \\ \mathbf{H}_{kj}^{KU} & \mathbf{H}_{kk}^{KU} \end{pmatrix}$ <p style="text-align: center;">or at least</p> $\mathbf{H}_{jj}^{KU}$	(34)

Among the first three formulations given in Table 2, Eq. (28) has been proved to be the one that yields the least error throughout the frequency range [57]. Likewise, Eq. (34) was confirmed as the best performer among the last three formulations given in the table [54]. Note also that, Eq. (31) is a particular case of the Eq. (32) as mentioned in reference [52]. As a result, it is decided to compare the performances of formulations given by Eq. (28), Eq. (30) and Eq. (34) in Table 2.

So, the problem given in section 2.2.1 is reinvestigated using Eq. (28), Eq. (30) and Eq. (34) in addition to the proposed decoupling formulations. It is assumed that FRFs of the coupled system and the known subsystem are available only at known subsystem coordinates, i.e., at and between coordinates  $j$  and  $k$ . Furthermore, five different sets of simulated coupled system FRFs are generated in order to examine the effects of gradually increased noise level on the performance of each decoupling method. Thus, exact coupled system FRFs are polluted by five different sets of random variables, i.e.,  $m_{ab,k}$  and  $n_{ab,k}$  in Eq. (26), with Gaussian distribution, zero mean and standard deviations ranging from  $5e-5$  m/N to  $25e-5$  m/N. Results obtained for  $15e-5$  m/N standard deviation (SD) of pollution are given in Figure 14 for illustration.

During calculations it is observed that different pollution sets with the same standard deviation may give slightly different results at each time. So, calculations via each method are repeated 100 times for each standard deviation of pollution, and the averages of the FRAC values are compared in Table 3.

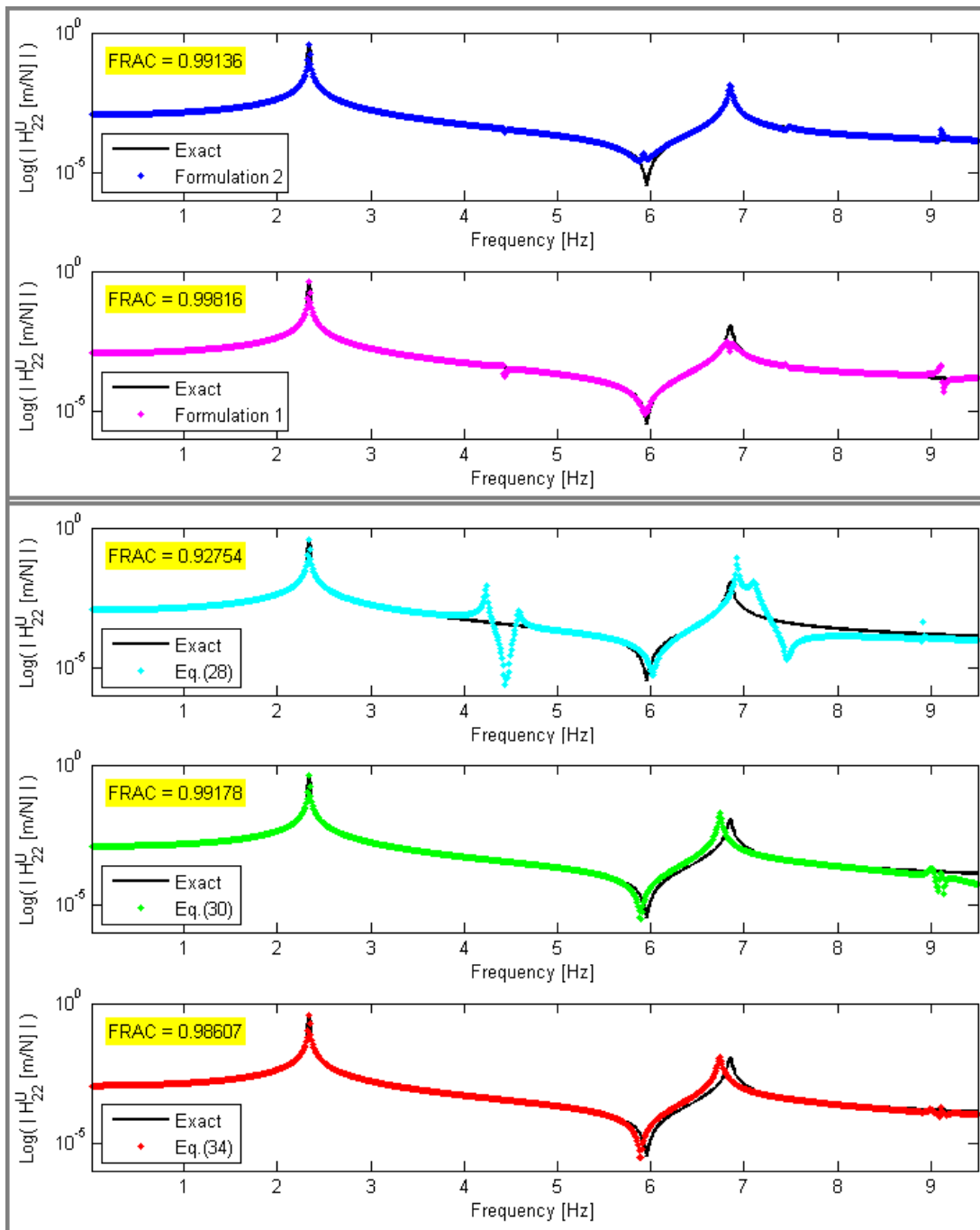


**Figure 14.** Point FRFs at the 2nd DOF of the unknown subsystem: exact (—, black), predicted via proposed formulations using data polluted with SD of  $15e-5$ : Formulation 2 (\*, blue), Formulation 1 (\*, magenta) and via formulations given in literature: Eq. (28) (\*, cyan), Eq. (30) (\*, green), Eq. (34) (\*, red)



**Table 3.** Mean and Standard Deviation (SD) of FRAC values for each method wrt varying pollution level

Method	FRAC Values (Mean $\pm$ SD values after 100 runs)				
	SD of 5e-5 m/N	SD of 10e-5 m/N	SD of 15e-5 m/N	SD of 20e-5 m/N	SD of 25e-5 m/N
Formulation 2	0.9979 $\pm$ 0.0019	0.9970 $\pm$ 0.0024	0.9900 $\pm$ 0.0234	0.9869 $\pm$ 0.0107	0.9792 $\pm$ 0.0184
Formulation 1	0.9948 $\pm$ 0.0218	0.9947 $\pm$ 0.0077	0.9912 $\pm$ 0.0096	0.9796 $\pm$ 0.0189	0.9744 $\pm$ 0.0238
Eq. (28)	0.9971 $\pm$ 0.0215	0.9759 $\pm$ 0.0274	0.9701 $\pm$ 0.0307	0.9601 $\pm$ 0.0404	0.9522 $\pm$ 0.0639
Eq. (34)	0.9928 $\pm$ 0.0192	0.9794 $\pm$ 0.0358	0.9767 $\pm$ 0.0529	0.9615 $\pm$ 0.1067	0.9778 $\pm$ 0.0340
Eq. (30)	0.9921 $\pm$ 0.0050	0.9859 $\pm$ 0.0183	0.9822 $\pm$ 0.0211	0.9736 $\pm$ 0.0435	0.9696 $\pm$ 0.0562

Table 3 shows that the overall performances of the proposed decoupling formulations are found to be better in terms of mean FRAC values. Particularly, Formulation 2 distinguishes itself as the statistically best performer among all formulations with higher FRAC values for the most of the different pollution levels. As mentioned previously, the comparison made here is for the case where one has FRFs of the coupled system and the known subsystem at and between all DOFs of the known subsystem, i.e., at and between coordinates  $j$  and  $k$ . However, this is not always the case in real life applications, since the number of DOFs of a system/subsystem is always limited to the number of measurement points and/or sensors in real-life engineering structures. Therefore, it is very important to investigate the performances of linear decoupling methods under the availability of limited number of internal measurement DOFs in the known subsystem.

For this purpose, the same calculation given above is repeated for the cases where one has the FRFs of the coupled system and the known subsystem at the following internal known subsystem coordinates:

- 1)  $m_4$  and  $m_5$
- 2) only at  $m_4$
- 3) only at  $m_5$
- 4) none

The results obtained are tabulated in Figure 15. Each grid of the plot is painted with the color of the linear decoupling method that gives the maximum mean FRAC value for a given pollution level – measured internal DOFs combination.

Figure 15 reveals that proposed decoupling formulations, particularly Formulation 2, seem to be the most successful ones for all levels of pollution, when FRFs of the coupled system and known subsystem at and between all the internal DOFs of the known subsystem are available. However, Eq. (34), the so-called Dual Formulation [54], performs better for almost all the cases when some or all the FRFs of the coupled system and known subsystem at and between the internal DOFs of the known subsystem are not available, irrespective of the pollution level.

Note also that, for the case where none of the FRFs of the coupled system and known subsystem at and between the internal DOFs of the known subsystem are available Formulation 1 and Formulation 2 cannot predict the unknown subsystem FRFs since these formulations are based on the transfer FRFs between connection coordinates  $j$  and internal coordinates  $k$  of the known subsystem. For this case, only Eq. (34) and Eq. (28) can predict the unknown subsystem FRFs with the same accuracy as can be observed from the double-colored last grid column in Figure 15.

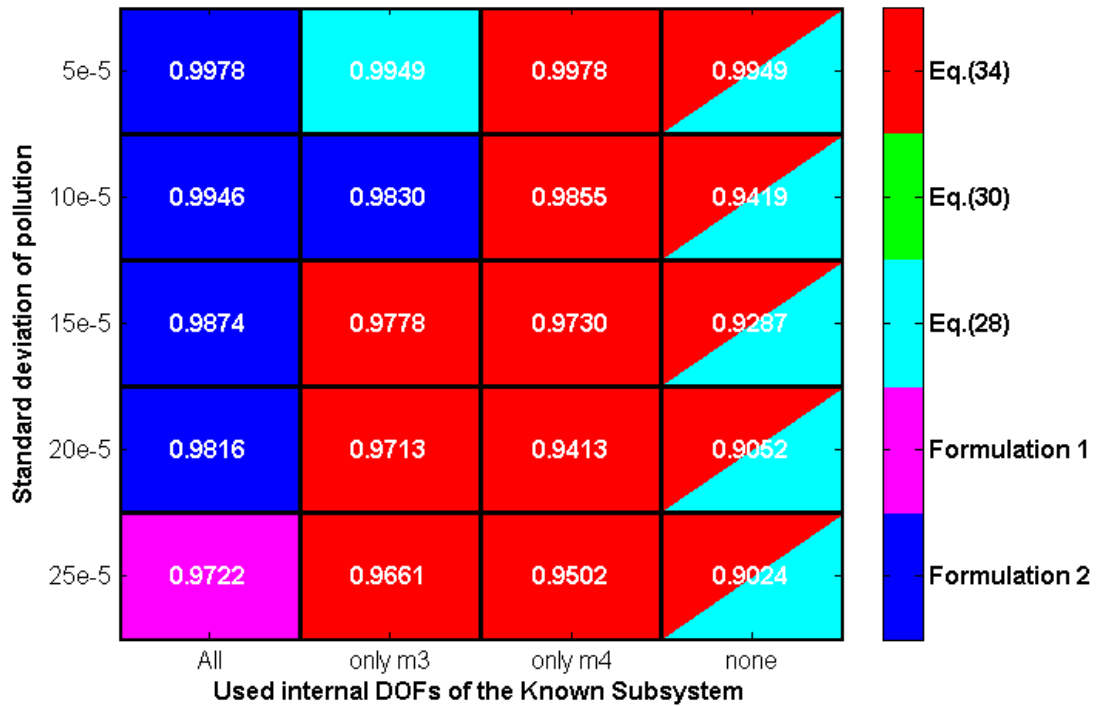


**Figure 15.** Maximum mean FRAC values obtained with the associated linear decoupling method for a given pollution level – measured internal known subsystem DOFs combination (Cell color indicates the method which gives the maximum FRAC value)

Being the prominent formulations, as concluded from Figure 15, only Eq. (34) and Formulation 2 are compared with each other in Figure 16. Again, each grid of the plot is painted with the color of linear decoupling method that gives the maximum mean FRAC value for a given pollution level – measured internal DOFs combination. This time, mean FRAC values obtained via both methods are given together at each grid of Figure 16 where the greater FRAC value is always given at the top.

As a final remark, in consideration of the results of this case study, use of Eq. (34), the so-called Dual Formulation [54], is employed in this study for decoupling of equivalent linear systems in this thesis.

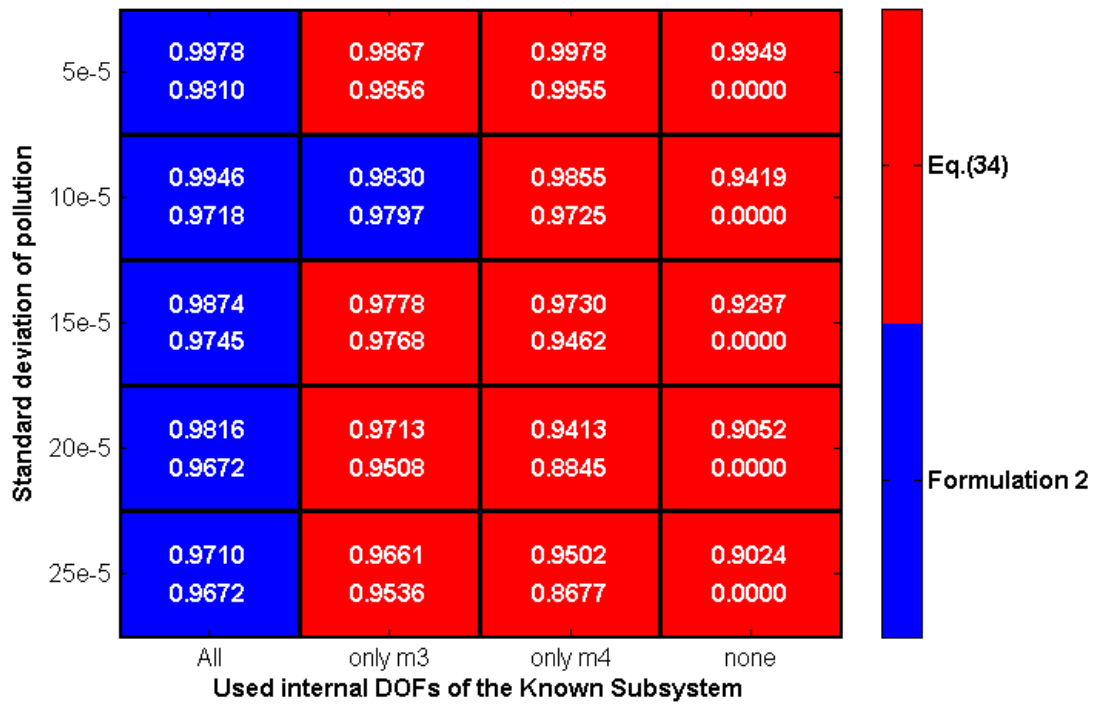


**Figure 16.** Mean FRAC values obtained via Eq. (34) and Formulation 2 for a given pollution level – measured internal known subsystem DOFs combination – greater FRAC value is always given on top of other at each grid (Cell color indicates the method which gives higher FRAC value)

## CHAPTER 3

### DECOUPLING OF NONLINEAR SYSTEMS - THEORY

In this chapter, firstly, Describing Function Method used for harmonic response calculation in nonlinear structures and measurement of FRFs in nonlinear systems are presented. Then, the parametric modal identification technique for nonlinear systems [66] which serves as one of the basis of this study is given. Finally, the theory of FRF Decoupling Method for Nonlinear Systems (FDM-NS) proposed for obtaining FRFs of a substructure decoupled from a coupled nonlinear structure is explained in detail.

#### 3.1. Harmonic Response Analysis in Nonlinear Systems

After a brief explanation of modelling nonlinearities, the theory of the Describing Function Method (DFM) used to calculate the harmonic response of a nonlinear system is given in this section.

##### 3.1.1. Dynamic Modeling of Systems with Nonlinear Elements

The equation of motion for a nonlinear MDOF system can be written as;

$$\mathbf{M}\ddot{\mathbf{x}}(t) + \mathbf{C}\dot{\mathbf{x}}(t) + i\mathbf{D}\mathbf{x}(t) + \mathbf{K}\mathbf{x}(t) + \mathbf{N}(x, \dot{x}) = \mathbf{f}(t) \quad (35)$$

where  $\mathbf{M}$ ,  $\mathbf{C}$ ,  $\mathbf{D}$  and  $\mathbf{K}$  represent mass, viscous damping, structural damping and stiffness matrices of the system, respectively. Here,  $\mathbf{x}(t)$  represents generalized displacement vector while  $\mathbf{f}(t)$  stands for the harmonic external forcing vector, and  $i$  and dot represent the unit imaginary number and derivation with respect to time, respectively. All nonlinear restoring forces are represented by  $\mathbf{N}(x, \dot{x})$  vector which

can be a function of displacement and velocity. The  $r^{\text{th}}$  element of the nonlinear restoring forcing vector,  $\mathbf{N}_r$ , can be expressed as

$$\mathbf{N}_r = \sum_{j=1}^n n_{rj} \quad r = 1, 2, 3, \dots, n \quad (36)$$

where  $n_{rj}$  represents the nonlinear restoring force between the coordinates  $r$  and  $j$ . Note that  $n_{rj}$  can be represented as a function of displacement  $x_{rj}$  and/or velocity  $\dot{x}_{rj}$  as

$$n_{rj} = n_{rj}(x_{rj}, \dot{x}_{rj}) \quad (37)$$

where  $x_{rj}$  represents the relative displacement between coordinates  $r$  and  $j$

$$x_{rj} = x_r - x_j \quad \text{for } r \neq j \quad (38)$$

and it corresponds to the displacement of grounded coordinates

$$x_{rj} = x_r \quad \text{for } r = j \quad (39)$$

The external forcing vector,  $\mathbf{f}(t)$ , can be expressed in complex vector form as

$$\mathbf{f}(t) = \mathbf{F}e^{i\theta} \quad (40)$$

where generic angle  $\theta$  can be defined as the product of angular frequency  $\omega$  and time  $t$  whereas  $\mathbf{F}$  represents the external forcing amplitude vector. Assuming that the nonlinear response to the external harmonic forcing is not essentially sinusoidal but composed of several harmonics, it can be written as a Fourier series in the form of

$$\mathbf{x}(t) = \sum_{m=0}^{\infty} \mathbf{x}(t)_m = \sum_{m=0}^{\infty} \mathbf{X}_m e^{im\theta} \quad (41)$$

where  $m$  represents the number of harmonics included and  $\mathbf{X}_m$  is the complex displacement response amplitude of the  $m^{\text{th}}$  harmonic. Then, the complex displacement response amplitude at coordinate  $r$  for the  $m^{\text{th}}$  harmonic can be defined as

$$(X_r)_m = (|X_r| \angle \psi_r)_m = |X_r|_m e^{i(\psi_r)_m} \quad (42)$$

where  $|X_r|_m$  is the magnitude and  $(\psi_r)_m$  is the phase of the complex displacement response. If we consider the Fourier series representation of the response given in Equation (42) by just considering the first  $p$  harmonics, the truncated (approximate) response can be written as

$$\mathbf{x}(t) \approx \sum_{m=0}^p \mathbf{x}(t)_m = \sum_{m=0}^p \mathbf{X}_m e^{im\theta} \quad (43)$$

### 3.1.2. Calculation of Nonlinear Response by Using DFM

In this section, the theory of determining harmonic response in nonlinear systems by using DFM [67] is presented. Considering  $n_{rj}$ , which is defined in Equation (37) as the nonlinear internal force between the coordinates  $r$  and  $j$ , and assuming for the sake of simplicity that  $n_{rj}$  is only displacement dependent, one can represent it in terms of Fourier series as

$$n_{rj} = n_{rj}(x_{rj}) = \sum_{m=0}^{\infty} (n_{rj}(x_{rj}))_m e^{im\theta} \quad (44)$$

The term  $(n_{rj}(x_{rj}))_m$  can be determined by using the following Fourier integral [67]

$$\left(n_{r_j}(x_{r_j})\right)_m = \frac{1}{2\pi} \int_0^{2\pi} n_{r_j}(x_{r_j}) d\theta \quad \text{for } m = 0 \quad (45)$$

$$\left(n_{r_j}(x_{r_j})\right)_m = \frac{i}{\pi} \int_0^{2\pi} n_{r_j}(x_{r_j}) e^{-im\theta} d\theta \quad \text{for } m \neq 0 \quad (46)$$

The terms  $\left(n_{r_j}(x_{r_j})\right)_m$  for even values of subscript  $m$  are due to nonlinearities with asymmetrical characteristics. In this study, interest is restricted to symmetrical nonlinearities only and higher harmonic terms are neglected assuming that they are much smaller compared to the fundamental harmonic. Considering only the fundamental harmonic, Equation (45) and (46) can be written as

$$n_{r_j}(x_{r_j}) = \left( \frac{i}{\pi} \int_0^{2\pi} n_{r_j}(x_{r_j}) e^{-i\theta} d\theta \right) e^{i\theta} \quad (47)$$

Similarly, Equation (43) reduces to

$$\mathbf{x}(t) = \mathbf{X} e^{i\omega t} \quad (48)$$

The nonlinear internal forces,  $n_{r_j}(x_{r_j})$ , can also be expressed in terms of describing functions,  $\nu_{r_j}$ , as follows

$$n_{r_j}(x_{r_j}) = \nu_{r_j}(X_{r_j}) X_{r_j} e^{i\theta} \quad (49)$$

where  $\nu_{r_j}$ , which can also be considered as an equivalent linear complex stiffness, is a function of the amplitude of complex displacement response. The following equation



can be derived from the nonlinear force representations given in the Equation (47) and (49) as

$$v_{rj}(|X_{rj}|) = \frac{i}{\pi |X_{rj}|} \int_0^{2\pi} n_{rj}(x_{rj}) e^{-i\theta} d\theta \quad (50)$$

Budak and Özgüven [68] suggested that nonlinear internal forces can be expressed as a multiplication of so called "nonlinearity matrix" by displacement vector. So, the internal nonlinear forces can be written as a matrix multiplication in the following form

$$\mathbf{N}(x, \dot{x}) = \mathbf{\Delta}(x, \dot{x}) \mathbf{X} e^{i\omega t} \quad (51)$$

Here,  $\mathbf{\Delta}(x, \dot{x})$  is the response dependent "nonlinearity matrix" which was first introduced by Budak and Özgüven [68] for particular types of nonlinearities. Later, it was extended by Tanrikulu et al. [69] for any type of nonlinearity in terms of DFs as given below

$$\Delta_{rr} = v_{rr} + \sum_{\substack{j=1 \\ j \neq r}}^n v_{rj} \quad r = 1, 2, 3, \dots, n \quad (52)$$

$$\Delta_{rj} = -v_{rj}, \quad r \neq j, \quad r = 1, 2, 3, \dots, n \quad (53)$$

When Equations (40), (51) and (48) are substituted into Equation (35), nonlinear internal forces can be introduced into the system as an additional equivalent stiffness matrix which is a function of unknown response amplitudes. Then, receptance matrix of the nonlinear system can be written in the following form:

$$\mathbf{H}^{\text{NL}} = \left( -\omega^2 \mathbf{M} + i\omega \mathbf{C} + i\mathbf{D} + \mathbf{K} + \mathbf{\Delta}(\mathbf{X}) \right)^{-1} \quad (54)$$

where the response of the nonlinear system can be expressed as

$$\mathbf{X} = \mathbf{H}^{\text{NL}} \mathbf{F} \quad (55)$$

It should be noted that  $\mathbf{H}^{\text{NL}}$  is a function of unknown displacement amplitude. Thus, solution of Equation (55) requires iterative methods. In this thesis, Fixed Point Iteration Method is used. The linear response of the system at a starting frequency which is calculated by omitting nonlinear terms in a nonlinear sub/system is taken as the initial guess for the displacement vector  $\mathbf{X}$  at that frequency. However, the solution obtained at a previous frequency step is taken as the initial guess at the following frequency steps. Iterations are to be repeated until the percentage displacement error drops below a specified value. Convergence is checked by calculating the maximum relative percentage error between two successive solutions which is given below:

$$e = \max \left( \left| \frac{\mathbf{X}_{i+1} - \mathbf{X}_i}{\mathbf{X}_i} \right| \right) \quad (56)$$

As to avoid divergence due to numerical instability, and also to obtain fast convergence, fixed point iteration is applied with the following relaxation [70]:

$$\mathbf{X}_{i+1}^* = (\lambda) \mathbf{X}_{i+1} + (1 - \lambda) \mathbf{X}_i, \quad 0 < \lambda < 1 \quad (57)$$

where  $\lambda$  is the relaxation coefficient employed to force a non-converging system to converge or improve convergence by damping out oscillations. Although FDM-NS uses experimental measurements, simulated experimental results which are calculated using the solution method described above are used in the case studies given in Chapter 4. In these case studies cubic stiffness and piecewise linear stiffness type of nonlinear elements are used, force-displacement characteristics of which are shown in Figure 17 and Figure 18, respectively.

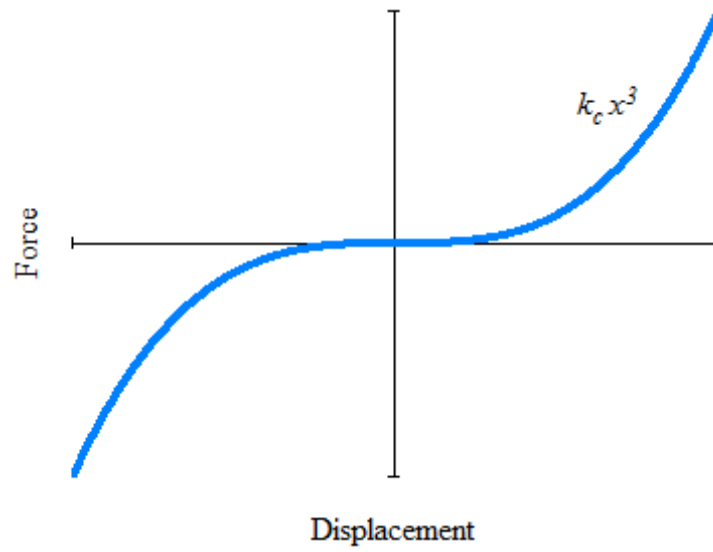


**Figure 17.** Force-displacement characteristic of cubic stiffness type of nonlinear element

Single harmonic DF representing the cubic stiffness type of nonlinearity having a force-displacement characteristic as given in Figure 17 can be expressed as:

$$v = \frac{3}{4} k_c X^2 \quad (58)$$

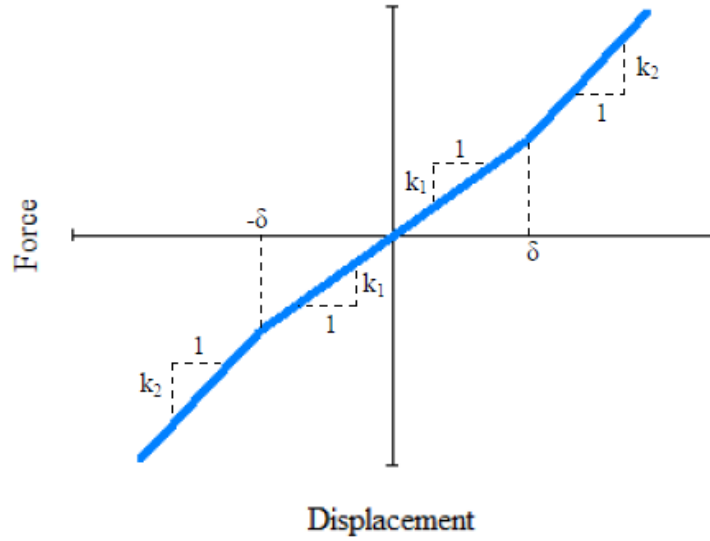


**Figure 18.** Force-displacement characteristic of piecewise linear stiffness type of nonlinear element

On the other hand, single harmonic DF representing the piecewise linear stiffness type of nonlinearity having a force-displacement characteristic as given in Figure 18 can be expressed as:

$$\begin{aligned}
 v &= k_1 && \text{for } X < \delta \\
 v &= \frac{2(k_1 - k_2)}{\pi} \left[ \arcsin\left(\frac{\delta}{X}\right) + \left(\frac{\delta}{X}\right) \sqrt{1 - \left(\frac{\delta}{X}\right)^2} \right] + k_2 && \text{for } X \geq \delta
 \end{aligned} \tag{59}$$

### 3.2. Measurement of FRFs in Nonlinear Structures

An FRF is simply a transfer function expressing the frequency domain relationship between the response of a system and the force applied on it. Furthermore, an FRF is invariant of both applied force and the response level for a linear system. However, it is not the case for a nonlinear system such that an FRF measured in a nonlinear system

is valid only for a specific force or response level maintained during the test. In the following subsections, two different measurement techniques are introduced depending on the control parameter.

### **3.2.1. Controlled Force Amplitude Test**

This test is mainly based on application of a constant amplitude harmonic excitation to a nonlinear system at each frequency step throughout a frequency span. As it is well-known, FRFs resulting from such a measurement is invariant of the force amplitude in a linear system. In other words, vibration measurements performed under different excitation levels yield the same FRF curve in linear systems. However, this is not the case for nonlinear systems. In case of a nonlinear system, vibration measurements performed under different excitation levels ends up with different FRF curves. When a constant amplitude harmonic excitation is applied to a nonlinear system over a frequency span, the equivalent damping and/or stiffness values introduced by the nonlinear elements into the structure varies as its response level changes with the changing frequency of constant amplitude harmonic excitation. This variation leads to the distortion of the FRF curve obtained which implies the presence of nonlinearity and thus can be used for nonlinearity detection. This can be observed in Figure 19 which gives FRFs of a nonlinear structure under constant harmonic excitation of different magnitudes.

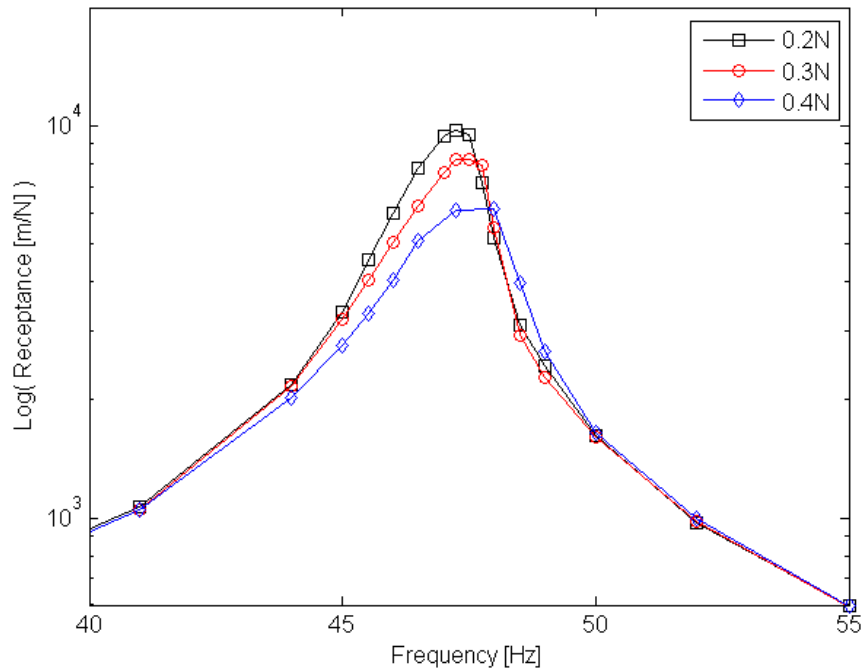


**Figure 19.** Measured FRFs of a nonlinear structure under constant harmonic excitation of different magnitudes

It should be noted that linear modal identification techniques are not applicable to FRFs obtained from such tests.

### 3.2.2. Controlled Displacement Amplitude Test

The idea behind this test is to keep the relative harmonic displacement between end coordinates of the nonlinear element constant at a given value throughout the frequency range of the test, as discussed in [71] and applied in practice in [72], so that the nonlinear element behaves linearly. In other words, controlled displacement amplitude test yields linear FRFs each corresponding to a different response level of the nonlinear element as illustrated in Figure 20. This can be mathematically seen from Equation (54): By controlling the response level of the single nonlinear element that exist in the system, the nonlinearity matrix ( $\Delta$ ) in this equation is transformed into an

additional equivalent stiffness matrix as long as the describing function for this nonlinearity is a function of the response amplitude only.

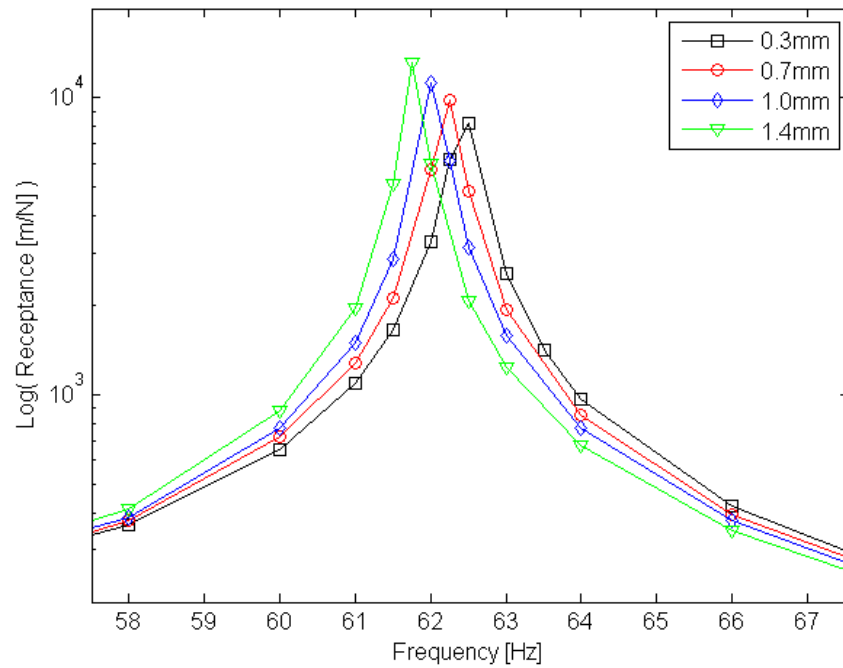


**Figure 20.** Measured FRFs of a nonlinear structure for different response levels of the nonlinear element involved

### 3.3. Theory of Parametric Identification Approach using Modal Model for Nonlinear Systems

Arslan et al. [66] suggested that if FRFs of a system having nonlinearity that can be modeled as a single nonlinear element are measured by keeping the response level of this single nonlinear element constant at a certain amplitude and this test is repeated for various different response levels, linear identification methods can be used and sets of modal parameters can be obtained, each set corresponding to a different response

level. As the identified modal parameters, natural frequencies ( $\omega_r$ ), loss factors ( $\eta_r$ ) and modal constants ( ${}_r A_{kl}$ ) vary with the response amplitude, they can be expressed as a function of the amplitude of the relative harmonic displacement between the end coordinates  $p$  and  $q$  of the nonlinear element ( $X_{pq}$ ) as follows [66]:

$$\omega_r = \omega_r(X_{pq}) \quad (60)$$

$$\eta_r = \eta_r(X_{pq}) \quad (61)$$

$${}_r A_{kl} = {}_r A_{kl}(X_{pq}) \quad (62)$$

So, obtained modal parameter variations can be used to write the pseudo receptance expression of the system as a modal summation at any given frequency as:

$$H_{kl}(\omega, X_{pq}) = \sum_{r=1}^n \frac{{}_r A_{kl}(X_{pq})}{\left( (\omega_r(X_{pq}))^2 - \omega^2 + i(\omega_r(X_{pq}))^2 \eta_r(X_{pq}) \right)} \quad (63)$$

Note that, Eq. (63) can be used in harmonic response prediction of the nonlinear system iteratively, as well as in decoupling analyses. Further details regarding the theory of this method can be found in [66].

### 3.4. Theory of FDM-NS

In this section, the underlying theory of the FDM-NS is given in detail, which is first presented and later experimentally verified in papers [73,74] written based on the work done in thesis study. The proposed method can predict FRFs of an unknown subsystem, whether linear or nonlinear, from the measured FRFs of the coupled nonlinear system and the measured or calculated FRFs of the remaining known



subsystem. Note that FDM-NS can decouple any coupled nonlinear structure provided that existing nonlinearity can be modelled as a single nonlinear element and its location is known.

The theory of FDM-NS is presented under three main headings, since it requires different approaches depending on the location of the nonlinear element in the coupled system: The nonlinearity can be either in the unknown subsystem or in the known subsystem, or it can connect these subsystems. Remind that the notation used throughout this thesis for all systems/subsystems and the coordinate sets are given in Figure 8 in section 2.1.1.

### **3.4.1. Nonlinearity in the Unknown Subsystem**

This is the case where the single nonlinear element is at a certain location in the unknown subsystem. Note that, the number of measurement points on the coupled system reduces depending on the location of the nonlinear element. When the nonlinear element is located between internal DOFs (i), complete FRF matrix of the coupled system for the coordinates of interest should be obtained through experimental measurements. However, if the nonlinear element is between an internal DOF (i) and a coupling DOF (j) of the unknown subsystem, it is not necessary to measure FRFs at and between internal DOFs (i) of the coupled system (i.e.,  $\mathbf{H}_{ii}^{KU}$ ) anymore. If the nonlinear element is located between coupling DOFs (j) of the unknown subsystem, only FRFs of the coupled system at and between coordinates j and k (i.e.,  $\mathbf{H}_{jj}^{KU}$ ,  $\mathbf{H}_{jk}^{KU}$  and  $\mathbf{H}_{kk}^{KU}$ ) should be measured.

The solution of this subproblem basically requires the sequential application of the following techniques:

- Controlled displacement amplitude vibration test at several different amplitudes.

- Application of a decoupling technique for linear systems (the dual assembly approach [54] is used in this thesis).
- Application of the parametric modal identification technique for nonlinear systems [66] discussed in Section 3.3.

The complete FRF matrix of the known subsystem for the coordinates of interest can be calculated by using its available system parameters or it can be obtained experimentally. On the other hand, the required FRFs of the coupled nonlinear system can be measured by conducting controlled displacement amplitude tests where the amplitude of the relative displacement between the end coordinates of the nonlinear element is kept constant at a different value for each FRF curve. This results in various different linear FRF curves for the coupled nonlinear system where each set corresponds to different response level of the nonlinear element. Then, one can come up with different FRF curves for the nonlinear unknown subsystem each of which represents a different equivalent linear system by performing linear decoupling. Here, the dual assembly approach [54] is used as the linear decoupling method, which results in the following equation:

$$\begin{aligned}
\mathbf{H}^U &= \begin{bmatrix} \mathbf{H}^{KU} & \mathbf{0} \\ \mathbf{0} & -\mathbf{H}^K \end{bmatrix} - \begin{bmatrix} \mathbf{H}^{KU} & \mathbf{0} \\ \mathbf{0} & -\mathbf{H}^K \end{bmatrix} \begin{bmatrix} \mathbf{B}_E^{KU^T} \\ \mathbf{B}_E^{K^T} \end{bmatrix} \\
&\times \left( \begin{bmatrix} \mathbf{B}_C^{KU} & \mathbf{B}_C^K \end{bmatrix} \begin{bmatrix} \mathbf{H}^{KU} & \mathbf{0} \\ \mathbf{0} & -\mathbf{H}^K \end{bmatrix} \begin{bmatrix} \mathbf{B}_E^{KU^T} \\ \mathbf{B}_E^{K^T} \end{bmatrix} \right)^+ \\
&\times \begin{bmatrix} \mathbf{B}_C^{KU} & \mathbf{B}_C^K \end{bmatrix} \begin{bmatrix} \mathbf{H}^{KU} & \mathbf{0} \\ \mathbf{0} & -\mathbf{H}^K \end{bmatrix}
\end{aligned} \tag{64}$$

where  $\mathbf{B}_C = \begin{bmatrix} \mathbf{B}_C^{KU} & \mathbf{B}_C^K \end{bmatrix}$  and  $\mathbf{B}_E = \begin{bmatrix} \mathbf{B}_E^{KU} & \mathbf{B}_E^K \end{bmatrix}$  represent signed Boolean matrices used to enforce compatibility and equilibrium at interface DOFs, and the symbol  $^+$

stands for the generalized inverse. Note here that, each FRF curve obtained for the unknown subsystem is valid only for a different level of the nonlinear element. So, one can use each FRF curve in order to parametrically identify the corresponding equivalent linear system and thus obtain the variation of modal parameters with respect to the response level of the nonlinear element [66]. Then, response dependent FRFs of the unknown nonlinear subsystem can be computed iteratively for any excitation level by using these modal parameter variations.

### 3.4.2. Nonlinearity in the Known Subsystem

This is the case where a single nonlinear element exists at any given location in the known subsystem. (i.e., at coordinates  $j$ ,  $k$  or between coordinates  $j$  and  $k$ ). In this case, the FRFs of the coupled system at and between coordinates  $j$  and  $k$  (i.e.,  $\mathbf{H}_{jj}^{KU}$ ,  $\mathbf{H}_{jk}^{KU}$  and  $\mathbf{H}_{kk}^{KU}$ ) are necessary, and the following techniques should be used sequentially for the solution of this subproblem:

- Controlled displacement amplitude vibration test at a specific amplitude.
- Application of a decoupling technique for linear systems (the dual assembly approach [54] is used in this thesis).

First of all, point and transfer FRFs of the coupled system along with those of the known subsystem at all coordinates  $j$  and  $k$  should be measured by keeping the amplitude of the relative harmonic displacement between the end coordinates of the nonlinear element at a certain value at each frequency step across a frequency range of interest. This will result in linear FRF curves for the coupled system and the known subsystem for a specific relative displacement amplitude. Moreover, it leads to the same nonlinearity matrix to be introduced into the dynamic stiffness matrices of the coupled system and the known subsystem at each frequency of measurement which can be expressed as follows, respectively:

$$\mathbf{Z}^K = \mathbf{K}^K - \omega^2 \mathbf{M}^K + i\omega \mathbf{C}^K + \Delta \quad (65)$$

$$\mathbf{Z}^{KU} = \mathbf{K}^{KU} - \omega^2 \mathbf{M}^{KU} + i\omega \mathbf{C}^{KU} + \begin{pmatrix} 0 & 0 & 0 \\ 0 & & \\ 0 & \Delta & \end{pmatrix} \quad (66)$$

where  $\Delta = \begin{pmatrix} \Delta_{jj} & \Delta_{jk} \\ \Delta_{kj} & \Delta_{kk} \end{pmatrix}$ .

Note that, addition of a fixed valued nonlinearity matrix into the dynamic stiffness matrices of the coupled system and the known subsystem throughout a frequency span is equivalent to modifying the stiffness matrix ( $\mathbf{K}^K$ ) of the known subsystem. Such a modification will not affect the unknown subsystem characteristics as well as the results of the decoupling process. So, the problem reduces to decoupling of linear systems. Consequently, FRFs of the unknown subsystem at its connection coordinates (j) can be obtained by just applying the dual assembly approach [54], for which the resulting formulation is given by Equation (64).

### 3.4.3. Nonlinearity at the Connection of Two Subsystems

When the nonlinear element connects two subsystems, the approach to be used for the solution differs depending on the availability of its parameters. If the parameters of the nonlinear connection element are not available, it can be included into the unknown subsystem. Then, a massless node can be considered at the free end of the nonlinear connection element which is rigidly connected to the known subsystem when coupled (Figure 21a). Note that, this approach has also been used in [38] previously. Thus, the system reduces to the one considered in section 3.4.1.

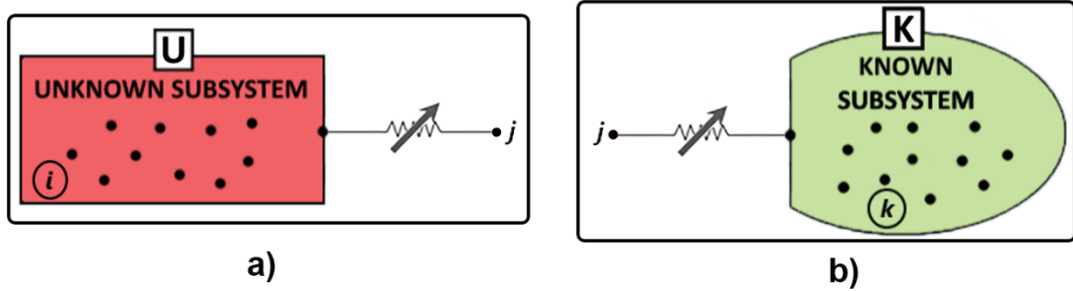


**Figure 21.** Inclusion of the connecting nonlinear element, a) in the unknown subsystem, b) in the known subsystem

Similarly, if the parameters of the nonlinear connection element are available, the nonlinear element can be included into the known subsystem. Again, a massless node can be considered at the free end of the nonlinear connection element which is rigidly connected to the unknown subsystem when coupled (Figure 21b). Then, the problem reduces to the one defined in section 3.4.2.



## CHAPTER 4

### APPLICATIONS OF FDM-NS TO NONLINEAR LUMPED PARAMETER MDOF SYSTEMS

In this chapter, applications of FDM-NS to nonlinear lumped parameter MDOF systems are given in order to demonstrate the validity and the performance of the proposed method on theoretical bases. The case studies are categorized depending on the location of the nonlinear element in the coupled nonlinear system. In other words, the same MDOF system with identical physical parameters is studied in each case study except the location and the type of the nonlinear element involved. Moreover, theoretically calculated data is not used directly, but polluted in each case study in order to simulate the experimental measurements more realistically.

#### 4.1. Case Study 1 - Nonlinearity in the Unknown Subsystem

In this case study, a 2 DOF nonlinear unknown subsystem is to be decoupled from a 3 DOF lumped parameter coupled nonlinear system via FDM-NS. Coupled nonlinear system consists of two subsystems connected to each other rigidly as illustrated in Figure 22. Physical parameters of the coupled system are given in Table 4.

**Table 4.** Physical parameters of the coupled system

Element Number ( $i$ )	$m_i$ [kg]	$k_i$ [N/m]	$c_i$ [Ns/m]
1	0.20	2000	0.50
2	0.10	1000	0.20
3	0.15	1000	0.30
4	0.20	1500	0.60

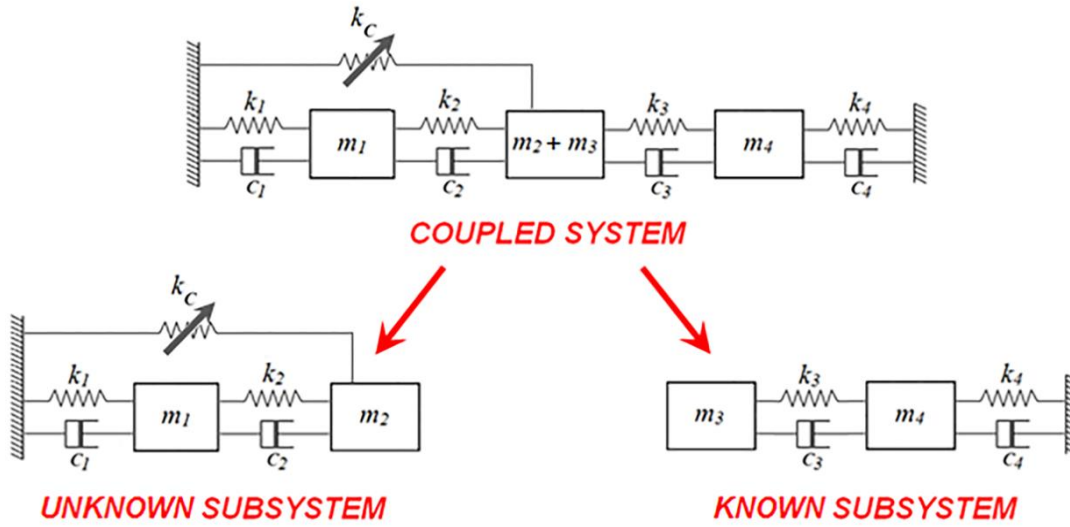


**Figure 22.** Decoupling of a nonlinear coupled system – nonlinearity is at the coupling DOF of the unknown subsystem

The existing nonlinearity in the unknown subsystem is of cubic stiffness type. Furthermore, its ends are connected to the coupling DOF of the unknown subsystem and the ground. The nonlinear internal force expression and related parameters for this nonlinear element are defined as follows:

$$n(x) = k_c x^3 \quad \text{where} \quad k_c = 2 \times 10^5 \text{ N/m}^3 \quad (67)$$

As the first step of FDM-NS, complete FRF matrix of the known subsystem is theoretically calculated from the known system parameters for the DOFs of interest ( $m_3$  and  $m_4$ ). Secondly, point and transfer FRF sets of the coupled system at the known subsystem DOFs ( $m_2+m_3$  and  $m_4$ ) are obtained by performing a set of controlled displacement amplitude experiments for different displacement levels of the nonlinear element. Thereby, exact FRF sets of the coupled system are obtained for 20 different harmonic displacement amplitudes of its second DOF ( $m_2+m_3$ ) ranging from 3 mm to



60 mm with 3 mm increment. A complex random number is added to each calculated FRF set in order to simulate measurement errors as follows:

$$\mathbf{H}_{ab}^{\text{KU}}(\omega_k) = \hat{\mathbf{H}}_{ab}^{\text{KU}}(\omega_k) + m_{ab,k} + i n_{ab,k} \quad (68)$$

In Equation (68),  $m_{ab,k}$  and  $n_{ab,k}$  are independent random variables with Gaussian distribution having a zero mean and a standard deviation of  $4 \times 10^{-6}$  m/N which brings a noticeable pollution on calculated FRFs. Now, one can obtain point FRFs of the unknown subsystem at its coupling DOF ( $m_2$ ) as given in Figure 23 by performing linear decoupling via dual assembly approach [54] for 20 different FRF sets of the coupled system. Since the calculated unknown subsystem FRFs still have the effect of measurement errors, curves in the form of an FRF are fitted to each of them as shown in Figure 23.

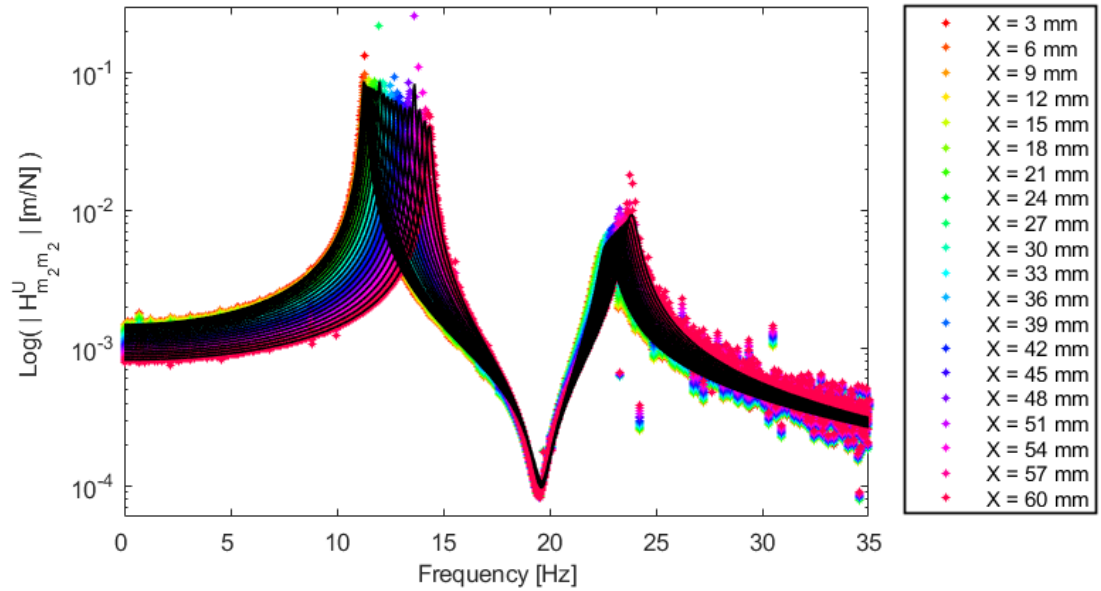


**Figure 23.** Point FRFs of the unknown subsystem at  $m_2$  (colored points) and fitted FRF curves (black lines)

From now on, parametric modal identification technique [66] can be applied step by step. First, modal parameters of each fitted FRF curve are extracted using the linear modal identification technique developed by Richardson and Formenti [75]. Then, their variations as a function of the amplitude of relative harmonic displacement between end coordinates of the nonlinear element are obtained as shown in Figure 24 and Figure 25 for the first and second modes, respectively. Note that, fitted curves to the obtained modal parameters are polynomials of third order. As a result, point response of the unknown nonlinear subsystem can easily be calculated for any forcing level using these modal parameter variations.

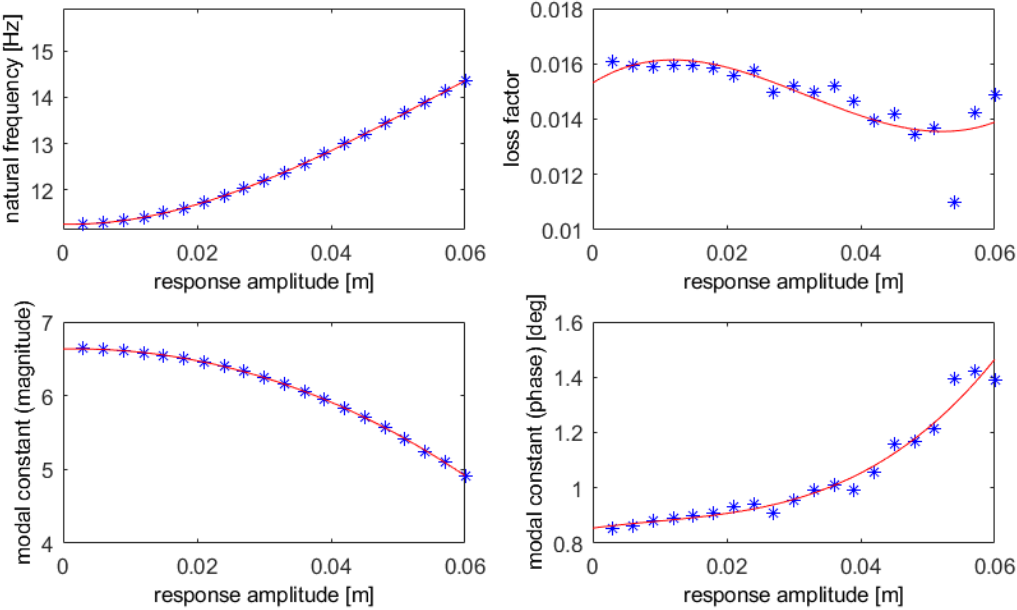


**Figure 24.** Modal parameter variations for the 1st mode wrt response amplitude of the nonlinear element (\*, identified parameters & —, fitted curves)

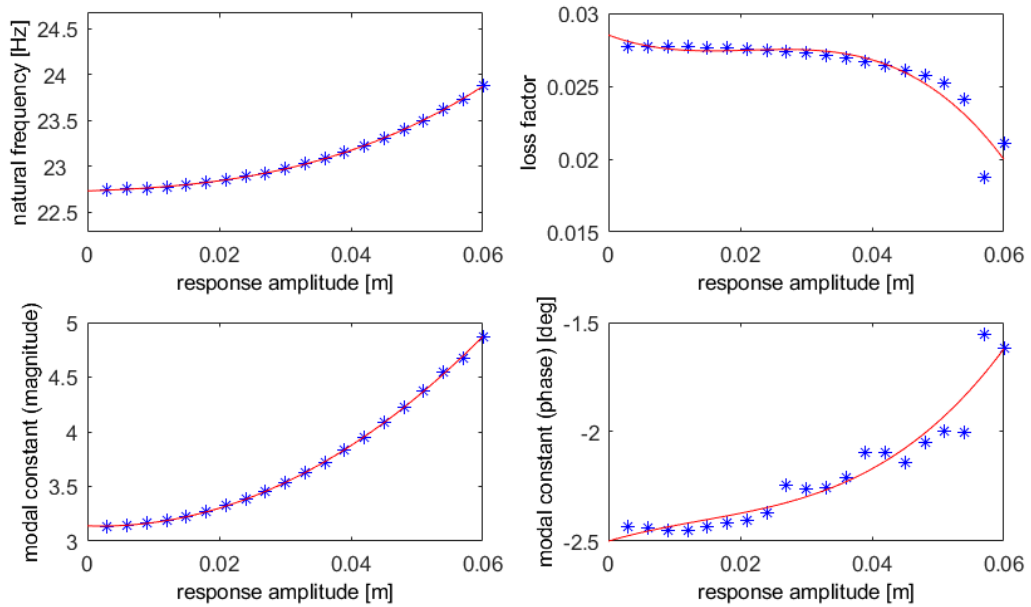


**Figure 25.** Modal parameter variations for the 2nd mode wrt response amplitude of the nonlinear element (\*, identified parameters & —, fitted curves)

In order to validate the results of FDM-NS, point response of the unknown subsystem at  $m_2$  is calculated for a harmonic excitation of magnitude 1 N, both by performing modal synthesis using the modal parameter variations given in Figure 24 and Figure 25 (as a function of response amplitude), and by applying DFM using all of the actual parameters of this subsystem. A frequency step size of 0.02 Hz is employed during numerical calculations. Note that both approaches are based on the basic assumption that harmonic excitation results in harmonic response at the same frequency. Obtained results are illustrated for both forward and backward frequency sweeps in Figure 26 and Figure 27. Agreement of the predicted and directly calculated responses proves the validity of the proposed method for this case where nonlinearity is in the unknown subsystem.

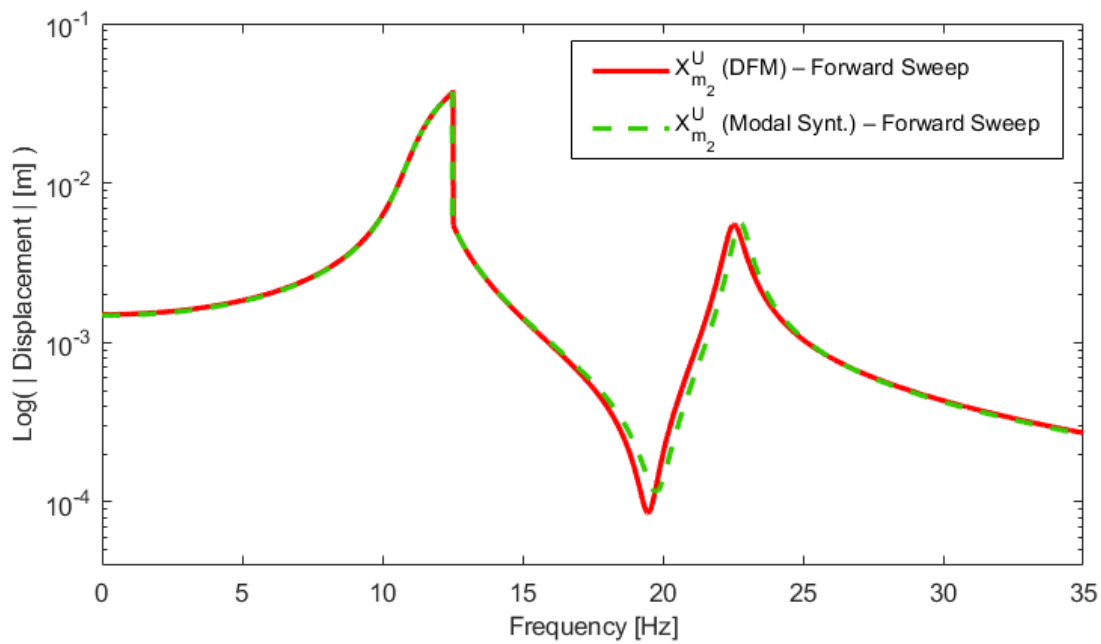


**Figure 26.** Forward frequency sweep response of the unknown subsystem at  $m_2$

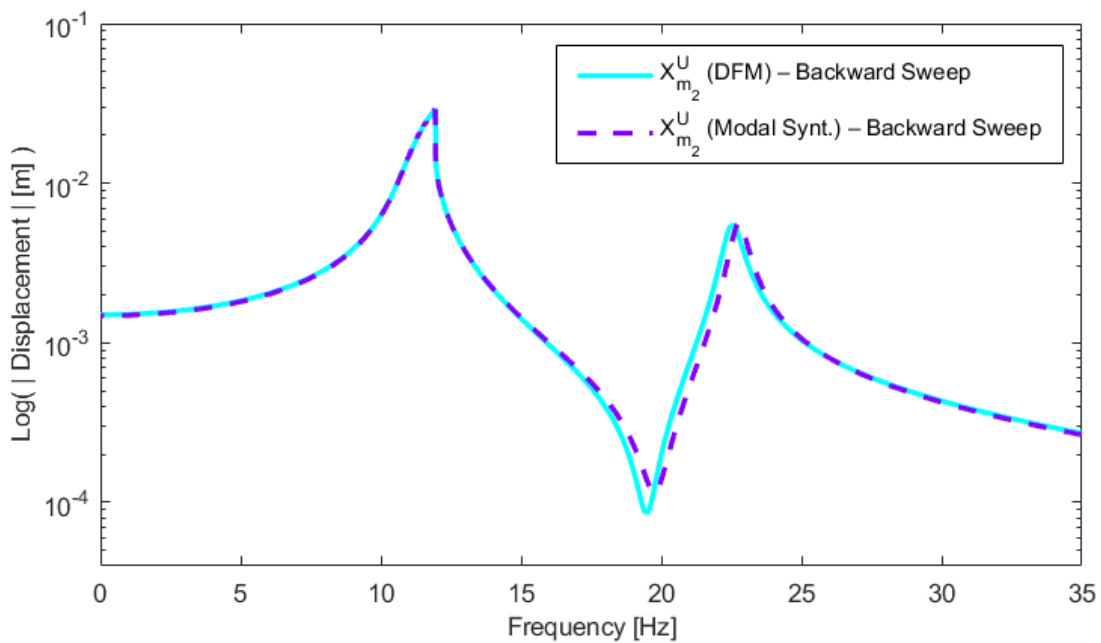


**Figure 27.** Backward frequency sweep response of the unknown subsystem at  $m_2$

## 4.2. Case Study 2 - Nonlinearity in the Known Subsystem

In this case study, a 2 DOF linear unknown subsystem is to be decoupled from a 3 DOF lumped parameter coupled nonlinear system using FDM-NS. Coupled nonlinear system consists of two subsystems connected to each other rigidly as illustrated in Figure 28. Physical parameters of the coupled system are identical to those given in Table 4. The nonlinearity in the known subsystem is again assumed to be of cubic stiffness type. The nonlinear internal force expression and the related parameters of the nonlinear element are the same as those given in Equation (67). But this time, its ends are connected to the internal DOF ( $m_4$ ) of the known subsystem and the ground.

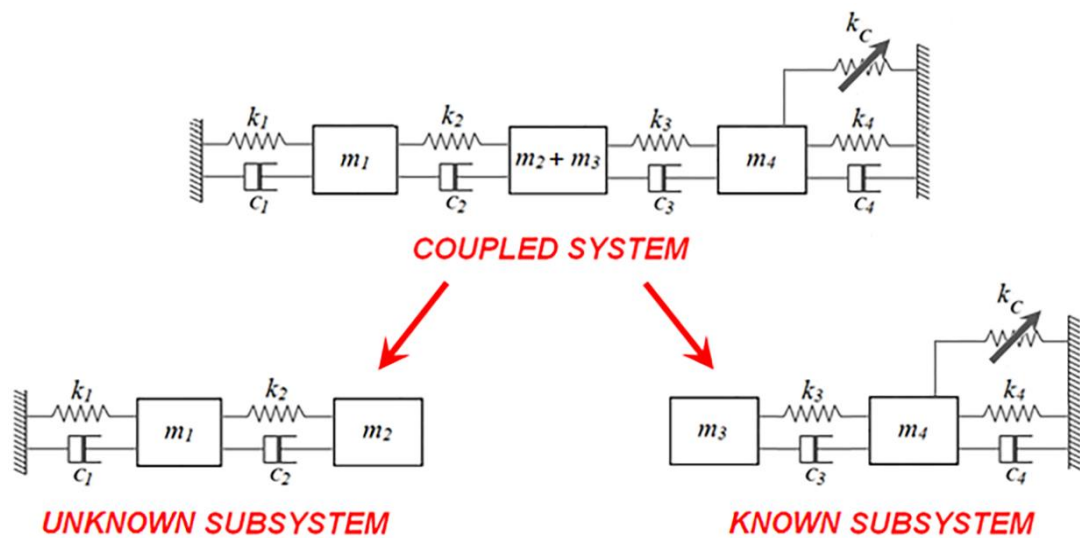


**Figure 28.** Decoupling of a nonlinear coupled system – nonlinearity is in the known subsystem

As the first step of FDM-MS, point and transfer FRFs of the coupled system and the known subsystem at and between known subsystem coordinates are obtained by carrying out a controlled displacement amplitude test throughout the desired frequency

span. For this application, exact FRFs of the coupled system ( $\hat{\mathbf{H}}^{\text{KU}}$ ) and of the known subsystem ( $\hat{\mathbf{H}}^{\text{K}}$ ) are calculated by using the physical parameters given in Table 4. In these calculations, the magnitude of the harmonic force is taken such that response level of the cubic nonlinearity remains constant (20 mm for both systems) at each frequency step. Note that a frequency step size of 0.01 Hz is employed during numerical calculations. Calculated FRFs are polluted by adding a complex random number in order to simulate measurement errors as follows:

$$\mathbf{H}_{\text{ab}}^{\text{KU}}(\omega_k) = \hat{\mathbf{H}}_{\text{ab}}^{\text{KU}}(\omega_k) + m_{\text{ab},k} + i n_{\text{ab},k} \quad (69)$$

$$\mathbf{H}_{\text{ab}}^{\text{K}}(\omega_k) = \hat{\mathbf{H}}_{\text{ab}}^{\text{K}}(\omega_k) + p_{\text{ab},k} + i q_{\text{ab},k} \quad (70)$$

In Equations (69) and (70),  $m_{\text{ab},k}$ ,  $n_{\text{ab},k}$ ,  $p_{\text{ab},k}$  and  $q_{\text{ab},k}$  are independent random variables with Gaussian distribution having zero mean and a standard deviation of  $3 \times 10^{-5}$  m/N which brings a noticeable pollution on calculated FRFs. Effects of such a pollution on point receptances of the coupled system and of the known subsystem at  $m_4$  are illustrated in Figure 29 together with FRF curves obtained just after curve fitting. Note that FRFs given in the figure show linear behavior since they are obtained via controlled displacement amplitude test. Otherwise, the responses of the coupled system and the known subsystem would behave nonlinearly as illustrated in Figure 30 which shows FRF curves obtained for both systems when a constant amplitude harmonic excitation of magnitude 4 N is applied to  $m_4$ .

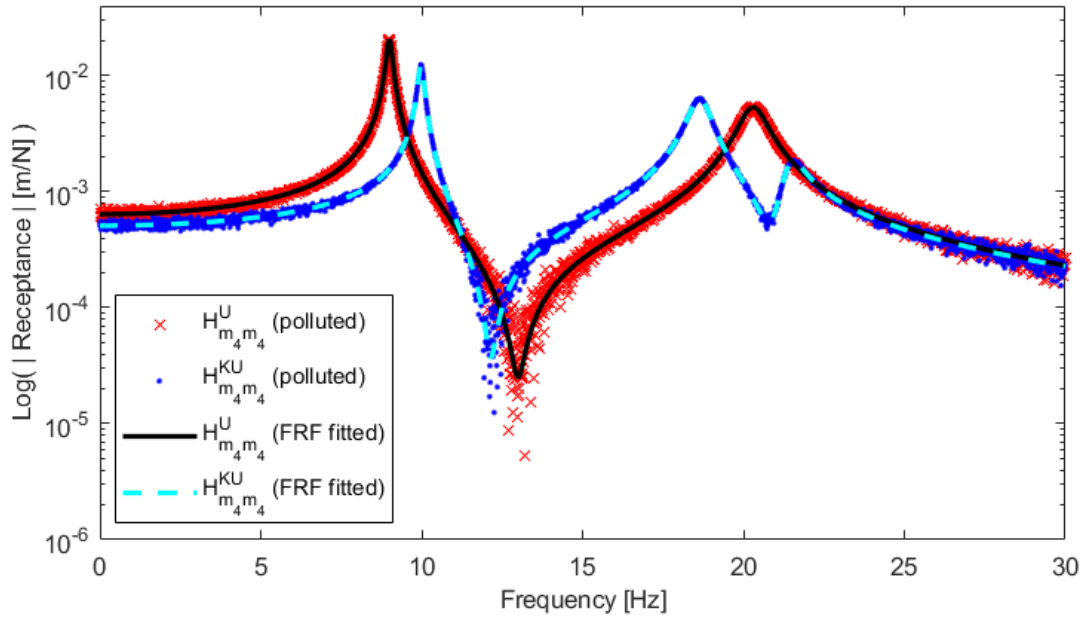


**Figure 29.** Polluted and curve fitted point receptances of the coupled system and the known subsystem at  $m_4$

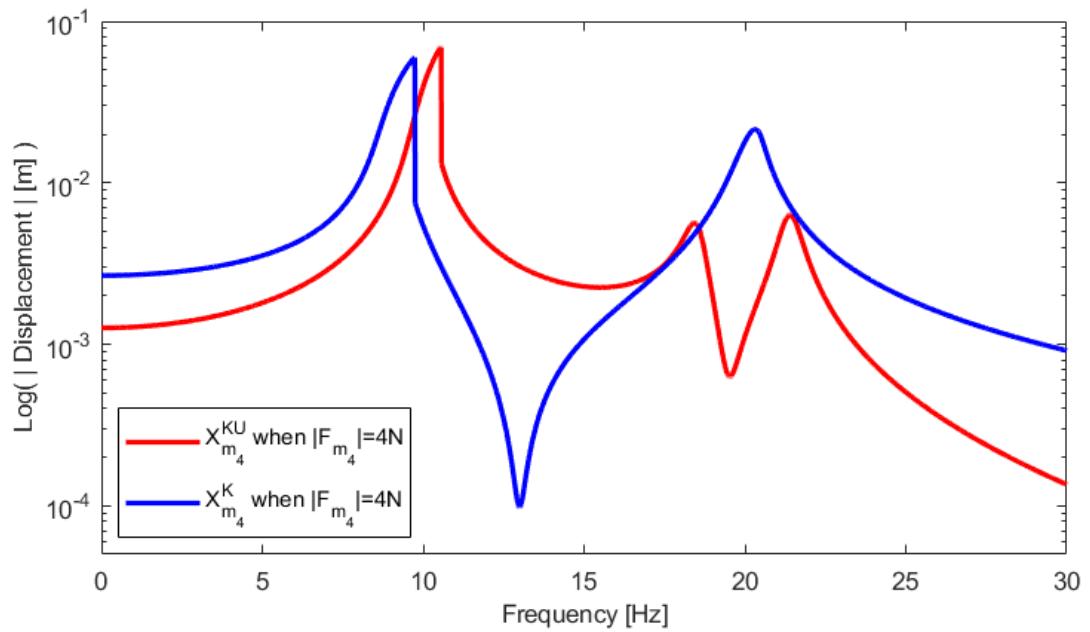


**Figure 30.** Frequency responses of the coupled system and the known subsystem at  $m_4$  under constant amplitude harmonic excitation

As of now, point receptances of the unknown subsystem at  $m_2$  are obtained via dual assembly approach [54] by employing FRF curves fitted to the calculated point and transfer receptances of the coupled system at  $m_2+m_3$  and  $m_4$ , along with those of the known subsystem at  $m_3$  and  $m_4$ . Exact and predicted point FRFs of the unknown subsystem at  $m_2$  are presented in Figure 31.

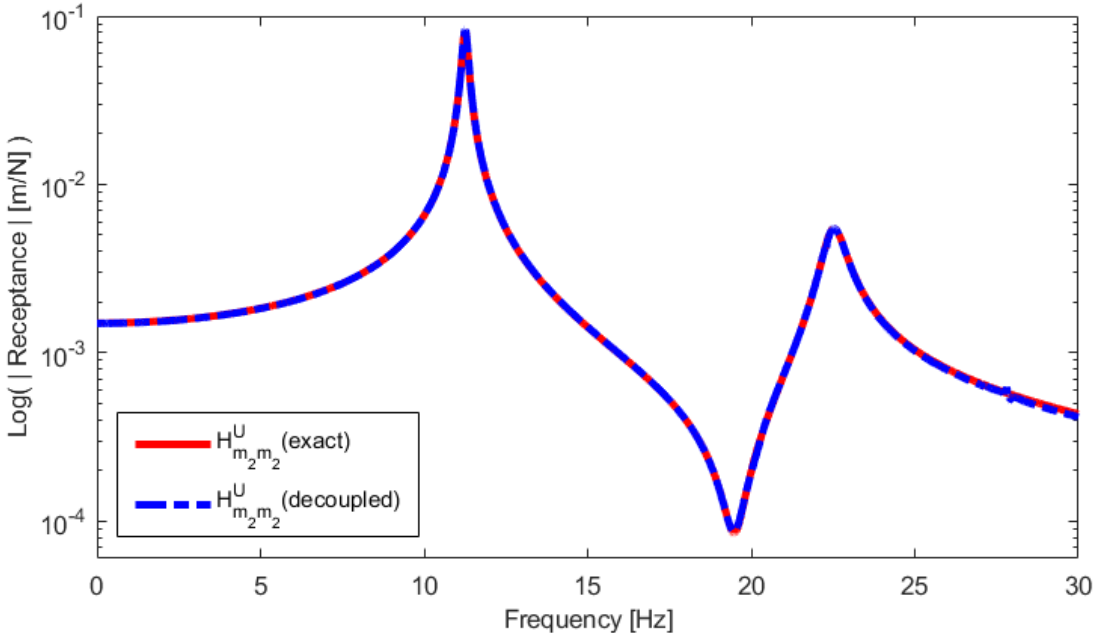


**Figure 31.** Exact and decoupled point receptances of the unknown subsystem at  $m_2$

One can observe from the Figure 31 that FRFs predicted by using FDM-NS shows almost perfect agreement with the exact ones. Consequently, the decoupling method developed is proved to yield satisfactory results in the case where nonlinearity is in the known subsystem.



### 4.3. Case Study 3 - Nonlinearity at the Connection of Subsystems

This case study is about decoupling of a coupled nonlinear MDOF system composed of two subsystems having 2 DOFs and coupled to each other via linear and nonlinear elastic elements as illustrated in Figure 32.

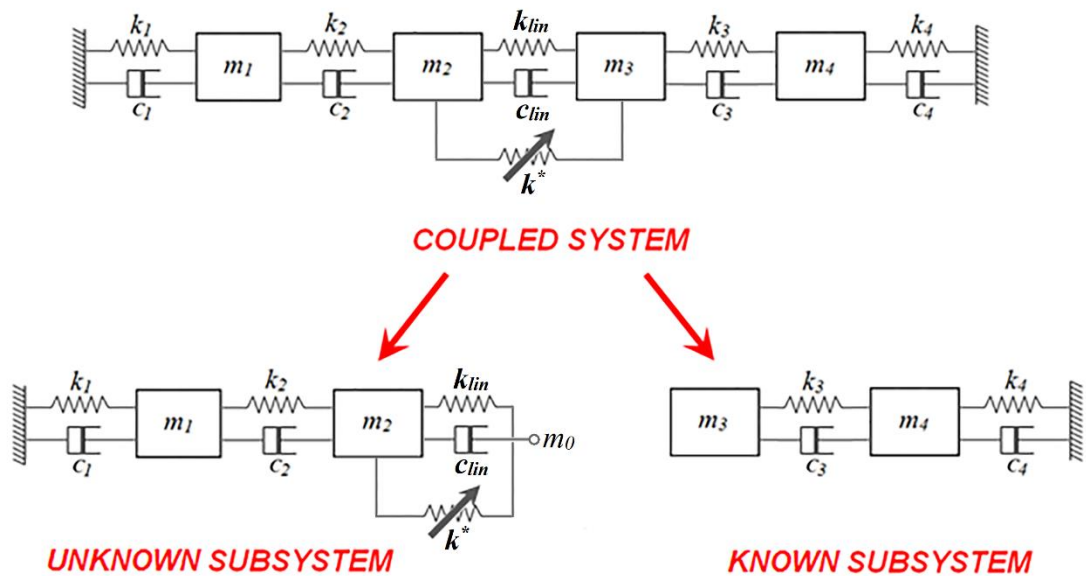


**Figure 32.** Decoupling of a nonlinear coupled system – nonlinearity is at the connection of subsystems

Physical parameters of the coupled system are identical to those given in Table 4 except the connection elements. Parameters of the linear elastic stiffness and viscous damping elements connecting two subsystems are taken as 800 N/m and 0.02 N/ms, respectively. The nonlinear connection element is assumed to be of gap type nonlinearity where the relation between nonlinear internal force and displacement can be expressed as:

$$\begin{aligned}
n(x, \dot{x}) &= 0 & \text{for } |x| < \delta \\
n(x, \dot{x}) &= k^* (x - \delta) & \text{for } x \geq \delta \\
n(x, \dot{x}) &= k^* (x + \delta) & \text{for } x \leq -\delta
\end{aligned} \tag{71}$$

Note that in Equation (71)  $k^*$  represents the stiffness at specified elongation intervals and  $\delta$  is the elongation corresponding to the point of transition from the gap to the stiffness  $k^*$ . Their values are set as 600 N/m and 1 mm, respectively. A graphical representation showing the force-displacement characteristic of this nonlinear element is given in Figure 33.

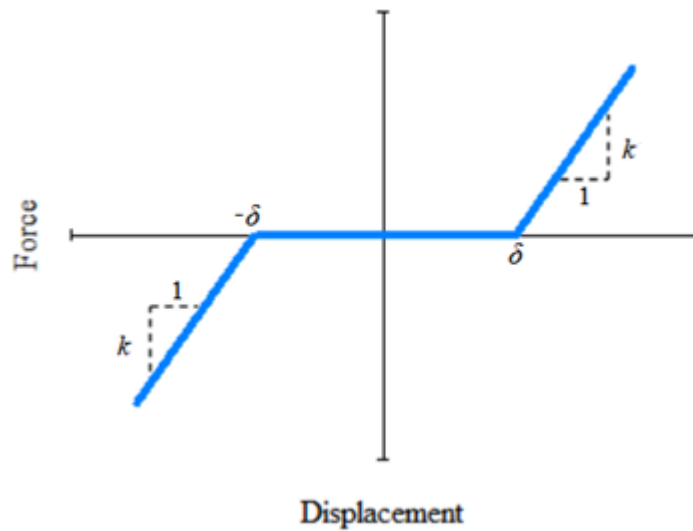


**Figure 33.** Force-displacement characteristic of gap nonlinearity

In this case study, it is assumed that coupled nonlinear system can only be excited from known subsystem coordinates ( $m_3$  and  $m_4$ ) and only responses of the  $m_2$ ,  $m_3$  and  $m_4$  are measurable. Moreover, it is assumed that the parameters of the linear and nonlinear connection elements are not available. Therefore, they are included in the unknown

subsystem as illustrated in Figure 32 such that a third node having zero mass, which is called  $m_0$ , is defined at the free end of the connection elements. As the first step of FDM-NS, the complete FRF matrix of the known subsystem is theoretically calculated from the known system parameters for the DOFs of interest ( $m_3$  and  $m_4$ ). Secondly, point and transfer FRFs of the coupled system at and between  $m_2$ ,  $m_3$  and  $m_4$  except point FRFs of  $m_2$  are obtained by performing a set of controlled displacement amplitude experiments for different displacement levels of the nonlinear element. Thereby, exact FRF sets of the coupled system are obtained for 30 different harmonic relative displacement amplitudes between  $m_2$  and  $m_3$  ranging from 0 mm to 3 mm with 0.2 mm increment. A complex random number is added to exact FRFs in order to reflect the effect of measurement errors as follows:

$$\mathbf{H}_{ab}^{\text{KU}}(\omega_k) = \hat{\mathbf{H}}_{ab}^{\text{KU}}(\omega_k) + m_{ab,k} + i n_{ab,k} \quad (72)$$

In Equation (72),  $m_{ab,k}$  and  $n_{ab,k}$  are independent random variables with Gaussian distribution having a zero mean and a standard deviation of  $8 \times 10^{-6}$  m/N which brings a noticeable pollution on calculated FRFs. Since calculated coupled system FRFs include simulated measurement errors, curves in the form of an FRF curve are fitted to each set. As an example, FRF curves fitted to the measured point FRF values at  $m_3$  are given in Figure 34. Moreover, point FRFs of the known subsystem at  $m_3$  are also illustrated in Figure 35 which is a single FRF curve since this subsystem is linear.

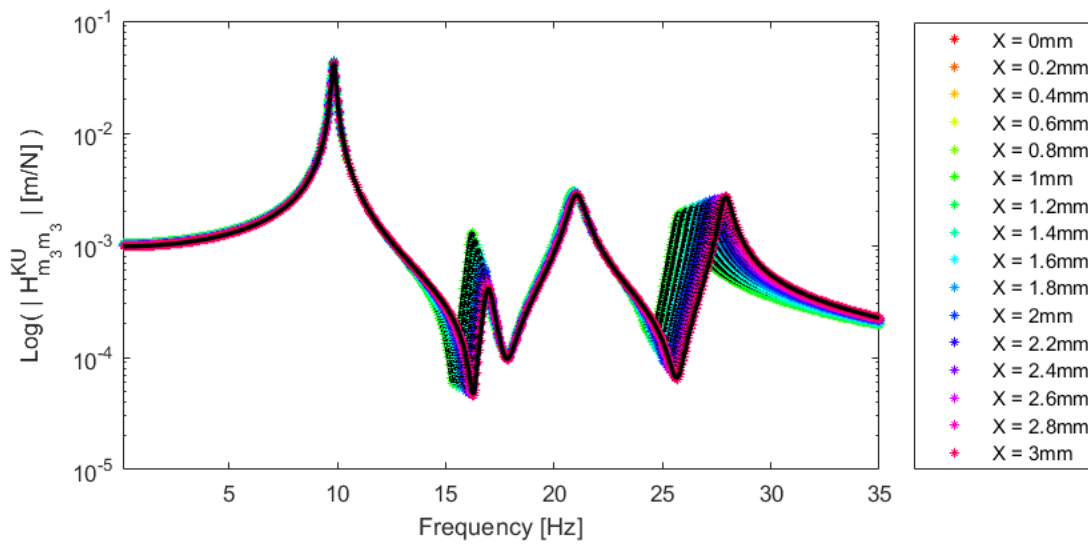


**Figure 34.** Point FRFs of the coupled system at  $m_3$  (colored points) and fitted FRF curves (black lines)

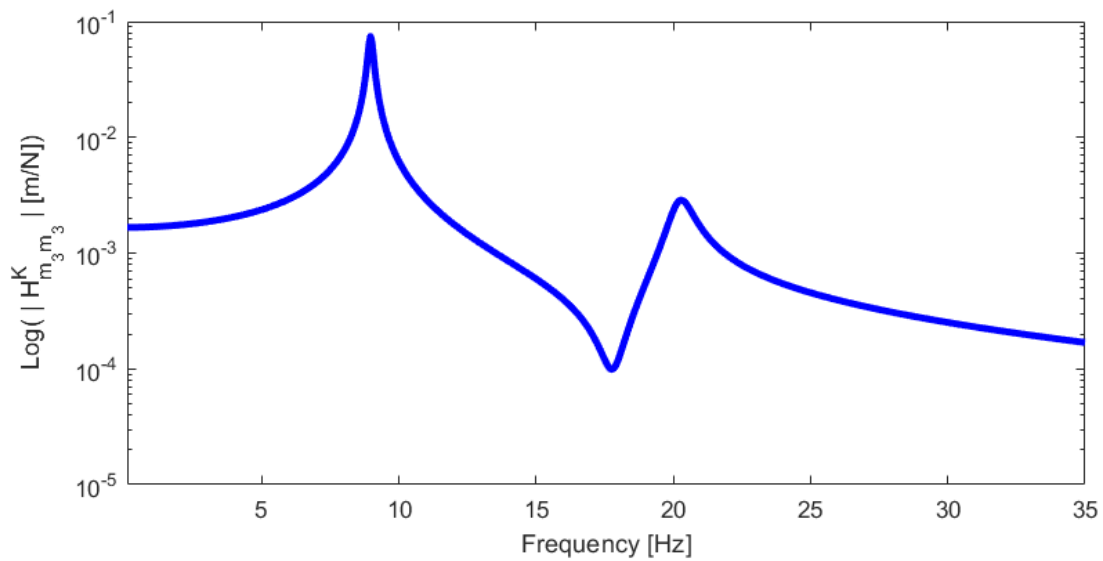


**Figure 35.** Point FRFs of the known subsystem at  $m_3$

Using all the available data obtained up to now, point FRFs of the unknown subsystem at  $m_0$  and also transfer FRFs between  $m_0$  and  $m_2$  can be calculated by performing linear decoupling via dual assembly approach [54] for 15 different displacement level of the gap nonlinearity. The results are given in Figure 36.

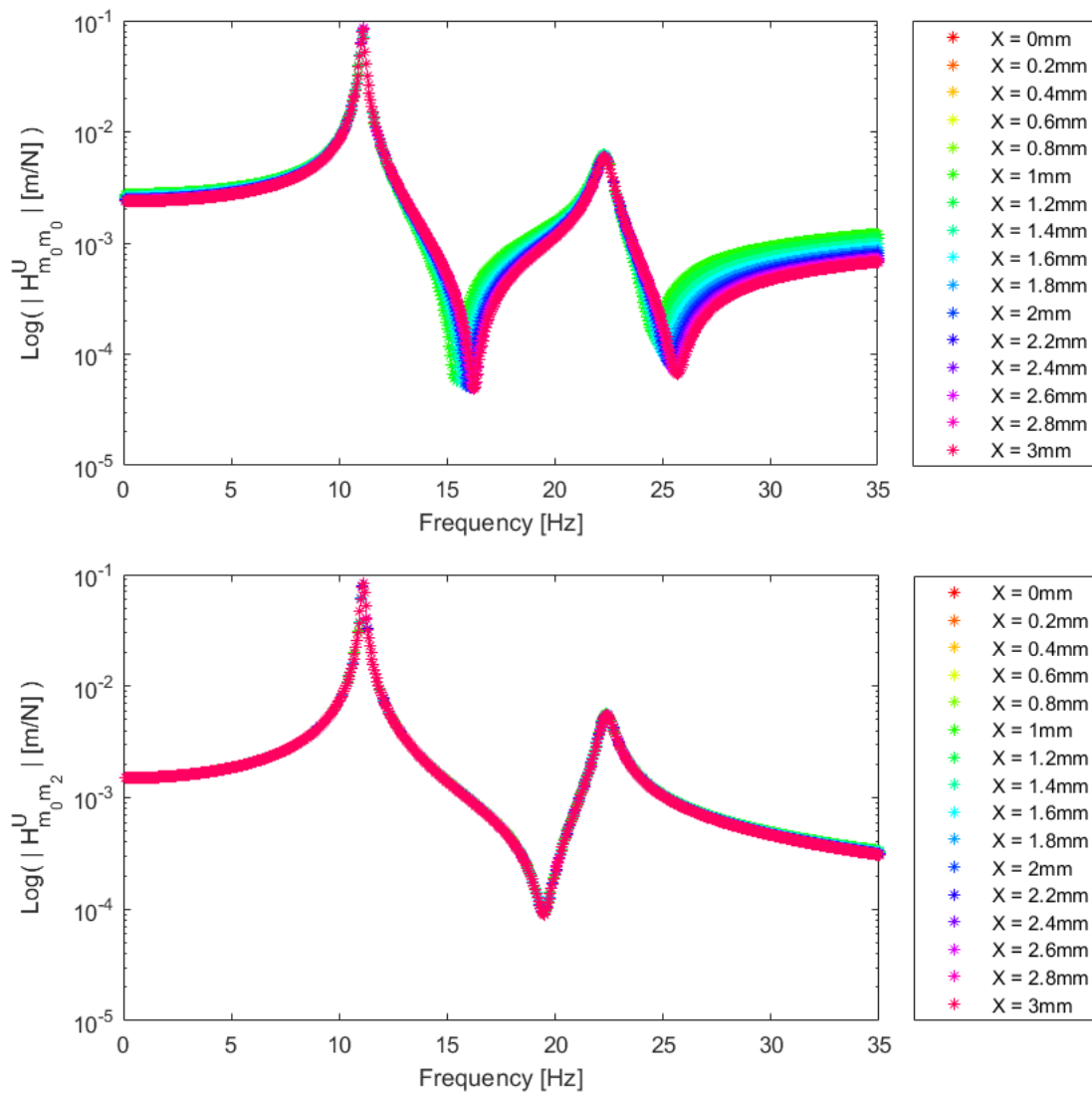


**Figure 36.** Point FRFs of the unknown subsystem at  $m_0$  (above) along with its transfer FRFs between  $m_0$  and  $m_2$  (below)

After this stage, parametric modal identification technique [66] can be applied step by step. First, modal parameters of each FRF curve are extracted using the linear modal identification technique developed by Richardson and Formenti [75]. Then, their variations as a function of the amplitude of relative harmonic displacement between end coordinates of the nonlinear element are obtained as shown in Figure 37 to Figure 42. Note that, fitted curves to the obtained modal parameters are smoothing splines of MATLAB® [81] with a smoothing parameter of 0.99999999998. So, one can calculate the response of the unknown nonlinear subsystem for any forcing level using these modal parameter variations.

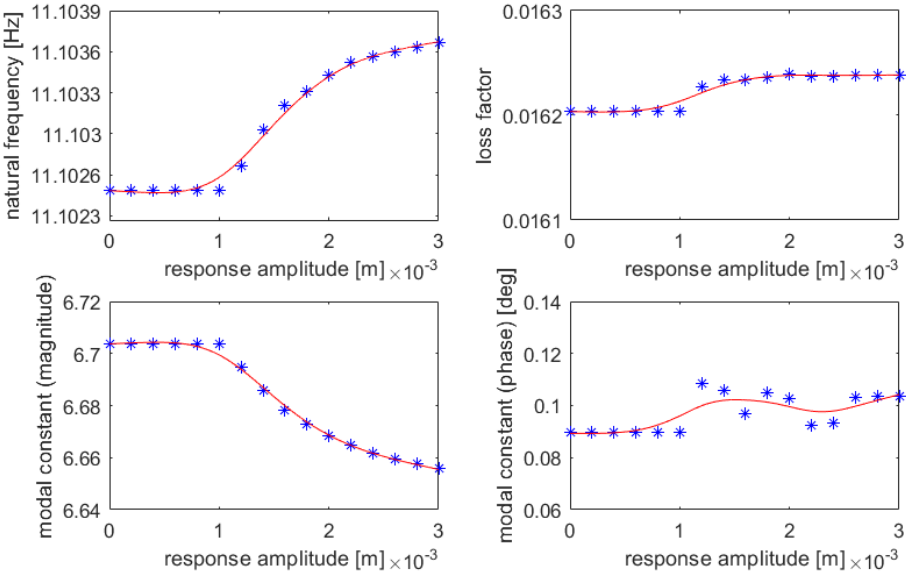


**Figure 37.** Modal parameter variations for the 1st mode of the transfer FRFs of the unknown subsystem between  $m_0$  and  $m_2$  wrt response amplitude of the nonlinear element (\*, identified parameters & —, fitted curves)

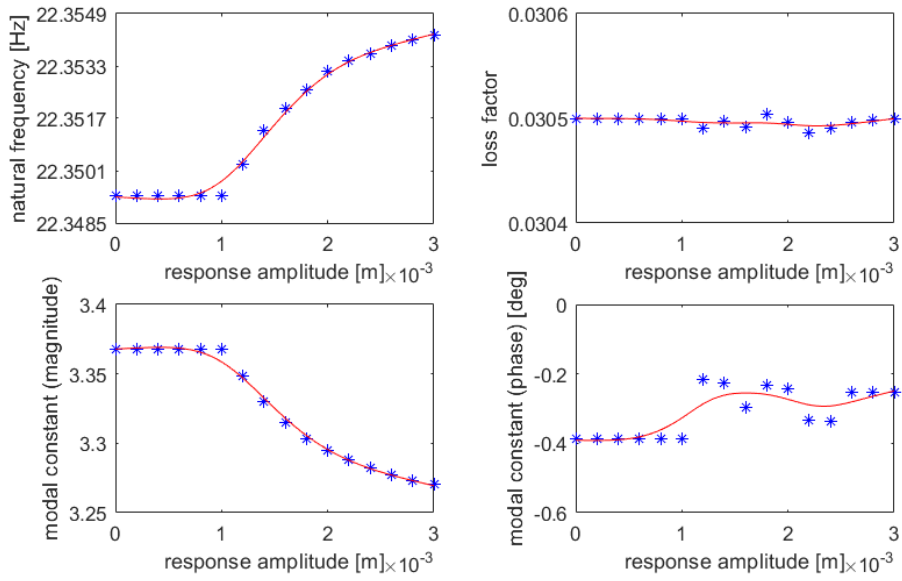


**Figure 38.** Modal parameter variations for the 2nd mode of the transfer FRFs of the unknown subsystem between  $m_0$  and  $m_2$  wrt response amplitude of the nonlinear element (\*, identified parameters & —, fitted curves)

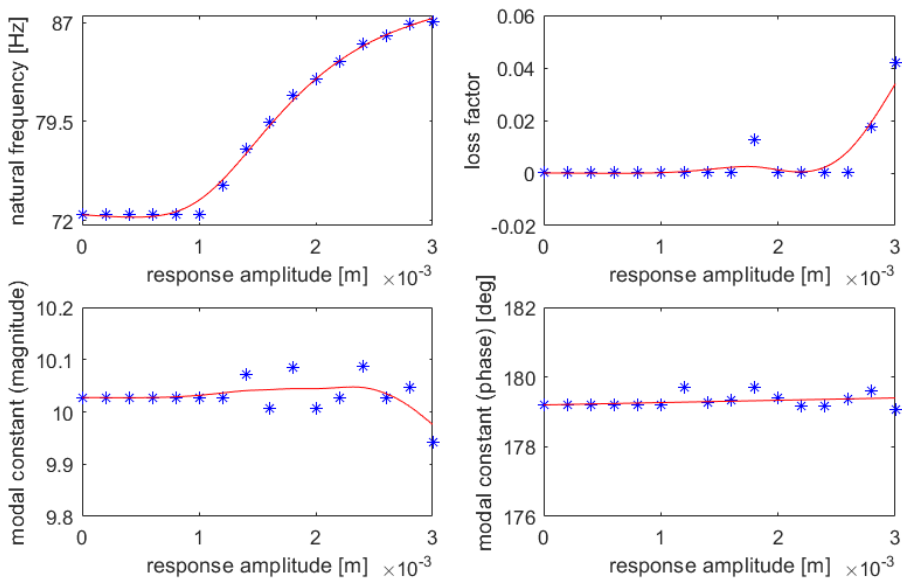


**Figure 39.** Modal parameter variations for the 3rd mode of the transfer FRFs of the unknown subsystem between  $m_0$  and  $m_2$  wrt response amplitude of the nonlinear element (\*, identified parameters & —, fitted curves)

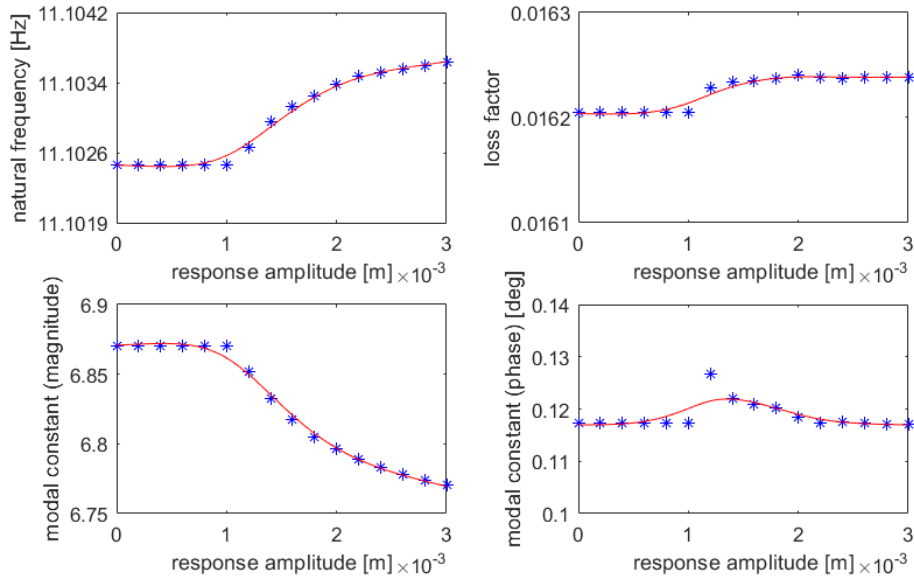


**Figure 40.** Modal parameter variations for the 1st mode of the point FRFs of the unknown subsystem at  $m_0$  wrt response amplitude of the nonlinear element (\*, identified parameters & —, fitted curves)

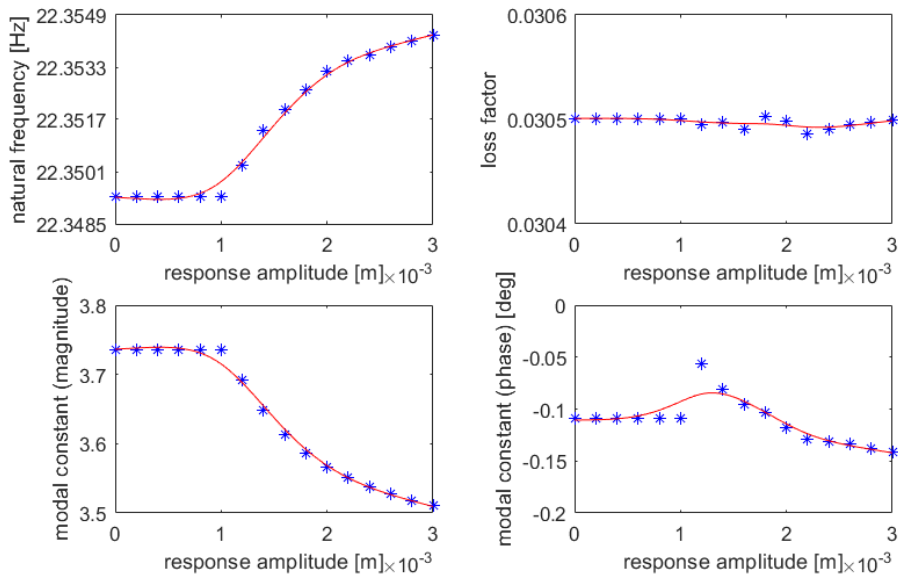


**Figure 41.** Modal parameter variations for the 2nd mode of the point FRFs of the unknown subsystem at  $m_0$  wrt response amplitude of the nonlinear element (\*, identified parameters & —, fitted curves)



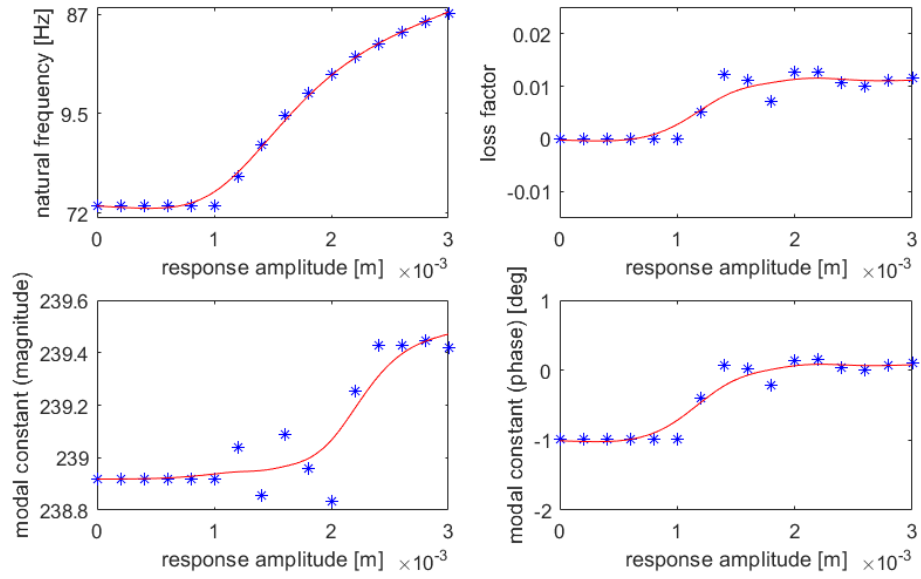


**Figure 42.** Modal parameter variations for the 3rd mode of the point FRFs of the unknown subsystem at  $m_0$  wrt response amplitude of the nonlinear element (\*, identified parameters & —, fitted curves)

In order to verify the results and thus validate the method, the decoupled subsystem is recoupled to a linear SDOF subsystem whose system parameters are given in Table 5. Construction of the new coupled system is shown in Figure 43. The response of this new coupled system is obtained first by performing FRF coupling [76] where FRFs of the unknown subsystem are resynthesized using the modal parameters given in Figure 37 to Figure 42. Then, they are also calculated directly via DFM using actual system parameters. Note that both approaches are based on the basic assumption that harmonic excitation results in harmonic response at the same frequency.

**Table 5.** Physical parameters of the known SDOF subsystem

Element Number ( $i$ )	$m_i$ [kg]	$k_i$ [N/m]	$c_i$ [Ns/m]
5	0.15	800	0.60

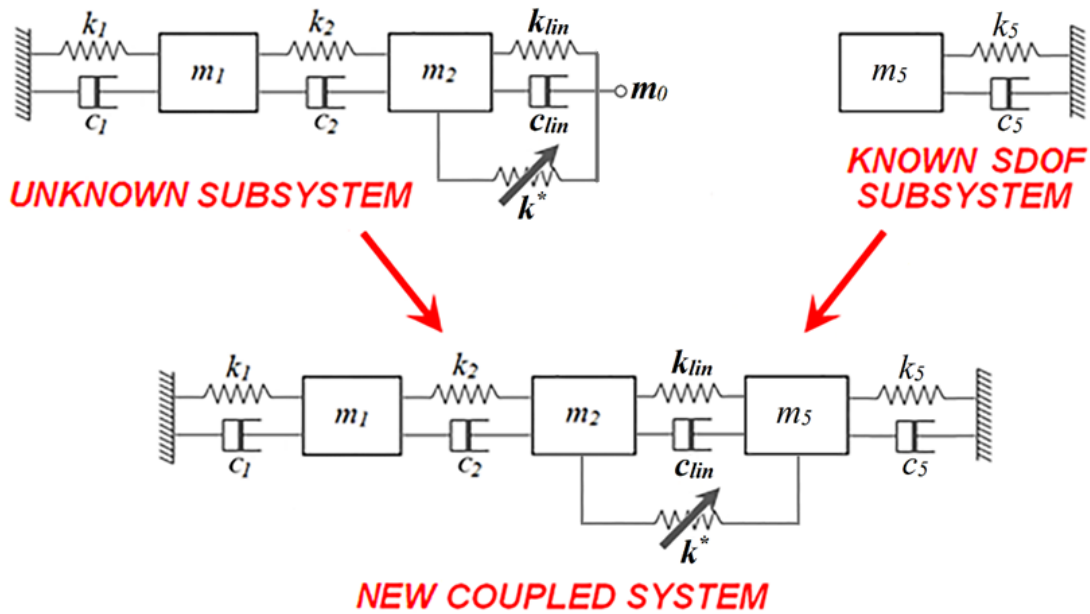


**Figure 43.** Construction of a new nonlinear coupled system - nonlinearity at the connection of two subsystems again

The response of the new coupled system at  $m_5$  is calculated when a harmonic excitation of amplitude 0.4 N is applied to  $m_5$ . Note that a frequency step size of 0.05 Hz is employed during numerical calculations. The results are given in Figure 44 and Figure 45 for both forward and backward frequency sweeps. In addition, linear response of the new coupled system is also given in these figures in order to show the distortion of calculated FRFs due to nonlinearity. It can be observed that predicted results after FRF coupling using results of FDM-NS closely match with those obtained directly through DFM. Small discrepancies at the frequency of jump phenomenon at the 2<sup>nd</sup> resonance are believed to be due to inaccurate modal parameters due to noise in the primary data. However, the general agreement between the predicted and directly calculated results proves the validity of the proposed decoupling approach for a system composed of two linear subsystems coupled through a nonlinear element.

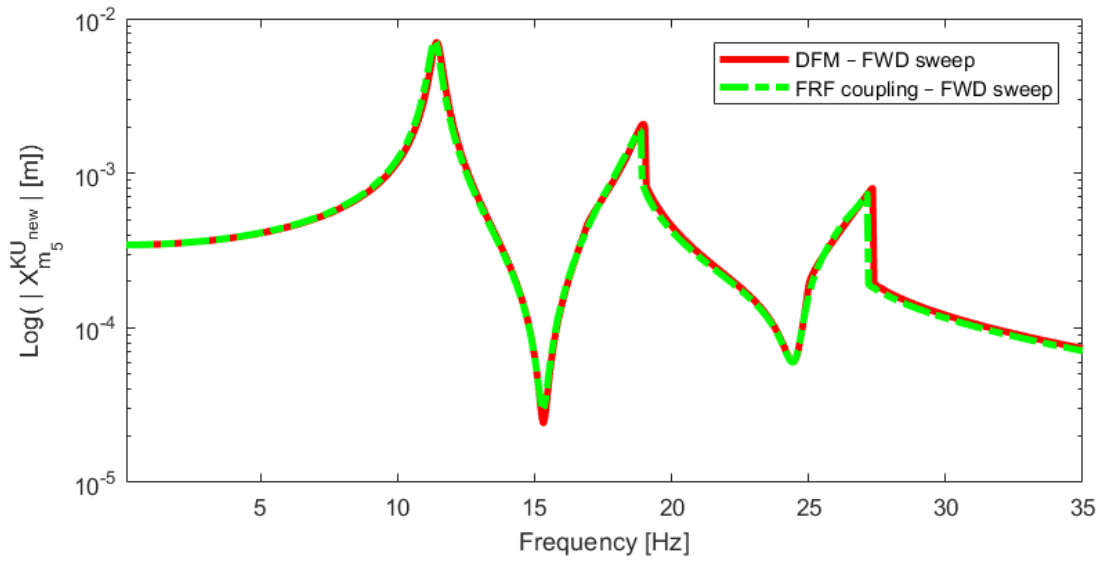


**Figure 44.** Predicted and directly calculated responses of the new coupled system at  $m_5$  obtained via forward frequency sweeping

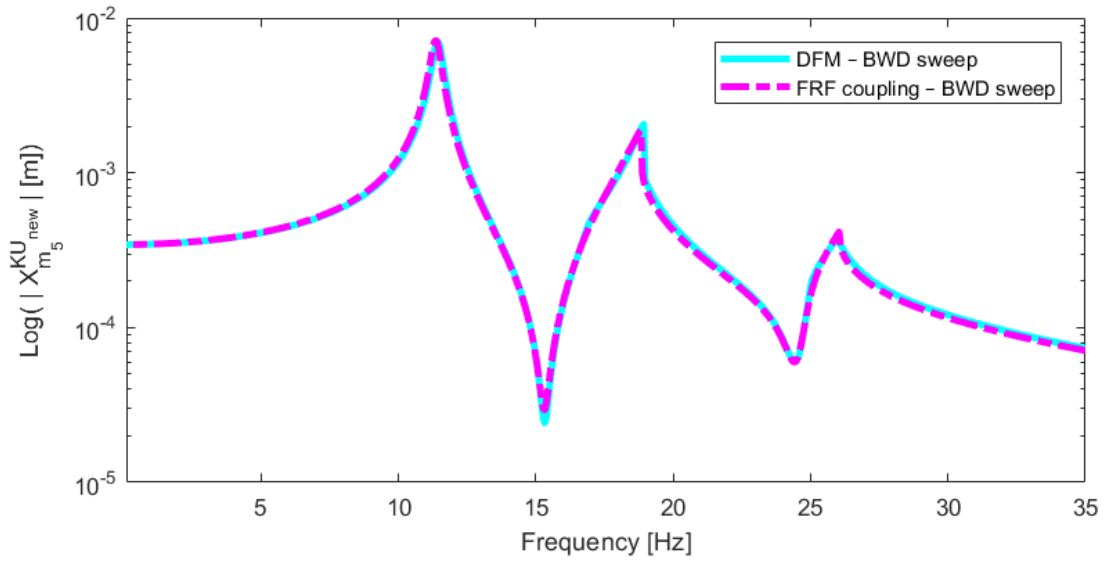


**Figure 45.** Predicted and directly calculated responses of the new coupled system at  $m_5$  obtained via backward frequency sweeping



## CHAPTER 5

### EXPERIMENTAL VERIFICATION OF FDM-NS

In this chapter, the proposed decoupling approach for nonlinear systems is applied to experimental test systems. The first experiment is conducted on a nonlinear T-beam which is similar to the test structure developed by Ferreira [76] and later used by Siller [77], and also used by Arslan et al. [66] for identification purposes. In this experimental case study, dynamics of a linear unknown substructure (a cantilever beam) is to be obtained by decoupling dynamics of a known nonlinear substructure from those of the complete T-beam structure. Whereas in the second experiment, decoupling of two cantilever beams, free ends of which are held between two thin identical beams is considered. In this application, dynamics of a nonlinear unknown substructure is obtained by decoupling the dynamics of a known linear substructure from those of the coupled structure composed of two cantilever beams connected each other with a nonlinear element.

#### **5.1. Application of FDM-NS to a Nonlinear T-Beam**

In this section, FDM-NS is applied to an experimental test system which involves a cantilever beam connected to a relatively thin fixed-fixed beam which together forms a T-beam assembly as shown in Figure 46. The thin fixed-fixed beam introduces nonlinearity into the system such that the center line of the beam elongates as it deflects and gets longer than its original length. This yields axial forces and thus increases the stiffness of the beam [78]. Firstly, FRFs of the T-beam assembly are measured via controlled displacement amplitude test for a particular displacement value at the connection point of two beams. As the system shows linear behavior for a constant displacement of the nonlinear element, the linear parameters of the thin fixed-fixed

beam are calculated analytically while its nonlinear parameters are separately identified. Using obtained data, FRFs of the linear cantilever beam are obtained first by using FDM-NS and then by conducting a modal test. In order to verify the real-life applicability and accuracy of FDM-NS, predicted and measured FRFs of the unknown subsystem are compared.

**5.1.1. Experimental Setup**

The test setup is composed of a linear cantilever beam, considered as the unknown subsystem, with its free end attached to the midpoint of a thin beam having fixed-fixed boundary conditions. The thin beam is referred to as the known nonlinear subsystem. Physical dimensions of the test setup are given in Figure 46.

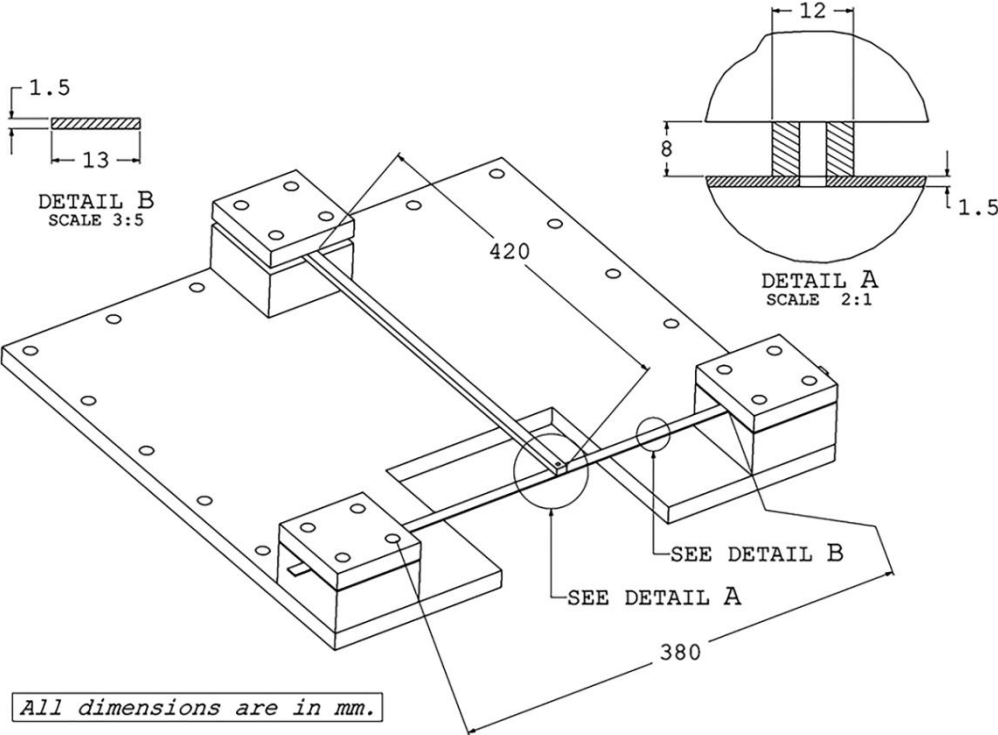


**Figure 46.** Physical dimensions of the test setup

Both beams are made of St37 steel. They are manufactured long enough that ends of the beams are sandwiched between steel blocks so as to maintain fixed boundary conditions. A picture of the test setup used in the experiment is given in Figure 47.

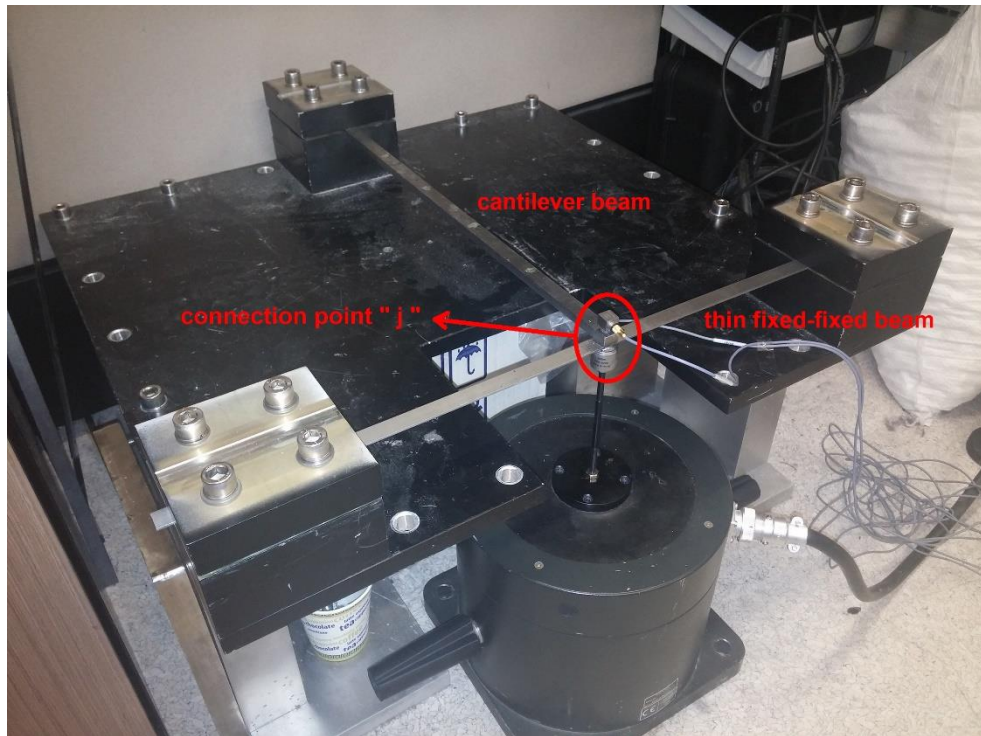


**Figure 47.** Picture of the test setup used in the experiment

B&K Type 4808 vibration exciter via a push-rod attached to the connection point of the beams is used to harmonically excite the test system. Due to the low level of voltage supplied from the signal generator, excitation force level of the vibration exciter is manually increased by using a B&K Type 2712 power amplifier. Acceleration response is measured using a B&K Type 4507B uniaxial accelerometer whereas externally applied harmonic forces are measured via B&K Type 8230-002 force transducer which is attached to the tip of the push-rod. Throughout all measurements,

B&K Type 3560C frontend system is used as a data acquisition system which also includes output channels that can be used as signal generators with a frequency range from 0 to 25.6 kHz. The equipment used in the experiment is graphically shown in Figure 48.



**Figure 48.** View of the equipment used in the experiment

**5.1.2. Preliminary Analyses**

Prior to experiment, preliminary modal analyses are performed by using a commercial FEA software called ANSYS R15.0<sup>®</sup> in order to decide the frequency range of interest we can use during the experiment. In this experiment, the fundamental resonance frequency of the coupled T-beam assembly is taken as the frequency around which the measurements are going to be carried out. It should also be noted that the modal analyses are performed under the linearity assumption where large deflections triggering nonlinearities are not allowed.



In order to minimize the modeling errors in the FEM of the test structure (Figure 49), the accelerometer and the force transducer used in the experiment are modeled as rigid masses such that modulus of elasticity for the accelerometer and force transducer are taken 10 times larger than that of the beams. Effective mass values, which is the overall mass for the accelerometer while it is the mass above the piezo element for the force transducer, are obtained from the datasheets of each transducer [79,80]. These values are given in Table 6.

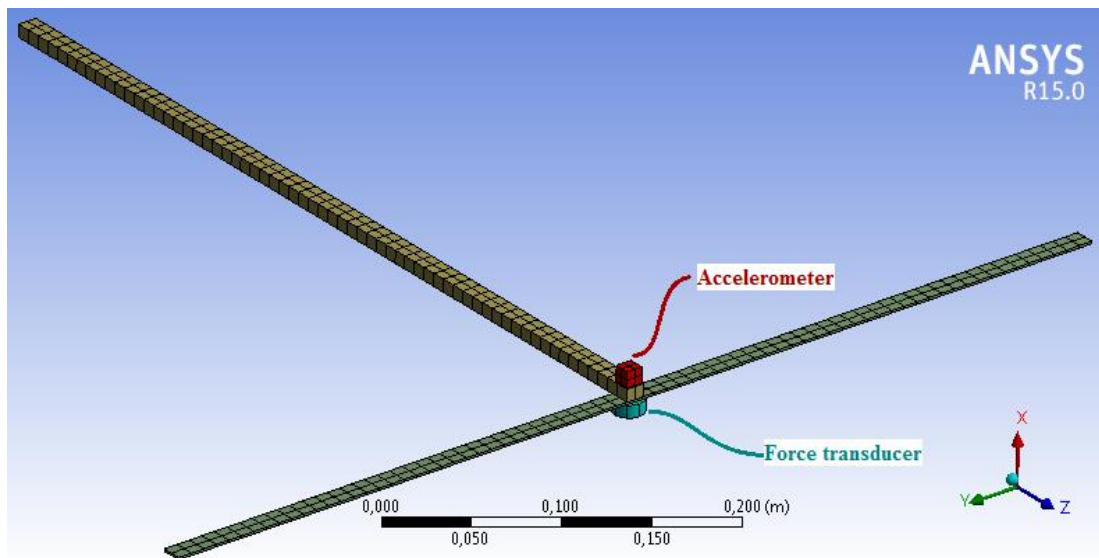


**Figure 49.** FEM of the test structure

**Table 6.** Mass of the accelerometer and force transducer

Transducer Type		Effective Mass [grams]
Accelerometer	Brüel&Kjaer Type 4507B	4.8
Force Transducer	Brüel&Kjaer Type 8230-002	9.5

First, by performing modal analysis in ANSYS R15.0<sup>®</sup> for the whole test setup, the first natural frequency of the T-beam assembly is calculated as 36 Hz results of which are also illustrated in Figure 50 together with the corresponding mode shape.

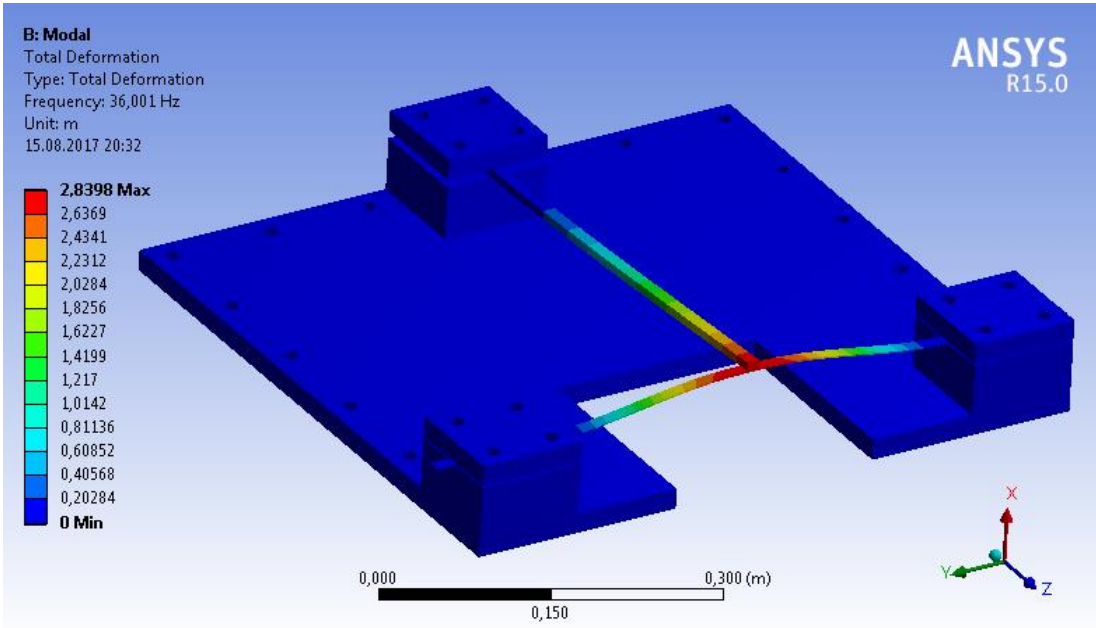


**Figure 50.** Modal analysis results of the T-beam assembly – its fundamental resonance

Since it is intended to obtain the FRFs of the linear cantilever beam, the frequency range of interest is taken such that it also covers the first natural frequency of the linear cantilever beam, which is obtained as 31.3 Hz by performing modal analysis in ANSYS R15.0<sup>®</sup>. These results are also illustrated in Figure 51 together with the corresponding mode shape.

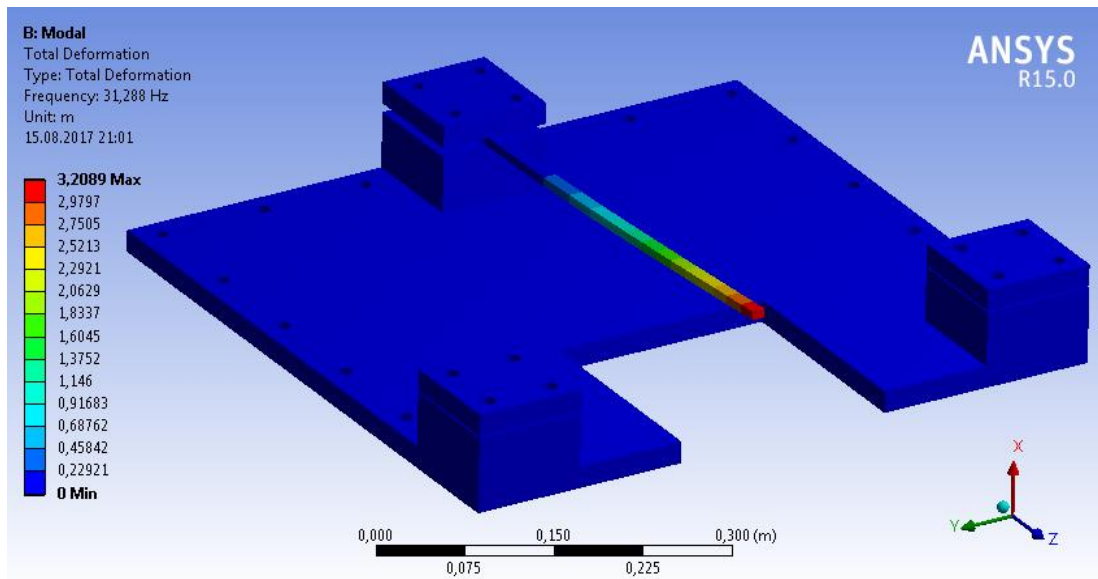


**Figure 51.** Modal analysis results of the cantilever beam by itself – its fundamental resonance

Consequently, the frequency range of interest throughout this experiment is determined as 20 - 55 Hz, considering the pre-estimated fundamental resonances of the coupled T-beam system and unknown subsystem.

### 5.1.3. Experimental Work and Application of FDM-NS

As the initial step, point FRFs of the T-beam assembly at the attachment point of the linear cantilever beam and of the thin fixed-fixed beam in transverse direction are measured experimentally. An adaptive frequency resolution is adopted such that the frequency resolution is increased in the close neighborhood of the resonance. Point FRFs at the connection point of two beams are measured as given in Figure 52 by conducting a controlled displacement amplitude test for the constant harmonic displacement amplitude of 1 mm.

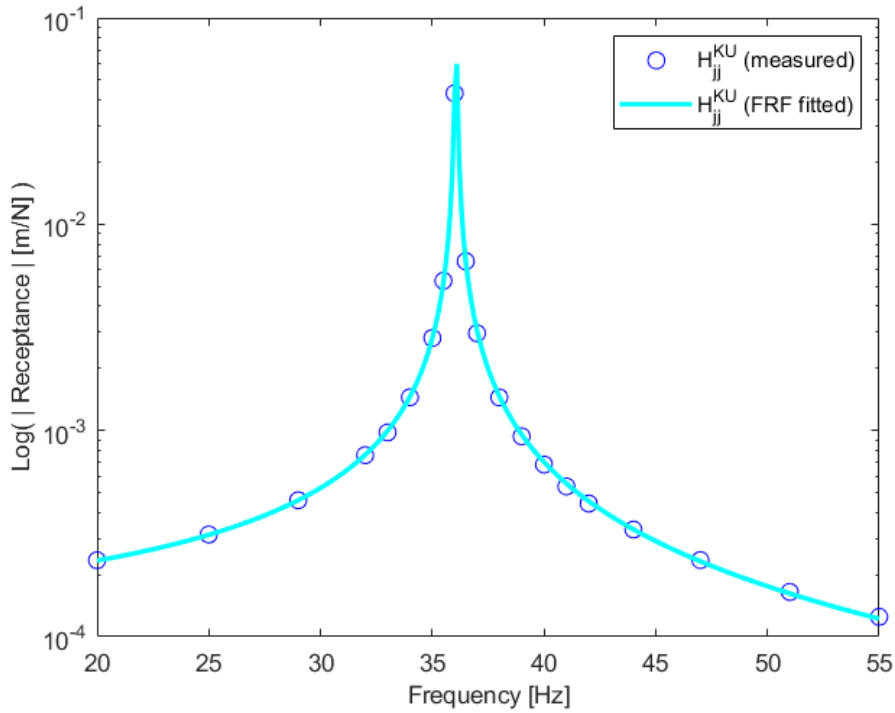


**Figure 52.** Point FRFs of the T-beam assembly at the connection point  $j$  under transverse loading for constant harmonic displacement amplitude of 1 mm

In Figure 52, experimentally obtained FRFs are illustrated together with the FRF curve fitted to these measured data points by using a code mainly based on a built-in function of MATLAB<sup>®</sup>, called “invfreqs” [81]. Note that fitted FRF curve with high frequency resolution is used hereafter in the calculations in lieu of the measured point FRFs of the coupled system at the connection point of two subsystems ( $\mathbf{H}_{jj}^{KU}$ ).

As the next step, the fixed-fixed thin beam is modeled as grounded linear and nonlinear transverse springs with their free ends attached to a concentrated equivalent mass as shown in Figure 53.

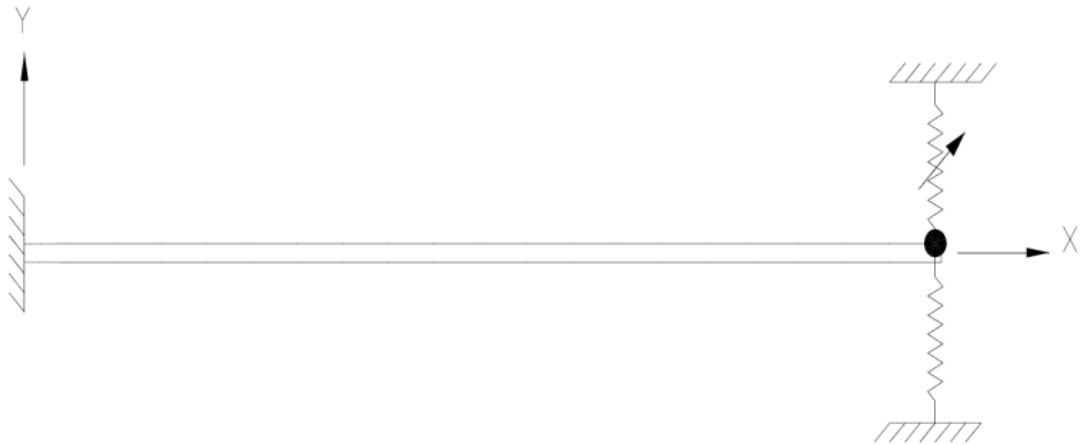


**Figure 53.** Model of the test rig

By using the material and geometric properties of the fixed-fixed thin beam, the equivalent linear spring stiffness and the equivalent mass values are calculated as 2558.7 N/m and 21.52 g, respectively. In addition, nonlinear stiffness of the thin fixed-fixed beam is identified through a nonlinear identification approach, called Direct Nonlinearity by Describing Functions (DDF) method, proposed by Aykan and Özgüven [82,83]. Initially, the nonlinear T-beam assembly is examined under two different constant amplitude harmonic excitations according to DDF method. In these tests, harmonic forces of magnitudes 0.25 N and 0.5 N is applied to the attachment point of two subsystems and point FRFs of the T-beam structure are measured at several frequencies as illustrated in Figure 54. The behaviors of the FRFs given in this figure indicates presence of a stiffening nonlinearity in the system. As expected, the jump phenomenon observed in both FRF curves occurs at higher frequencies for the higher excitation force level which is the characteristic of a stiffening nonlinearity.

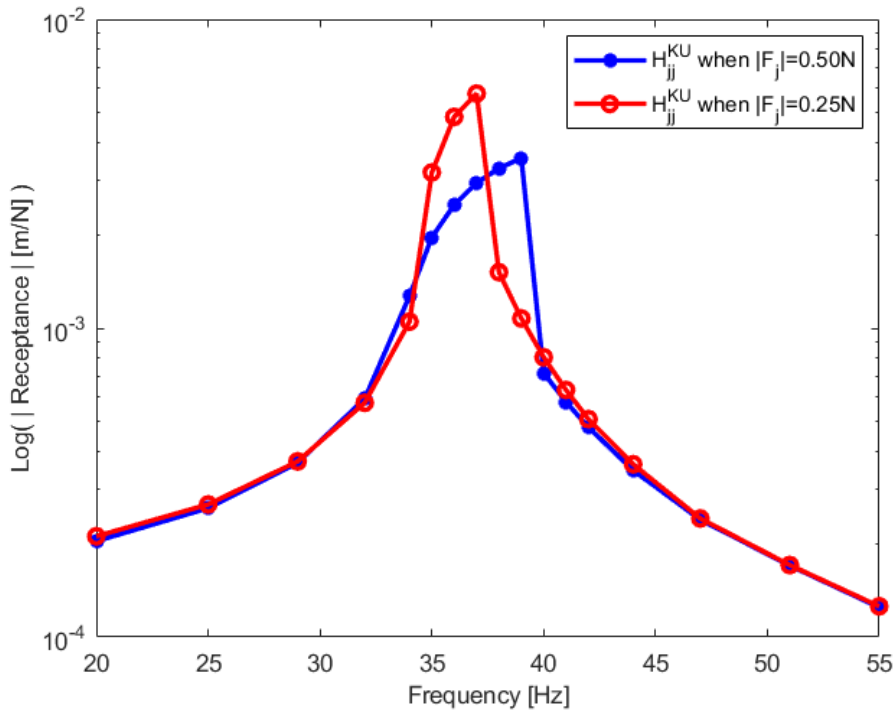


**Figure 54.** Point FRFs of the T-beam assembly at the connection point  $j$  under harmonic loading of constant magnitudes 0.25 N and 0.5 N in transverse direction

Using the measurement results given in Figure 54, DF values representing the grounded nonlinear element attached to the tip of the cantilever beam are obtained by applying DDF method [82,83] which can perform nonlinear identification directly from a series of measured nonlinear FRFs. By using DDF method, the DFs representing the nonlinear element are calculated from the experimental FRFs given in Figure 54 with respect to the displacement amplitude of point  $j$ . The real and imaginary parts of the DF values obtained, which respectively correspond to stiffness and damping nonlinearities, are illustrated in Figure 55. Note that, DF curves shown in Figure 55 are obtained via polynomial curve fitting up to third degree. The polynomial coefficients of DF curves are also listed in Table 7.

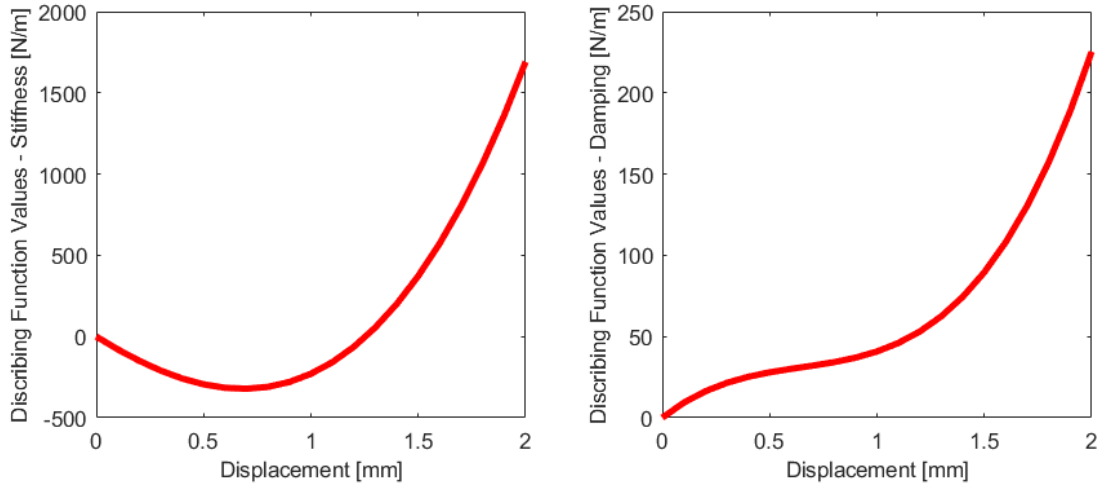


**Figure 55.** DF values obtained via DDF Method [82,83] for stiffness (left) and damping (right) nonlinearities

**Table 7.** Identified parameters for the nonlinear element

	Linear Coefficient ( $k_1$ )	Quadratic Coefficient ( $k_2$ )	Cubic Coefficient ( $k_3$ )
Real part of DF	-8.2898e+05	3.6177e+08	2.3771e+11
Imaginary part of DF	1.0504e+05	-1.3231e+08	6.8055e+10

Using the parameters identified in Table 7, DF representing the nonlinear element can be formulated as follows:

$$\nu = k_1 X + k_2 X^2 + k_3 X^3 \quad (73)$$

where  $X$  represents the harmonic displacement amplitude of the nonlinear element.

Now, all necessary data is available in order to obtain FRFs of the known nonlinear subsystem. By employing FDM-NS using the FRFs measured from the coupled T-

beam assembly and those calculated for the fixed-fixed beam at a constant harmonic displacement amplitude of 1 mm, point FRFs of the linear cantilever beam alone at its tip point ( $\mathbf{H}_{jj}^U$ ) are obtained. Results found are compared with those obtained via modal testing of the cantilever beam itself in Figure 56.

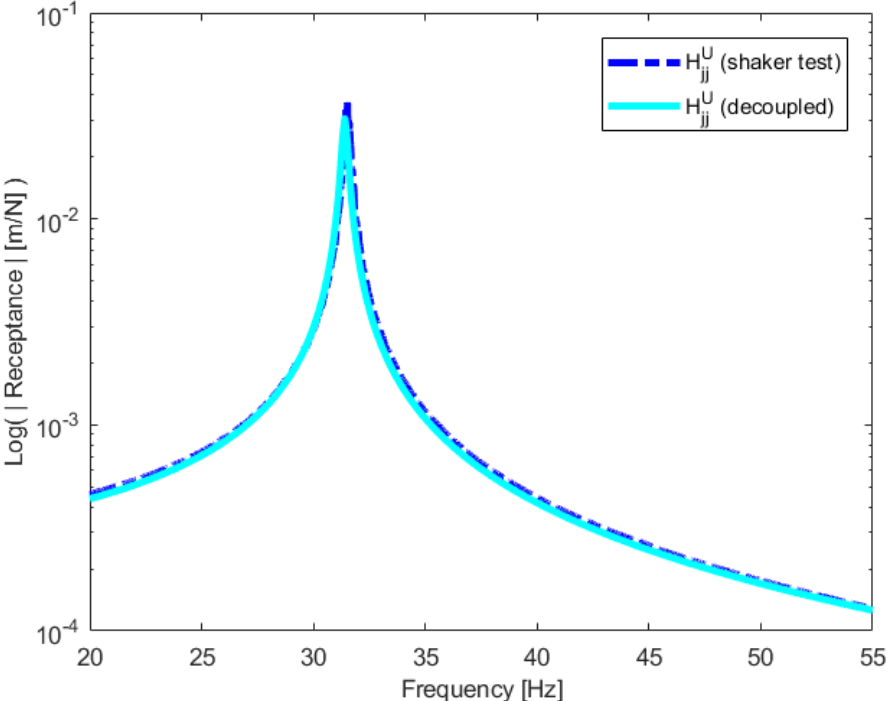


**Figure 56.** Point FRFs of the cantilever beam alone at its tip point  $j$  in transverse direction

It can be observed from Figure 56 that the FRF curve obtained through FDM-NS and the FRFs directly measured through modal testing of the linear cantilever beam itself shows a very good agreement. So, it can be verified that FDM-NS is a practical tool to decouple a nonlinear subsystem from a given nonlinear coupled system.



## **5.2. Application of FDM-NS to a Coupled Cantilever Beam System with a Nonlinear Element**

In this section, application of the FDM-NS to another nonlinear experimental test system is presented to demonstrate real life applicability and validity of FDM-NS. This experimental test system consists of cantilever beams connected to each other from their tip by two thin beams which yields nonlinearity to the coupled system. Note that, this test is a real-life application of the theory given for the case where nonlinearity is in the unknown subsystem.

### **5.2.1. Experimental Setup**

The setup is composed of a cantilever beam coupled to a shorter cantilever beam by connecting their free ends to each other with two thin identical beams which yield nonlinear stiffness effect. The cantilever beams are manufactured from St37 alloy steel whereas the thin beams are made of 6061-T3 aluminum alloy. Furthermore, fixed joints between each cantilever beam and two thin identical beams are obtained by riveting. A picture of the setup used in this experiment is given in Figure 57. The dimensions and technical details of the test system are also given in Figure 58.

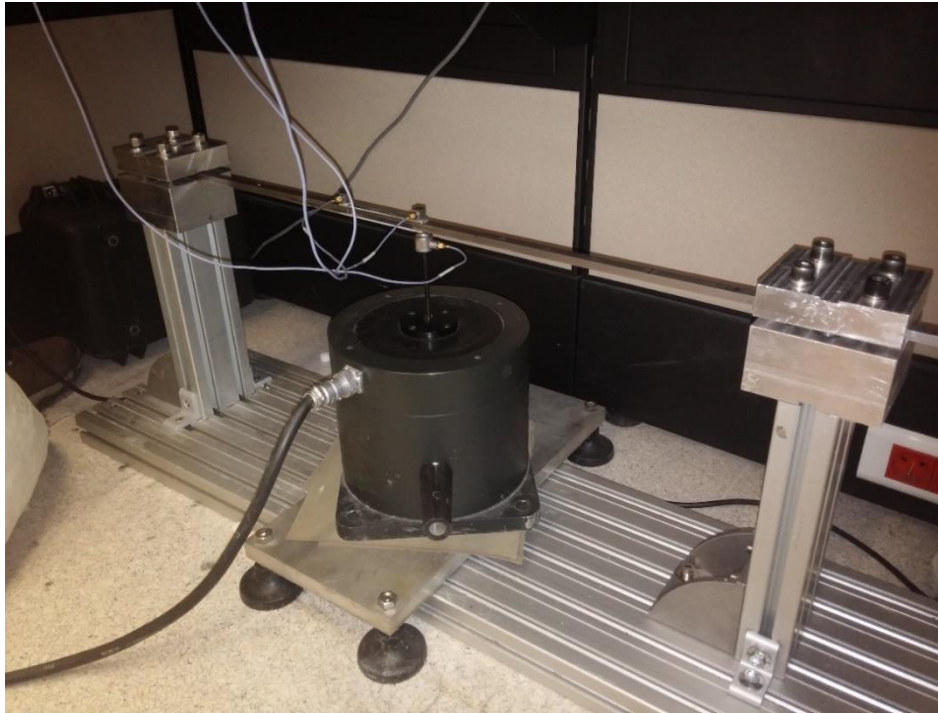


**Figure 57.** Setup used in the experiment

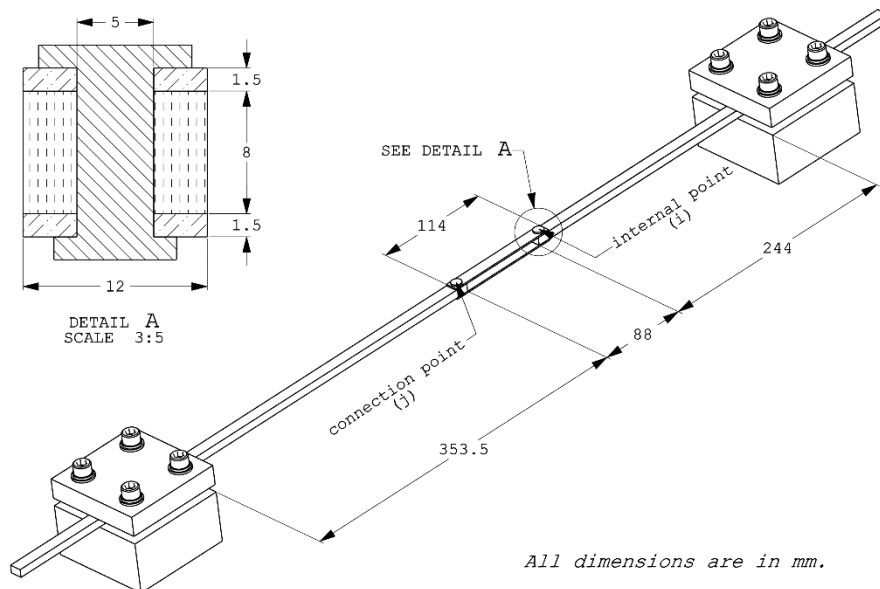


**Figure 58.** Dimensions and technical details of the test system

Maintaining perfect fixed boundary conditions are very difficult in real life applications. In order to maintain the fixed boundary conditions in the experimental setup, dimensions of the beams are longer than their effective lengths of 353.5 mm and 244 mm, so that adequate parts of the beams are clamped between fixture blocks. Equipment used in the experiment is listed in Table 8.

**Table 8.** Equipment used in the modal testing

Data Acquisition System	Brüel&Kjaer Type 3560 C Frontend
Shaker	Brüel&Kjaer Type 4808
Force Transducer	Brüel&Kjaer Type 8230-002
Power Amplifier	Brüel&Kjaer Type 2712
Accelerometer	Brüel&Kjaer 4507B

### 5.2.2. Preliminary Analyses

Prior to the experiment for decoupling, preliminary modal analyses are performed by using a commercial FEA software ANSYS R15.0<sup>®</sup> in order to decide a suitable frequency range of interest to be used in the experiment. In this experiment, the fundamental resonance of the coupled cantilever beams assembly is taken as the frequency around which the measurements are going to be carried out. It should again be noted that the modal analyses are performed under the linearity assumption where large deflections triggering nonlinearities are not allowed during the analyses with ANSYS R15.0<sup>®</sup>.

In order to minimize the modeling errors in the FEM of the test structure (Figure 59), accelerometer and force transducer used in the experiment are modeled as rigid masses so that modulus of elasticity for the accelerometer and force transducer are taken 10

times larger than that of the beams. Effective mass values given in Table 6 are used in the analyses.

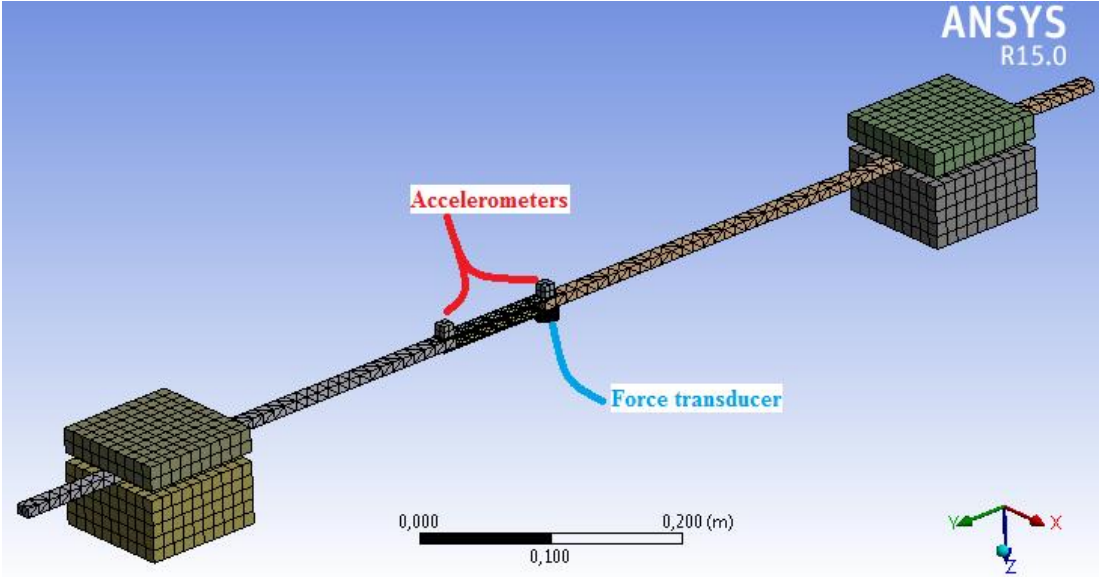


**Figure 59.** FEM of the test structure

First, by performing modal analysis with ANSYS R15.0<sup>®</sup> for the whole test setup, the first natural frequency of the cantilever beams assembly is calculated as 72.2 Hz results of which are also illustrated in Figure 60 together with the corresponding mode shape.

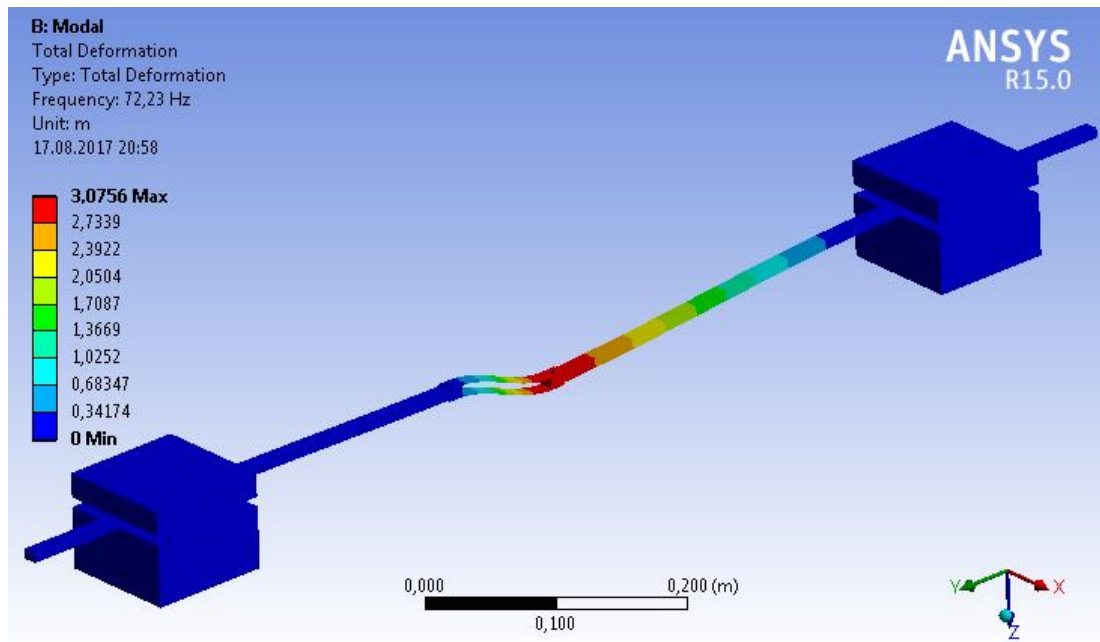


**Figure 60.** Fundamental mode of the coupled cantilever beams assembly

Since the long cantilever beam is to be decoupled from the assembly as the known subsystem, it is intended to arrange the frequency range of interest such that it also covers the first natural frequency of the long cantilever beam alone. So, its fundamental natural frequency is calculated as 52.9 Hz by performing modal analysis with ANSYS R15.0<sup>®</sup> results of which are also illustrated in Figure 61 together with the corresponding mode shape.

Consequently, the frequency range of interest to be used throughout this experiment is determined as 35 - 91 Hz considering the natural frequencies obtained for the coupled cantilever beams system and of the known subsystem.

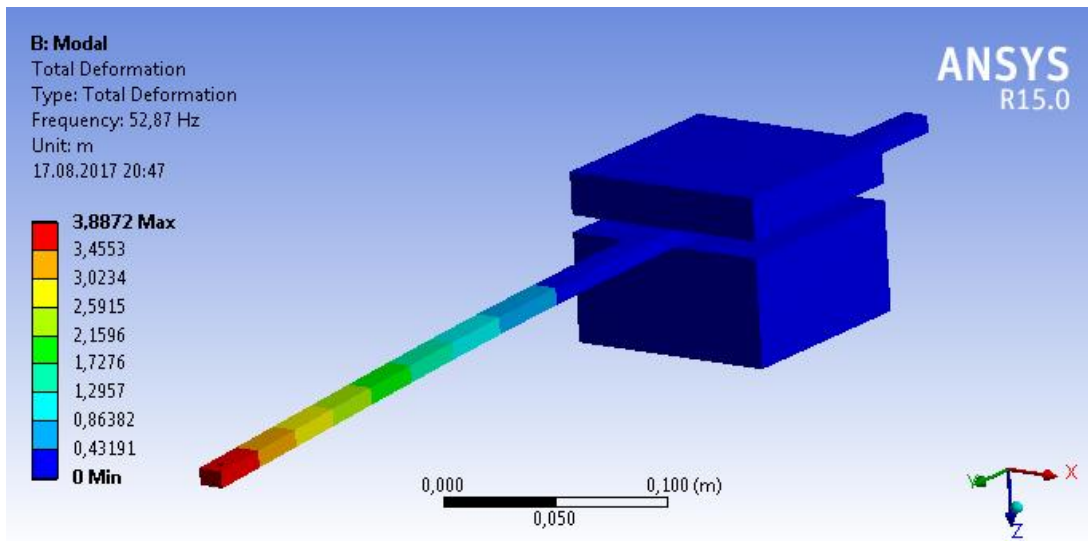


**Figure 61.** Fundamental mode of the long cantilever beam alone

### 5.2.3. Experimental Work and Application of FDM-NS

In this experiment, the long cantilever beam is considered as the linear known substructure. Two thin identical beams, which introduces nonlinearity into the test structure, are the connection elements between long and short cantilever beams. Since the type and parameters of the nonlinear connection elements are not available, short cantilever beam together with the two thin identical beams are considered as the unknown substructure. So, this unknown substructure is to be decoupled from the coupled nonlinear structure. It should be additionally noted that an adaptive frequency resolution is used in the measurements which is further decreased in the immediate vicinity of the fundamental resonance.

First of all, point ( $\mathbf{H}_{jj}^{KU}$ ) and transfer ( $\mathbf{H}_{ji}^{KU}$ ) FRFs of the coupled nonlinear system in transverse direction are measured experimentally employing the controlled displacement amplitude test procedure given in Figure 62.

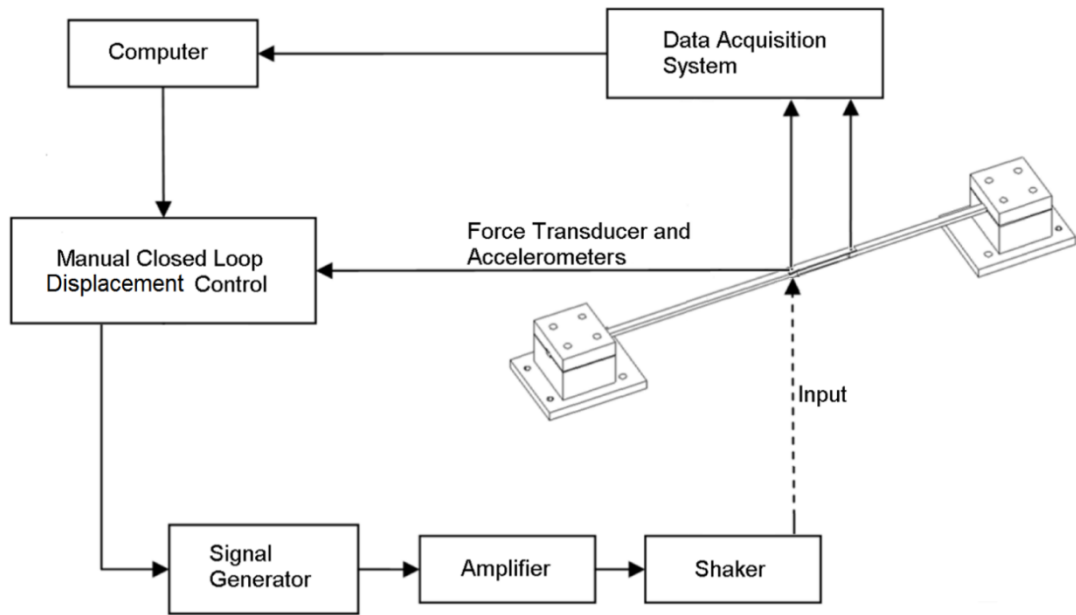


**Figure 62.** Experimental procedure followed during controlled displacement amplitude test

Note that additional measurement from the tip of the short cantilever beam is required in order to obtain the relative deformation between the two ends of the nonlinear connection element. Modal tests are performed for the relative displacement amplitudes of 0.1 mm, 0.3 mm, 0.5 mm, 0.7 mm and 1.0 mm between two ends of the nonlinear element ( $|\mathbf{X}_j - \mathbf{X}_i|$ ). Results of the tests are given in Figure 63 and Figure 64. In these figures, FRF curves fitted to the experimental data are given as well.

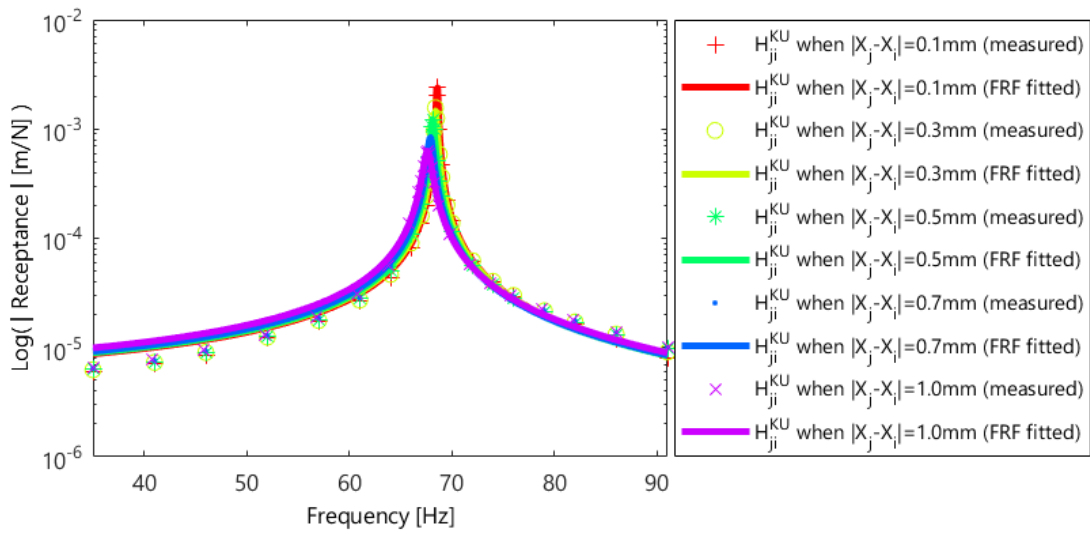


**Figure 63.** Measured transfer FRFs (symbols) and fitted FRF curves (lines) of the coupled system between internal point (i) and connection point (j) in transverse direction for various response levels of the nonlinear element

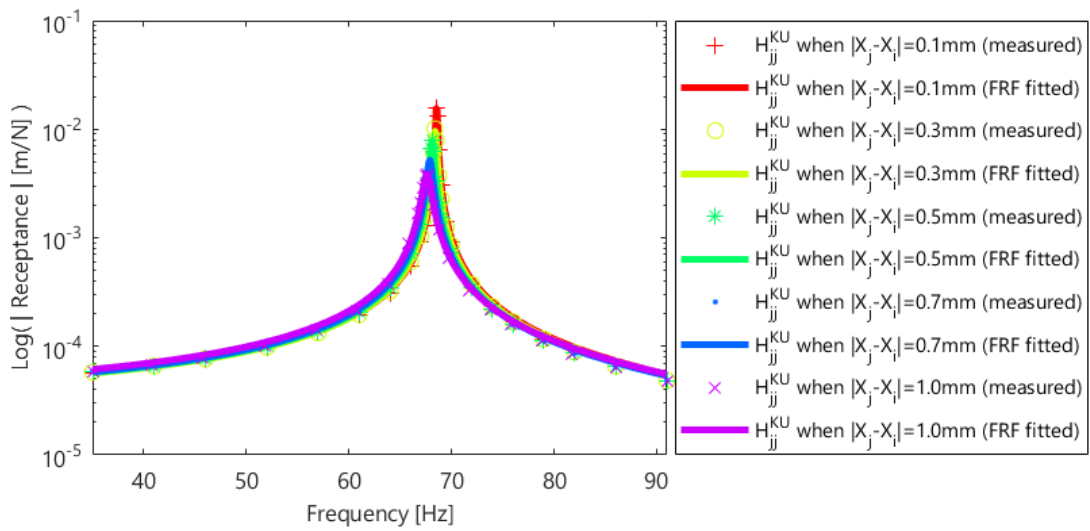


**Figure 64.** Measured point FRFs (symbols) and fitted FRF curves (lines) of the coupled system at connection point (j) in transverse direction for various response levels of the nonlinear element



At this stage, tip point FRFs of the long cantilever beam as the known linear substructure can be obtained through modal tests using modal hammer. Results are shown in Figure 65.

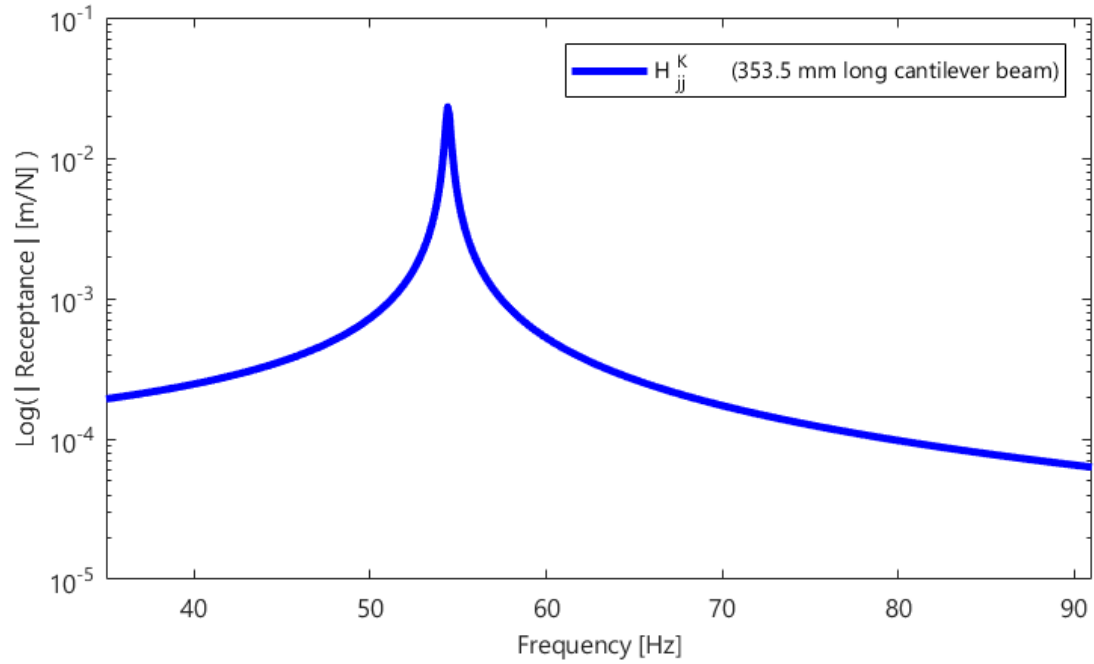


**Figure 65.** Measured point FRFs of the known subsystem alone at its coupling DOF (j) in transverse direction

Note that in Figure 65, the FRF curve fitted to the experimental data is given. So, by using all available FRFs obtained up to here, one can obtain the response of unknown substructure at its coupling DOF by applying FDM-NS. During decoupling calculations via FDM-NS, dual assembly approach [54] is used as the linear decoupling tool. Results are given in Figure 66.

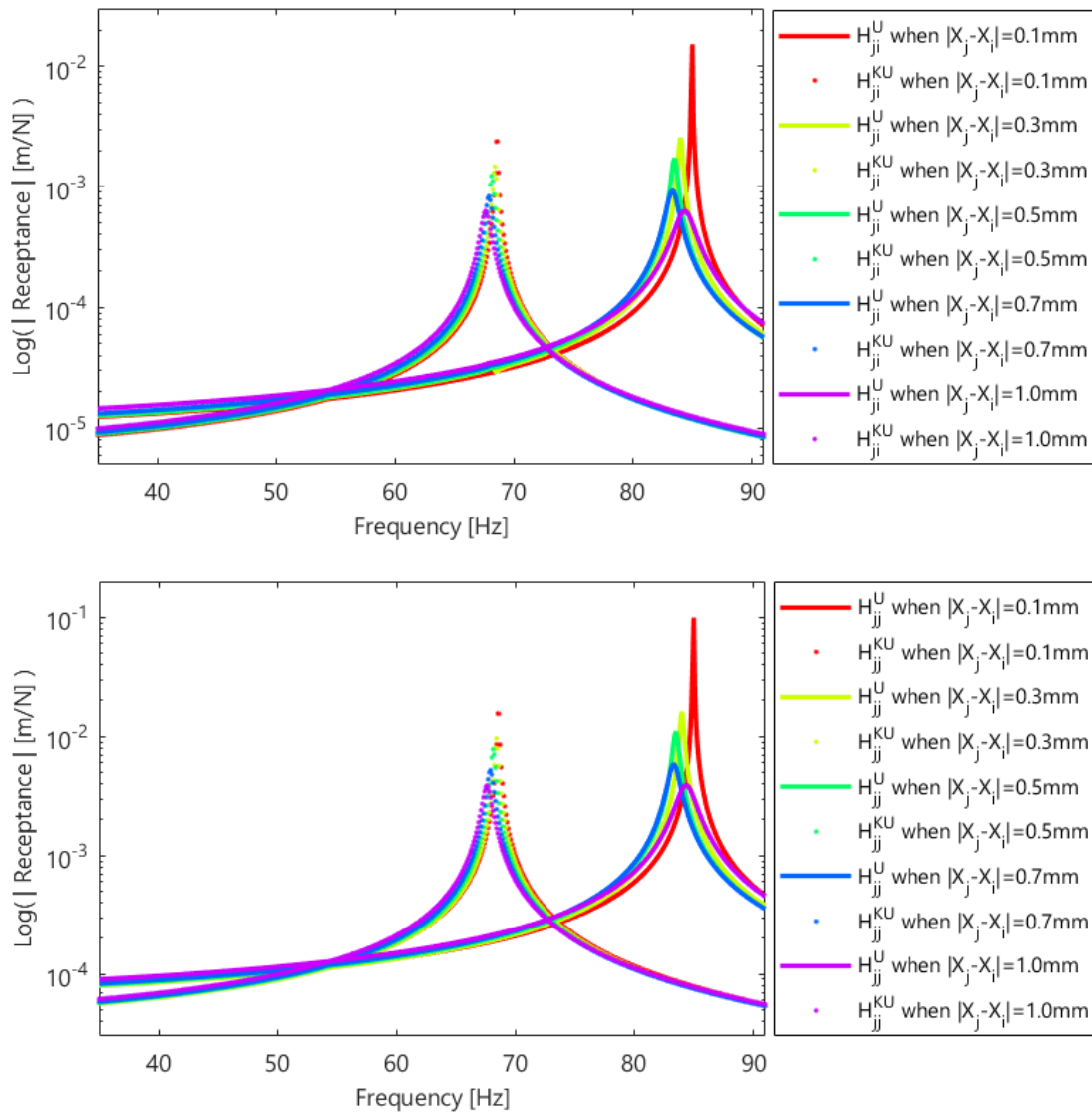


**Figure 66.** Calculated point (above) and transfer (below) FRFs of unknown subsystem (lines) and those measured for coupled system (dots) in transverse direction when excited from connection point (j)

In Figure 66, point ( $\mathbf{H}_{ji}^{KU}$ ) and transfer ( $\mathbf{H}_{ji}^{KU}$ ) FRFs of the coupled nonlinear system are given together with obtained point ( $\mathbf{H}_{ji}^U$ ) and transfer ( $\mathbf{H}_{ji}^U$ ) FRFs of the unknown nonlinear subsystem. As expected, decoupling of a linear FRF curve that belongs to

the long cantilever beam from each of the linear FRF curves that belong to the nonlinear coupled structure results in several FRF curves again each corresponding to a different displacement level of the nonlinear connection element. Note also that, decoupled FRF curves of the unknown subsystem includes the nonlinear connection dynamics due to two thin identical beams.

As explained in section 3.3, decoupled FRF curves in Figure 66 are to be used to identify the modal properties of each equivalent linear system in order to obtain the modal model of the unknown nonlinear subsystem. Modal parameters corresponding to each FRF curve are extracted using modal identification. As mentioned earlier, linear identification can be easily used with these FRFs since they show linear behavior. Identification of the modal parameters is performed by the formulation presented by Richardson and Formenti [75]. Natural frequencies, damping ratios and modal constants of the system are obtained using this technique. Magnitudes and phases of modal constants are identified as two separate parameters, as a modal constant is a complex quantity for a damped system. Identified modal parameters corresponding to the first modes of the unknown nonlinear subsystem are given for point ( $\mathbf{H}_{jj}^U$ ) and transfer ( $\mathbf{H}_{ji}^U$ ) FRFs in Figure 67 and Figure 68 as a function of displacement level of the nonlinear element. Note that, fitted curves to the obtained modal parameters are polynomials of third order.

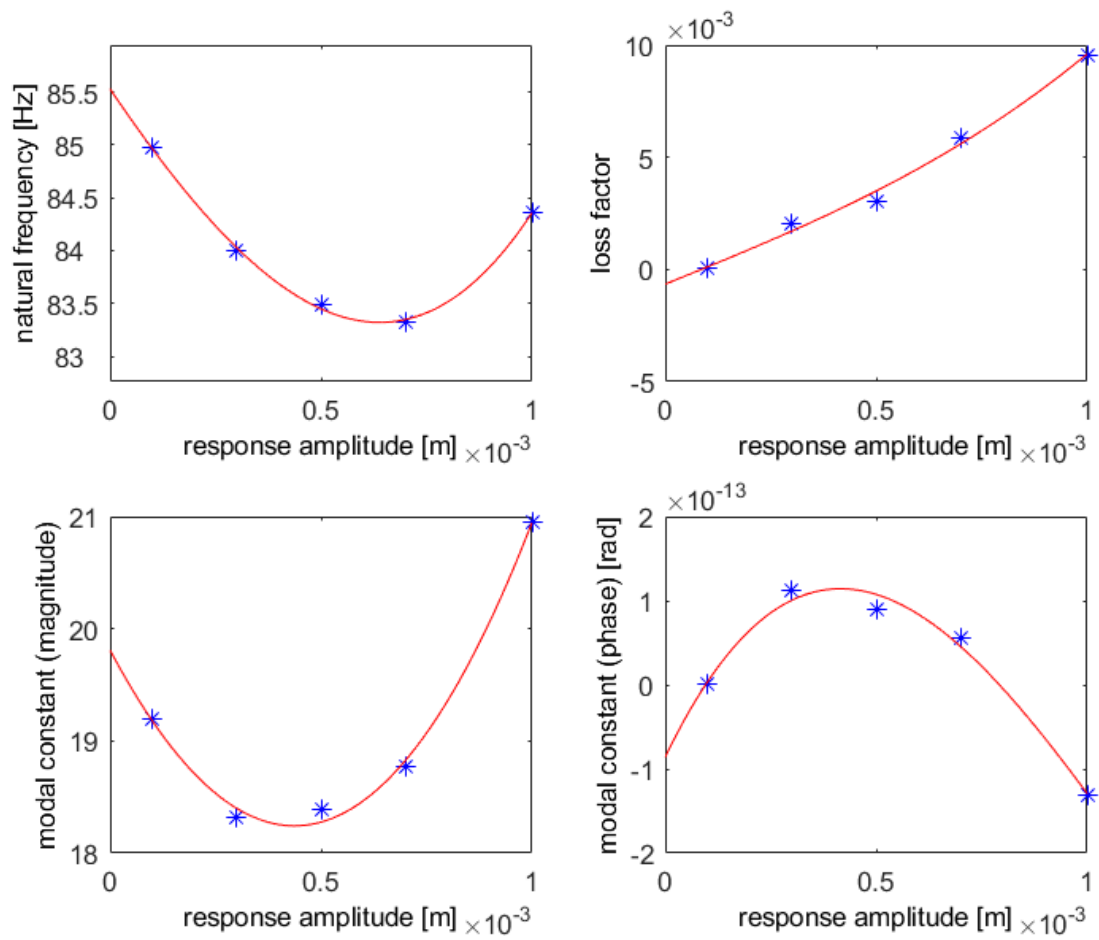


**Figure 67.** Variation of the modal parameters of the first mode of the unknown nonlinear subsystem for  $\mathbf{H}_{jj}^U$  wrt relative response amplitude,  $|\mathbf{X}_j - \mathbf{X}_i|$  (\*, identified parameters & —, fitted curves)

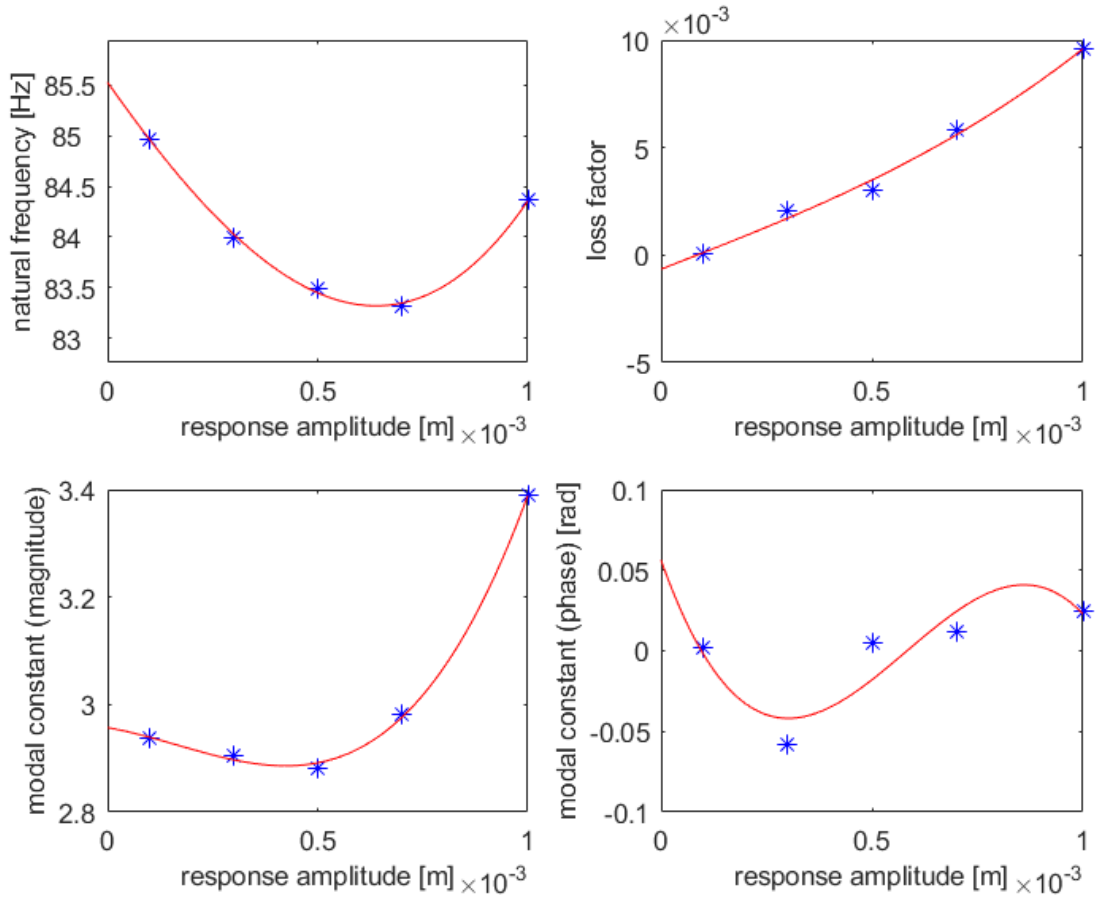


**Figure 68.** Variation of the modal parameters of the first mode of the unknown nonlinear subsystem for  $\mathbf{H}_{ji}^U$  wrt relative response amplitude,  $|\mathbf{X}_j - \mathbf{X}_i|$  (\*, identified parameters & —, fitted curves)

#### 5.2.4. Verification of FDM-NS Results

Here, decoupling results obtained via FDM-NS in section 5.2.3 are compared with those obtained directly via experimentation. Since stand-alone modal testing of the unknown subsystem by exciting it from the free tip of the two thin identical beams does not simulate the exact dynamics of this subsystem, the test system is modified as illustrated in Figure 69.

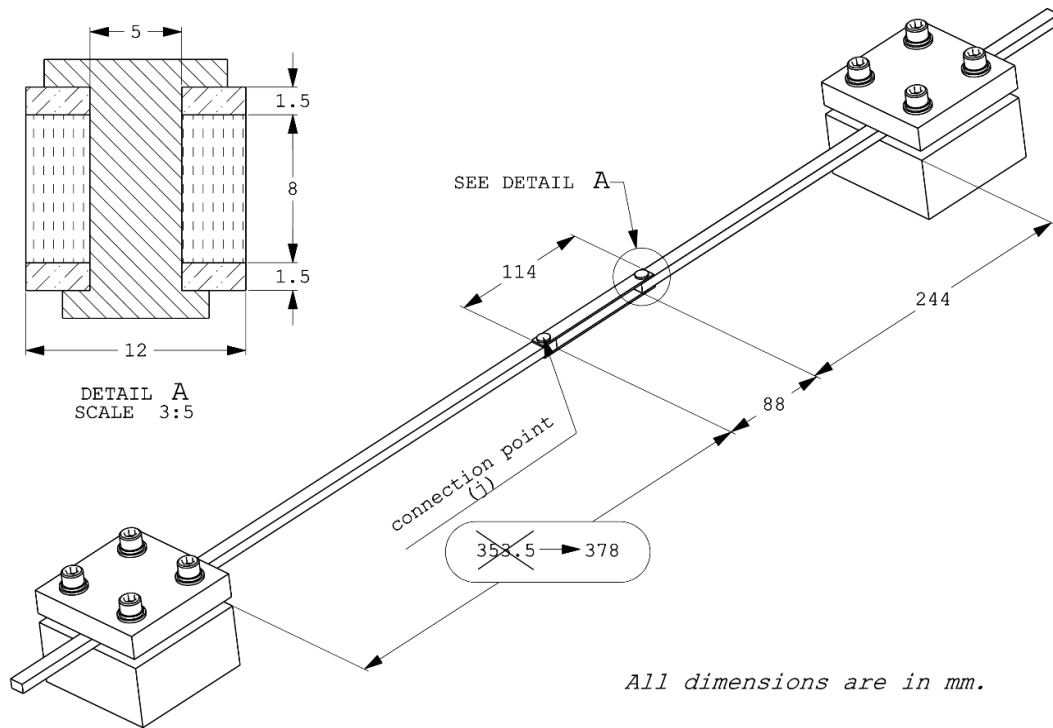


**Figure 69.** Dimensions and technical details of the modified test system

In this modified test system, the unknown subsystem is again coupled to a modified long cantilever beam whose length is increased to 378 mm this time. A step by step procedure for the verification process can be given as follows:

- First, measure stand-alone FRFs of the 378 mm long modified cantilever beam at its coupling point (tip point of the beam).
- Apply coupling theory by using the modal parameters of the unknown subsystem obtained in section 5.2.3 and FRFs of the 378 mm long modified cantilever beam. Note that an iterative solution will be required as the modal parameters are calculated as a function of displacement of the nonlinear

element. Thus, calculate response of the modified test system for harmonic excitation of magnitude 0.4 N applied at its coupling DOF.

- Measure the response of the modified test system for harmonic excitation of magnitude 0.4 N applied at its coupling DOF.
- Finally, compare the obtained results with each other. Agreement of the results will verify the method developed (FDM-NS) in this thesis.

As the first step, stand-alone FRFs of the 378 mm long modified cantilever beam are measured at its tip by carrying out a modal test with a modal hammer. The results obtained are given in Figure 70 together with those obtained for 353.5 mm long cantilever beam used in section 5.2.3.

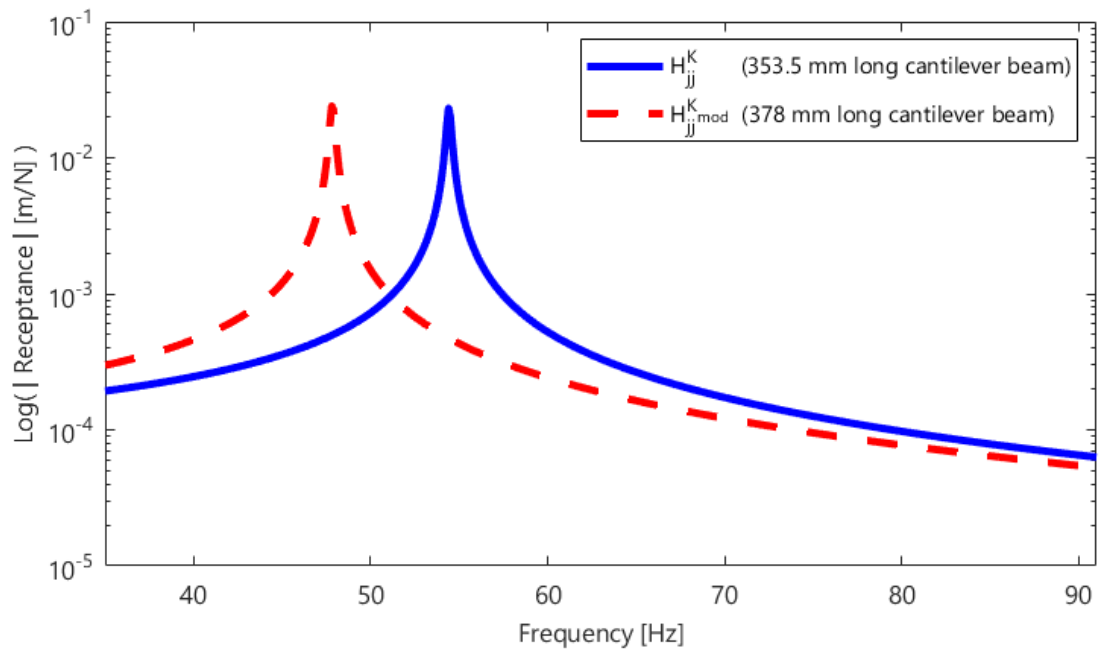


**Figure 70.** Measured point FRFs of the modified known subsystem by itself at its coupling DOF (j) in transverse direction

Since the modified test system is again nonlinear, its FRF will vary with the harmonic excitation level. Therefore, the modal test is performed using constant harmonic excitation of amplitude 0.4 N. During experiment, a similar procedure to the one given in Figure 62 for controlled force displacement testing is followed. But this time, harmonic forcing level is controlled manually by adjusting the voltage level through power amplifier at each frequency step. Measured and numerically calculated responses of the modified test system at its coupling DOF ( $\mathbf{X}_j^{KU_{mod}}$ ) for harmonic excitation of amplitude 0.4 N in transverse direction are given in Figure 71 and Figure 72.

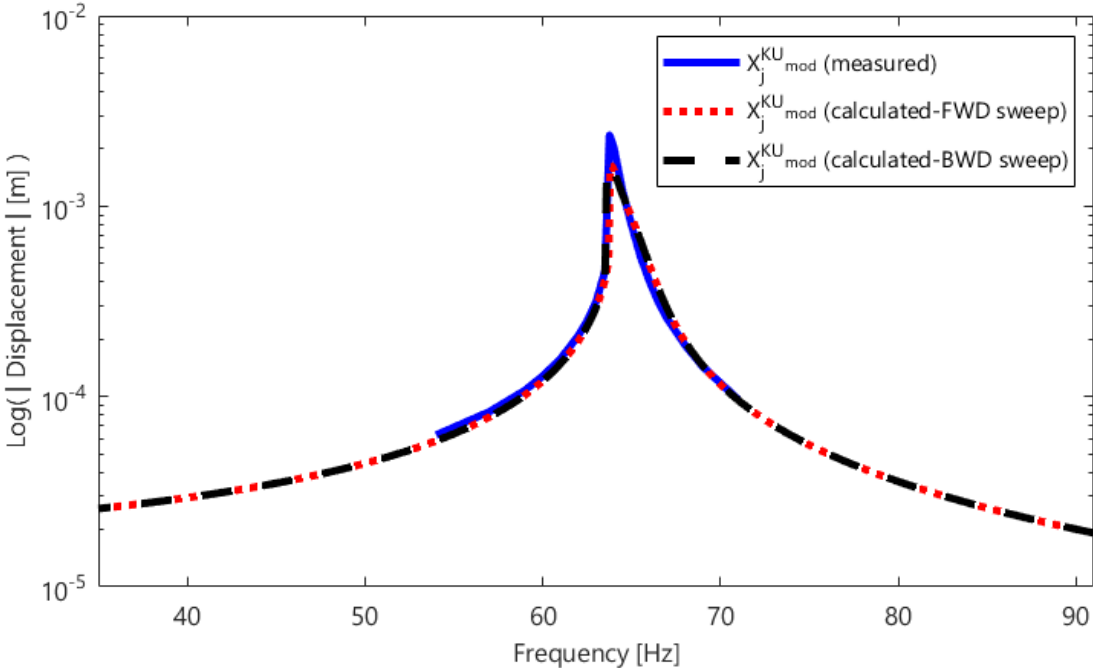


**Figure 71.** Measured and calculated responses of the modified test system at its coupling DOF (j) for harmonic excitation of amplitude 0.4 N in transverse direction



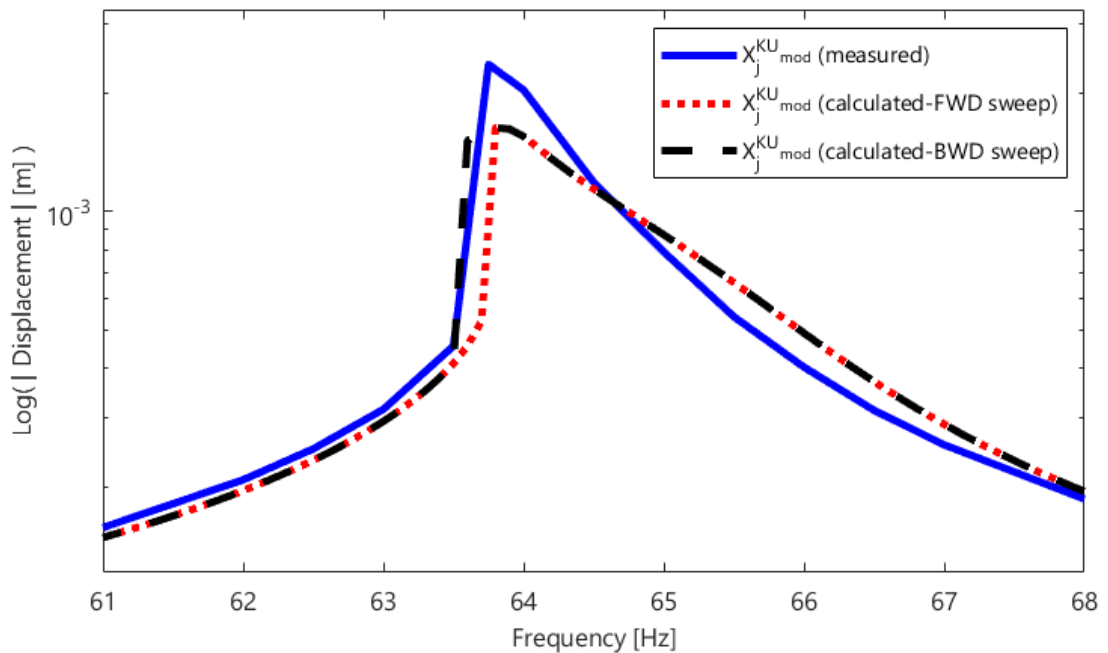


**Figure 72.** Measured and calculated responses of the modified test system at its coupling DOF (j) for harmonic excitation of amplitude 0.4 N in transverse direction – zoomed around resonance

It can be seen from Figure 71 and Figure 72 that obtained response shows nonlinear behavior which is typical when a system has softening stiffness type of nonlinearity. It is also observed that a good agreement is obtained between measured response and numerically calculated responses through forward and backward sweeping, especially at frequencies where the jump phenomenon occurs. A small difference can be observed between the amplitudes of the resonances. This may be due to misestimating the loss factors while extracting modal parameters from unknown subsystem FRFs. Recall that unknown subsystem FRFs are obtained by using experimental FRFs of the coupled system and the known subsystem. Unlike the modal testing of linear systems, limited number of frequency points can be used during controlled force amplitude testing of nonlinear systems. Although number of frequency points are increased in the immediate vicinity of the resonance, the resolution may not be sufficient to catch the

frequency where the peak amplitude occurs. Therefore, the unknown subsystem FRFs obtained via decoupling using these measured FRFs may have some errors which may result in some error in identified damping values.

## CHAPTER 6

### APPLICATION OF FDM-NS ON A REAL ENGINEERING SYSTEM

In this chapter, the proposed decoupling approach for nonlinear systems is applied to a real engineering system. This system is composed of an Inertial Measurement Unit (IMU) and its mechanical interface plate placed upon a tray grounded with elastomer isolators which has been used as such in several aerospace platforms in defense industry. Since elastomer isolators behave nonlinearly as they deflect, they introduce nonlinearity to the overall engineering system. In this application, point FRFs at the connection interface between mechanical interface plate of IMU and the tray are predicted by decoupling the FRFs of IMU from those of the overall nonlinear system via FDM-NS.

#### 6.1. Coupled Nonlinear System, its Subsystems and the Test Setup

In this application, FDM-NS is used in decoupling of a real engineering structure in order to observe the efficiency of the method on an industrial case. This engineering structure consists of an IMU rigidly connected to an interface plate which is connected to the ground via elastomer isolators as shown in Figure 73.

IMUs are frequently utilized on aerospace applications [84]. They provide reliable position and motion discernment for stabilization and navigation applications. They measure linear acceleration, angular position and angular velocity in six DOFs by using a combination of accelerometers and gyroscopes. However, these sensors can adversely be affected by mitigating effects of transferred disturbances due to the environmental vibrations and noise. Excessive vibration energy may reveal itself as measurement errors in the inertial data. Therefore, IMUs must be protected from high

level excitations, especially from those transmitted through mounting base. Moreover, the data collected by IMU sensors allow a computer in a navigation system to calculate its current position based on velocity and time. Therefore, it is crucial to predict transmissibility characteristics of the vibration isolated IMU, since the computer corrects the data measured by IMU using this transmissibility information and thus calculates current acceleration, angular position and angular velocity of the platform.

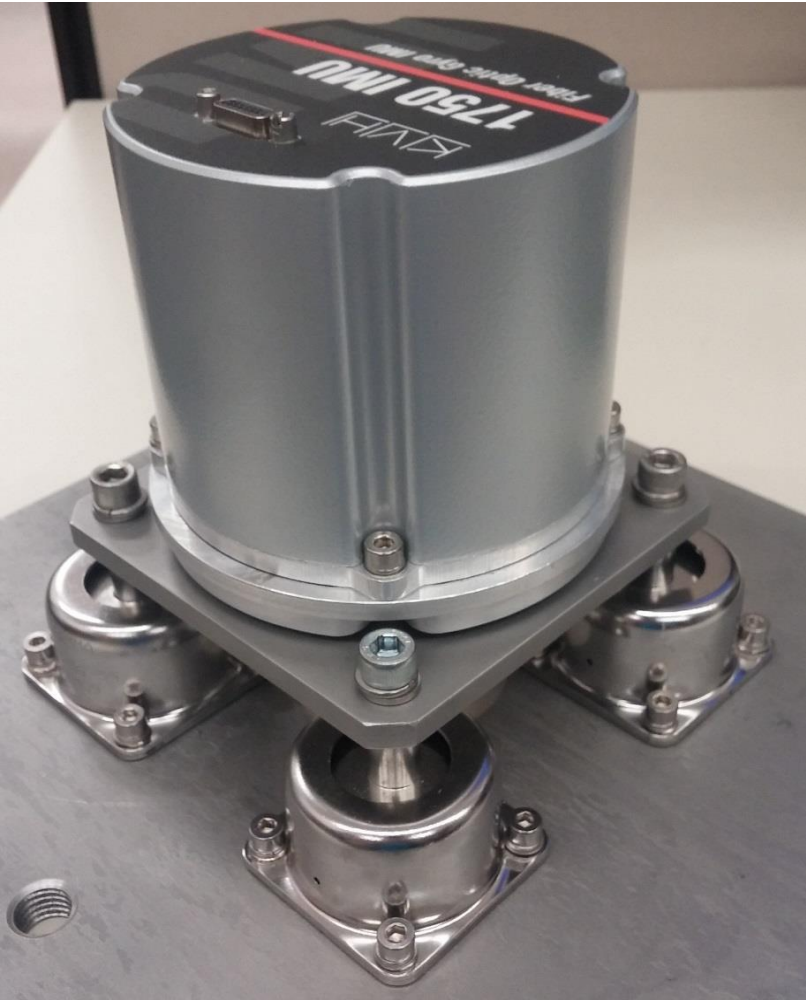


**Figure 73.** Coupled engineering structure – passive isolated IMU system

In this system, the IMU is isolated from the base excitations by use of a rigid tray on top of elastomer vibration isolators. Note that these elastomer isolators have been proved to show softening behavior as they deflect [85], thus introduces nonlinearity to the overall system. This nonlinear behavior should be taken into consideration for precise estimate of the transmissibility characteristics of the vibration isolated IMU.

The mounting tray is manufactured from St37 alloy steel whereas the mechanical interface plate of the IMU is made of 6061-T3 aluminum alloy. In this study, the assembly of IMU with its mechanical interface plate shown in Figure 74 is considered as the known linear subsystem whose FRFs at and between the connection point  $j$  and the internal point  $i$  are to be calculated through FEA and to be used in decoupling calculations directly.

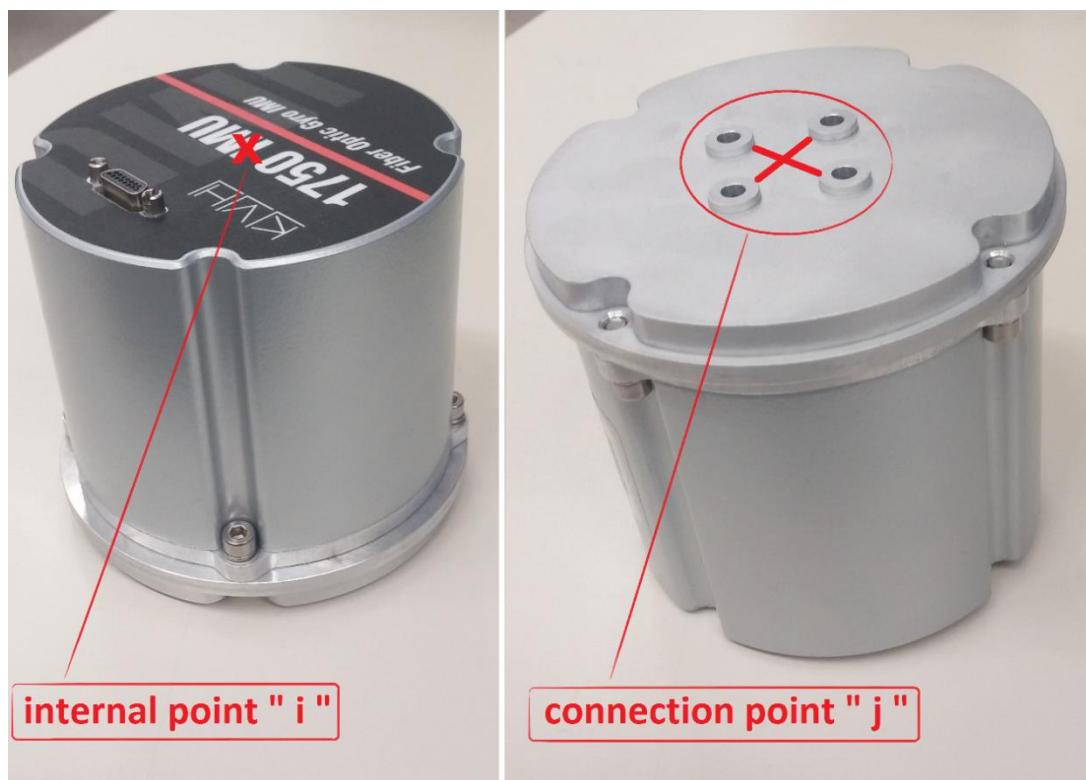


**Figure 74.** Known linear subsystem – IMU and its mechanical interface plate

On the other hand, the tray grounded with elastomer isolators shown in Figure 75 is taken as the unknown nonlinear subsystem whose point FRFs at its connection interface, which is referred to as point j, are to be predicted via proposed decoupling method for nonlinear systems.

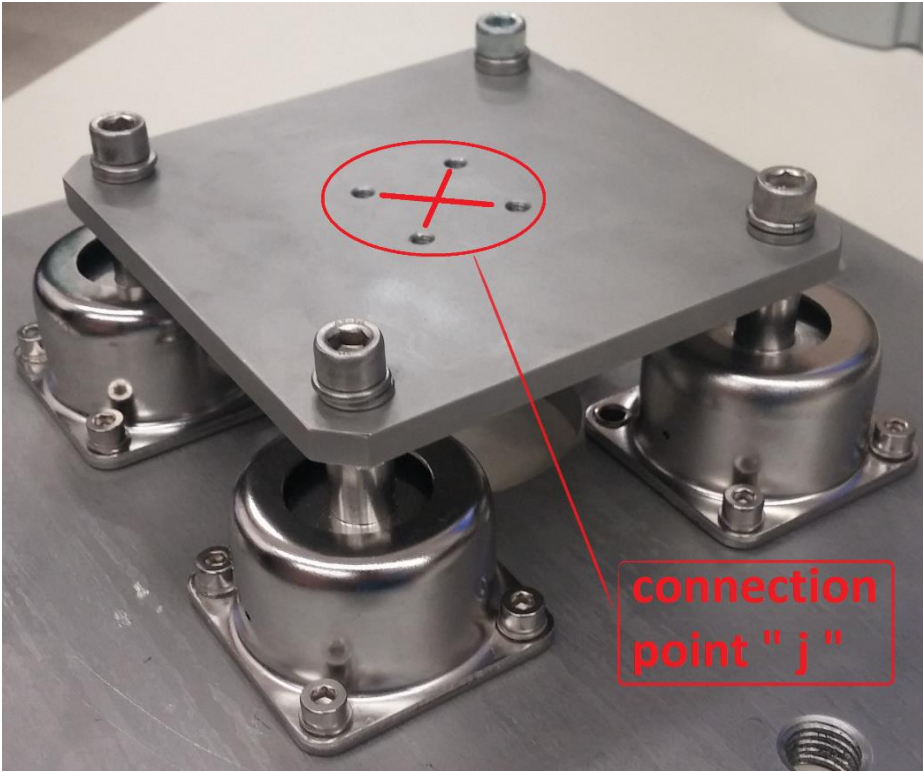


**Figure 75.** Unknown nonlinear subsystem – tray grounded with elastomer isolators

Furthermore, fixed connection between the tray and the mechanical interface plate of IMU is achieved by use of 4 bolted joints as illustrated in Figure 76.

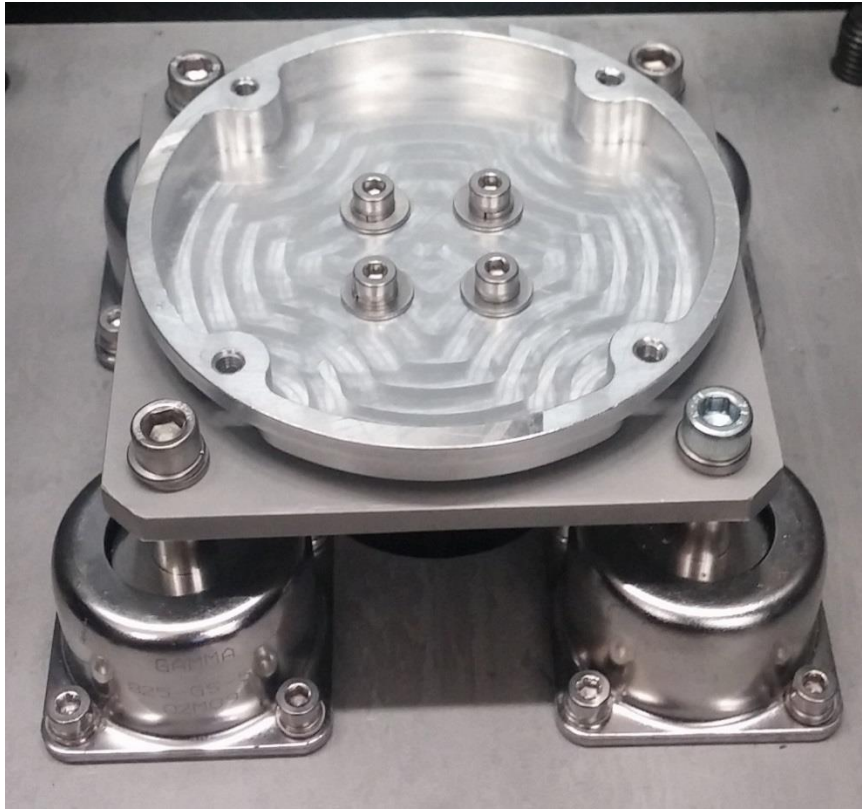


**Figure 76.** View of the fixed connection between two subsystems

A picture of the test setup is also given in Figure 77. It can be observed from this figure that the overall coupled test system is mounted on a rigid base with fixed-fixed boundary conditions. In other words, the overall coupled test system is grounded as it is the case in the aerospace platforms in which it is being used.

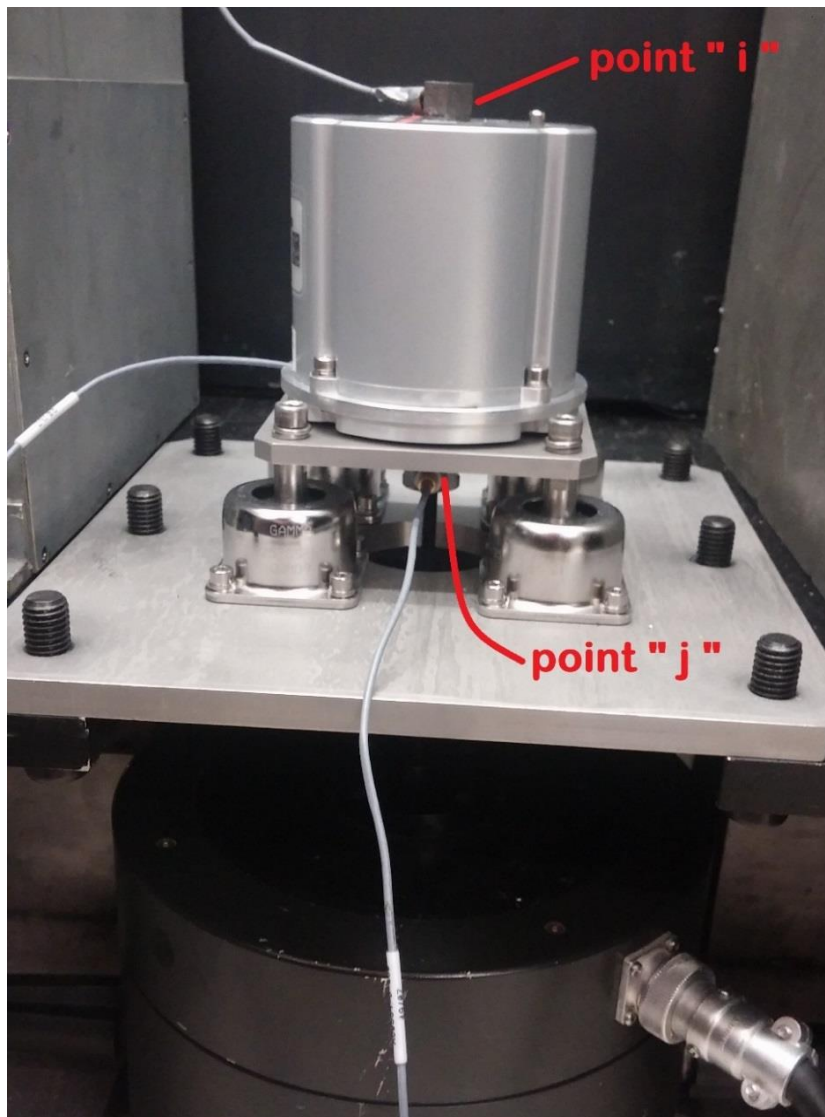


**Figure 77.** Coupled nonlinear system under testing

B&K Type 4808 vibration exciter is used to harmonically excite the coupled system via a push-rod attached to point j as shown in Figure 77. Due to the low level of voltage supplied from the signal generator, excitation force level of the vibration exciter is increased by using a B&K Type 2712 power amplifier. Frequency responses are measured using B&K Type 4507B uniaxial accelerometers. One of the accelerometers is located at point j of two subsystems in order to measure point FRFs of the connection



interface in the direction of harmonic excitation. The second accelerometer is attached to the point  $i$ , which is in line with the axis of excitation, in order to measure transfer FRFs at an internal coordinate of the known linear subsystem. On the other hand, externally applied harmonic forces are measured via a B&K Type 8230-002 force transducer which is attached to the tip of the push-rod. Throughout all measurements, B&K Type 3560C frontend system is used as a data acquisition system which also includes output channels that can be used as signal generators with a frequency range from 0 to 25.6 kHz.

## **6.2. Preliminary FEA and Test on the Coupled System**

In this application, the center of gravity of overall coupled system and all its subsystems are on the axis of excitation in order not to have rotational and transverse vibrations. In order to check the validity of the assumption of rigid tray, a preliminary harmonic analysis is carried out on the coupled system. In this analysis, a FEM of the coupled system (Figure 78) is constructed where elastomer isolators are modeled as grounded identical springs. Then, responses at point  $j$  and  $q$  are calculated for a constant amplitude harmonic forcing from point  $j$ .

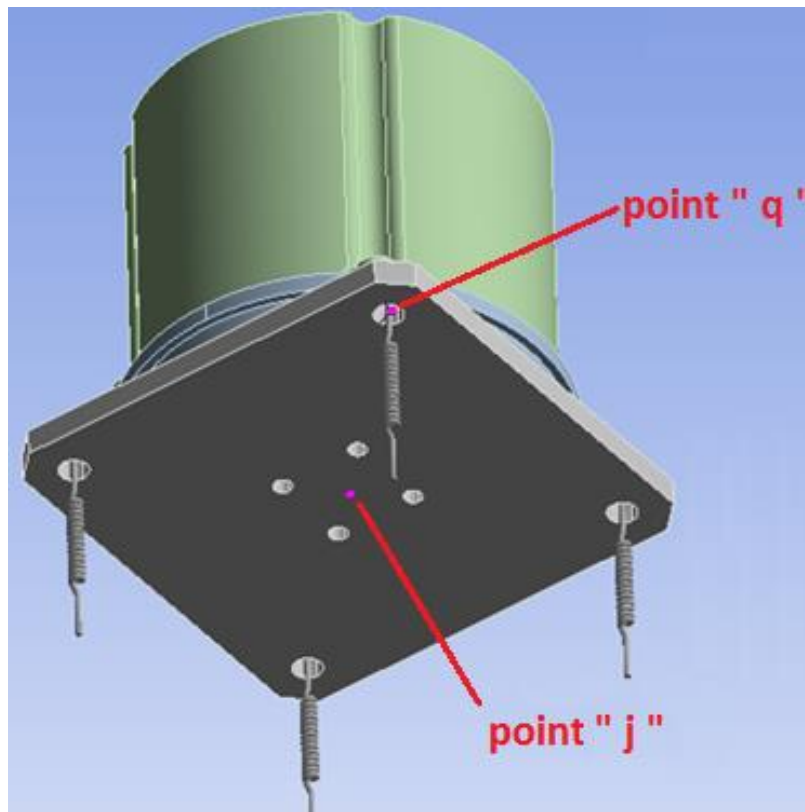


**Figure 78.** Linear FEM of the coupled system

Responses of point j and q ( $\mathbf{X}_j^{\text{KU}}$  and  $\mathbf{X}_q^{\text{KU}}$ ) are calculated and compared with each other in Figure 79. Results show that the responses of each isolator located at each corner of the tray are almost the same as that of the point of excitation throughout the frequency span of interest which ranges from 30 to 112 Hz.

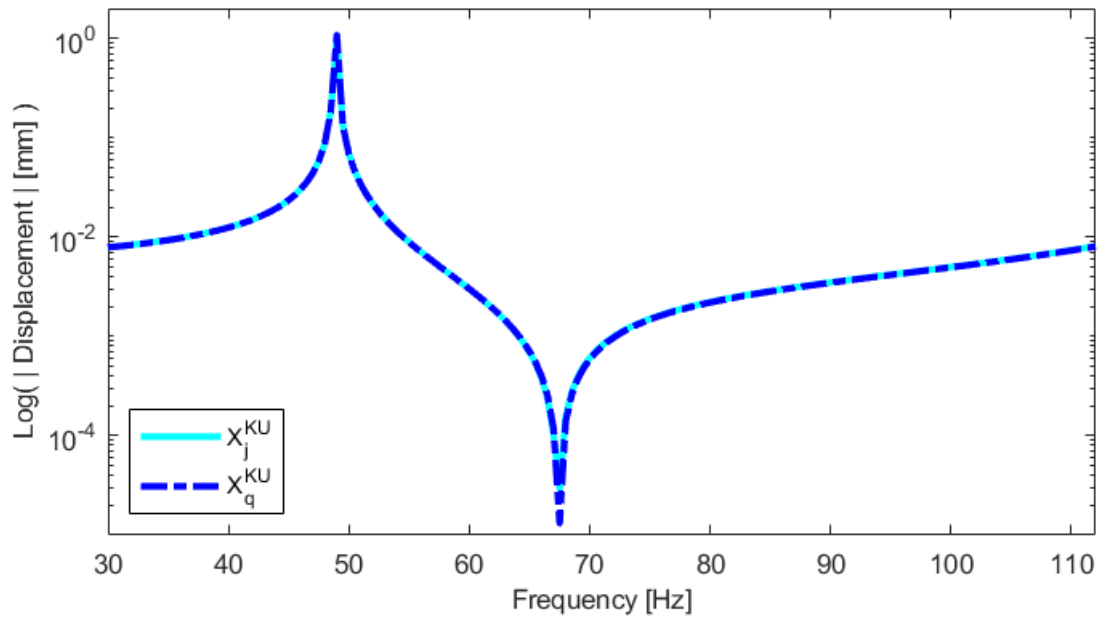


**Figure 79.** Comparison of harmonic responses at point  $j$  and  $q$  of the linear FEM of the coupled system

As a preliminary experiment, the coupled system which is expected to behave nonlinearly is tested under harmonic excitations with different constant amplitudes in order to observe its nonlinear dynamic behavior. Three sets of controlled force amplitude tests are performed. Measured point FRFs of the coupled system at point  $j$  ( $\mathbf{H}_{jj}^{KU}$ ) are given in Figure 80 for harmonic excitations of amplitude 5 N, 7.5 N and 10 N. It can be observed from the figure that fundamental resonance of the coupled system shifts to the left-hand side as the amplitude of harmonic excitation increases. This behavior is a sign of a softening stiffness type nonlinearity, which is due to the elastomer isolators in the system.

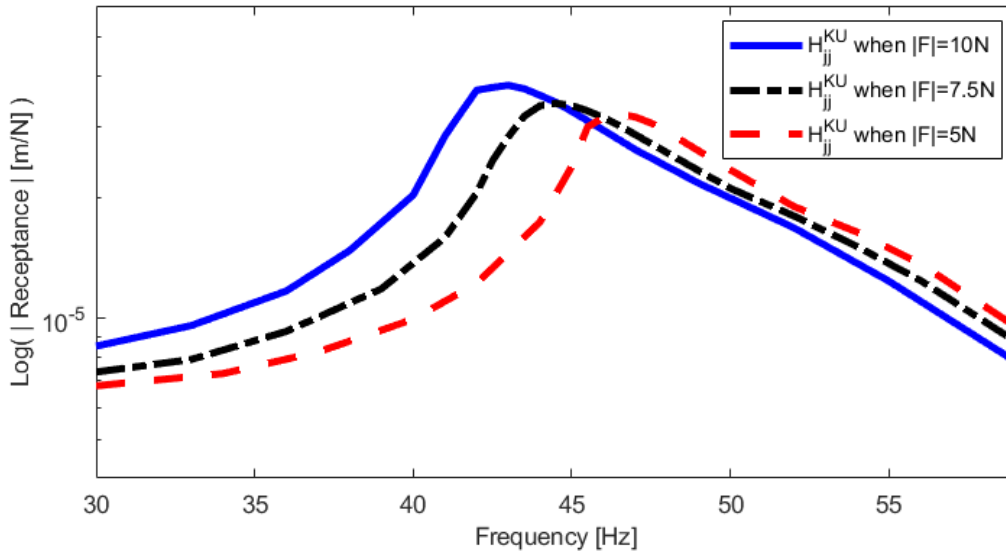


**Figure 80.** Measured point FRFs of the coupled system at point j via controlled force amplitude test

### 6.3. Application of FDM-NS

Firstly, a controlled displacement amplitude test is performed on the coupled nonlinear system. The measured FRFs are later used in decoupling calculations. Secondly, FRFs of the known linear subsystem are obtained through FEA. As the last step of FDM-NS, the FRFs of the unknown nonlinear subsystem are obtained via FRF decoupling.

For verification, however, it is not possible to measure the FRFs of the unknown subsystem directly, since the unknown subsystem includes nonlinear elastomer isolators whose stiffness changes depending on the static load on it. In order to overcome this problem a dummy mass is placed on the unknown subsystem while measuring its FRFs, and mass cancellation is applied. As it is not convenient to apply mass cancellation to measured FRFs showing nonlinear behavior [86] when force controlled FRFs are measured, comparison is made for FRFs measured with controlled displacement amplitude testing. Therefore, a single set of coupled system FRFs is measured for a specific harmonic displacement level of its nonlinear element, as this

will be sufficient to predict the unknown subsystem FRFs only for a specific displacement level of its nonlinear element for verification purposes.

### 6.3.1. Experimental Measurements on the Coupled System

In this experiment, point FRFs of the coupled nonlinear system at point  $j$  ( $\mathbf{H}_{jj}^{KU}$ ) together with its transfer FRFs between point  $i$  and  $j$  ( $\mathbf{H}_{ji}^{KU}$ ) are measured by performing a controlled displacement amplitude test. During the test, harmonic displacement amplitude of point  $j$  is kept constant at 0.05 mm for each frequency point of measurement which is almost the same as the displacement amplitude of each elastomer isolator as demonstrated in Figure 79. Measured point and transfer FRFs of the coupled nonlinear system ( $\mathbf{H}_{jj}^{KU}$  and  $\mathbf{H}_{ji}^{KU}$ ) are respectively given in Figure 81 and Figure 82 together with the FRF curves fitted to obtained data by mainly using “invfreqs” command of MATLAB® [81].

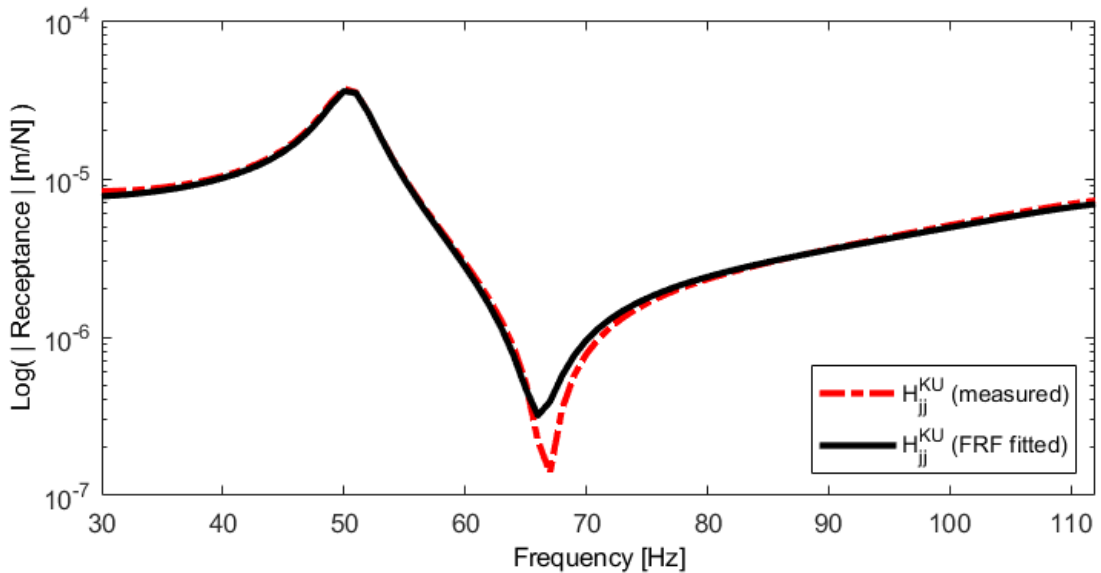


**Figure 81.** Measured point FRFs and the fitted FRF curve of the coupled nonlinear system at point  $j$  for 0.05 mm displacement amplitude of elastomer isolators

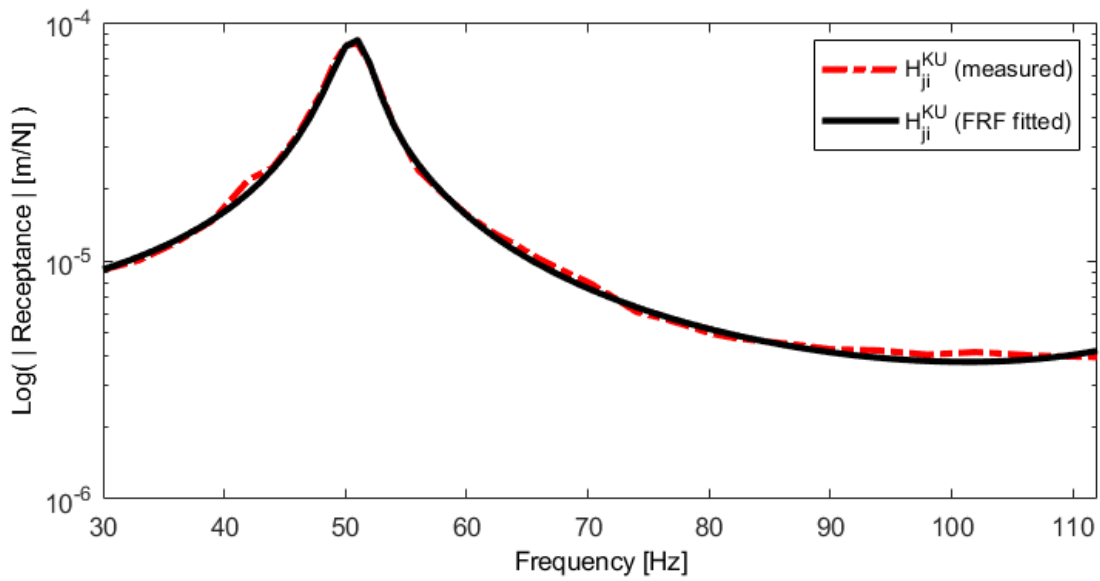


**Figure 82.** Measured transfer FRFs and the fitted FRF curve of the coupled nonlinear system between point  $i$  and  $j$  for 0.05 mm displacement amplitude of elastomer isolators

### 6.3.2. Harmonic Analyses on the Known Linear Subsystem

In order to obtain FRFs of the known linear subsystem, its FEM is constructed. Firstly, constructed FEM is verified by performing a modal test on the known subsystem under free-free boundary condition using a modal hammer. Figure 83 shows the measured known subsystem FRFs ( $\mathbf{H}_{ij}^K$ ) along with those numerically obtained via harmonic analysis in FE environment.

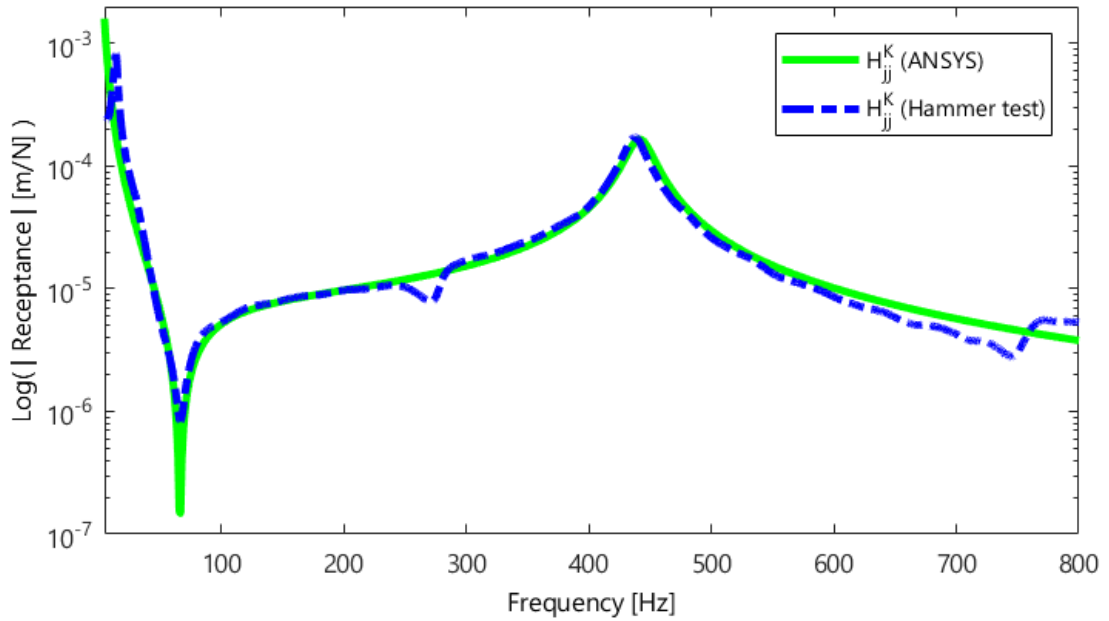


**Figure 83.** Point FRFs of the known linear subsystem at point  $j$  calculated via FEA and measured via hammer test

In Figure 83, constructed FEM of the known subsystem is verified for a wide frequency range that covers its first natural frequency. However, the frequency range of interest in this study is 30 Hz to 110 Hz. Then, a harmonic analysis is conducted using this verified FEM in order to obtain point and transfer FRFs of the known linear subsystem at and between point  $i$  and  $j$  ( $\mathbf{H}_{jj}^K$ ,  $\mathbf{H}_{ji}^K$  and  $\mathbf{H}_{ii}^K$ ) under free-free boundary condition via ANSYS R15.0<sup>®</sup>. Results are given in Figure 84 in the form of receptances.

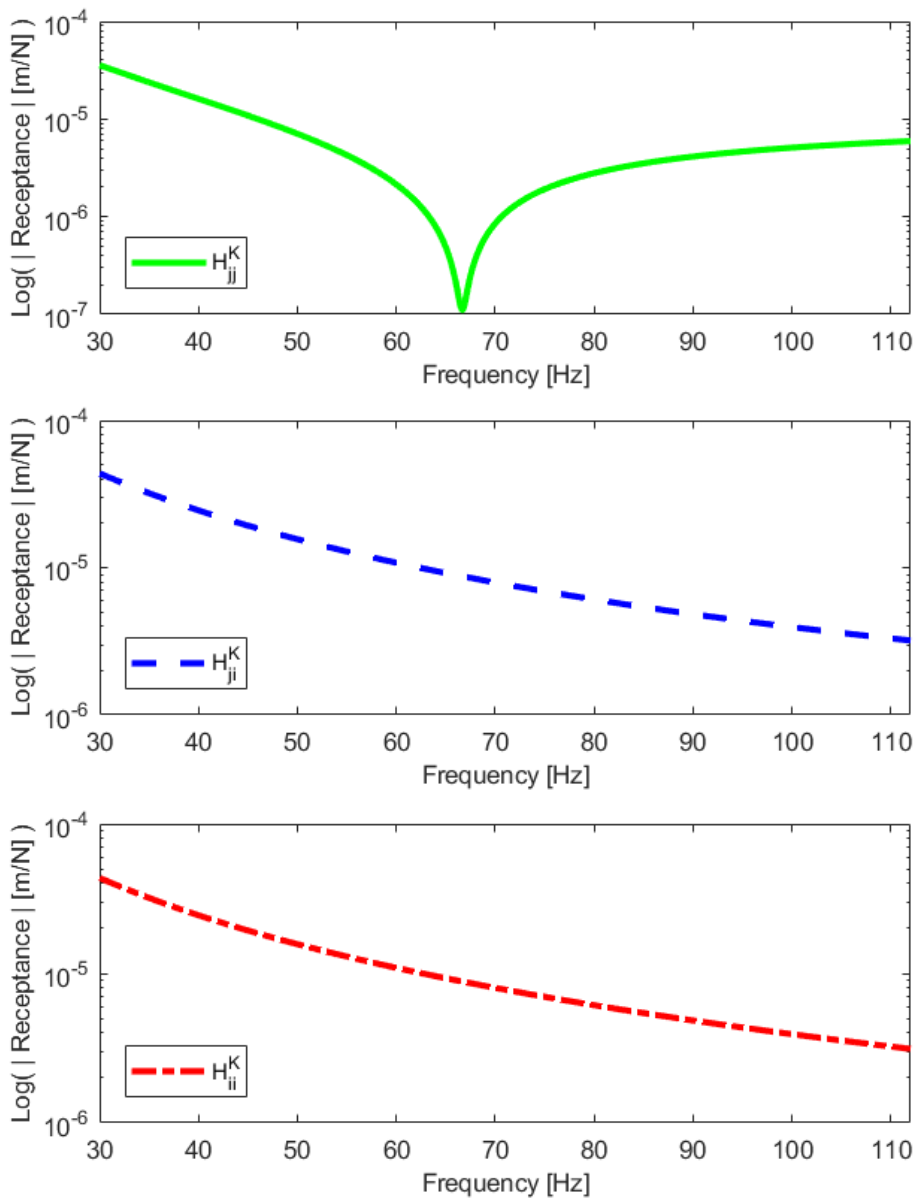


**Figure 84.** Point and transfer FRFs of the known linear subsystem at and between point i and j calculated via FEA

Now one can decouple known subsystems FRFs from coupled nonlinear system FRFs in order to predict unknown nonlinear subsystem FRFs at point j ( $\mathbf{H}_{jj}^U$ ) for 0.05 mm constant displacement amplitude of elastomer isolators.



### 6.3.3. Implementation of FRF Decoupling

In this section, unknown nonlinear subsystem FRFs are going to be predicted by applying the dual assembly approach [54] as the last step of FDM-NS. Decoupling calculations are performed using two sets of data:

- Standard interface (i.e., by using only  $\mathbf{H}_{jj}^{KU}$  and  $\mathbf{H}_{jj}^K$  ).

- Extended interface (i.e., by using  $\begin{bmatrix} \mathbf{H}_{jj}^{KU} & \mathbf{H}_{ji}^{KU} \\ \mathbf{H}_{ij}^{KU} & \mathbf{H}_{ii}^{KU} \end{bmatrix}$  and  $\begin{bmatrix} \mathbf{H}_{jj}^K & \mathbf{H}_{ji}^K \\ \mathbf{H}_{ij}^K & \mathbf{H}_{ii}^K \end{bmatrix}$  )

Here, the use of extended interface is expected to improve the results predicted via standard interface, as suggested in reference [54].

#### 6.3.3.1. FRF Decoupling using Standard Interface

Here, point FRFs of the unknown nonlinear system at point  $j$  ( $\mathbf{H}_{jj}^U$ ) are calculated via dual assembly approach [54] using standard interface. Predicted FRFs are given in Figure 85. It can be observed from the figure that predicted FRFs are ill-conditioned and noise is greatly amplified around the frequency of 66.7 Hz.

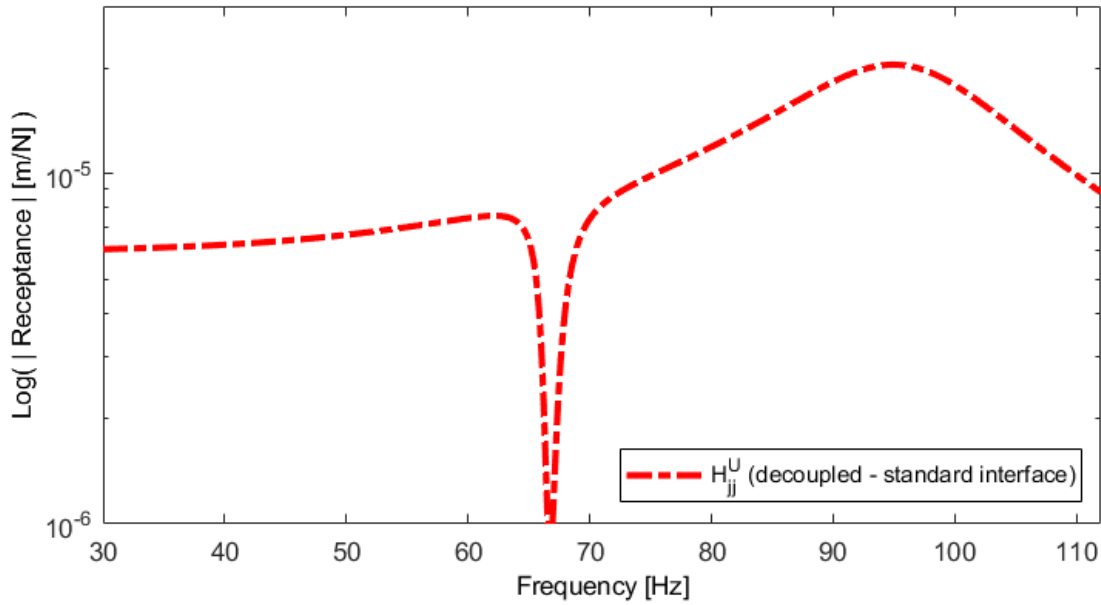


**Figure 85.** Predicted point FRFs of the unknown subsystem at point j by using standard interface for 0.05 mm displacement amplitude of elastomer isolators

### 6.3.3.2. FRF Decoupling using Extended Interface

To circumvent ill-conditioning around the frequency of 66.7 Hz, D'Ambrogio et al. suggest [54] the use of FRFs at some internal DOFs of the known subsystem. Therefore, point FRFs of the unknown nonlinear system are recalculated via dual assembly approach [54] using extended interface. In this approach, the point FRFs of the coupled system and the known subsystem at point i ( $\mathbf{H}_{ii}^{KU}$  and  $\mathbf{H}_{ii}^K$ ) and their transfer FRFs between point i and j ( $\mathbf{H}_{ji}^{KU}$  and  $\mathbf{H}_{ji}^K$ ) are also included in the decoupling calculations in addition to the standard interface.

Even though all the required FRFs are obtained for the known linear subsystem as given in Figure 84, point FRFs of the coupled nonlinear system at point i ( $\mathbf{H}_{ii}^{KU}$ ) are

not available. So,  $\mathbf{H}_{ii}^{KU}$  is generated via FRF synthesis using the modal parameters extracted from  $\mathbf{H}_{jj}^{KU}$  and  $\mathbf{H}_{ji}^{KU}$ , which are illustrated in Figure 86 altogether.

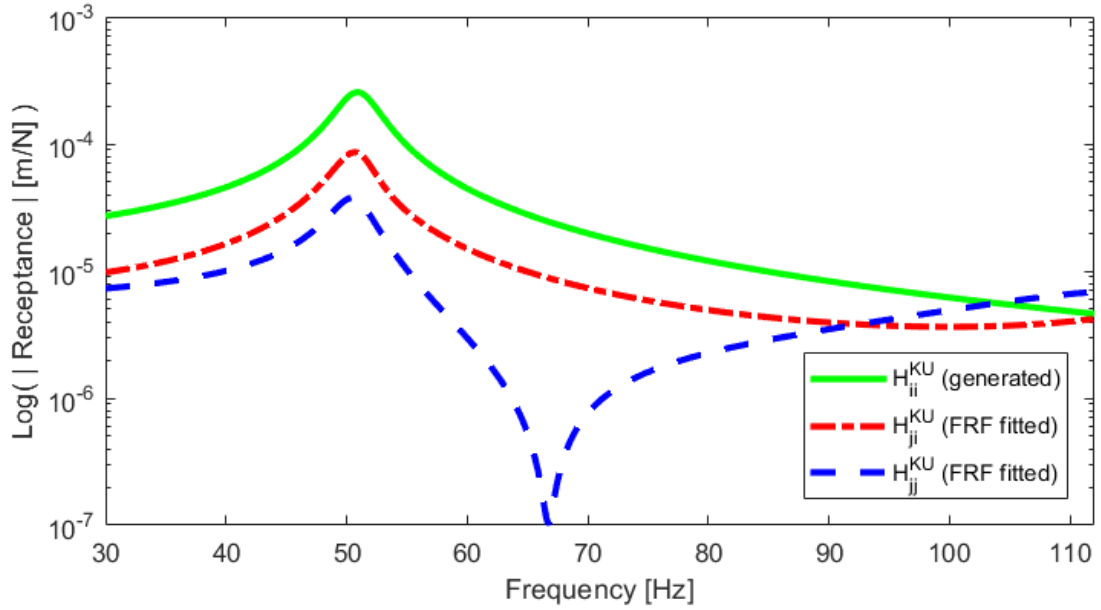


**Figure 86.** FRFs of the coupled nonlinear system at and between point i and j for 0.05 mm displacement amplitude of elastomer isolators

So, one can perform decoupling using all the available data at the extended interface. Predicted FRFs of the unknown nonlinear subsystem at point j ( $\mathbf{H}_{jj}^U$ ) are given in Figure 87. It is observed that amplification of the noise due to the ill-conditioning around the frequency of 66.7 Hz is quite reduced.

Note that the rate of improvement in this ill-conditioning problem depends on the number and choice of the measurement points at the internal DOFs of the known

subsystem [54]. So, further improvement may be obtained by taking additional measurements on internal DOFs of the known subsystem.

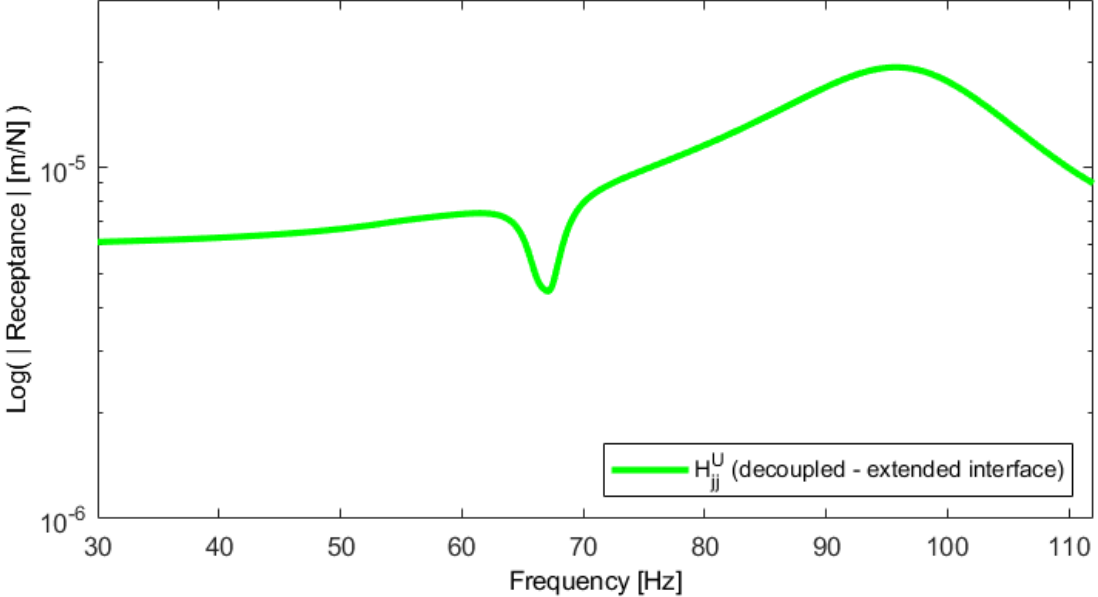


**Figure 87.** Predicted point FRFs of the unknown subsystem at point j by using extended interface for 0.05 mm displacement amplitude of elastomer isolators

**6.4. Verification of FDM-NS Results**

Here, point FRFs of the “unknown” nonlinear subsystem at point j ( $\mathbf{H}_{jj}^U$ ) are obtained via controlled displacement amplitude testing for the purpose of comparison with the results of decoupling calculations. It should be recalled that the resonant frequency, and thus linear stiffness of the elastomer isolator being used (825-GS-55) varies depending on the static load carried by itself (Figure 88). Therefore, unknown subsystem FRFs obtained after decoupling will not be the same as those directly measured from the unknown nonlinear subsystem given in the Figure 75. In other

words, decoupling calculations will result in the unknown nonlinear subsystem response while the elastomer isolators are in the strained condition, which cannot be measured directly.

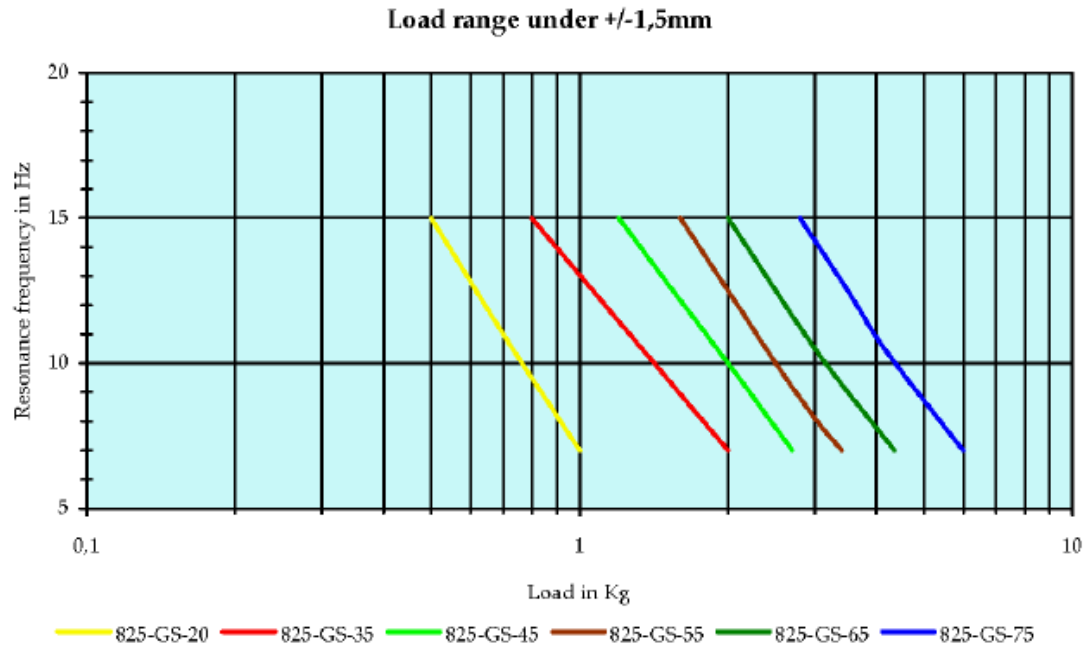


**Figure 88.** Variation of resonance frequency wrt load carried by an elastomer isolator (825-GS-55) [87]

Therefore, verification of the decoupling results should be made by comparing them with the values measured by preloading them. This is achieved by loading isolators by using a dummy mass; however, then the mass effect of the dummy mass is cancelled from the measured response of the unknown nonlinear subsystem. For this purpose, a rigid block which is made up of tungsten and has the same mass as the known linear subsystem is manufactured and mounted on the unknown nonlinear system during

testing (Figure 89). In this test, the harmonic displacement amplitude of the elastomer isolators is kept constant again at 0.05 mm.

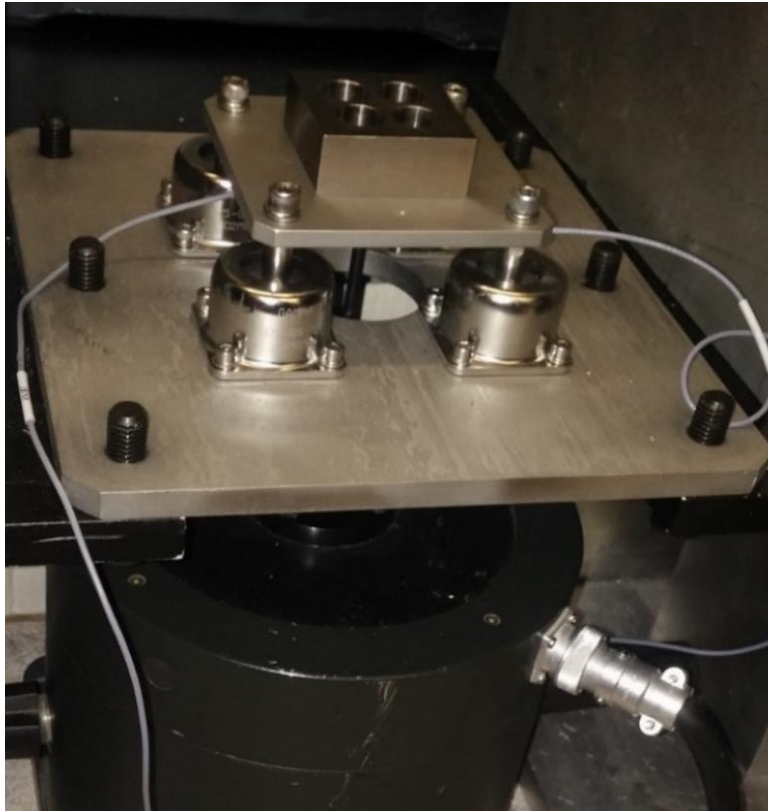


**Figure 89.** Unknown nonlinear subsystem under testing

In order to eliminate the mass loading effect of this dummy block from the measured point FRFs of the unknown subsystem at point  $j$  ( $\mathbf{H}_{jj}^U$ ), the well-known formula for mass cancellation is used [1]:

$$\mathbf{A}_{jj}^U = \frac{{}^m \mathbf{A}_{jj}^U}{1 - m_d \cdot {}^m \mathbf{A}_{jj}^U} \quad (74)$$

where  ${}^m \mathbf{A}_{jj}^U$  and  $\mathbf{A}_{jj}^U$  represent the measured and corrected point accelerances at point  $j$ , respectively, whereas  $m_d$  corresponds to mass of the rigid dummy block.

Measured point FRFs and the FRF curve fitted to this data using MATLAB<sup>®</sup> [81] are given in Figure 90 together with the FRF curve obtained after cancellation of the mass effect of the dummy mass.

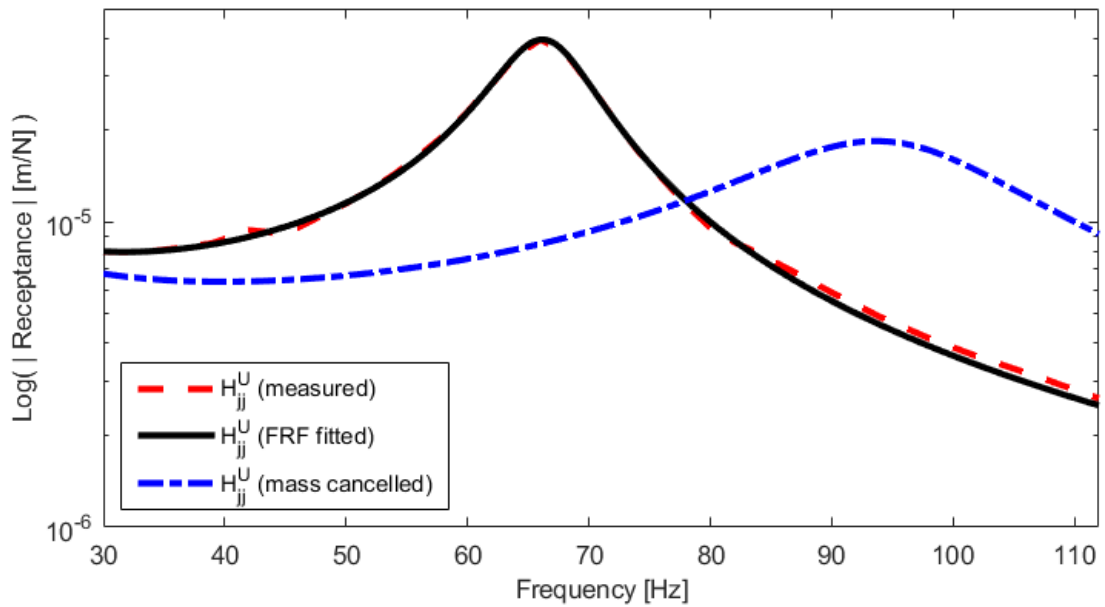


**Figure 90.** Measured point FRFs, fitted FRF curve and FRF curve obtained after mass cancellation of the unknown nonlinear subsystem at point  $j$  for 0.05 mm displacement amplitude of elastomer isolators

Now, one can compare the predicted point FRFs of the unknown nonlinear subsystem at point  $j$  ( $\mathbf{H}_{jj}^U$ ) given in Figure 85 and Figure 87 with those obtained in Figure 90

through mass cancellation just after measurement. The comparison is depicted in Figure 91.

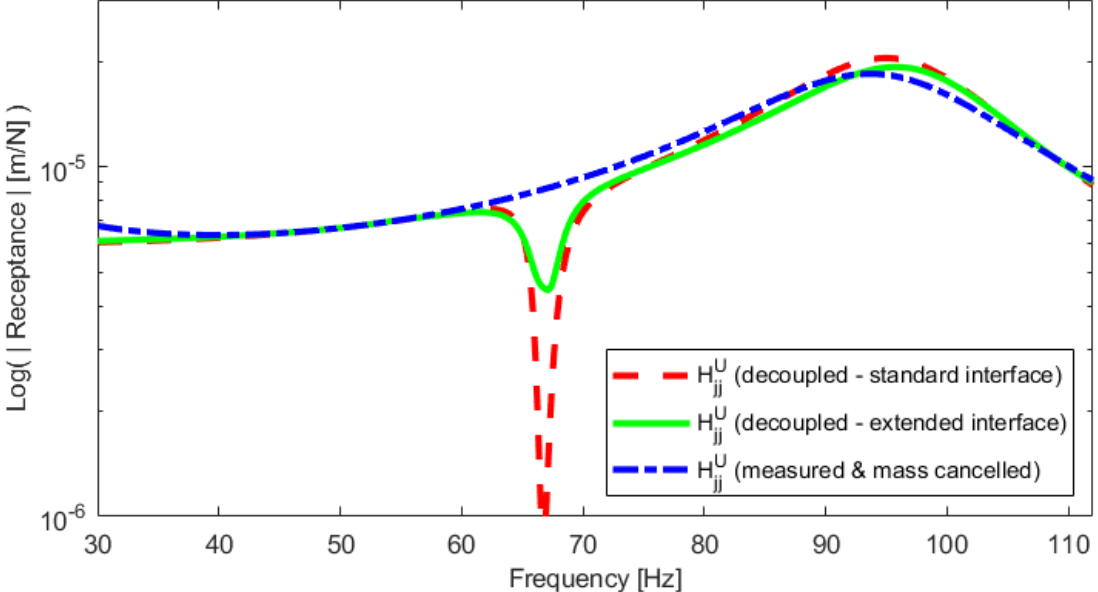


**Figure 91.** Predicted (using standard and extended interfaces) and measured point FRFs of the unknown nonlinear subsystem at point j by for 0.05 mm displacement amplitude of elastomer isolators

Figure 91 gives a clear view of the amplification of noise due to the ill-conditioning around the frequency of 66.7 Hz. As expected, FRF decoupling using extended interface provides more correlated results with those measured. Furthermore, a slight frequency shift around the resonance occurs which is believed to be due to the cumulative effect of the errors in experimental measurements and curve fitting processes of the coupled system FRFs along with the modeling errors of the known subsystem in FE environment. Eventually, the acceptable results obtained using FDM-NS shows the applicability of the method on a real engineering system.



## CHAPTER 7

### SUMMARY AND CONCLUSIONS

In this thesis, the decoupling problem, i.e., predicting dynamic behavior of a particular substructure from the knowledge of the dynamics of the coupled structure and those of the other substructures, is considered. FRFs of the whole structure are assumed to be known from experiments, along with the measured or theoretically calculated FRFs of the known substructure. Both sets of FRFs are assumed to be known at only known subsystem coordinates. Although the decoupling of linear systems has been well investigated for three decades and led to several decoupling methods, the decoupling of nonlinear systems yet seems to remain untouched. So, this study focuses mainly on the decoupling of nonlinear systems, even though some work on decoupling of linear systems is also presented.

Firstly, two different formulations for decoupling of linear systems are proposed. Both methods give exact results, as it is the case in most of the decoupling methods, when exact FRFs are used in all equations. However, the problem in all of such methods is the sensitivity of the formulations to even very slight errors which are inevitable due to the use of measured data. All formulations usually include matrix inversions, and depending on the nature of the equations, some methods are more sensitive to measurement errors and therefore do not perform well. Hence, it is important to test the performance of any new decoupling technique and compare its performance with existing best ones. Application of the proposed decoupling formulations is presented on a lumped parameter system. In this case study simulated experimental results are used, and in order to simulate experimentally measured FRFs of the coupled system, theoretically calculated exact FRFs are polluted. In studying the performances of the

proposed methods, Frequency Response Assurance Criteria are used which show the correlation between the predicted and the true FRFs of the unknown subsystem.

Furthermore, performances of the proposed formulations together with some of those available in the literature are evaluated on the same case study. Also, effect of noise on the performance of the decoupling methods is examined by polluting the exact FRFs of the coupled system using different sets of independent random variables with the same mean and gradually increased standard deviations. However, decoupling methods under investigation yield FRAC values that show an uneven trend with the increasing level of noise. In order to make a sound comparison, results are calculated for 100 runs for each method with a different pollution set with the same mean and standard deviation at each time. Result of this statistical comparison shows that proposed methods come up with the most correlated results for each of the five-different standard deviation of pollution. Thus far, all the FRF information of the coupled system and the known subsystem at the internal coordinates of the known subsystem are used during calculations. Since this is not the case for decoupling of real life structures whose number of DOFs is limited to the number of coordinates that can practically be measured, the former statistical comparison is expanded for the cases where only some or none of the FRFs at the internal coordinates of the known subsystem are available. It is observed from the results that the so-called Dual Formulation [54] performs best in case of unavailability of FRFs at some or all internal coordinates of the known subsystem.

Later, the dynamic decoupling problem for nonlinear structures is addressed. A method is developed to decouple a nonlinear or linear substructure from a given coupled nonlinear structure. The so-called “FRF Decoupling Method for Nonlinear Systems (FDM-NS)” is believed to be the first method proposed for nonlinear decoupling. It is capable of decoupling nonlinear systems having a nonlinearity of any type that can be modeled as a single element. Yet, the method is flexible as far as the location of the nonlinear element is concerned. That is, the nonlinearity can be either

in the known or unknown subsystem, or it can connect both subsystems. Depending on the location of the nonlinearity, whether in the known or unknown substructure, two different formulations are suggested. For the case where the nonlinear element is at the connection of two subsystems, it is shown how to reduce this problem to that where the nonlinear element is connected to the internal DOFs of the known or unknown subsystems.

Firstly, FDM-NS is tested on simulated case studies. Three different case studies are presented using a MDOF lumped parameter system and simulated experimental data. The same MDOF system with identical physical parameters is used in each case study by changing the location and the type of the nonlinear element. In the first numerical case study, FDM-NS is applied to a MDOF nonlinear system where the unknown subsystem includes a cubic stiffness type of nonlinear element. By using the FRFs measured through displacement controlled experiments, sets of modal parameters are identified for the unknown subsystem through linear modal identification, each set corresponding to a different response level of the cubic stiffness element. Then, harmonic response of the unknown subsystem can be calculated for any given forcing level iteratively using the modal parameter sets obtained. It is shown that the nonlinear response predicted by using FDM-NS is almost the same as the one obtained directly by employing DFM.

In the second simulated case study, FDM-NS is applied to the same MDOF lumped parameter nonlinear system where the nonlinear element is in the known subsystem this time. In this study, FRFs of the coupled nonlinear system, as well as the known nonlinear subsystem are obtained at a chosen specific relative displacement level of the two ends of the nonlinear cubic stiffness element. Again, simulated experimental data is used for the coupled system FRFs. Then, the unknown subsystem FRFs are obtained by applying linear decoupling. Results obtained show perfect agreement with the exact ones.

As the last simulated case study, FDM-NS is applied to the same MDOF lumped parameter nonlinear system where the nonlinear element connects two subsystems this time. In this study, the unknown gap type of nonlinear connection element is included in the unknown subsystem by adding a massless node to the free end of the nonlinear connection element. Thereby, the problem is reduced to the case where the nonlinear element is in the unknown subsystem. Predicted results closely match with those obtained directly through DFM except small discrepancies at the frequency where jump phenomenon is observed. This is believed to be due to inaccurately estimated modal parameters due to noise in the primary data.

Later, FDM-NS is applied to structural test systems in order to demonstrate its real-life applicability. In the first experimental case study, a linear cantilever beam is decoupled from the nonlinear T-beam assembly composed of a linear cantilever beam attached to the mid-point of a thin beam of which both ends are fixed and therefore introduces a nonlinear stiffness. The transverse dynamic response of the coupled system is measured experimentally for a specific relative displacement amplitude of the nonlinear element through controlled displacement amplitude testing. Then, the fixed-fixed thin beam is taken as the known nonlinear substructure and it is modeled as a concentrated nonlinear stiffness in transverse direction with a concentrated equivalent mass and linear stiffness. Linear parameters of this single DOF model of the fixed-fixed thin beam are theoretically calculated whereas its nonlinear parameters are experimentally identified. After obtaining the known substructure FRFs for the same specific relative displacement level of the nonlinear element, linear decoupling is performed to obtain the unknown tip point FRFs of the linear cantilever beam. A very good agreement is observed between the predicted FRFs by using FDM-NS and those obtained from the shaker test of the cantilever beam alone, even though fixed-fixed thin beam is modeled as a single DOF mass-nonlinear spring system.

FDM-NS is also applied to another experimental test system composed of two cantilever beams coupled with two thin identical beams. In this test case, FDM-NS is

verified for a case where the unknown nonlinear element couples two linear structures such that the nonlinear subsystem cannot be tested alone. In that respect, this is a typical real-life case where there is no alternative to using nonlinear decoupling method if one would like to measure the dynamics of the nonlinear subsystem. In this application, firstly, FRFs of the coupled system are measured through controlled displacement amplitude testing, while those of the known cantilever beam are obtained via classical modal testing. Then, modal parameter variations of the unknown subsystem are obtained as a function of the displacement level of the nonlinear connection beams by applying FDM-NS. In order to verify these results, the experimental test system is modified such that the length of the known subsystem is increased. Then first FRFs of the new cantilever beam are obtained via classical modal testing. Finally, FRFs of the new coupled nonlinear system are calculated for a constant amplitude harmonic force by using the modal parameter variations obtained for the unknown nonlinear subsystem along with FRFs of the new cantilever beam. From the comparison of the calculated values with those measured directly, it is concluded that the overall agreement is quite well although slight deviations were observed around resonance.

Lastly, the decoupling method developed is applied on a real engineering system. The engineering system used is an IMU placed upon a tray grounded with rubber isolators having nonlinear characteristics. In this study, point FRFs at the connection point of two subsystems are predicted by decoupling the dynamics of IMU from the dynamics of the overall nonlinear system via FDM-NS. The satisfactory results obtained show the applicability of FDM-NS on real engineering systems.

To conclude, first of all, two new formulations are proposed for decoupling of linear systems in this thesis. Although these methods perform best only when complete dynamics of the coupled system and the known subsystem are available at all DOFs of the known subsystem, they can remain as alternative methods for decoupling of linear systems.

This thesis, to the best of author's knowledge, represents the first attempt to decouple a nonlinear or linear substructure from a given coupled nonlinear structure. A method, called FRF Decoupling Method for Nonlinear Systems (FDM-NS), is proposed in order to obtain substructure dynamics of a nonlinear structure, starting from experimentally measured FRFs of the coupled nonlinear structure and experimentally measured or theoretically calculated dynamic response of its known substructure. It is assumed in this method that the nonlinearity in the coupled system can be modeled as a single nonlinear element and its location is available. Note that, FDM-NS distinguishes itself as the only alternative to obtain the dynamics of a nonlinear subsystem that cannot be measured separately but only when coupled to neighboring structure(s). In this study, FDM-NS is first employed through some numerical case studies using simulated experimental data. Then, its real-life applicability is demonstrated through some experimental cases performed on test rigs involving nonlinearity. Finally, the method is successfully applied to decouple a real engineering system which consists of an IMU and its passive vibration isolation system usually used in aerospace applications.

As a future work, this study may be extended for decoupling of nonlinear systems involving multiple nonlinear elements. This seems to be possible only if the controlled displacement amplitude test procedure may be improved so that displacement levels of the multiple nonlinear elements can be controlled at the same time.

## REFERENCES

- [1] D.J. Ewins, *Modal Testing: Theory and Practice*, John Willey & Sons, London, England, 1984.
- [2] N. Okubo, M. Miyazaki, *Development of Uncoupling Technique and Its Application*, Proceedings of 4th International Modal Analysis Conference, 1986.
- [3] P. Sjövall, T. Abrahamsson, *Substructure System Identification from Coupled System Test Data*, *Mechanical Systems and Signal Processing*, 22 (1) (2008) 15-33.
- [4] N.M.M. Maia, J.M.M. Silva, A.M.R. Ribeiro, *Some Applications of Coupling/Uncoupling Techniques in Structural Dynamics - Part 1: Solving the Mass Cancellation Problem*, in: *Proceeding of the 15th International Modal Analysis Conference*, 1997.
- [5] C.G. Koh, L.M. See, T. Balendra, *Estimation of Structural Parameters in Time Domain: A Substructure Approach*, *Earthquake Engineering and Structural Dynamics*, 20 (1991) 787-801.
- [6] T.R. Kim, K.F. Ehmann, S.M. Wu, *Identification of Joint Structural Parameters between Substructures*, *Journal of Engineering for Industry*, 113 (1991) 419-424.
- [7] T. Yang, S.H. Fan, C.S. Lin, *Joint Stiffness Identification Using FRF Measurements*, *Computers and Structures*, 81 (2003) 2549-2556.

- [8] C.G. Koh, K. Shankar, Substructural Identification Method without Interface Measurement, *Journal of Engineering Mechanics*, 129 (7) (2003) 769-776.
- [9] G. Kerschen, K. Worden, A.F. Vakakis, J.C. Golinval, Past, Present and Future of Nonlinear System Identification in Structural Dynamics, *Mechanical Systems and Signal Processing*, 20 (3) (2006) 505-592.
- [10] D.M. Storer, Dynamic Analysis of Non-Linear Structures Using Higher Order Frequency Response Functions, Ph.D. Thesis, Department of Engineering, University of Manchester, October 1991.
- [11] J. Cattarius, Numerical Wing/Store Interaction Analysis of a Parametric F16 Wing, Ph.D. Thesis, Department of Engineering Science and Mechanics, Virginia Polytechnic Institute and State University, September 1999.
- [12] Y. R. Yang, KBM Method of Analyzing Limit Cycle Flutter of a Wing with an External Store and Comparison with a Wind-Tunnel Test, *Journal of Sound and Vibration*, 187 (2) (1995) 271-280.
- [13] R.N. Desmarais, W.H. Reed, Wing Store Flutter with Nonlinear Pylon Stiffness, *Journal of Aircraft*, 18 (11) (1981) 984-987.
- [14] R. Craig, M. Bampton, Coupling of Substructures for Dynamic Analysis, *AIAA Journal*, 6 (7) (1968) 1313-1319.
- [15] J. Hallquist, V.W. Snyder, Synthesis of Two Discrete Vibratory Systems Using Eigenvalue Modification, *AIAA Journal*, 11 (2) (1973) 247-249.



- [16] J.H. Crowley, G.T. Rocklin, A.L. Klosterman, H. Vold, Direct Structural Modification Using Frequency Response Functions, in: Proceedings of the 2nd International Modal Analysis Conference, Orlando, Florida, 1984, pp.58–65.
- [17] M. İmregün, D.A. Robb, D.J. Ewins, Structural Modification and Coupling Dynamic Analysis Using FRF Data, in: Proceedings of the 5th International Modal Analysis Conference, London, UK, 1987.
- [18] B. Jetmundsen, R.L. Bielawa, W.G. Flannelly, Generalized Frequency Domain Substructure Synthesis, *Journal of the American Helicopter Society*, 33 (1) (1988) 55-64.
- [19] A.P.V. Urgueira, Dynamic Analysis of Coupled Structures Using Experimental Data, Ph.D. Thesis, Department of Mechanical Engineering, Imperial College London, London, England, 1989 (<http://www.imperial.ac.uk/dynamics/phd-theses/>).
- [20] A. Sestieri, W. D'Ambrogio, A Modification Method for Vibration Control of Structures, *Mechanical Systems and Signal Processing*, 3 (3) (1989) 229-253.
- [21] H.N. Özgüven, Structural Modifications Using Frequency Response Functions, *Mechanical Systems and Signal Processing*, 4 (1) (1990) 53-63.
- [22] Y. Ren, C.F. Beards, On Substructure Synthesis with FRF Data, *Journal of Sound and Vibration*, 185 (5) (1995) 845-866.
- [23] Y.H. Park, Y.S. Park, Structural Modification Based on Measured Frequency Response Functions: An Exact Eigenproperties Reallocation, *Journal of Sound and Vibration*, 237 (2000) 411-426.

- [24] J.E. Mottershead, C. Mares, M.I. Friswell, An Inverse Method for the Assignment of Vibration Nodes, *Mechanical Systems and Signal Processing*, 15 (2001) 87-100.
- [25] W. Liu, D.J. Ewins, Substructure Synthesis via Elastic Media, *Journal of Sound and Vibration*, 257 (2) (2002) 361-379.
- [26] W. D'Ambrogio, A. Sestieri, A Unified Approach to Substructuring and Structural Modification Problems, *Shock and Vibration*, 11 (3-4) (2004) 295-310.
- [27] A. Kyrianiou, J.E. Mottershead, H. Ouyang, Assignment of Natural Frequencies by an Added Mass and One or More Springs, *Mechanical Systems and Signal Processing*, 18 (2) (2004) 263-289.
- [28] D. De Klerk, D.J. Rixen, J. de Jong, Frequency Based Substructuring (FBS) Method Reformulated According to the Dual Domain Decomposition Method, in: *Proceedings of the 24th International Modal Analysis Conference*, 2006.
- [29] D. De Klerk, D.J. Rixen, S.N. Voormeeren, General Framework for Dynamic Substructuring: History, Review, and Classification of Techniques, *AIAA Journal*, 46 (5) (2008) 1169-1181.
- [30] H. Hang, K. Shankar, J.C.S. Lai, Prediction of the Effects on Dynamic Response due to Distributed Structural Modification with Additional Degrees of Freedom, *Mechanical Systems and Signal Processing*, 22 (8) (2008) 1809-1825.
- [31] R.L. Mayes, Tutorial on Experimental Dynamic Substructuring Using the Transmission Simulator Method, in: *Proceedings of the 30th International Modal Analysis Conference*, 2012.

- [32] B. Sayın, E. Ciğeroğlu, A New Structural Modification Method with Additional Degrees of Freedom for Dynamic Analysis of Large Systems, in: Proceedings of the 31st International Modal Analysis Conference, 2013.
- [33] K. Watanabe, H. Sato, A Modal Analysis Approach to Nonlinear Multi-Degrees-of Freedom System, ASME Journal of Vibration, Acoustics, Stress and Reliability in Design, 110 (1988) 410-411.
- [34] J.V. Ferreira, D.J. Ewins, Nonlinear Receptance Coupling Approach Based on Describing Functions, in: Proceedings of the 14th International Modal Analysis Conference, Dearborn, Michigan, USA, 1996, pp.1034-1040.
- [35] Y.H. Chong, M. İmregün, Coupling of Non-Linear Substructures Using Variable Modal Parameters, Mechanical Systems and Signal Processing, 14 (2000) 731-746.
- [36] S. Huang, Dynamic Analysis of Assembled Structures with Nonlinearity, Ph.D. Thesis, Department of Mechanical Engineering, Imperial College London, London, England, 2007 (<http://www.imperial.ac.uk/dynamics/phd-theses/>).
- [37] R.J. Kuether, M.S. Allen, Structural Modification of Nonlinear FEA Subcomponents Using Nonlinear Normal Modes, in: Proceedings of the 31st International Modal Analysis Conference, Garden Grove, California, USA, 2013.
- [38] T. Kalaycıoğlu, H.N. Özgüven, Nonlinear Structural Modification and Nonlinear Coupling, Mechanical Systems and Signal Processing, 46 (2) (2014) 289-306, <https://doi.org/10.1016/j.ymssp.2014.01.016>.

- [39] F. Wenneker, P. Tiso, A Substructuring Method for Geometrically Nonlinear Structures, in: Proceedings of the 32nd International Modal Analysis Conference, Orlando, Florida, USA, 2014.
- [40] C. Tepe, E. Ciğeroğlu, Structural Coupling of Two-Nonlinear Structures, in: Proceedings of the 33rd International Modal Analysis Conference, Orlando, Florida, USA, 2015.
- [41] R.J. Kuether, M.S. Allen, Modal Substructuring of Geometrically Nonlinear Finite-Element Models, *AIAA Journal*, 54 (2) (2016) 691-702.
- [42] S. Gray, J. Starkey, Dynamic Substructure Separation Using Physical and Modal Models, in: Proceedings of the 6th International Modal Analysis Conference, Kissimmee, Florida, 1988.
- [43] C. Gontier, M. Bensaïbi, Time Domain Identification of a Substructure from in situ Analysis of the Whole Structure, *Mechanical Systems and Signal Processing*, 9 (4) (1995) 379-396.
- [44] J.M.M. Silva, N.M.M. Maia, P.M.L. Ribeiro, Dynamic Modeling: Application of Uncoupling Techniques, in: Proceedings of the 14th International Modal Analysis Conference, 1996.
- [45] N.M.M. Maia, J.M.M. Silva, A.M.R. Ribeiro, P.L.C. Silva, On the Dynamic Characterization of Joints Using Uncoupling Techniques, in: Proceedings of the 16th International Modal Analysis Conference, 1998.
- [46] P. Kalling, T. Abrahamsson, T. McKelvey, Subsystem State-Space Model Identification and its Sensitivity to Test Variability, in: P. Sas, M. De Munck

(Eds.), Proceedings of ISMA 2004 - International Conference on Noise and Vibration Engineering, Leuven, Belgium, 2004, pp. 2729-2744.

- [47] J. Zhen, T.C. Lim, G. Lu, Determination of System Vibratory Response Characteristics Applying a Spectral-Based Inverse Sub-Structuring Approach. Part I: Analytical Formulation, *International Journal of Vehicle Noise and Vibration*, 1 (2004) 1-30.
- [48] Z.W. Wang, J. Wang, Y.B. Zhang, C.Y. Hu, Y. Zhu, Application of the Inverse Substructure Method in the Investigation of Dynamic Characteristics of Product Transport System, *Packaging Technology and Science*, 25 (6) (2012) 351-362.
- [49] J. Wang, L. Lu, Z. Wang, Modeling the Complex Interaction between Packaged Product and Vehicle, *Advanced Science Letters*, 4 (6-7) (2011) 2207-2212.
- [50] Z.W. Wang, J. Wang, Inverse Substructure Method of Three Substructures Coupled System and its Application in Product Transport-System, *Journal of Vibration and Control*, 17 (6) (2011) 943-952.
- [51] J. Wang, X. Hong, Y. Qian, Z.W. Wang, L.X. Lu, Inverse Sub-Structuring Method for Multi-Coordinate Coupled Product Transport System, *Packaging Technology and Science*, 27 (5) (2014) 385-408.
- [52] W. D'Ambrogio, A. Fregolent, Promises and Pitfalls of Decoupling Procedures, in: *Proceedings of the 26th International Modal Analysis Conference*, 2008.
- [53] D. Cloutier, P. Avitabile, Investigation on the Use of Various Decoupling Approaches, in: *Proceedings of the 28th International Modal Analysis Conference*, 2010.

- [54] W. D'Ambrogio, A. Fregolent, The Role of Interface DOFs in Decoupling of Substructures Based on the Dual Domain Decomposition, *Mechanical Systems and Signal Processing*, 24 (7) (2010) 2035-2048.
- [55] S.N. Voormeeren, D.J. Rixen, A Dual Approach to Substructure Decoupling Techniques, in: *Proceedings of the 28th International Modal Analysis Conference*, 2010.
- [56] W. D'Ambrogio, A. Fregolent, Direct Decoupling of Substructures Using Primal and Dual Formulation, in: *Proceedings of the 29th International Modal Analysis Conference*, 2011.
- [57] F.C. Batista, N.M.M. Maia, Uncoupling Techniques for the Dynamic Characterization of Sub-Structures, in: *Proceedings of the 29th International Modal Analysis Conference*, 2011.
- [58] W. D'Ambrogio, A. Fregolent, Inverse Dynamic Substructuring Using Direct Hybrid Assembly in the Frequency Domain, *Mechanical Systems and Signal Processing*, 45 (2) (2014) 360-377.
- [59] M. Law, H. Rentzsch, S. Ihlenfeldt, M. Putz, Application of Substructure Decoupling Techniques to Predict Mobile Machine Tool Dynamics: Numerical Investigations, *Procedia CIRP*, 46 (2016) 537-540.
- [60] M. Law, H. Rentzsch, S. Ihlenfeldt, Predicting Mobile Machine Tool Dynamics by Experimental Dynamic Substructuring, *International Journal of Machine Tools and Manufacture*, 108 (2016) 127-134.

- [61] J. Brunetti, A. Culla, W. D'Ambrogio, A. Fregolent, Experimental Dynamic Substructuring of the Ampair Wind Turbine Test Bed, in: Proceedings of the 32nd International Modal Analysis Conference, 2014.
- [62] W. D'Ambrogio, A. Fregolent, Predicting the Dynamics of Flexible Space Payloads under Different Boundary Conditions through Substructure Decoupling, in: Proceedings of the 35th International Modal Analysis Conference, 2017.
- [63] J.P. Noël, G. Kerschen, 10 Years of Advances in Nonlinear System Identification in Structural Dynamics: A Review, in: Proceedings of ISMA 2016 - International Conference on Noise and Vibration Engineering, Leuven, Belgium, 2016.
- [64] M. Tahtalı, H.N. Özgüven, Vibration Analysis of Dynamic Structures Using a New Structural Modification Method, in: Proceedings of the 6th International Machine Design and Production Conference, METU, Ankara, pp. 511-520, September 21-23, 1994.
- [65] W. Heylen, S. Lammens, FRAC: A Consistent Way of Comparing Frequency Response Functions, in: Proceedings of the International Conference on Identification in Engineering, Swansea, pp. 48-57, 1996.
- [66] Ö. Arslan, M. Aykan, H.N. Özgüven, Parametric Identification of Structural Nonlinearities from Measured Frequency Response Data, *Mechanical Systems and Signal Processing*, 25 (4) (2011) 1112-1125.
- [67] A. Gelb, W.E. Van der Velde, *Multiple-Input Describing Functions and Nonlinear System Design*, McGraw Hill, New York, 1968.

- [68] E. Budak, H.N. Özgüven, Iterative Receptance Method for Determining Harmonic Response of Structures with Symmetrical Non-linearities, *Mechanical Systems and Signal Processing*, 7 (1) (1993) 75-87.
- [69] Ö. Tanrikulu, B. Kuran, H.N. Özgüven, M. İmregün, Forced Harmonic Response Analysis of Non-Linear Structures Using Describing Functions, *AIAA Journal*, 31 (7) (1993) 1313-1320.
- [70] E. Ciğeroğlu, H.N. Özgüven, Non-linear Vibration Analysis of Bladed Disks with Dry Friction Dampers, *Journal of Sound and Vibration*, 295 (2006) 1028-1043.
- [71] J. He, D. J. Ewins, A Simple Method of Interpretation for the Modal Analysis of Nonlinear Systems, 5th International Modal Analysis Conference, London, England, 626-634, 1987.
- [72] S. Perinpanayagam, D. Robb, D.J. Ewins, J.M. Barragan, Nonlinearities in an Aero-engine Structure: From Test to Design, 2004 International Conference on Modal Analysis Noise and Vibration Engineering, Leuven, Belgium, 3167–3182, 2004.
- [73] T. Kalaycıoğlu, H.N. Özgüven, Dynamic Decoupling of Nonlinear Systems, in: *Dynamics of Coupled Structures*, vol. 4, Proceedings of the 35th IMAC, A Conference on Structural Dynamics, Springer, New York, 2017, pp 199-203, [https://doi.org/10.1007/978-3-319-54930-9\\_17](https://doi.org/10.1007/978-3-319-54930-9_17).
- [74] T. Kalaycıoğlu, H.N. Özgüven, FRF Decoupling of Nonlinear Systems, *Mechanical Systems and Signal Processing*, 102 (2018) 230-244, <https://doi.org/10.1016/j.ymssp.2017.09.029>.



- [75] M.N. Richardson, D.L. Formenti, Parameter Estimation from Frequency Response Measurements Using Rational Fraction Polynomials, in: Proceedings of the 1st International Modal Analysis Conference, 1982.
- [76] J.V. Ferreira, Dynamic Response Analysis of Structures with Nonlinear Components, Ph.D. Thesis, Department of Mechanical Engineering, Imperial College London, 1998.
- [77] H.R.E. Siller, Non-linear Modal Analysis Methods for Engineering Structures, Ph.D. Thesis, Department of Mechanical Engineering, Imperial College London, 2004.
- [78] Q. Jing, T. Mukherjee, G. K. Fedder, Large-Deflection Beam Model for Schematic-Based Behavioral Simulation in NODAS, in Nanotech: Technical Proceedings of the 5th International Conference on Modeling and Simulation of Microsystems (MSM -02), vol. 1. San Juan, Puerto Rico: NSTI, Apr. 22-25 2002, pp. 136-139.
- [79] <https://www.bksv.com/-/media/literature/Product-Data/bp1841.ashx>, visited on August 2017.
- [80] <https://www.bksv.com/-/media/literature/Product-Data/bp2080.ashx>, visited on August 2017.
- [81] MATLAB R2013a Help Manual.
- [82] M. Aykan, Identification of Localized Nonlinearity for Dynamic Analysis of Structures, Ph.D. Thesis, Department of Mechanical Engineering, Middle East Technical University, 2013.

- [83] M. Aykan, H.N. Özgüven, Parametric Identification of Nonlinearity in Structural Systems Using Describing Function Inversion, *Mechanical Systems and Signal Processing*, 40 (1) (2013) 356-376.
- [84] G.D. Pasquale, A. Somà, Reliability Testing Procedure for MEMS IMUs Applied to Vibrating Environments, Department of Mechanics, Politecnico di Torino, Torino, Italy, 2010.
- [85] A.K. Mallik, V. Kher, M. Puri, H. Hatwal, On the Modelling of Non-Linear Elastomeric Vibration Isolators, *Journal of Sound and Vibration* 219 (2) (1999) 239-253.
- [86] M.R. Ashory, High Quality Modal Testing Methods, Ph.D. Thesis, Department of Mechanical Engineering, Imperial College London, London, England, 1999 (<http://www.imperial.ac.uk/dynamics/phd-theses/>).
- [87] [http://sdsolutions.ru/d/546908/d/fiche\\_technique\\_825.pdf](http://sdsolutions.ru/d/546908/d/fiche_technique_825.pdf), visited on March 2018.

## APPENDICES

### A. PUBLISHED PAPERS DURING PHD

#### New FRF Based Methods for Substructure Decoupling

Taner Kalaycıoğlu<sup>1,2</sup>, H. Nevzat Özgüven<sup>1</sup>

<sup>1</sup>Department of Mechanical Engineering, Middle East Technical University, 06800 Ankara, TURKEY

<sup>2</sup>MGEO Sector, ASELSAN Inc., 06011 Ankara, TURKEY

e-mail: tkalayci@aselsan.com.tr, ozguven@metu.edu.tr

#### ABSTRACT

Substructuring methods are well known and are widely used in predicting dynamics of coupled structures. In theory, there is no reason why the same techniques could not be used in a reverse problem of predicting the dynamic behavior of a particular substructure from the knowledge of the dynamics of the coupled structure and of all the other substructures. However, the reverse problem, known as decoupling, usually requires matrix inversions, and therefore even small measurement errors may easily affect the accuracy of such methods. In this study two new FRF based approaches are presented for decoupling. The methods proposed require coupled system FRFs at coordinates that belong to the known subsystem as well as the measured or calculated FRFs of the known subsystem alone. Formulations are based on the reverse application of the structural coupling method proposed in a previous publication co-authored by one of the authors of this paper. The performances of the proposed methods are demonstrated and then compared with those of some well-known recent methods in the literature through a case study.

**Keywords:** Decoupling, uncoupling, inverse substructuring, subsystem identification, subsystem subtraction

#### 1 INTRODUCTION

The modal analysis and testing is widely used to analyze the dynamic characteristics of a whole machine or its components [1]. Since engineering structures are generally designed as an assembly of several components, a lot of effort has been devoted to structural coupling methods that predict the total dynamic behavior of a complex machine from those of its components in recent decades. Conversely, in some cases, the dynamic characteristics of a whole system may be known but that of its component may be hard to measure because of the difficulty of performing measurements or excitation on a subsystem individually under its normal operating conditions.

In this study, the decoupling problem, the identification of the dynamic behavior of a structural subsystem that is part of a larger system is addressed. One of the earliest studies on the substructure decoupling is performed by Okubo and Miyazaki [2] in 1986. In their solution, FRFs of the complete system and the known subsystem is used to obtain FRF of the unknown subsystem. After a long break, Gontier and Bensaibi [3] presented a decoupling technique based on time domain approach which still remains as the only technique in time domain. Silva et al. [4] presented a study regarding joint identification. They used decoupling methodology in order to eliminate difficulties in measurement and experimenting for joint identification. Later, they proposed a different technique for joint identification [5]. In this technique, they used coupling formulation of Jetmundsen et al. [6] and obtained a better formulation in terms of the number of matrix inversions. In this formulation, joint (i.e. connection) degrees of freedom (DoFs) are not taken into account. Ind and Ewins [7] presented an approach similar to that of Silva et al. [5]. Kalling et al. [8] studied the decoupling problem by performing state-space model identification. D'Ambrogio and Fregolent [9] presented a modal based approach for decoupling analyses which suffers from modal truncation problems.

D'Ambrogio and Fregolent [10] presented an FRF based decoupling technique similar to that of Okubo and Miyazaki [2]. In this work, they pointed out the problems due to unmeasured rotational DoFs as well. Afterwards, D'Ambrogio and Fregolent [11] proposed two decoupling procedures; namely, impedance based and mobility based approaches, which calculate the FRFs of the connection DoF on an unknown subsystem by using the FRFs of the coupled system and the residual subsystem

---

\* T. Kalaycıoğlu, H.N. Özgüven, New FRF Based Methods for Substructure Decoupling, in: Dynamics of Coupled Structures, vol. 4, Proceedings of the 34th IMAC, A Conference on Structural Dynamics, Springer, New York, 2016, pp. 463-472, [https://doi.org/10.1007/978-3-319-29763-7\\_46](https://doi.org/10.1007/978-3-319-29763-7_46).

at residual subsystem DoFs. The latter is equivalent to the approach presented by Sjövall and Abrahamsson [12]. A general framework for dynamic substructuring is provided in [13] and [14] in which the so called dual domain decomposition technique that allows retaining the full set of global DoFs by ensuring equilibrium at the interface between substructures is introduced. When performing substructuring by using the dual domain decomposition, the coupling problem can be directly formulated from [14], whereas a similar formulation for the decoupling problem is developed and discussed in [15] for collocated approach where DoFs used to enforce equilibrium are the same as DoFs used to enforce compatibility, and in [16] and [17] for non-collocated approach where DoFs used to enforce equilibrium are not the same as DoFs used to enforce compatibility.

Batista and Maia [18] proposed three different decoupling formulations based on the classical decoupling procedure of Jetmundsen et al. [6]. They consider the effects of including different sets of DoF of the coupled system: (i) exclusion of connection DoFs, (ii) inclusion of connection DoFs only and (iii) inclusion of connection DoFs and internal DoFs of the residual subsystem. Cloutier and Avitabile [19] presented inverse frequency based substructuring approach that requires measurements on the unknown substructure. Later, D'Ambrogio and Fregolent [20] proposed the so called hybrid assembly approach. They compared dual [15] and hybrid assembly approaches through an experimental case study and ended up with very similar results in terms of predicted FRFs of the unknown subsystem.

In this paper, two new FRF based decoupling approaches are developed which are based on the structural modification method suggested by Tahtalı and Özgüven [21] two decades ago. The approaches developed can predict the FRFs of an unknown subsystem from the measured FRFs of the coupled system and the measured or calculated FRFs of the other subsystem. The methods are tested on a simple lumped parameter system by using simulated experimental data. Results are compared with those obtained through some well-known decoupling methods.

## 2 THEORY

In this section, the theory of the decoupling approaches proposed is given. In this approach, the structural modification method suggested by Tahtalı and Özgüven [21] is revisited and modified to be used for substructure decoupling. The notation used throughout the paper for all systems/subsystems and the coordinate sets are given in Fig. 1.

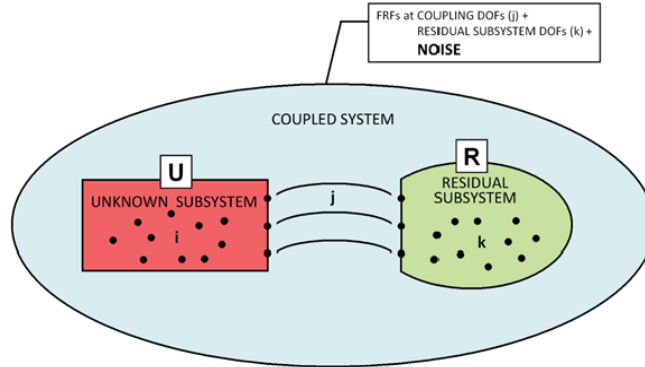


Fig. 1 Notation used for systems and sets of coordinates

Here, first, the basic equations of the Coupling Force Method suggested by Tahtalı and Özgüven [21] will be given. The displacement vectors for the unknown and the residual subsystems can be written, respectively, as:

$$\begin{Bmatrix} \mathbf{X}_i^U \\ \mathbf{X}_j^U \end{Bmatrix} = \begin{pmatrix} \mathbf{H}_{ii}^U & \mathbf{H}_{ij}^U \\ \mathbf{H}_{ji}^U & \mathbf{H}_{jj}^U \end{pmatrix} \begin{Bmatrix} \mathbf{F}_i^U \\ \mathbf{F}_j^U + \mathbf{f} \end{Bmatrix} \quad (1)$$

$$\begin{Bmatrix} \mathbf{X}_j^R \\ \mathbf{X}_k^R \end{Bmatrix} = \begin{pmatrix} \mathbf{H}_{jj}^R & \mathbf{H}_{jk}^R \\ \mathbf{H}_{kj}^R & \mathbf{H}_{kk}^R \end{pmatrix} \begin{Bmatrix} -\mathbf{f} \\ \mathbf{F}_k^R \end{Bmatrix} \quad (2)$$

where superscripts U and R refer to the vectors related to the unknown and the residual subsystems, respectively. Subscript i refers to the coordinates of the unknown subsystem only, subscript j refers to the coordinates that are common to the unknown and residual subsystem, and finally subscript k refers to the coordinates of the residual subsystem only (Fig. 1). Here,  $\mathbf{f}$ ,  $\mathbf{F}$  and  $\mathbf{H}$  represent coupling reaction force vector, external force vector and the FRF matrix, respectively. Expanding Eq. (1) and (2) leads to following equations:

$$\mathbf{X}_i^U = \mathbf{H}_{ii}^U \mathbf{F}_i^U - \mathbf{H}_{ij}^U (\mathbf{F}_j^U + \mathbf{f}) \quad (3)$$

$$\mathbf{X}_j^U = \mathbf{H}_{jj}^U \mathbf{F}_j^U + \mathbf{H}_{ij}^U (\mathbf{F}_i^U + \mathbf{f}) \quad (4)$$

$$\mathbf{X}_j^R = -\mathbf{H}_{jj}^R \mathbf{f} + \mathbf{H}_{jk}^R \mathbf{F}_k^R \quad (5)$$

$$\mathbf{X}_k^R = -\mathbf{H}_{kj}^R \mathbf{f} + \mathbf{H}_{kk}^R \mathbf{F}_k^R \quad (6)$$

Note that, when two subsystems are rigidly coupled,  $\mathbf{X}_j^U = \mathbf{X}_j^R$ , which represents the displacement vector at the coupling coordinates. Therefore Eq. (4) and Eq. (5) are equal to each other. Thus, by equating the right hand sides of these equations coupling reaction force can be written as follows:

$$\mathbf{f} = \left[ \mathbf{H}_{jj}^U + \mathbf{H}_{jj}^R \right]^{-1} \left[ \mathbf{H}_{jk}^R \mathbf{F}_k^R - \mathbf{H}_{ji}^U \mathbf{F}_i^U - \mathbf{H}_{jj}^U \mathbf{F}_j^U \right] \quad (7)$$

After having obtained the coupling reaction force  $\mathbf{f}$ , the response of the coupled system can be obtained by substituting  $\mathbf{f}$  in equations (3), (5) and (6) as follows:

$$\mathbf{X}_i^U = \mathbf{H}_{ii}^U \mathbf{F}_i^U + \mathbf{H}_{ij}^U \left( \mathbf{F}_j^U + \left[ \mathbf{H}_{jj}^U + \mathbf{H}_{jj}^R \right]^{-1} \left[ \mathbf{H}_{jk}^R \mathbf{F}_k^R - \mathbf{H}_{ji}^U \mathbf{F}_i^U - \mathbf{H}_{jj}^U \mathbf{F}_j^U \right] \right) \quad (8)$$

$$\mathbf{X}_j^R = -\mathbf{H}_{jj}^R \left[ \mathbf{H}_{jj}^U + \mathbf{H}_{jj}^R \right]^{-1} \left[ \mathbf{H}_{jk}^R \mathbf{F}_k^R - \mathbf{H}_{ji}^U \mathbf{F}_i^U - \mathbf{H}_{jj}^U \mathbf{F}_j^U \right] + \mathbf{H}_{jk}^R \mathbf{F}_k^R \quad (9)$$

$$\mathbf{X}_k^R = -\mathbf{H}_{kj}^R \left[ \mathbf{H}_{jj}^U + \mathbf{H}_{jj}^R \right]^{-1} \left[ \mathbf{H}_{jk}^R \mathbf{F}_k^R - \mathbf{H}_{ji}^U \mathbf{F}_i^U - \mathbf{H}_{jj}^U \mathbf{F}_j^U \right] + \mathbf{H}_{kk}^R \mathbf{F}_k^R \quad (10)$$

Note that the response of the coupled system can also be written as follows:

$$\begin{pmatrix} \mathbf{X}_i^U \\ \mathbf{X}_j^R \\ \mathbf{X}_k^R \end{pmatrix} = \begin{pmatrix} \mathbf{H}_{ii} & \mathbf{H}_{ij} & \mathbf{H}_{ik} \\ \mathbf{H}_{ji} & \mathbf{H}_{jj} & \mathbf{H}_{jk} \\ \mathbf{H}_{ki} & \mathbf{H}_{kj} & \mathbf{H}_{kk} \end{pmatrix} \begin{pmatrix} \mathbf{F}_i^U \\ \mathbf{F}_j^U \\ \mathbf{F}_k^R \end{pmatrix} \quad (11)$$

The above formulation gives the basic equations of the Coupling Force Method proposed by Tahtalı and Özgüven [21]. From now on, formulation to be given will be about the derivation of decoupling formulations. In the following section the use of these equations for decoupling will be given.

## 2.1 Formulation Using Equation (9)

Let us assume that external forcing is applied only to the  $k^{\text{th}}$  coordinates of the coupled system and the rest of the external forcing is equal to zero;

$$\begin{pmatrix} \mathbf{F}_i^U \\ \mathbf{F}_j^U \\ \mathbf{F}_k^R \end{pmatrix} = \begin{pmatrix} \mathbf{0}_{i \times l} \\ \mathbf{0}_{j \times l} \\ \mathbf{F}_{k \times l} \end{pmatrix} \quad (12)$$

By using Eq. (11) and Eq. (12), Eq. (9) can be rewritten as follows:

$$\mathbf{H}_{jk} \mathbf{F}_{k \neq j} = -\mathbf{H}_{jj}^R \left( \mathbf{H}_{jj}^U + \mathbf{H}_{jj}^R \right)^{-1} \mathbf{H}_{jk}^R \mathbf{F}_{k \neq j} + \mathbf{H}_{jk}^R \mathbf{F}_{k \neq j} \quad (13)$$

By multiplying both sides of Eq. (13) with  $(\mathbf{F}_{k \neq j})^{-1}$  from right hand side, one can obtain

$$\mathbf{H}_{jk}^R - \mathbf{H}_{jk} - \mathbf{H}_{jj}^R \left( \mathbf{H}_{jj}^U + \mathbf{H}_{jj}^R \right)^{-1} \mathbf{H}_{jk}^R \quad (14)$$

Premultiplying all terms of Eq. (14) by  $(\mathbf{H}_{jj}^R)^{-1}$  and post multiplying them by  $(\mathbf{H}_{jk}^R)^{-1}$  yields

$$\left( \mathbf{H}_{jj}^R \right)^{-1} \left( \mathbf{H}_{jk}^R - \mathbf{H}_{jk} \right) \left( \mathbf{H}_{jk}^R \right)^{-1} = \left( \mathbf{H}_{jj}^U + \mathbf{H}_{jj}^R \right)^{-1} \quad (15)$$

Taking inverse of the both sides of Eq. (15), the following equation can be written:

$$\mathbf{H}_{jk}^R \left( \mathbf{H}_{jk}^R - \mathbf{H}_{jk} \right)^{-1} \mathbf{H}_{jj}^R = \mathbf{H}_{jj}^U + \mathbf{H}_{jj}^R \quad (16)$$

Rearranging Eq. (16) yields the final equation which gives the FRF matrix of the unknown subsystems in terms of those of coupled system and residual subsystem:

$$\mathbf{H}_{jj}^U = \mathbf{H}_{jk}^R \left( \mathbf{H}_{jk}^R - \mathbf{H}_{jk} \right)^{-1} \mathbf{H}_{jj}^R - \mathbf{H}_{jj}^R \quad (17)$$

It is interesting to note that if it is assumed that external forcing is applied only to the  $j^{\text{th}}$  coordinates of the coupled system while the rest of the external forces are zero, that is

$$\begin{pmatrix} \mathbf{F}_i^U \\ \mathbf{F}_j^U \\ \mathbf{F}_k^R \end{pmatrix} = \begin{pmatrix} \mathbf{0}_{i \neq j} \\ \mathbf{F}_{j \neq j} \\ \mathbf{0}_{k \neq j} \end{pmatrix} \quad (18)$$

one will end up with the decoupling formulation given by Batista and Maia [18]:

$$\mathbf{H}_{jj}^U = \mathbf{H}_{jj}^R \left( \left( \mathbf{H}_{jj}^R \right)^{-1} \mathbf{H}_{jj}^R - \mathbf{I}_{j \neq j} \right)^{-1} \quad (19)$$

## 2.2 Formulation Using Equation (10)

Let us assume again that external forcing is applied only to the  $j^{\text{th}}$  coordinates of the coupled system and the rest of the external forces are zero as given in Eq. (18), and let us use Eq. (10) rather than Eq. (9). Then by using Eq. (11) and Eq. (18), one can rewrite Eq. (10) as follows:

$$\mathbf{H}_{kj} \mathbf{F}_{j \neq j} = \mathbf{H}_{kj}^R \left( \mathbf{H}_{jj}^U + \mathbf{H}_{jj}^R \right)^{-1} \mathbf{H}_{jj}^U \mathbf{F}_{j \neq j} \quad (20)$$

By multiplying both sides of Eq. (20) with  $(\mathbf{F}_{j \neq j})^{-1}$  from right hand side, one can obtain:

$$\mathbf{H}_{kj} - \mathbf{H}_{kj}^R \left( \mathbf{H}_{jj}^U + \mathbf{H}_{jj}^R \right)^{-1} \mathbf{H}_{jj}^U \quad (21)$$

Premultiplying all terms of Eq. (21) by  $(\mathbf{H}_{kj}^R)^{-1}$  and post multiplying them by  $(\mathbf{H}_{jj}^U)^{-1}$  gives

$$\left( \mathbf{H}_{kj}^R \right)^{-1} \mathbf{H}_{kj} \left( \mathbf{H}_{jj}^U \right)^{-1} = \left( \mathbf{H}_{jj}^U + \mathbf{H}_{jj}^R \right)^{-1} \quad (22)$$

Taking inverse of both sides of Eq. (22), the following equation can be obtained

$$\mathbf{H}_{jj}^U (\mathbf{H}_{kj})^{-1} \mathbf{H}_{kj}^R = \mathbf{H}_{jj}^U + \mathbf{H}_{jj}^R \quad (23)$$

Then, the final equation which gives the FRF matrix of the unknown subsystems in terms of those of coupled system and residual subsystem can be obtained as follows:

$$\mathbf{H}_{jj}^U = \mathbf{H}_{jj}^R \left( (\mathbf{H}_{kj})^{-1} \mathbf{H}_{kj}^R - \mathbf{I}_{j \times j} \right)^{-1} \quad (24)$$

Again it is interesting to note that if it is assumed that external forcing is applied only to the  $k^{\text{th}}$  coordinates of the coupled system as shown in Eq. (12), the formulation given by Maia et al. [5] can be easily obtained:

$$\mathbf{H}_{jj}^U = \mathbf{H}_{jk}^R \left( \mathbf{H}_{kk}^R - \mathbf{H}_{kk} \right)^{-1} \mathbf{H}_{kj}^R - \mathbf{H}_{jj}^R \quad (25)$$

### 3 CASE STUDIES

In this section, application of the proposed decoupling formulations to a lumped parameter system is presented. Furthermore, performances of the proposed formulations are compared with those of some well-known techniques by using the same case study.

#### 3.1 Application of the Approaches to a Lumped Parameter System

The coupled system considered in this application is composed of two subsystems rigidly connected to each other as shown in Fig. 2. Physical parameters of the residual and the unknown subsystem are given in Table 1. Note that  $\mathbf{k}$ ,  $\mathbf{m}$  and  $\mathbf{c}$  represent stiffness, mass and viscous damping parameters, respectively.

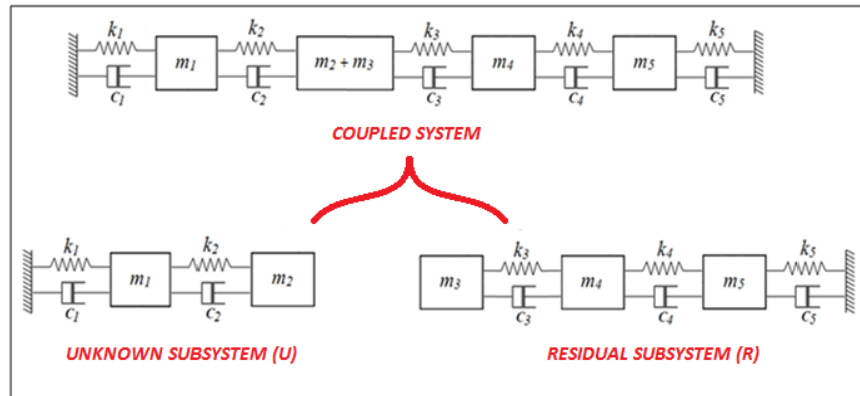


Fig. 2 Lumped parameter system model

Table 1 Physical parameters

Element Number ( $i$ )	$m_i$ [kg]	$k_i$ [N/m]	$c_i$ [Ns/m]
1	2.5	1500	0.15
2	3	2000	0.20
3	2	2100	0.21
4	3	1900	0.19
5	2.5	2200	0.22

Here, it is assumed that the FRFs of the coupled system are experimentally measured and the physical model of the residual subsystem is available. It is aimed to determine the FRF of the unknown subsystem at its connection coordinate. In order to

simulate the measured FRFs of the coupled system, first the exact FRFs of the coupled system ( $\hat{\mathbf{H}}$ ) are calculated by using the physical parameters given in Table 1 and then they are polluted by simply adding complex random variables as shown below:

$$\mathbf{H}_{ij}(\omega_k) = \hat{\mathbf{H}}(\omega_k) + p_{ij,k} + i q_{ij,k} \quad (26)$$

Here,  $p_{ij,k}$  and  $q_{ij,k}$  are independent random variables with Gaussian distribution, zero mean and a standard deviation of  $5 \times 10^{-5}$  m/N. The effect of such a pollution on the driving point FRF at the 2<sup>nd</sup> DoF (the coupling DoF) of the coupled system is shown in Fig. 3 together with the FRF obtained after curve fitting.

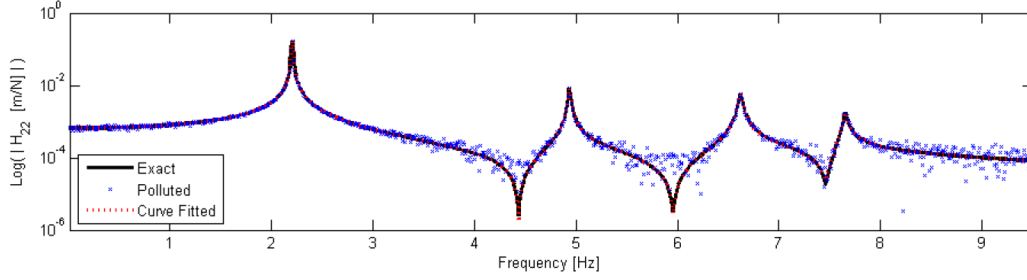


**Fig. 3** Driving point FRF of the coupled system at the 2<sup>nd</sup> DoF: true (—, black), polluted (\*\*\*, blue) and curve fitted (---, red)

Then, by using the curves fitted to the polluted FRFs of the coupled structure, driving point FRF at the coupling DoF of the unknown subsystem is calculated using the proposed formulations, and the results are given in Fig. 4 and Fig. 5.

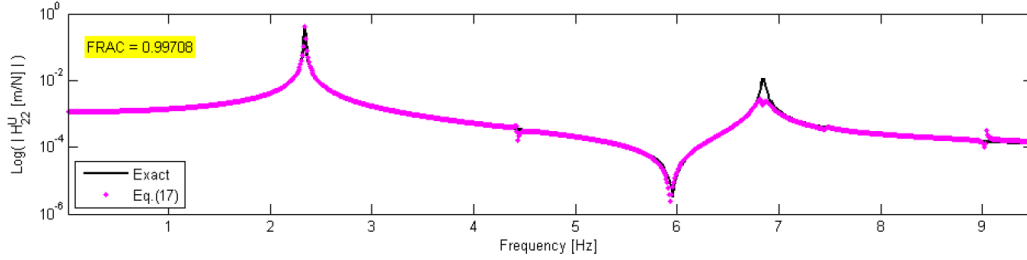


**Fig. 4** Driving point FRF at the 2<sup>nd</sup> DoF of the unknown subsystem: true (—, black), predicted using Eq. (17) (\*\*\*, magenta)

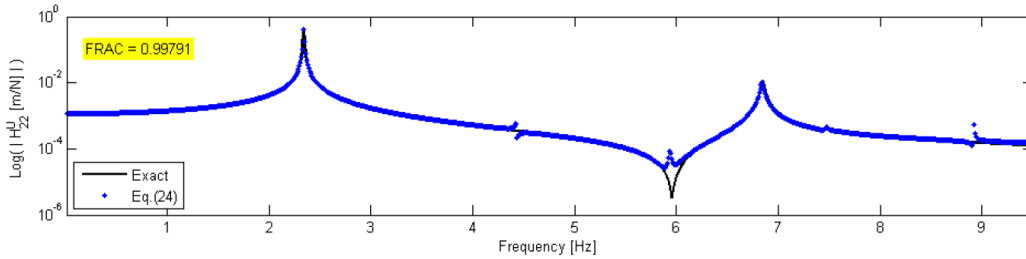


**Fig. 5** Driving point FRF at the 2<sup>nd</sup> DoF of the unknown subsystem: true (—, black), predicted using Eq. (24) (\*\*\*, blue)

Fig. 4 and Fig. 5 show that both approaches predict the unknown subsystem FRF satisfactorily. If the performances of both approaches are compared with each other around resonances, the predicted FRF via Eq. (24) seem to fit better to the true FRF by visual inspection.



However, in order to make a reliable and sound comparison, it is required to use a metric rather than making visual inspection. For that purpose, the Frequency Response Assurance Criterion (FRAC) [22] is used. The FRAC values calculated for FRFs calculated by using Eq. (17) and Eq. (24) are 0.99708 and 0.99791, respectively. So, it can be said again that, at least for the example case given here, both equations can successfully be used for decoupling, and Eq. (24) gives slightly better results compared to Eq. (17).

### 3.2 A Comparison of the Approaches with well-known Existing Methods

In this section, the performances of proposed methods are compared with those of well-known recent methods. The final equations for these methods, their references and the input data required for each of them are summarized in Table 2.

**Table 2** List of most recent decoupling methods

Ref.	Final Equation	Needs (Residual)	Needs (Coupled)	Equation
[18]	$\mathbf{H}_{jj}^U = \mathbf{H}_{jk}^R \mathbf{H}_{kj}^R \left( \mathbf{H}_{jk}^R (\mathbf{H}_{kk}^R - \mathbf{H}_{kk}) \mathbf{H}_{kj}^R \right)^{-1} \mathbf{H}_{jk}^R \mathbf{H}_{kj}^R - \mathbf{H}_{jj}^R$	$\begin{pmatrix} \mathbf{H}_{jj}^R & \mathbf{H}_{jk}^R \\ \mathbf{H}_{kj}^R & \mathbf{H}_{kk}^R \end{pmatrix}$	$\mathbf{H}_{kk}$	(27)
[18]	$\mathbf{H}_{jj}^U = \left( \mathbf{H}_{jj}^R (\mathbf{H}_{jj}^R - \mathbf{H}_{jj}) \right)^{-1} \mathbf{I}_{jj} \mathbf{H}_{jj}^R$	$\mathbf{H}_{jj}^R$	$\mathbf{H}_{jj}$	(28)
[18]	$\mathbf{H}_{jj}^U = \mathbf{H}_{jj}^R \mathbf{H}_{jj}^R \left( \mathbf{H}_{jk}^R (\mathbf{H}_{kj}^R - \mathbf{H}_{kj}) \mathbf{H}_{jj}^R \right)^{-1} \mathbf{H}_{jk}^R \mathbf{H}_{kj}^R - \mathbf{H}_{jj}^R$	$\begin{pmatrix} \mathbf{H}_{jj}^R & \mathbf{H}_{jk}^R \\ \mathbf{H}_{kj}^R & \mathbf{H}_{kk}^R \end{pmatrix}$	$\mathbf{H}_{kj}$	(29)
[5]	$\mathbf{H}_{jj}^U = \mathbf{H}_{jk}^R (\mathbf{H}_{kk}^R - \mathbf{H}_{kk})^{-1} \mathbf{H}_{kj}^R - \mathbf{H}_{jj}^R$	$\begin{pmatrix} \mathbf{H}_{jj}^R & \mathbf{H}_{jk}^R \\ \mathbf{H}_{kj}^R & \mathbf{H}_{kk}^R \end{pmatrix}$	$\mathbf{H}_{kk}$	(30)
[2]	$\mathbf{H}_{jj}^U = \left( \mathbf{I} - \mathbf{H}_{jj} [\mathbf{H}_{jj}^R]^{-1} \right)^{-1} \mathbf{H}_{jj}$	$\mathbf{H}_{jj}^R$	$\mathbf{H}_{jj}$	(31)
[11]	$\mathbf{H}_{jj}^U = \begin{pmatrix} \mathbf{I} - \mathbf{H}_{jj} \mathbf{Z}_{jj}^R - \mathbf{H}_{jk} \mathbf{Z}_{kj}^R \\ -\mathbf{H}_{kj} \mathbf{Z}_{jj}^R - \mathbf{H}_{kk} \mathbf{Z}_{kj}^R \end{pmatrix}^+ \begin{pmatrix} \mathbf{H}_{jj} \\ \mathbf{H}_{kj} \end{pmatrix}$	$\begin{pmatrix} \mathbf{Z}_{jj}^R \\ \mathbf{Z}_{kj}^R \end{pmatrix}$	$\begin{pmatrix} \mathbf{H}_{jj} & \mathbf{H}_{jk} \\ \mathbf{H}_{kj} & \mathbf{H}_{kk} \end{pmatrix}$	(32)
[11]	$\mathbf{H}_{jj}^U = \begin{pmatrix} \mathbf{H}_{jj} \\ \mathbf{H}_{jk} \end{pmatrix}^T \left( \begin{pmatrix} \mathbf{I}_{jj} & \mathbf{0}_{jk} \\ \mathbf{H}_{kj}^R & \mathbf{H}_{kk}^R - \mathbf{H}_{kk} \end{pmatrix}^{-1} \begin{pmatrix} \mathbf{H}_{jj} & \mathbf{H}_{jk} - \mathbf{H}_{jk}^R \\ \mathbf{H}_{kj} & \mathbf{H}_{kk} - \mathbf{H}_{kk}^R \end{pmatrix} \right)^+$	$\begin{pmatrix} \mathbf{H}_{jj}^R & \mathbf{H}_{jk}^R \\ \mathbf{H}_{kj}^R & \mathbf{H}_{kk}^R \end{pmatrix}$	$\begin{pmatrix} \mathbf{H}_{jj} & \mathbf{H}_{jk} \\ \mathbf{H}_{kj} & \mathbf{H}_{kk} \end{pmatrix}$	(33)
[15]	$\mathbf{H}^U = \begin{pmatrix} \mathbf{H} & \mathbf{0} \\ \mathbf{0} & -\mathbf{H}^R \end{pmatrix} - \begin{pmatrix} \mathbf{H} & \mathbf{0} \\ \mathbf{0} & -\mathbf{H}^R \end{pmatrix} \begin{pmatrix} \mathbf{B}^T \\ (\mathbf{B}^R)^T \end{pmatrix} \dots$ $\left( \begin{pmatrix} \mathbf{B} & \mathbf{B}^R \end{pmatrix} \begin{pmatrix} \mathbf{H} & \mathbf{0} \\ \mathbf{0} & -\mathbf{H}^R \end{pmatrix} \begin{pmatrix} \mathbf{B}^T \\ (\mathbf{B}^R)^T \end{pmatrix} \right)^{-1} \begin{pmatrix} \mathbf{B} & \mathbf{B}^R \end{pmatrix} \begin{pmatrix} \mathbf{H} & \mathbf{0} \\ \mathbf{0} & -\mathbf{H}^R \end{pmatrix}$	$\begin{pmatrix} \mathbf{H}_{jj}^R & \mathbf{H}_{jk}^R \\ \mathbf{H}_{kj}^R & \mathbf{H}_{kk}^R \end{pmatrix}$	$\begin{pmatrix} \mathbf{H}_{jj} & \mathbf{H}_{jk} \\ \mathbf{H}_{kj} & \mathbf{H}_{kk} \end{pmatrix}$	(34)

Among the first three formulations given in the table, Eq. (28) was shown to be the one that produces the smallest error throughout the frequency range [18]. Moreover, among the last three formulations given in the table, Eq. (34) was shown to give better results [15]. Note also that Eq. (31) is a special case of the Eq. (32) as also mentioned in reference [11]. Consequently, it will be more to the point to compare the proposed formulations with Eq. (28), Eq. (30) and Eq. (34) in Table 2.

So, the problem given in Section 3.1 is also solved by using Eq. (28), Eq. (30) and Eq. (34) in addition to employing the proposed formulations, i.e., Eq. (23) and Eq. (24). Moreover in order to see the effect of increasing noise level in measured

FRFs on the performances of different methods, coupled system FRFs are polluted by five different sets of random variables,  $p_{ij,k}$  and  $q_{ij,k}$  in Eq. (26), with Gaussian distribution, zero mean and standard deviations ranging from  $5 \times 10^{-5}$  m/N to  $25 \times 10^{-5}$  m/N. Results obtained for the standard deviation of  $15 \times 10^{-5}$  m/N are given in Fig. 6.

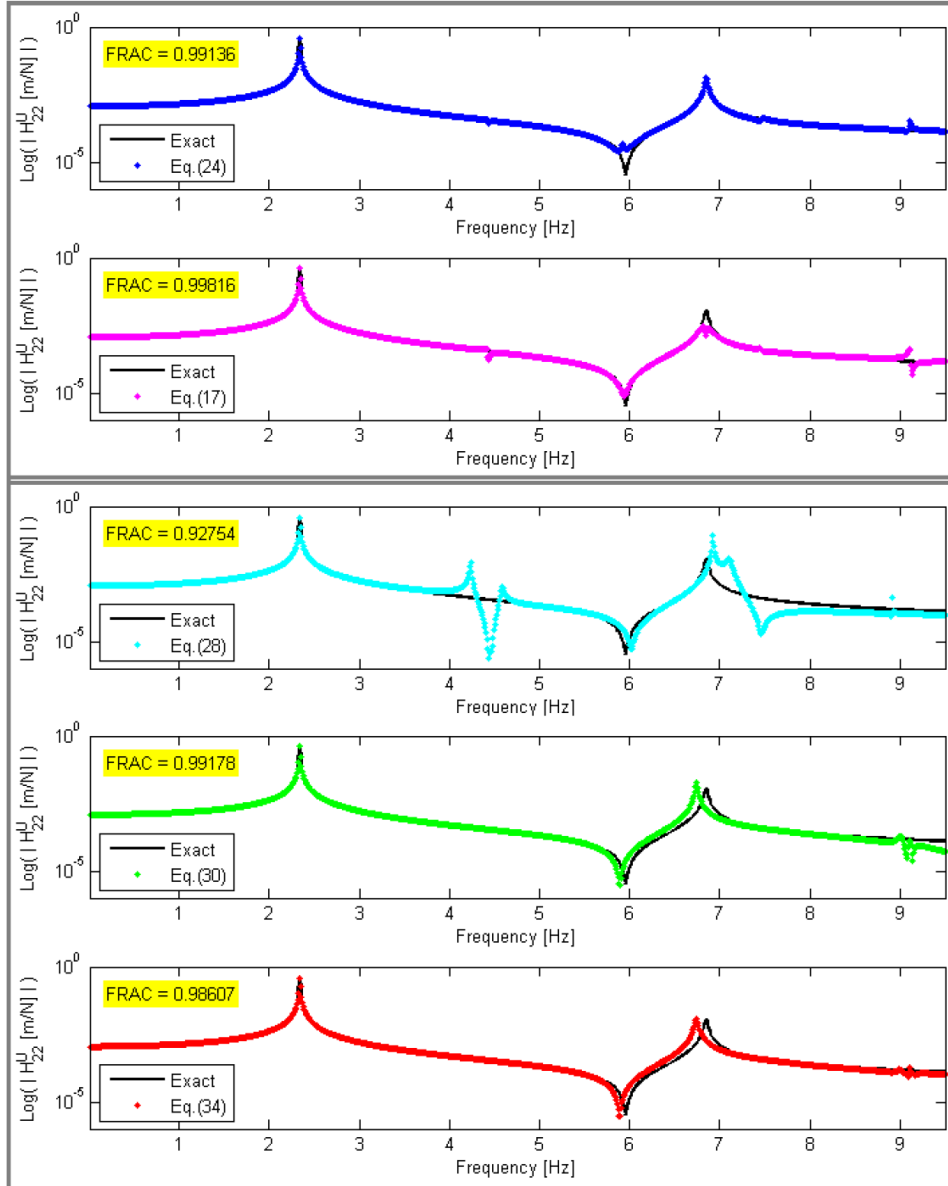


**Fig. 6** Driving point FRF at the 2<sup>nd</sup> DoF of the unknown subsystem: true (—, black), predicted using standard deviation of  $15 \times 10^{-5}$  via proposed formulations: Eq. (24) (—, blue), Eq. (17) (—, magenta) and via formulations given in literature: Eq. (28) (—, cyan), Eq. (30) (—, green), Eq. (34) (—, red)

It is observed that using different pollution sets with the same standard deviation may give slightly different results. Therefore, in order to compare the performances of different formulations and to study the effect of increasing measurement errors (increasing standard deviation of pollution), calculations with each method are repeated 100 times for each standard deviation of pollution, and the averages of the FRAC values are compared in Table 3.

**Table 3** Mean (M) and Standard Deviation (SD) of FRAC values obtained for each method

Method	FRAC Values (M $\pm$ SD values calculated for 100 runs)				
	SD of $5 \times 10^{-5}$ m/N	SD of $1 \times 10^{-4}$ m/N	SD of $15 \times 10^{-5}$ m/N	SD of $2 \times 10^{-4}$ m/N	SD of $25 \times 10^{-5}$ m/N
Eq. (24)	0.9979 $\pm$ 0.0019	0.9970 $\pm$ 0.0024	0.9900 $\pm$ 0.0234	0.9869 $\pm$ 0.0107	0.9792 $\pm$ 0.0184
Eq. (17)	0.9948 $\pm$ 0.0218	0.9947 $\pm$ 0.0077	0.9912 $\pm$ 0.0096	0.9796 $\pm$ 0.0189	0.9744 $\pm$ 0.0238
Eq. (28)	0.9971 $\pm$ 0.0215	0.9759 $\pm$ 0.0274	0.9701 $\pm$ 0.0307	0.9601 $\pm$ 0.0404	0.9522 $\pm$ 0.0639
Eq. (34)	0.9928 $\pm$ 0.0192	0.9794 $\pm$ 0.0358	0.9767 $\pm$ 0.0529	0.9615 $\pm$ 0.1067	0.9778 $\pm$ 0.0340
Eq. (30)	0.9921 $\pm$ 0.0050	0.9859 $\pm$ 0.0183	0.9822 $\pm$ 0.0211	0.9736 $\pm$ 0.0435	0.9696 $\pm$ 0.0562

When mean FRAC values given in the Table 3 are compared to each other, the overall performances of the proposed formulations (i.e., Eq. (24) and Eq. (17)) are found to be better. Especially, Eq. (24) proved to be statistically the best performer among all formulations.

#### 4 DISCUSSION AND CONCLUSIONS

In this paper the decoupling problem, i.e. the prediction of the dynamic behavior of a structural subsystem, starting from information about the remaining subsystems (residual subsystems) and from the known dynamic behavior of the complete system, is considered. The dynamic behavior of the whole structure is assumed to be known from experiments, together with the experimentally measured or theoretically calculated dynamics of the residual substructure.

In this work, two different decoupling formulations derived from the work of Tahtah and Özgüven [21] are presented and thus two new methods are proposed. Both methods give exact results, as it is the case in most of the decoupling methods, when exact FRFs are used in all equations. However, the problem in all of such methods is the sensitivity of the formulations to even very slight errors which are inevitable due to the use of measured data. All formulations usually include matrix inversions, and depending on the nature of the equations, some methods are more sensitive to measurement errors and therefore do not perform well. Hence, it is important to test the performance of any new decoupling technique, and compare its performance with existing best ones. Application of the proposed decoupling formulations is presented on a lumped parameter system. In this case study simulated experimental results are used, and in order to simulate experimentally measured FRFs of the coupled system, theoretically calculated exact FRFs are polluted. In studying the performances of the proposed methods, Frequency Response Assurance Criteria, which shows the correlation between the predicted FRFs and the true FRFs of the unknown subsystem, are used.

Furthermore, performances of the proposed formulations together with some of those available in the literature are investigated through the same case study. Also, effect of noise on the performance of the decoupling methods is examined by polluting the true FRFs of the coupled system using different sets of independent random variables with same mean but gradually increased standard deviations. However, decoupling methods in question do not yield FRAC values in regular trend to the increasing level of noise. Thus, an appropriate statistical comparison becomes essential to establish comparability between the decoupling methods investigated. It is observed from the results of the statistical comparison that proposed methods come up with the most correlated results for each of five standard deviation of pollution.

Consequently, it can be said that proposed methods can be used as alternative approaches results of which should be taken into consideration during decoupling studies. The applicability and accuracy of the methods proposed are demonstrated only on a simple lumped parameter system and additionally they need to be tested on real structures.

## 5 REFERENCES

- [1] Ewins, D.J., "Modal Testing: Theory Practice and Application", Research Studies Press Ltd., Baldock, Hertfordshire, England, 2000.
- [2] Okubo, N., Miyazaki, M., "Development of Uncoupling Technique and Its Application", Proceedings of 4<sup>th</sup> International Modal Analysis Conference, 1986.
- [3] Gontier, C., Bensaïbi, M., "Time Domain Identification of a Substructure from in situ Analysis of the Whole Structure", Mechanical Systems and Signal Processing, Vol. 9, No. 4, pp. 379-396, 1995.
- [4] Silva, J.M.M., Maia, N.M.M., Ribeiro, P.M.L., "Dynamic Modeling: Application of Uncoupling Techniques", Proceedings of the 14<sup>th</sup> International Modal Analysis Conference, 1996.
- [5] Maia, N.M.M., Silva, J.M.M., Ribeiro, A.M.R., Silva, P.L.C., "On the Dynamic Characterization of Joints Using Uncoupling Techniques", Proceedings of the 16<sup>th</sup> International Modal Analysis Conference, 1998.
- [6] Jtmundsen, B., Bielawa, R.L., Flannelly, W.G., "Generalized Frequency Domain Substructuring Synthesis", Journal of American Helicopter Society, Vol. 33, No. 1, pp 55-64, 1988.
- [7] Ind, P.R., Ewins, D.J., "Impedance Based Decoupling and Its Application to Indirect Modal Testing and Component Measurement: A Numerical Investigation", Proceedings of the 21<sup>st</sup> International Modal Analysis Conference, 2003.
- [8] Kalling, P., Abrahamsson, T., McKelvey, T., "Subsystem State-Space Model Identification and its Sensitivity to Test Variability", Proceedings of ISMA 2004 - International Conference on Noise and Vibration Engineering, edited by Sas, P. and De Munck, M., pp. 2729-2744, Leuven (Belgium), Sep. 2004.
- [9] D'Ambrogio, W., Fregolent, A., "Decoupling of a Substructure from Modal Data of the Complete Structure", Proceedings of ISMA 2004 - International Conference on Noise and Vibration Engineering, edited by Sas, P. and De Munck, M., pp. 2693-2706, Leuven (Belgium), Sep. 2004.
- [10] D'Ambrogio, W., Fregolent, A., "Prediction of Substructure Properties Using Decoupling Procedures, Structural Dynamics", Proceedings of Eurodyn 2005 - International Conference on Structural Dynamics, edited by Soize, C. and Schüeller, G., pp. 1893-1898, Paris (France), Sep. 2005.
- [11] D'Ambrogio, W., Fregolent, A., "Promises and Pitfalls of Decoupling Techniques", Proceedings of the 26<sup>th</sup> International Modal Analysis Conference, 2008.
- [12] Sjövall, P., Abrahamsson, T., "Substructure System Identification from Coupled System Test Data", Mechanical Systems and Signal Processing, Vol. 22, No. 1, pp. 15-33, 2008.
- [13] De Klerk, D., Rixen, D.J., and de Jong, J., "Frequency Based Substructuring (FBS) Method Reformulated According to the Dual Domain Decomposition Method" Proceedings of the 24<sup>th</sup> International Modal Analysis Conference, 2006.
- [14] De Klerk, D., Rixen, D.J. and Voormeeren, S., "General Framework for Dynamic Substructuring: History, Review, and Classification of Techniques", AIAA Journal, Vol. 46, No. 5, pp. 1169-1181, 2008.
- [15] D'Ambrogio, W., Fregolent, A., "The Role of Interface DoFs in Decoupling of Substructures based on the Dual Domain Decomposition", Mechanical Systems and Signal Processing, Vol. 24, No. 7, pp. 2035-2048, 2010.
- [16] Voormeeren, S.N., Rixen, D.J., "A Dual Approach to Substructure Decoupling Techniques", Proceedings of the 28<sup>th</sup> International Modal Analysis Conference, 2010.
- [17] D'Ambrogio, W., Fregolent, A., "Direct Decoupling of Substructures Using Primal and Dual Formulation", Proceedings of the 29<sup>th</sup> International Modal Analysis Conference, 2011.
- [18] Batista, F.C., Maia, N.M.M., "Uncoupling Techniques for the Dynamic Characterization of Sub-structures", Proceedings of the 29<sup>th</sup> International Modal Analysis Conference, 2011.
- [19] Cloutier, D., Avitabile, P., "Dynamic Uncoupling of a System Model for Component Identification", Proceedings of the 29<sup>th</sup> International Modal Analysis Conference, 2011.
- [20] D'Ambrogio, W., Fregolent, A., "Inverse Dynamic Substructuring Using Direct Hybrid Assembly in the Frequency Domain", Mechanical Systems and Signal Processing, Vol. 45, No. 2, pp. 360-377, 2014.
- [21] Tahtali, M., Özgüven, H.N., "Vibration Analysis of Dynamic Structures Using a New Structural Modification Method", Proceedings of the 6<sup>th</sup> International Machine Design and Production Conference, METU, Ankara, pp. 511-520, September 21-23, 1994.
- [22] Heylen, W., Lammens, S., "FRAC: A Consistent Way of Comparing Frequency Response Functions", Proceedings of the International Conference on Identification in Engineering, Swansea, pp. 48-57, 1996.

# Dynamic Decoupling of Nonlinear Systems

Taner Kalaycıoğlu<sup>1,2</sup>, H. Nevzat Özgüven<sup>1</sup>

<sup>1</sup>Department of Mechanical Engineering, Middle East Technical University, 06800 Ankara, TURKEY

<sup>2</sup>MGEO Business Sector, ASELSAN Inc., 06011 Ankara, TURKEY

e-mail: tkalayci@aselsan.com.tr, ozguven@metu.edu.tr

## ABSTRACT

Structural decoupling problem has been well investigated for three decades and led to several decoupling methods. In spite of the inherent nonlinearities in a structural system in various forms all decoupling studies are for linear systems. In this study, decoupling problem for nonlinear systems is addressed for the first time and a method is proposed for calculating the frequency response functions of a substructure decoupled from a coupled nonlinear structure where nonlinearity can be modelled as a single nonlinear element. The method proposed is validated through simulated case studies.

**Keywords:** Nonlinear decoupling, nonlinear uncoupling, nonlinear inverse substructuring, nonlinear subsystem identification, nonlinear substructure decoupling

## 1 INTRODUCTION

Since engineering structures are generally designed as an assembly of several components, considerable effort has been devoted to structural decoupling of linear systems, some of those worth mentioning is listed in references [1-3]. However, the problem where system to be decoupled includes a nonlinear element such as clearance, friction and nonlinear stiffness remains untouched. In this paper, a method is developed for the decoupling problem of nonlinear systems. The method is tested on simple lumped parameter systems by using simulated experimental data.

## 2 THEORY

The uncoupling problem is studied as three separate problems, depending on the location of the nonlinear element in the coupled system. The nonlinearity can be either in the unknown subsystem or in the known subsystem, or it can connect two subsystems. The method proposed for the solution of this problem is mainly based on the application of the following techniques:

- ✓ The *controlled displacement amplitude testing* technique proposed by Arslan et al. [4] for nonlinear systems.
- ✓ The decoupling technique proposed by D'Ambrogio et al. [1] for linear systems.
- ✓ The parametric modal identification technique proposed by Arslan et al. [4] for nonlinear systems.

The method proposed is applicable to systems where the nonlinearity can be modelled as a single nonlinear element. It is also assumed that the location of this nonlinear element is known.

### 2.1 Nonlinearity in the Unknown Subsystem

In this case, it is assumed that known subsystem is linear whereas unknown subsystem is nonlinear and the location of the nonlinear element is known. Firstly, the complete FRF matrix of the known subsystem for the coordinates we are interested in is obtained by using the known system parameters. Then, various different sets of linear FRFs of the coupled system for the coordinates we are interested in are obtained by keeping the amplitude of the relative harmonic displacement between the end coordinates of the nonlinear element constant at a different value for each set of FRFs [4]. Note that, depending on the location of the nonlinearity, the number of coordinates at which FRFs should be measured in the coupled system can be reduced. Using available FRFs, sets of linear FRF curves for the unknown subsystem can be obtained by applying the decoupling formulation proposed by D'Ambrogio et al. [1] for linear systems, each set corresponding to a different response level. Then, by applying the modal identification technique developed by Richardson and Formenti [5], a set of modal parameters will be obtained from each FRF curve. As the identified modal parameters vary with the response amplitude, they can be expressed as a function of

---

\* T. Kalaycıoğlu, H.N. Özgüven, Dynamic Decoupling of Nonlinear Systems, in: Dynamics of Coupled Structures, vol. 4, Proceedings of the 35th IMAC, A Conference on Structural Dynamics, Springer, New York, 2017, pp. 199-203, [https://doi.org/10.1007/978-3-319-54930-9\\_17](https://doi.org/10.1007/978-3-319-54930-9_17).

the amplitude of the relative harmonic displacement between the end coordinates of the nonlinear element [4]. Then, the FRFs of the unknown subsystem can be calculated at different response levels by using the modal parameter variations obtained.

## 2.2 Nonlinearity in the Known Subsystem

In this case, it is assumed that known subsystem is nonlinear whereas unknown subsystem is linear. Nonlinear element may be located at any place in the known subsystem. Firstly, the point and transfer FRFs of the coupled system as well as of the known subsystem at coordinates that belong to the known subsystem should be obtained by keeping the amplitude of the relative harmonic displacement between the end coordinates of the nonlinear element at a specific value throughout the desired frequency range [4]. FRFs of the known system will be calculated whereas those of the coupled system should be measured by making controlled displacement amplitude testing. This will yield a set of linear FRF curves for the coupled system, as well as for the known subsystem. Note that the nonlinearity matrices, first introduced by Tanrikulu et al. [7] and then used in many applications, added to the dynamic stiffness matrices of the coupled system and the known subsystem will have the same values at each frequency throughout the desired frequency range. Hence, the existence of nonlinearity will be the same as adding a linear stiffness matrix to the known part of the system, and thus the problem will be reduced into decoupling of linear systems. Consequently, the FRFs of the unknown subsystem at its coupling DOFs can be calculated using the FRFs of the known and coupled systems obtained above by applying the decoupling formulation proposed by D'Ambrogio et al. [1].

## 2.3 Nonlinearity in the Connection of Two Subsystems

When the nonlinear element connects two subsystems, the problem can be reduced into the one of those defined in section 2.1 or section 2.2, depending on the availability of the properties of the nonlinear element. If the parameters of the nonlinear connection element are not known, it should be taken as a part of the unknown subsystem with a massless node at the other end, which is rigidly connected to the connection node of the known subsystem. A similar approach has been followed by the authors in [6]. Thus, the system will be reduced into the system considered in section 2.1. In case where the parameters of the nonlinear element are known, the system can be reduced into the system considered in section 2.2 in the same vein.

## 3 SIMULATED CASE STUDIES

In this section, applications of the proposed decoupling method to a lumped parameter system are presented in order to demonstrate the validity and the efficiency of the method developed.

### 3.1 Decoupling of a Lumped Parameter Nonlinear System – Nonlinearity at the Unknown Subsystem

In this case study, decoupling of a 2 DOF nonlinear subsystem from a 3 DOF lumped parameter system is demonstrated by applying the decoupling method proposed. The nonlinear element is assumed to be a grounded cubic stiffness connected to the coupling DOF of the unknown subsystem. Firstly, the complete FRF matrix (for the DOFs we are interested in) of the known subsystem are theoretically obtained from the known subsystem parameters. Secondly, we need to obtain point and transfer FRFs of the coupled system at coordinates that belong to the known subsystem experimentally through a controlled displacement amplitude test in the frequency range of interest for different constant harmonic displacement amplitudes of the second DOF of the coupled system. These values are theoretically obtained, but in order to include the effect of experimental errors, they are polluted by adding a complex random number. Then the decoupling formulation proposed by D'Ambrogio et al. [1] for linear systems is applied for each 20 different sets of point and transfer FRF curves of the coupled subsystem at coordinates that belong to the known subsystem in order to obtain the point FRF of the unknown subsystem at its coupling DOF. The results are given in Fig. 1.

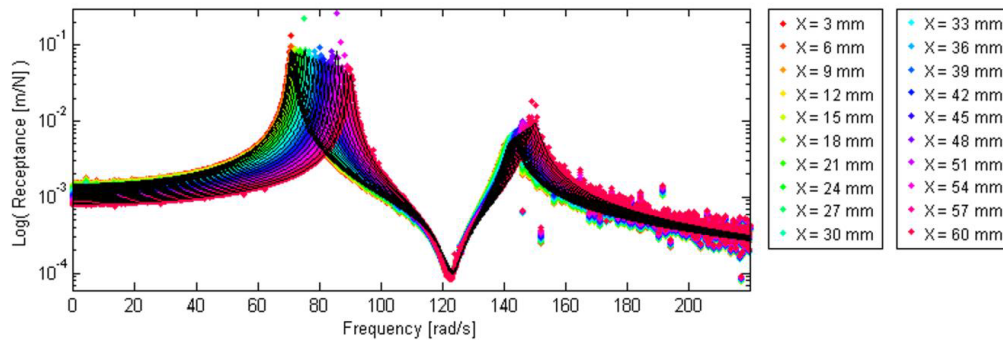
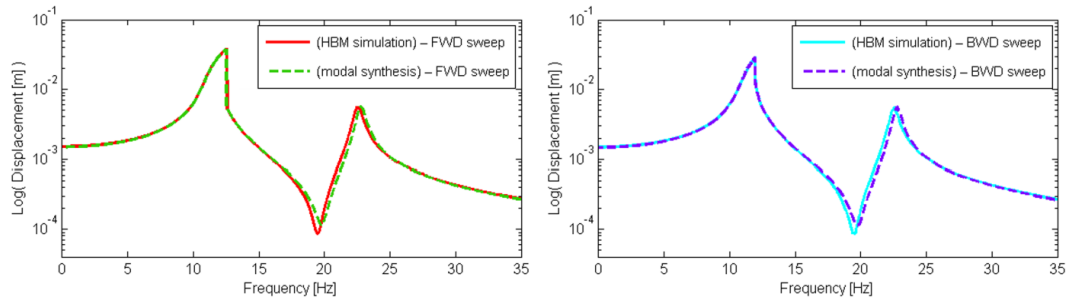


Fig. 1. Point FRFs of the unknown subsystem at its coupling DOF (colored points) and fitted FRF curves (—, black)

Note in Fig. 1 that, each FRF curve shows linear behavior, as it is obtained for a constant harmonic displacement amplitude of the nonlinear element. Firstly, the variation of modal parameters with respect to the amplitude of the relative harmonic displacement between the end coordinates of the nonlinear element is obtained by first fitting FRF curves to the calculated FRF values and then identifying modal parameters for each FRF curve by applying linear modal identification. Then, harmonic response of the unknown subsystem at its coupling DOF is calculated for a harmonic excitation of magnitude 1 N applied at the same point, by employing the approach proposed by Arslan et al. [4] and using the modal parameters calculated above (as a function of response amplitude). The same calculation is also performed through the application of the Harmonic Balance Method (HBM) by using the actual data for the unknown subsystem. These results are compared in Fig. 2. An excellent agreement of two response curves for both forward and backward sweeps in the whole frequency range demonstrates the validity of the method proposed.



**Fig. 2.** Forward (FWD) and backward (BWD) frequency sweep responses of the unknown subsystem at its coupling DOF

### 3.2 Decoupling of a Lumped Parameter Nonlinear System – Nonlinearity at the Known Subsystem

In this case study, decoupling of a 2 DOF linear subsystem from a 3 DOF lumped parameter nonlinear system is demonstrated by applying the decoupling method proposed. The nonlinear element is again assumed to be a grounded cubic stiffness connected to the internal DOF of the known subsystem. Then, the exact point and transfer FRFs of the coupled system and the known subsystem at coordinates that belong to the known subsystem are calculated by keeping the amplitude of the relative harmonic displacement between end coordinates of the cubic nonlinearity at a specific constant value (20 mm for both systems). In order to include the effect of noise in real testing, a complex random perturbation is added to the calculated FRFs. Finally, the decoupling formulation proposed by D'Ambrogio et al. [1] for linear systems is applied to obtain the point receptance of the unknown subsystem at its coupling DOF by using the FRF curves fitted to the point and transfer receptances of the coupled system obtained through simulated experiment, and receptances of the known subsystem. The results are given in Fig. 3.

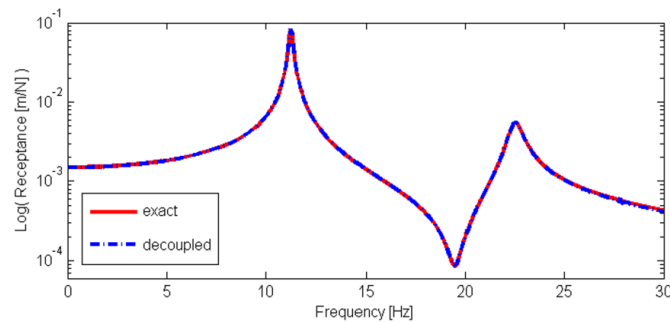


**Fig. 3.** Exact and decoupled point receptances of the unknown subsystem at its coupling DOF

Fig. 3 shows that the FRF obtained using the decoupling method proposed almost the same as the exact FRF. Then it can be concluded that the decoupling method developed yields very good results for the case where the nonlinearity is in the known subsystem.

#### 4 DISCUSSION AND CONCLUSIONS

Although there are some accuracy problems, the dynamic decoupling problem of linear structures is well addressed in literature. However, there has been almost no effort to tackle the dynamic decoupling problem of nonlinear structures. This paper presents the first attempt to solve this problem by suggesting a method that can be applied when the nonlinearity can be modelled as a single element. It is also assumed in this method that the location of nonlinearity is known. The approach proposed can be applied for all possible cases as far as the location of the nonlinear element is concerned, i.e. nonlinearity can be either in the known or unknown subsystem, or it can be at the connection. The method proposed is validated through simulated case studies.

#### 5 REFERENCES

- [1] D'Ambrogio, W., Fregolent, A., "The Role of Interface DOFs in Decoupling of Substructures based on the Dual Domain Decomposition", *Mechanical Systems and Signal Processing*, Vol. 24, No. 7, pp. 2035-2048, 2010.
- [2] Batista, F.C., Maia, N.M.M., "Uncoupling Techniques for the Dynamic Characterization of Sub-structures", *Proceedings of the 29<sup>th</sup> International Modal Analysis Conference*, 2011.
- [3] Voormeeren, S.N., Rixen, D.J., "A Family of Substructure Decoupling Techniques based on a Dual Assembly Approach", *Mechanical Systems and Signal Processing*, Vol. 27, pp. 379-396, 2012.
- [4] Arslan, Ö., Aykan, M., Özgüven, H.N., "Parametric Identification of Structural Nonlinearities from Measured Frequency Response Data", *Mechanical Systems and Signal Processing*, Vol. 25, No. 4, pp. 1112-1125, 2011.
- [5] Richardson, M.N., Formenti, D.L., "Parameter Estimation from Frequency Response Measurements Using Rational Fraction Polynomials", *Proceedings of the 1<sup>st</sup> International Modal Analysis Conference*, 1982.
- [6] Kalaycıoğlu, T., Özgüven, H.N., "Nonlinear Structural Modification and Nonlinear Coupling", *Mechanical Systems and Signal Processing*, Vol. 46, No. 2, pp. 289-306, 2014.
- [7] Tanrikulu Ö., Kuran B., Özgüven H.N., İmregün M., "Forced Harmonic Response Analysis of Non-linear Structures using Describing Functions", *AIAA Journal*, Vol. 31, No. 7, pp. 1313-1320, 1993.





Contents lists available at ScienceDirect

## Mechanical Systems and Signal Processing

journal homepage: [www.elsevier.com/locate/ymssp](http://www.elsevier.com/locate/ymssp)

## FRF decoupling of nonlinear systems

Taner Kalaycıoğlu<sup>a,b</sup>, H. Nevzat Özgüven<sup>a,\*</sup><sup>a</sup> Department of Mechanical Engineering, Middle East Technical University, 06800 Ankara, Turkey<sup>b</sup> Microelectronics, Guidance and Electro-Optics Business Sector, ASELSAN Inc., 06011 Ankara, Turkey

## ARTICLE INFO

## Article history:

Received 23 April 2017

Received in revised form 8 September 2017

Accepted 16 September 2017

## Keywords:

Nonlinear decoupling

Nonlinear uncoupling

Nonlinear inverse substructuring

Nonlinear subsystem identification

Nonlinear substructure decoupling

## ABSTRACT

Structural decoupling problem, i.e. predicting dynamic behavior of a particular substructure from the knowledge of the dynamics of the coupled structure and the other substructure, has been well investigated for three decades and led to several decoupling methods. In spite of the inherent nonlinearities in a structural system in various forms such as clearances, friction and nonlinear stiffness, all decoupling studies are for linear systems. In this study, decoupling problem for nonlinear systems is addressed for the first time. A method, named as FRF Decoupling Method for Nonlinear Systems (FDM–NS), is proposed for calculating FRFs of a substructure decoupled from a coupled nonlinear structure where nonlinearity can be modeled as a single nonlinear element. Depending on where nonlinear element is, i.e., either in the known or unknown subsystem, or at the connection point, the formulation differs. The method requires relative displacement information between two end points of the nonlinear element, in addition to point and transfer FRFs at some points of the known subsystem. However, it is not necessary to excite the system from the unknown subsystem even when the nonlinear element is in that subsystem. The validation of FDM–NS is demonstrated with two different case studies using nonlinear lumped parameter systems. Finally, a nonlinear experimental test structure is used in order to show the real-life application and accuracy of FDM–NS.

© 2017 Elsevier Ltd. All rights reserved.

## 1. Introduction

Since engineering structures are generally designed as an assembly of several components, it is expensive and time consuming to constitute FE model each time especially when several design alternatives are to be studied. Therefore, various structural coupling methods have been developed in order to reduce the effort involved in the dynamic reanalysis of such systems [1–19]. Although there are several different coupling methods based on the linearity assumption in the literature, most of the engineering structures are inherently nonlinear. During the past three decades, structural coupling of nonlinear subsystems has been investigated and led to several coupling methods taking the nonlinear effect into account [20–28].

Several studies have also been carried out for structural decoupling of linear systems, which becomes an important problem when the dynamic behavior of a system is known, but it is difficult to measure the dynamic characteristics of one of its components due to geometric constraints (i.e., due to difficulty in measuring and/or exciting a subsystem individually). The investigation on decoupling problem dates back to three decades ago, when the first attempt to extract objective component's dynamics in an assembly was performed by Okubo and Miyazaki [29]. Afterwards, Gontier and Bensaïbi [30] presented a time domain method for in situ identification of a substructure that is part of a known greater structure. Maia

\* Corresponding author.

E-mail address: [ozguven@metu.edu.tr](mailto:ozguven@metu.edu.tr) (H.N. Özgüven).<https://doi.org/10.1016/j.ymssp.2017.09.029>

0888-3270/© 2017 Elsevier Ltd. All rights reserved.

\* T. Kalaycıoğlu, H.N. Özgüven, FRF Decoupling of Nonlinear Systems, Mechanical Systems and Signal Processing, 102 (2018) 230–244, <https://doi.org/10.1016/j.ymssp.2017.09.029>.

et al. [31] presented a decoupling methodology as a means of modeling the dynamic behavior of structural elements, more specifically, for the dynamic characterization of joints. Kalling et al. [32] also studied the decoupling problem by performing state-space model identification including a sensitivity analysis to uncertainties in the known models. D'Ambrogio and Fregoleto [33] proposed two decoupling procedures; namely, impedance based and mobility based approaches that suffers from ill-conditioning problems. Sjövall and Abrahamsson [34] presented a frequency-based subsystem identification method that utilizes responses away from the connection point. A general framework for dynamic substructuring is provided in [15,16] in which the so called dual domain decomposition technique that allows retaining the full set of global degrees of freedom (DOFs) by ensuring equilibrium at the interface between substructures is introduced. When performing substructuring by using the dual domain decomposition, the coupling problem can be directly formulated from [16], whereas a similar formulation for the decoupling problem is developed and discussed in [35] for collocated approach where DOFs used to enforce equilibrium are the same as DOFs used to enforce compatibility, and in [36,37] for non-collocated approach where DOFs used to enforce equilibrium are not the same as DOFs used to enforce compatibility. Batista and Maia [38] proposed three different formulations based on the classical decoupling procedure of Jetmundsen et al. [5] considering the effects of including different sets of DOFs on the coupled system: (i) exclusion of connection DOFs, (ii) inclusion of connection DOFs only and (iii) inclusion of connection DOFs and internal DOFs of the known subsystem. The inverse substructuring approach presented by Cloutier and Avitabile [39] needs measurements from the unknown substructure. Later, D'Ambrogio and Fregoleto [40] proposed the so-called hybrid assembly approach. They compared dual [35] and hybrid assembly approaches by applying them to an experimental test bed and come up with similar results regarding predicted FRFs of the unknown subsystem. In later applications, the dual assembly approach [35] was successfully used to predict the subsystem dynamics in machine tools [41,42], wind turbines [43] and flexible space payloads [44].

Even though there are some accuracy problems, the dynamic decoupling problem of linear structures is well investigated in literature. However, the dynamic decoupling problem of nonlinear structures still remains untouched. The further challenge in nonlinear decoupling problem is that the existence of a nonlinearity in a coupled system leads to different system FRFs depending on the level of excitation. So, application of linear decoupling approaches will also result in different FRFs for an unknown substructure at each time. In order to overcome this challenge, nonlinear system identification techniques are consulted where reviews of those are given by Kerschen et al. [45] and Noël et al. [46].

In this paper, a method, named as FDM-NS (FRF Decoupling Method for Nonlinear Systems), is developed for the dynamic decoupling problem of nonlinear structures for the first time. This method can predict the FRFs of an unknown subsystem, whether linear or nonlinear, from the measured FRFs of the coupled nonlinear system and the measured or calculated FRFs of the remaining known subsystem. Note that this approach can be applied to decouple nonlinear structures, only if the nonlinearity can be modeled as a single nonlinear element and its location is known. However, there is no limitation in the type of nonlinear element in the system. The validity of FDM-NS is demonstrated on lumped multi degrees of freedom (MDOF) systems by using simulated experimental data. For the case where the unknown subsystem is linear, the results obtained are compared with the exact ones. On the other hand, for the case where the unknown subsystem is nonlinear, the results obtained via FDM-NS are again compared with the exact ones which are obtained by calculating FRFs of the nonlinear subsystem by using harmonic balance approach. Finally, a nonlinear experimental test rig is used in order to demonstrate the applicability and accuracy of FDM-NS when applied to real systems.

## 2. Theory

In this section, the theory of FDM-NS is given in detail. The uncoupling problem is studied as three separate problems depending on the location of the nonlinear element in the coupled system under consideration: The nonlinearity can be either in the unknown subsystem or in the known subsystem, or it can connect these subsystems. The notation used throughout the paper for all systems/subsystems and the coordinate sets are given in Fig. 1.

As can be seen from Fig. 1, superscripts U and K refer to unknown and known subsystems, respectively whereas superscript KU represents coupled system. Subscript  $i$  denotes the coordinates that belong to the unknown subsystem only, subscript  $j$  refers to the connection coordinates (connection may be rigid or elastic) between the unknown and known

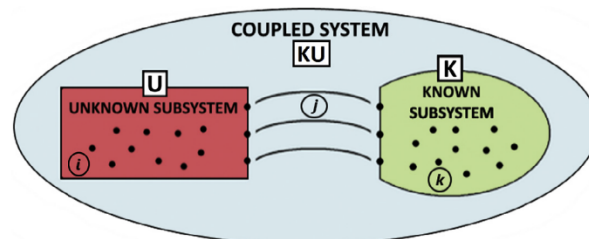


Fig. 1. Notation used for coupled system, subsystems and the coordinate sets.

subsystems, and finally subscript  $k$  represents the coordinates that belong to the known subsystem only. Furthermore,  $\mathbf{H}$  represents a FRF matrix in the following formulation. It should finally be stated for the following formulation that only a single nonlinear element is assumed to be included in the coupled system and its location is known.

### 2.1. Nonlinearity in the unknown subsystem

In this case, it is assumed that known subsystem is linear whereas unknown subsystem is nonlinear and the location of the nonlinear element is known. Here, depending on the location of the nonlinear element, the number of coordinates at which FRFs should be measured in the coupled system will change. When the nonlinear element is located between internal DOFs ( $i$ ), complete FRF matrix of the coupled system for the coordinates being interested in should be obtained through experimental measurements. However, in case where the nonlinear element is located between internal DOFs ( $i$ ) and coupling DOFs ( $j$ ) of the unknown subsystem, it is not required to measure FRFs between internal DOFs ( $i$ ) of the coupled system (i.e.,  $\mathbf{H}_{ii}^{ku}$ ). Nonlinear element can also be located between coupling DOFs ( $j$ ) of the unknown subsystem. When this is the case, only the FRFs of the coupled system at and between coordinates  $j$  and  $k$ , (i.e.,  $\mathbf{H}_{jj}^{ku}$ ,  $\mathbf{H}_{jk}^{ku}$  and  $\mathbf{H}_{kk}^{ku}$ ) are required to be measured experimentally.

This subproblem can be handled through successive applications of the following techniques:

- Controlled displacement amplitude vibration testing.
- A decoupling technique for linear systems (the dual assembly approach [35] is used in this paper).
- The parametric modal identification technique proposed by Arslan et al. [47] for nonlinear systems.

The complete FRF matrix of the known subsystem for the coordinates being interested in can be obtained by using its known system parameters. All the required FRFs of a coupled system can be obtained via experimental measurements. However, since the coupled system is nonlinear, various different linear FRF curves will be obtained via testing by keeping the amplitude of the relative harmonic displacement between end coordinates of the nonlinear element constant at a different value for each FRF curve. By applying a linear decoupling method using all available FRFs, one can obtain different FRF curves for the nonlinear unknown subsystem, each of which represents a linear system. Here, the dual assembly approach [35] is used as the linear decoupling method, resulting formulation of which is given below:

$$\mathbf{H}^U = \begin{bmatrix} \mathbf{H}^{ku} & \mathbf{0} \\ \mathbf{0} & -\mathbf{H}^k \end{bmatrix} - \begin{bmatrix} \mathbf{H}^{ku} & \mathbf{0} \\ \mathbf{0} & -\mathbf{H}^k \end{bmatrix} \begin{bmatrix} \mathbf{B}_E^{kuT} \\ \mathbf{B}_E^{kT} \end{bmatrix} \times \left( \begin{bmatrix} \mathbf{B}_C^{ku} & \mathbf{B}_C^k \end{bmatrix} \begin{bmatrix} \mathbf{H}^{ku} & \mathbf{0} \\ \mathbf{0} & -\mathbf{H}^k \end{bmatrix} \begin{bmatrix} \mathbf{B}_E^{kuT} \\ \mathbf{B}_E^{kT} \end{bmatrix} \right)^+ \times \begin{bmatrix} \mathbf{B}_C^{ku} & \mathbf{B}_C^k \end{bmatrix} \begin{bmatrix} \mathbf{H}^{ku} & \mathbf{0} \\ \mathbf{0} & -\mathbf{H}^k \end{bmatrix} \quad (1)$$

where  $\mathbf{B}_C = \begin{bmatrix} \mathbf{B}_C^{ku} & \mathbf{B}_C^k \end{bmatrix}$  and  $\mathbf{B}_E = \begin{bmatrix} \mathbf{B}_E^{ku} & \mathbf{B}_E^k \end{bmatrix}$  are signed Boolean matrices used to enforce compatibility and equilibrium at interface DOFs, and the symbol  $^+$  refers to the generalized inverse.

Each FRF curve obtained via linear decoupling will correspond to a different harmonic displacement amplitude of the nonlinear element. Then, sets of modal parameters will be obtained through the application of the modal identification technique developed by Richardson and Formenti [48] successively to each FRF curve. As the identified modal parameters - natural frequencies ( $\omega_r$ ), damping ratios ( $\eta_r$ ) and modal constants ( ${}_r A_{kl}$ ) - vary with response amplitude, they can be expressed as a function of the amplitude of the relative harmonic displacement between end coordinates of the nonlinear element ( $X_{pq}$ ) by fitting curves to these calculated data points. Fitted curves can be in the form of continuous or discontinuous functions depending on the type of nonlinearity. Resulting expressions are given below [47]

$$\omega_r = \omega_r(X_{pq}) \quad (2)$$

$$\eta_r = \eta_r(X_{pq}) \quad (3)$$

$${}_r A_{kl} = {}_r A_{kl}(X_{pq}) \quad (4)$$

Then, FRFs of the unknown subsystem can be computed at any response level by using the modal parameters at this level.

### 2.2. Nonlinearity in the known subsystem

In this case, it is assumed that known subsystem is nonlinear whereas unknown subsystem is linear. Nonlinear element may be located at any place on the known subsystem (i.e., at coordinates  $j$ ,  $k$  or between coordinates  $j$  and  $k$ ). Note here that, it is required to measure FRFs of the coupled system at and between coordinates  $j$  and  $k$  (i.e.,  $\mathbf{H}_{jj}^{ku}$ ,  $\mathbf{H}_{jk}^{ku}$  and  $\mathbf{H}_{kk}^{ku}$ ) experimentally. This subproblem can be handled through successive applications of the following techniques:

- Controlled displacement amplitude vibration testing
- A decoupling technique for linear systems (the dual assembly approach [35] is used in this paper).

Firstly, point and transfer FRFs of the coupled system as well as the known subsystem at coordinates  $j$  and  $k$  should be experimentally obtained by keeping the amplitude of the relative harmonic displacement between end coordinates of the nonlinear element at a specific value throughout the desired frequency range. Thereby, FRF curves for the coupled system and for the known subsystem will show linear behaviors. Furthermore, since displacement level of the nonlinear element is the same for both systems at every frequency all through one set of experiments, the Nonlinearity Matrices introduced to their dynamic stiffness matrices,  $\mathbf{Z}$ , will be the same at each frequency throughout the desired frequency range. So, dynamic stiffness matrices of the known subsystem and the coupled system can be written as follows, respectively:

$$\mathbf{Z}^K = \mathbf{K}^K - \omega^2 \mathbf{M}^K + i\omega \mathbf{C}^K + \mathbf{\Delta} \tag{5}$$

$$\mathbf{Z}^{KU} = \mathbf{K}^{KU} - \omega^2 \mathbf{M}^{KU} + i\omega \mathbf{C}^{KU} + \begin{pmatrix} 0 & 0 & 0 \\ 0 & & \\ & \mathbf{\Delta} & \\ 0 & & \end{pmatrix} \tag{6}$$

where  $\mathbf{\Delta} = \begin{pmatrix} \Delta_{ij} & \Delta_{jk} \\ \Delta_{kj} & \Delta_{kk} \end{pmatrix}$ .

Here,  $\mathbf{K}$ ,  $\mathbf{M}$  and  $\mathbf{C}$  correspond to mass, stiffness and damping matrices whereas  $\mathbf{\Delta}$  is the Nonlinearity Matrix introduced by Tanrikulu et al. [49] and once again, it has the same constant value at each frequency in this case. So, the existence of nonlinearity, under these circumstances, will be the same as adding a linear stiffness matrix to the known part of the system, and therefore the problem will be reduced into decoupling of linear systems. Consequently, the FRFs of the unknown subsystem at its coupling DOFs ( $j$ ) can be calculated by using the FRFs of the known subsystem and the coupled system obtained above and applying the dual assembly approach [35], formulation of which is given by Eq. (1).

### 2.3. Nonlinearity in the connection of two subsystems

When the nonlinear element connects two subsystems, the solution depends on whether or not the properties of this nonlinear elastic element is known. If the parameters of the nonlinear connection element are not known, it should be taken as a part of the unknown subsystem. Then it can be taken as an elastic element with a massless node at the other end, which is rigidly connected to the connection node of the known subsystem as depicted in Fig. 2. A similar approach has been used by the authors in [25]. Thus, the system will be reduced into the system considered in Section 2.1.

If the parameters of the nonlinear connection element are known, the nonlinear element can be taken as a part of the known subsystem with a massless node at its other end, which is rigidly connected to the unknown subsystem (Fig. 2). Then, the problem will be reduced into the one defined in Section 2.2.

## 3. Simulated case studies

In this section, applications of FDM-NS to lumped parameter systems are presented in order to demonstrate the validity and the efficiency of the method.

### 3.1. Decoupling of a lumped parameter nonlinear system – nonlinearity in the unknown subsystem

In this case study, decoupling of a 2 DOF nonlinear system from a 3 DOF lumped parameter nonlinear system will be demonstrated by applying FDM-NS. The coupled system is composed of two subsystems: A 2 DOF linear subsystem (known) and another 2 DOF nonlinear subsystem (unknown). These subsystems are rigidly connected to each other as shown in Fig. 3. Physical parameters of the coupled system are given in Table 1.

The type of nonlinearity in the system is assumed to be cubic stiffness. The grounded cubic stiffness nonlinearity connected to the coupling DOF of the unknown subsystem is defined as follows:

$$n(x)_{NL} = k_c x^3 \text{ where } k_c = 2 \times 10^5 \text{ N/m}^3 \tag{7}$$

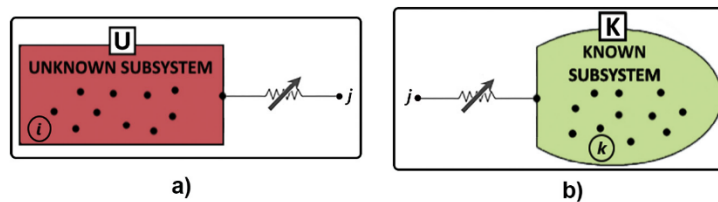


Fig. 2. Inclusion of the connecting nonlinear element, (a) in the unknown subsystem, (b) in the known subsystem.

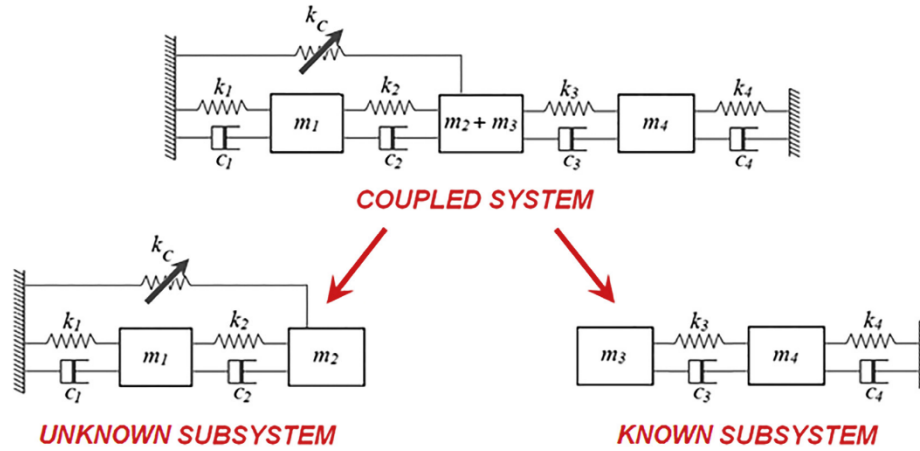


Fig. 3. Decoupling of a nonlinear coupled system - nonlinearity at the coupling DOF of the unknown subsystem.

**Table 1**  
Physical parameters of the coupled system.

Element number ( <i>i</i> )	$m_i$ [kg]	$k_i$ [N/m]	$c_i$ [Ns/m]
1	0.20	2000	0.50
2	0.10	1000	0.20
3	0.15	1000	0.30
4	0.20	1500	0.60

The first step in the application of FDM-NS is to obtain the complete FRF matrix (for the DOFs being interested in) of the known subsystem theoretically from the known system parameters. Secondly, point and transfer FRF sets of the coupled system at coordinates  $j$  and  $k$  should be obtained by conducting controlled displacement amplitude experiments for different relative displacement levels of the nonlinear element. Here, exact FRF sets are obtained for 20 different harmonic displacement amplitudes of the second DOF ( $m_2 + m_3$ ) of the coupled system. The values of the constant harmonic displacement amplitudes,  $|X_2^U|$ , start from 3 mm and continue with 3 mm increment up to 60 mm. In order to include the effect of experimental errors, the calculated FRF sets are polluted by adding a complex random number as follows:

$$\mathbf{H}_{ab}^{KU}(\omega_k) = \hat{\mathbf{H}}_{ab}^{KU}(\omega_k) + m_{ab,k} + i n_{ab,k} \quad (8)$$

In Eq. (8),  $m_{ab,k}$  and  $n_{ab,k}$  are independent random variables with Gaussian distribution having a zero mean and a standard deviation of  $4 \times 10^{-6}$  m/N.

At this stage, the dual assembly approach [35] for decoupling of linear systems is applied for each 20 different point and transfer FRF sets of the coupled system at its second ( $m_2 + m_3$ ) and the third ( $m_4$ ) DOFs in order to obtain point FRFs of the unknown subsystem at its coupling DOF. The results are given in Fig. 4. Note that, FRF curves of the unknown nonlinear subsystem show linear behavior, as each is obtained for a constant harmonic displacement amplitude of the nonlinear element.

Now, first fitting FRF curves to the calculated FRF values and then identifying linear modal parameters for each FRF curve, the variation of modal parameters can be obtained as a function of the amplitude of the relative harmonic displacement between end coordinates of the nonlinear element. The results are shown in Figs. 5 and 6 for the first and second modes, respectively. Modal parameters are extracted from FRF curves by using the modal identification technique developed by Richardson and Formenti [48]. Once the modal properties of the unknown subsystem are obtained, then the point receptance of the unknown nonlinear subsystem can easily be calculated for any forcing level by using the approach proposed by Arslan et al. [47].

In order to show the accuracy of the results obtained by using FDM-NS, driving point response of the unknown subsystem at second mass is calculated for a harmonic forcing with an amplitude of 1 N, first by performing modal synthesis using the modal parameter variations given in Figs. 5 and 6 (as a function of response amplitude), and then by applying Harmonic Balance Method (HBM) using the actual data for the subsystem. Note that both approaches are based on the basic assumption that harmonic excitation results in harmonic response at the same frequency. The comparisons of the results are presented in Figs. 7 and 8. An excellent agreement of two response curves for both forward and backward sweeps in the whole frequency range demonstrates the validity of the method proposed.

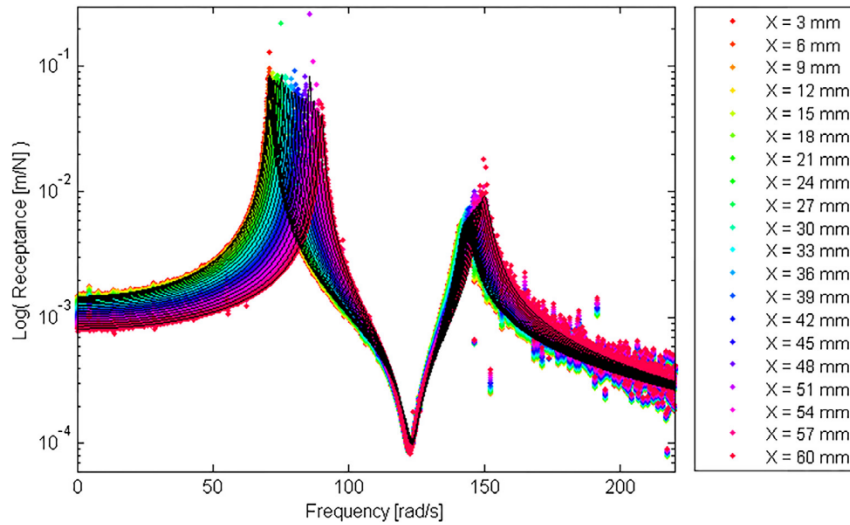


Fig. 4. Point FRFs of the unknown subsystem at its coupling DOF (colored points) and fitted FRF curves (–, black). (For interpretation of the references to color in this figure legend, the reader is referred to the web version of this article.)

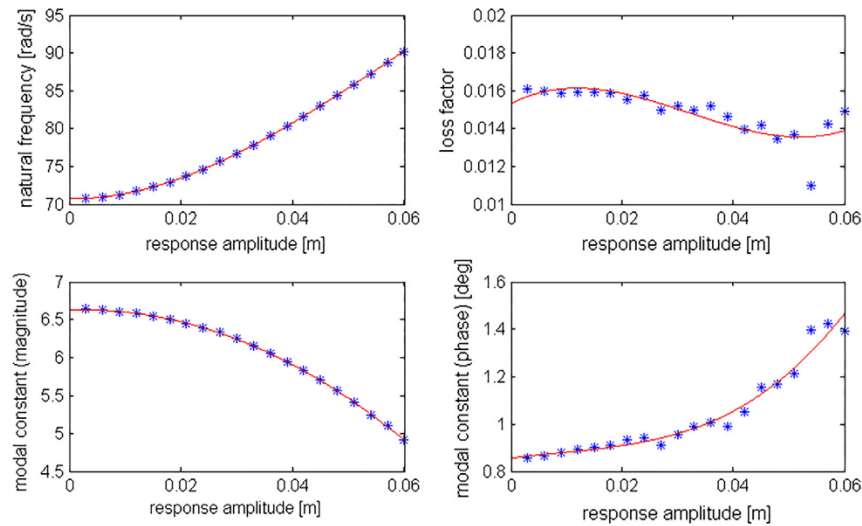


Fig. 5. Variation of the modal parameters of the first mode with response amplitude,  $|X_2^j|$  (\*, identified parameters & –, fitted curves) – Modal constant is given for point receptance of  $m_2$ .

### 3.2. Decoupling of a lumped parameter nonlinear system – nonlinearity in the known subsystem

In this case study, decoupling of a 2 DOF linear system from a 3 DOF lumped parameter nonlinear system will be demonstrated by applying FDM-NS. The coupled system is composed of two subsystems: A 2 DOF nonlinear subsystem (known) and another 2 DOF linear subsystem (unknown). These subsystems are rigidly connected to each other as shown in Fig. 9. Physical parameters of the coupled system are given in Table 1.

The type of nonlinearity in the known subsystem is again assumed to be cubic stiffness and described as given in Eq. (7).

Firstly, point and transfer FRFs of the coupled system and the known subsystem at coordinates  $j$  and  $k$  should be obtained experimentally by conducting a controlled displacement amplitude test in the frequency range of interest. In this

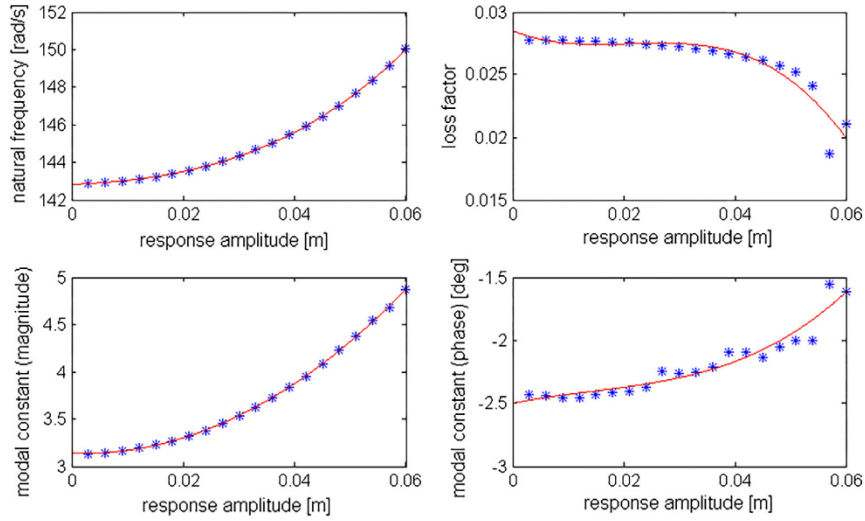


Fig. 6. Variation of the modal parameters of the second mode with response amplitude,  $|X_2^U|$  (\*, identified parameters & –, fitted curves) – Modal constant is given for point receptance of  $m_2$ .

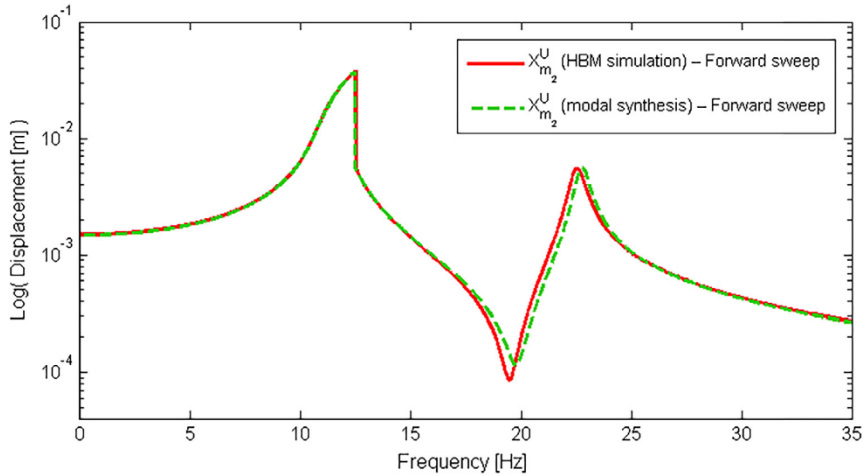


Fig. 7. Forward frequency sweep response of the unknown subsystem at  $m_2$ .

application, exact FRFs of the coupled system ( $\hat{\mathbf{H}}^{KU}$ ) and of the known subsystem ( $\hat{\mathbf{H}}^K$ ) are calculated by using the physical parameters given in Table 1. For each excitation frequency, the force amplitude is adjusted such that the amplitude of the relative harmonic displacement between end coordinates of the cubic nonlinearity is kept constant (20 mm for both systems). In order to include the effect of experimental errors in real testing, a complex random perturbation is added to the calculated FRFs in the following form:

$$\mathbf{H}_{ab}^{KU}(\omega_k) = \hat{\mathbf{H}}_{ab}^{KU}(\omega_k) + m_{ab,k} + in_{ab,k} \tag{9}$$

$$\mathbf{H}_{ab}^K(\omega_k) = \hat{\mathbf{H}}_{ab}^K(\omega_k) + p_{ab,k} + iq_{ab,k} \tag{10}$$

In Eq. (9) and (10),  $m_{ab,k}$ ,  $n_{ab,k}$ ,  $p_{ab,k}$  and  $q_{ab,k}$  are independent random variables with Gaussian distribution having zero mean and a standard deviation of  $3 \times 10^{-5}$  m/N. The effect of such perturbation on the point receptances of the coupled system and of the known subsystem at  $m_4$  is shown in Fig. 10 along with the FRFs obtained after curve fitting.

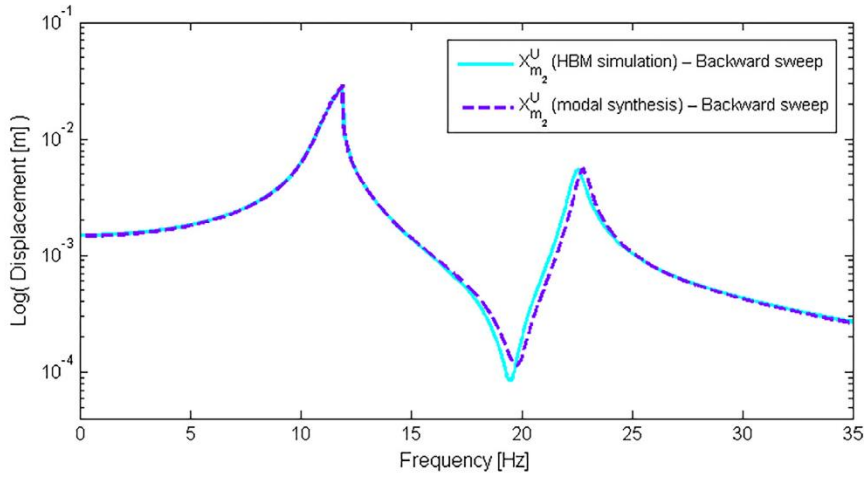


Fig. 8. Backward frequency sweep response of the unknown subsystem at  $m_2$ .

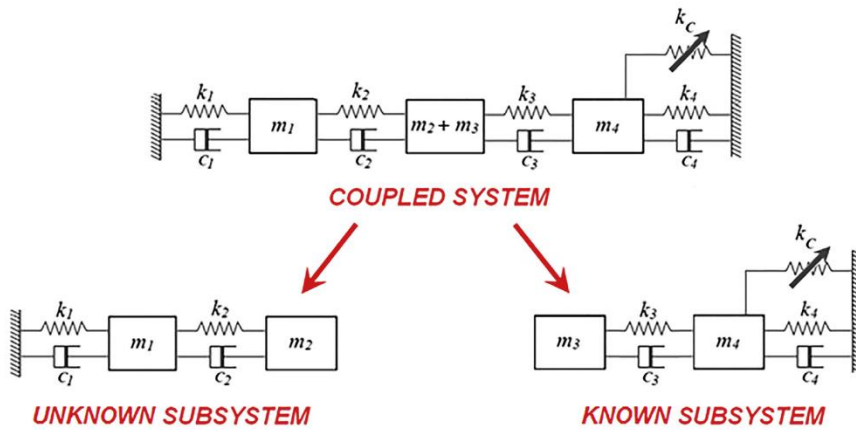


Fig. 9. Decoupling of a nonlinear coupled system - nonlinearity in the known subsystem.

Note that the FRFs given in Fig. 10 show linear behavior since they represent FRFs obtained through a controlled displacement amplitude test at which the nonlinear element will behave linearly. Otherwise, that is for a constant amplitude harmonic forcing of 4 N, the responses of the coupled system and the known subsystem would show nonlinear behavior as shown in Fig. 11.

Hereafter the dual assembly approach [35] for decoupling of linear systems can be applied in order to obtain the point receptance of the unknown subsystem at  $m_2$  by using fitted FRF curves to the calculated point and transfer receptances of the coupled system at  $m_2 + m_3$  and  $m_4$ , along with those of the known subsystem at  $m_3$  and  $m_4$ . The results are given in Fig. 12.

As can be seen from Fig. 12, the FRF obtained using FDM-NS is almost the same as the exact FRF. It can be concluded that the decoupling method developed yields very good results for the case where the nonlinearity is in the known subsystem. It should be noted that if the amplitude of the relative harmonic displacement between end coordinates of the cubic nonlinearity is kept constant at a different value, the equivalent linear systems for nonlinear subsystem and nonlinear coupled system will be different, but application of the linear decoupling theory will give the same FRF curve for the unknown linear subsystem.



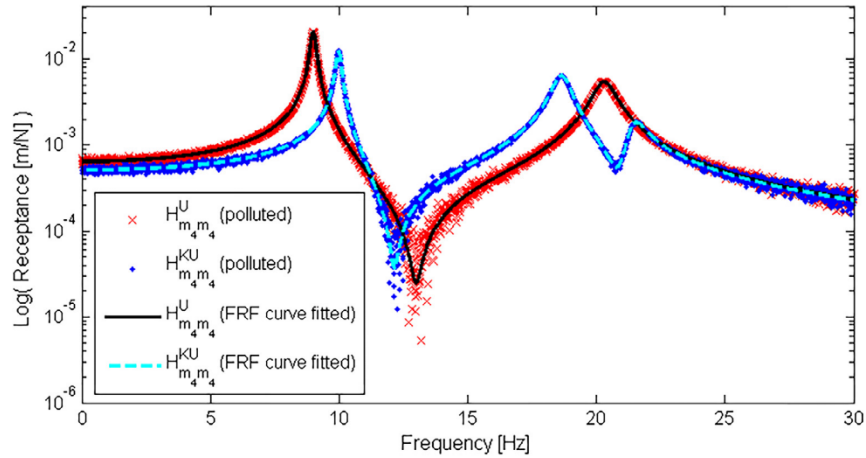


Fig. 10. Polluted and curve fitted point receptances of the coupled system and the known subsystem at  $m_4$ .

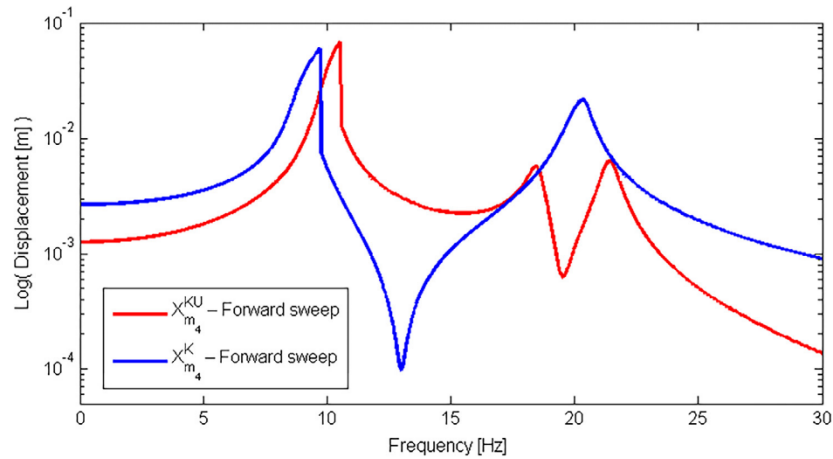


Fig. 11. Frequency responses of the coupled system and the known subsystem at  $m_4$  under constant amplitude harmonic excitation.

#### 4. Experimental case study

In this section, the method developed is applied to a real experimental test system which consists of a cantilever beam connected to another thin beam forming a T-beam configuration. The thin beam introduces nonlinear stiffness. First, linear FRFs of the coupled nonlinear test system are measured through controlled displacement amplitude testing, and the nonlinear part of the system is separately identified. Then, FRFs of the linear unknown subsystem are obtained first by using the method developed and then by performing a shaker test. Finally, predicted and measured FRFs of the unknown subsystem are compared in order to demonstrate the real-life applicability and accuracy of FDM-NS.

##### 4.1. Experimental setup

The setup consists of a linear cantilever beam, which is referred to as the unknown subsystem, with its free end connected to the midpoint of a thin beam having fixed-fixed boundary conditions. The thin beam introduces nonlinear stiffness to the cantilever beam, and it is treated as the known subsystem. The dimensions of the test beams are given in Fig. 13.

Both beams are made of St37 steel. In order to ensure fixed boundary conditions, beams are manufactured sufficiently long and the ends of the beams are squeezed between steel blocks. A picture of the test setup is shown in Fig. 14.

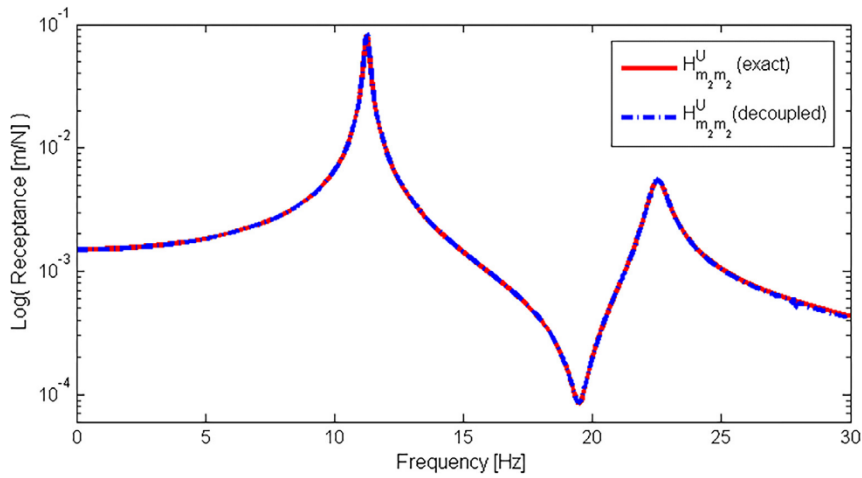


Fig. 12. Exact and decoupled point receptances of the unknown subsystem at  $m_2$ .

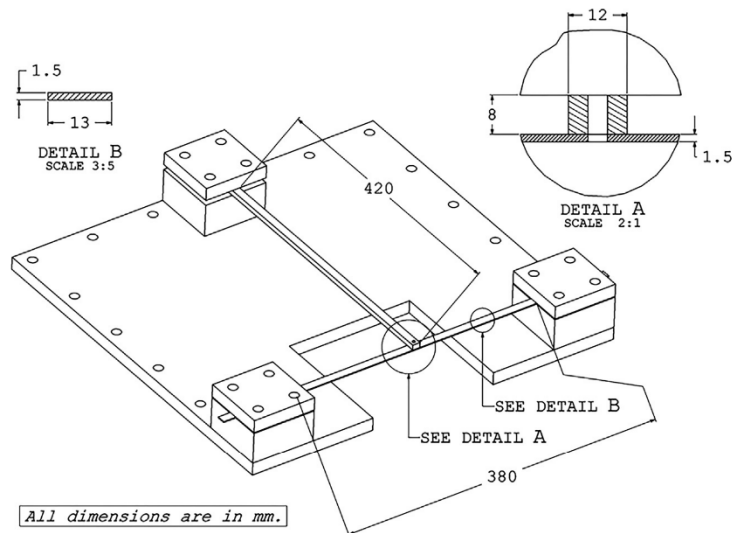


Fig. 13. The dimensions of the test setup.

The structure is excited with B&K Type 4808 shaker via a push-rod connected to the connection point of two beams. Excitation level of the shaker is manually adjusted by using B&K Type 2712 power amplifier. Acceleration responses are measured by using B&K Type 4507B uniaxial accelerometer, and the force applied is measured with B&K Type 8230-002 force transducer which is at the tip of the push-rod. B&K Type 3560C frontend system is used as a data acquisition system in all measurements.

#### 4.2. Experimental results and application of FDM-NS

In this experiment, point FRFs of the T-beam assembly at the connection point of the cantilever beam and the thin fixed-fixed beam are measured in transverse direction. In order to determine the frequency range of interest, a quick test with a random excitation is performed. The frequency range of interest is selected as 20–55 Hz which covers the first mode of the coupled structure. An adaptive frequency resolution is used in the final measurements. After performing a controlled

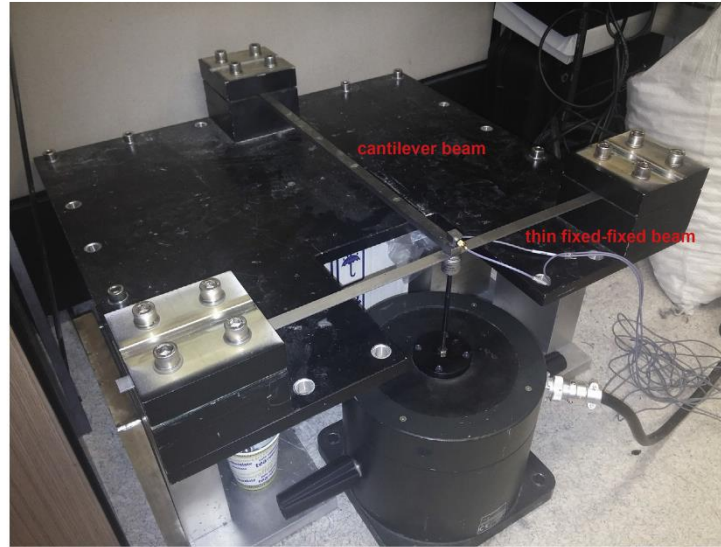


Fig. 14. Picture of the test setup.

displacement amplitude vibration measurement for the constant displacement amplitude of 1 mm, point FRFs at the connection point of two beams are obtained as shown in Fig. 15. It should be noted here that displacement data is obtained by integrating the measured acceleration data without using a filter.

In Fig. 15, experimentally measured FRFs are given together with the FRF curve fitted to these points. Note that fitted FRF curve is henceforth used in the calculations as the point FRF of the coupled system at the connection point of two subsystems ( $\mathbf{H}_{ij}^{ku}$ ).

The thin fixed-fixed beam is modeled as a discrete nonlinear spring in transverse direction with a concentrated equivalent mass. From the material and geometric properties of this beam, the linear part of its equivalent spring stiffness and the equivalent mass values are analytically calculated as 2558.7 N/m and 21.52 g, respectively. In order to identify nonlinear stiffness of the thin fixed-fixed beam, the nonlinear identification approach, called Direct Nonlinearity by Describing Functions (DDF) method, proposed by Aykan and Özgüven is used [50]. As the first step of DDF method, the nonlinear T-beam assembly is tested at two different excitation levels. In these tests, the connection point of two beams is excited with forces

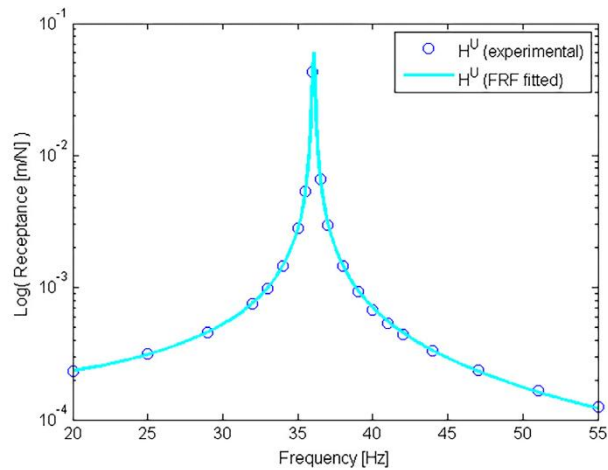


Fig. 15. Point FRFs at the connection point of two beams in transverse direction for the constant.

of magnitudes 0.25 N and 0.5 N, in turn, and point FRFs of the T-beam assembly are measured at various frequencies as shown in Fig. 16.

By applying DDF method [50] and using the experimental results given in Fig. 16, the Describing Function (DF) values representing the nonlinear element connected to the tip of the cantilever beam are calculated. The nonlinearity coefficients for the real and imaginary parts of DF are found by curve fitting, using polynomials up to the third order. The real and imaginary parts of DF which correspond to stiffness and damping nonlinearities, respectively, are plotted in Fig. 17. The coefficients of DF curves are given in Table 2.

The describing function representing the nonlinear element whose parameters are identified in Table 2 can be formulated as given below:

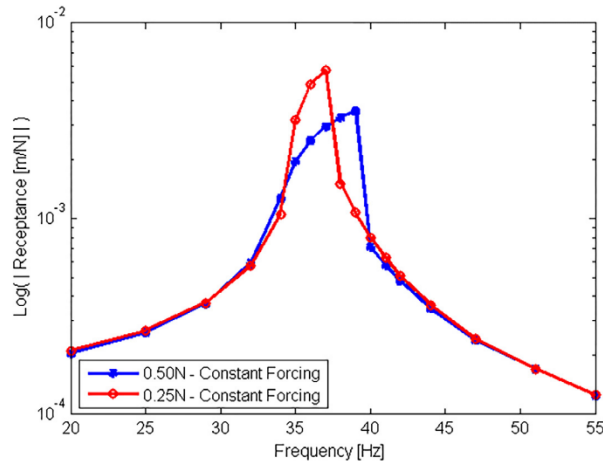


Fig. 16. Point FRFs at the connection point of two beams in transverse direction for excitations of constant magnitudes 0.25 N and 0.5 N.

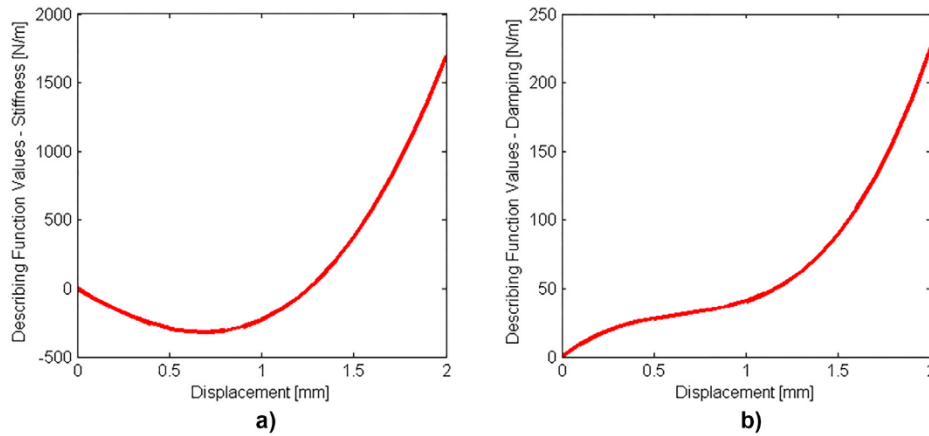


Fig. 17. Calculated DF values by DDF Method [50], (a) stiffness, (b) damping.

Table 2  
Parametric identification results for the nonlinear element.

	Linear coefficient ( $k_1$ )	Quadratic coefficient ( $k_2$ )	Cubic coefficient ( $k_3$ )
Real part of DF	$-8.2898e + 05$	$3.6177e + 08$	$2.3771e + 11$
Imaginary part of DF	$1.0504e + 05$	$-1.3231e + 08$	$6.8055e + 10$

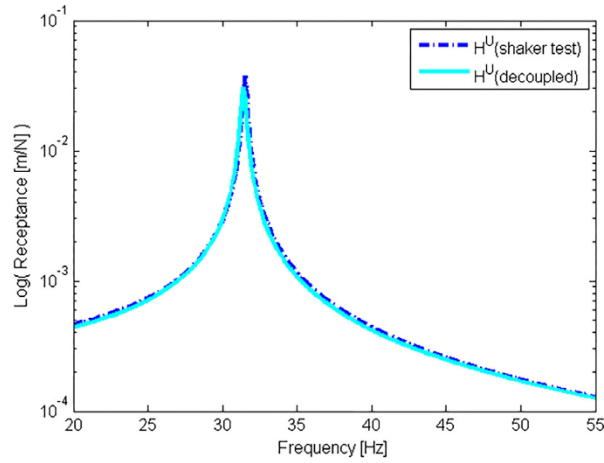


Fig. 18. Point FRFs at the tip of the cantilever beam in transverse direction.

$$v(X, \dot{X}) = k_1 X + k_2 X^2 + k_3 X^3 \quad (11)$$

where  $X$  represents the relative displacement amplitude between end coordinates of the nonlinear element. After identifying nonlinear parameters of the nonlinear subsystem as given in Table 2, FRFs of the known subsystem are calculated for the constant displacement amplitude of 1 mm. Then, FDM-NS is used to obtain point FRFs at the tip of the cantilever beam which is taken as the unknown subsystem. Results are compared with those obtained through shaker test of the cantilever beam alone in Fig. 18.

As can be seen from Fig. 18, a very good agreement is obtained between the FRF curve obtained via decoupling method proposed and FRFs directly measured through shaker test of the linear cantilever beam. It can be concluded that FDM-NS can be successfully and efficiently used for decoupling of a nonlinear subsystem from a given nonlinear coupled system.

## 5. Discussion and conclusions

In this study, dynamic decoupling problem for nonlinear structures is addressed. To the best of authors' knowledge, this paper represents the first attempt to decouple a nonlinear or linear substructure from a given coupled nonlinear structure. The method developed, "FRF Decoupling Method for Nonlinear Systems (FDM-NS)", can be applied when the nonlinearity in a system can be modeled as a single element. It is also assumed in this method that the location of nonlinearity is known.

FDM-NS can be applied to all possible cases regardless of the location of the nonlinear element, i.e. nonlinearity can be either in the known or unknown subsystem, or it can be at the connection. Depending on the location of nonlinearity, whether in the known or unknown substructure, two different formulations are used. For the case where the nonlinear element is at the connection of two subsystems, it is shown how to reduce this problem to that where the nonlinear element is connected to internal DOFs of the known or unknown subsystem.

FDM-NS is validated through simulated and real experimental case studies. Firstly, two different case studies using lumped parameter systems and simulated experimental data are presented. In the first numerical case study, FDM-NS is applied to a MDOF nonlinear system where nonlinearity is in the unknown subsystem. The FRF matrix of the known subsystem is calculated theoretically from known system parameters. Then, sets of linear FRFs are obtained for the coupled system. Each FRF set corresponds to a case where the relative displacement amplitude of two ends of the nonlinear element is kept at a specific value. Performing linear decoupling for each FRF set separately yields a different FRF curve for the unknown subsystem each time. As a result, sets of modal parameters are identified for the unknown subsystem through linear modal identification, each set corresponding to a different response level of the nonlinear element. By using these sets of modal parameters, harmonic response of the unknown subsystem is calculated for a given forcing level iteratively. It is shown in this numerical case study that the nonlinear response predicted by using the decoupling method suggested is almost the same as the one obtained directly by employing HBM.

In the second numerical case study, FDM-NS is applied to a similar MDOF nonlinear system where this time nonlinearity is in the known subsystem. In this case, linear FRFs of the coupled nonlinear system, as well as the known nonlinear subsystem are obtained at a chosen specific displacement level of the nonlinear element. Again, simulated experimental data is used in this study. Then, the unknown subsystem FRFs are obtained by applying linear decoupling. Results obtained show perfect agreement with the exact ones.

Finally, an experimental case study is presented in order to show the real-life application of FDM-NS to structural systems. In this study, a linear cantilever beam is decoupled from the nonlinear T-beam assembly composed of a linear cantilever beam attached to the mid-point of a thin beam of which both ends are fixed and therefore introduces a nonlinear stiffness. The transverse dynamic response of the coupled system is measured experimentally for a specific displacement level of the nonlinear element through controlled displacement amplitude testing. Then, the fixed-fixed thin beam is taken as the known nonlinear substructure and it is modeled as a concentrated nonlinear stiffness in transverse direction with a concentrated equivalent mass and linear stiffness. Linear parameters of this single DOF model of the fixed-fixed thin beam are theoretically calculated whereas its nonlinear parameters are experimentally identified. After obtaining the known substructure FRFs for the same specific displacement level of the nonlinear element, linear decoupling is performed to obtain tip point FRFs of the linear cantilever beam. A very good agreement is observed between the predicted FRFs by using the method developed in this study and those obtained from the shaker test of the cantilever beam alone, even though fixed-fixed thin beam is modeled as a single DOF mass-nonlinear spring system. Consequently, it can be said that the method proposed is a powerful tool for nonlinear structural decoupling problems of similar nature.

It is concluded in this study that, although it has some limitations, considering that it is a first attempt for decoupling a nonlinear structure, FDM-NS may be regarded as a promising tool in obtaining substructure dynamics of a nonlinear structure, starting from experimentally measured FRFs of the coupled nonlinear structure and experimentally measured or theoretically calculated dynamic response of its known substructure.

## References

- [1] R. Craig, M. Bampton, Coupling of substructures for dynamic analysis, *Amer. Inst. Aero. Astro. J.* 6 (7) (1968) 1313–1319.
- [2] J. Hallquist, V.W. Snyder, Synthesis of two discrete vibratory systems using eigenvalue modification, *AIAA J.* 11 (2) (1973) 247–249.
- [3] J.H. Crowley, G.T. Rocklin, A.L. Klosterman, H. Vold, Direct structural modification using frequency response functions, in: Proceedings of the 2nd International Modal Analysis Conference, Orlando, Florida, 1984, pp. 58–65.
- [4] M. Imregün, D.A. Robb, D.J. Ewins, Structural modification and coupling dynamic analysis using FRF data, in: Proceedings of the 5th International Modal Analysis Conference, London, UK, 1987.
- [5] B. Jetmundsen, R.L. Bielawa, W.G. Flannelly, Generalized frequency domain substructure synthesis, *J. Am. Helicopter Soc.* 33 (1) (1988) 55–64.
- [6] A.P.V. Urqueira, Dynamic analysis of coupled structures using experimental data (Ph.D. thesis), Department of Mechanical Engineering, Imperial College London, London, England, 1989 (<http://www.imperial.ac.uk/dynamics/phd-theses/>).
- [7] A. Sestieri, W. D'Ambrogio, A modification method for vibration control of structures, *Mech. Syst. Signal Process.* 3 (3) (1989) 229–253.
- [8] H.N. Özgüven, Structural modifications using frequency response functions, *Mech. Syst. Signal Process.* 4 (1) (1990) 53–63.
- [9] Y. Ren, C.F. Beards, On substructure synthesis with FRF data, *J. Sound Vib.* 185 (5) (1995) 845–866.
- [10] Y.H. Park, Y.S. Park, Structural modification based on measured frequency response functions: An exact eigenproperties reallocation, *J. Sound Vib.* 237 (2000) 411–426.
- [11] J.E. Mottershead, C. Mares, M.I. Friswell, An inverse method for the assignment of vibration nodes, *Mech. Syst. Signal Process.* 15 (2001) 87–100.
- [12] W. Liu, D.J. Ewins, Substructure synthesis via elastic media, *J. Sound Vib.* 257 (2) (2002) 361–379.
- [13] W. D'Ambrogio, A. Sestieri, A unified approach to substructuring and structural modification problems, *Shock Vib.* 11 (3–4) (2004) 295–310.
- [14] A. Kyrianiou, J.E. Mottershead, H. Ouyang, Assignment of natural frequencies by an added mass and one or more springs, *Mech. Syst. Signal Process.* 18 (2) (2004) 263–289.
- [15] D. De Klerk, D.J. Rixen, J. de Jong, Frequency based substructuring (FBS) method reformulated according to the dual domain decomposition method, in: Proceedings of the 24th International Modal Analysis Conference, 2006.
- [16] D. De Klerk, D.J. Rixen, S.N. Voormeeren, General framework for dynamic substructuring: history, review, and classification of techniques, *AIAA J.* 46 (5) (2008) 1169–1181.
- [17] H. Hang, K. Shankar, J.C.S. Lai, Prediction of the effects on dynamic response due to distributed structural modification with additional degrees of freedom, *Mech. Syst. Signal Process.* 22 (8) (2008) 1809–1825.
- [18] R.L. Mayes, Tutorial on experimental dynamic substructuring using the transmission simulator method, in: Proceedings of the 30th International Modal Analysis Conference, 2012.
- [19] B. Sayın, E. Cigeroğlu, A new structural modification method with additional degrees of freedom for dynamic analysis of large systems, in: Proceedings of the 31st International Modal Analysis Conference, 2013.
- [20] K. Watanabe, H. Sato, A modal analysis approach to nonlinear multi-degrees-of freedom system, *ASME J. Vib., Stress, Reliab. Des.* 110 (1988) pp. 410–411.
- [21] J.V. Ferreira, D.J. Ewins, Nonlinear receptance coupling approach based on describing functions, in: Proceedings of the 14th International Modal Analysis Conference, Dearborn, Michigan, USA, 1996, pp. 1034–1040.
- [22] Y.H. Chong, M. Imregün, Coupling of non-linear substructures using variable modal parameters, *Mech. Syst. Signal Process.* 14 (2000) 731–746.
- [23] S. Huang, Dynamic analysis of assembled structures with nonlinearity (Ph.D. thesis), Department of Mechanical Engineering, Imperial College London, London, England, 2007 (<http://www.imperial.ac.uk/dynamics/phd-theses/>).
- [24] R.J. Kuether, M.S. Allen, Structural modification of nonlinear FEA subcomponents using nonlinear normal modes, in: Proceedings of the 31st International Modal Analysis Conference, Garden Grove, California, USA, 2013.
- [25] T. Kalaycıoğlu, H.N. Özgüven, Nonlinear structural modification and nonlinear coupling, *Mech. Syst. Signal Process.* 46 (2) (2014) 289–306.
- [26] F. Wenneker, P. Tiso, A substructuring method for geometrically nonlinear structures, in: Proceedings of the 32nd International Modal Analysis Conference, Orlando, Florida, USA, 2014.
- [27] C. Tepe, E. Cigeroğlu, Structural coupling of two-nonlinear structures, in: Proceedings of the 33rd International Modal Analysis Conference, Orlando, Florida, USA, 2015.
- [28] R.J. Kuether, M.S. Allen, Modal substructuring of geometrically nonlinear finite-element models, *AIAA J.* 54 (2) (2016) 691–702.
- [29] N. Okubo, M. Miyazaki, Development of uncoupling technique and its application, in: Proceedings of 4th International Modal Analysis Conference, 1986.
- [30] C. Gontier, M. Bensaïbi, Time domain identification of a substructure from in situ analysis of the whole structure, *Mech. Syst. Signal Process.* 9 (4) (1995) 379–396.
- [31] N.M.M. Maia, J.M.M. Silva, A.M.R. Ribeiro, P.L.C. Silva, On the dynamic characterization of joints using uncoupling techniques, in: Proceedings of the 16th International Modal Analysis Conference, 1998.
- [32] P. Kalling, T. Abrahamsson, T. McKelvey, Subsystem state-space model identification and its sensitivity to test variability, in: P. Sas, M. De Munck (Eds.), Proceedings of ISMA 2004 – International Conference on Noise and Vibration Engineering, Leuven, Belgium, 2004, pp. 2729–2744.

- [33] W. D'Ambrogio, A. Fregolent, Promises and pitfalls of decoupling procedures, in: Proceedings of the 26th International Modal Analysis Conference, 2008.
- [34] P. Sjövall, T. Abrahamsson, Substructure system identification from coupled system test data, *Mech. Syst. Signal Process.* 22 (1) (2008) 15–33.
- [35] W. D'Ambrogio, A. Fregolent, The role of interface DOFs in decoupling of substructures based on the dual domain decomposition, *Mech. Syst. Signal Process.* 24 (7) (2010) 2035–2048.
- [36] S.N. Voormeeren, D.J. Rixen, A dual approach to substructure decoupling techniques, in: Proceedings of the 28th International Modal Analysis Conference, 2010.
- [37] W. D'Ambrogio, A. Fregolent, Direct decoupling of substructures using primal and dual formulation, in: Proceedings of the 29th International Modal Analysis Conference, 2011.
- [38] F.C. Batista, N.M.M. Maia, Uncoupling techniques for the dynamic characterization of sub-structures, in: Proceedings of the 29th International Modal Analysis Conference, 2011.
- [39] D. Cloutier, P. Avitabile, Dynamic uncoupling of a system model for component identification, in: Proceedings of the 29th International Modal Analysis Conference, 2011.
- [40] W. D'Ambrogio, A. Fregolent, Inverse dynamic substructuring using direct hybrid assembly in the frequency domain, *Mech. Syst. Signal Process.* 45 (2) (2014) 360–377.
- [41] M. Law, H. Rentzsch, S. Ihlenfeldt, M. Putz, Application of substructure decoupling techniques to predict mobile machine tool dynamics: numerical investigations, *Procedia CIRP* 46 (2016) 537–540.
- [42] M. Law, H. Rentzsch, S. Ihlenfeldt, Predicting mobile machine tool dynamics by experimental dynamic substructuring, *Int. J. Mach. Tools Manuf* 108 (2016) 127–134.
- [43] J. Brunetti, A. Culla, W. D'Ambrogio, A. Fregolent, Experimental dynamic substructuring of the Ampair wind turbine test bed, in: Proceedings of the 32nd International Modal Analysis Conference, 2014.
- [44] W. D'Ambrogio, A. Fregolent, Predicting the dynamics of flexible space payloads under different boundary conditions through substructure decoupling, in: Proceedings of the 35th International Modal Analysis Conference, 2017.
- [45] G. Kerschen, K. Worden, A.F. Vakakis, J.C. Golinval, Past, present and future of nonlinear system identification in structural dynamics, *Mech. Syst. Signal Process.* 20 (3) (2006) 505–592.
- [46] J.P. Noël, G. Kerschen, 10 years of advances in nonlinear system identification in structural dynamics: a review, in: Proceedings of ISMA 2016 – International Conference on Noise and Vibration Engineering, Leuven, Belgium, 2016.
- [47] Ö. Arslan, M. Aykan, H.N. Özgüven, Parametric identification of structural nonlinearities from measured frequency response data, *Mech. Syst. Signal Process.* 25 (4) (2011) 1112–1125.
- [48] M.N. Richardson, D.L. Formenti, Parameter estimation from frequency response measurements using rational fraction polynomials, in: Proceedings of the 1st International Modal Analysis Conference, 1982.
- [49] Ö. Tannıkulu, B. Kuran, H.N. Özgüven, M. İmregün, Forced harmonic response analysis of non-linear structures using describing functions, *AIAA J.* 31 (7) (1993) 1313–1320.
- [50] M. Aykan, H.N. Özgüven, Parametric identification of nonlinearity in structural systems using describing function inversion, *Mech. Syst. Signal Process.* 40 (1) (2013) 356–376.

# Experimental Verification of a Recently Developed FRF Decoupling Method for Nonlinear Systems

Taner Kalaycıoğlu<sup>1,2</sup>, H. Nevzat Özgüven<sup>1</sup>

<sup>1</sup>Department of Mechanical Engineering, Middle East Technical University, 06800 Ankara, TURKEY

<sup>2</sup>MGEO Business Sector, ASELSAN Inc., 06011 Ankara, TURKEY

e-mail: tkalayci@aselsan.com.tr, ozguven@metu.edu.tr

## ABSTRACT

The FRF Decoupling Method for Nonlinear Systems (FDM-NS), recently proposed by the authors of this paper, is a technique based on predicting the dynamic behavior of a particular substructure of a coupled nonlinear structure from the knowledge of the measured FRFs of the coupled nonlinear structure and calculated or measured FRFs of the other substructure. The uncoupled substructure can be linear or nonlinear. The method is applicable to systems where the nonlinearity can be represented as a single nonlinear element. The method has been experimentally verified for a structure having a grounded nonlinear element. In this work, the applicability of the method to a structure having an internal nonlinearity is demonstrated. The test system used in this study is composed of two cantilever beams where their free ends are connected to each other with two identical thin beams which introduce an internal nonlinearity to the coupled structure. In this test, the FRFs of the coupled nonlinear assembly are measured in a frequency range for various different constant displacement levels of the nonlinear connection element. Tip point transverse FRFs of one of the cantilever beam, which is taken as the known subsystem, are also measured. By using the decoupling method proposed the modal parameters of the unknown nonlinear subsystem are calculated as a function of the relative displacement amplitude between ends of the nonlinear connection element, from which the dynamic response of the decoupled subsystem can be calculated for any harmonic excitation. In order to demonstrate the accuracy of the method, the decoupled system is connected to a cantilever beam with a different length, and firstly, the FRFs of the coupled new system are calculated for constant amplitude harmonic forcing. Then, the calculated FRF curves are compared with those which are directly measured.

**Keywords:** Nonlinear decoupling, nonlinear uncoupling, nonlinear inverse substructuring, nonlinear subsystem identification, nonlinear substructure decoupling

## 1 INTRODUCTION

Most of the engineering structures are designed as an assembly of several parts and usually various alternatives are studied within design period. It is computationally expensive to perform FE analysis each time while reviewing these design alternatives. Hence, several structural coupling methods have been developed in order to reduce the computational effort in dynamic reanalysis of such systems [1-19]. Although there are several different coupling methods based on the linearity assumption in literature, engineering structures are usually nonlinear by nature. In the past three decades, structural coupling of nonlinear subsystems has been well investigated and various coupling methods have been developed considering the nonlinear effect [20-28].

Likewise, considerable effort has also been devoted to the reverse problem, i.e. structural decoupling of linear systems. This problem arises when the dynamic behavior of a subsystem cannot be measured due to difficulty in measuring and/or exciting it individually, yet it is possible to test the whole system as well as the other subsystems. The first investigation on decoupling problem was made by Okubo and Miyazaki [29] where they have proposed an uncoupling method to extract the dynamics of a bearing itself. Later, Gontier and Bensaïbi [30] presented a time domain method for in situ identification of joints through modal analysis of their assembled structure. Maia et al. [31] presented a decoupling methodology particularly for the dynamic

---

\* T. Kalaycıoğlu, H.N. Özgüven, FRF Decoupling Method for Nonlinear Systems – An Experimental Application, in: Proceedings of the 36th IMAC, A Conference on Structural Dynamics, Orlando, Florida, USA, 2018.



characterization of joints without making any FRF measurement at the joints. Kalling et al. [32] also worked on the decoupling problem by performing state-space model identification along with a sensitivity analysis showing possible ill-conditioning due to inertia ratios at the interface. D'Ambrogio and Fregolent [33] proposed impedance and mobility based approaches that suffers from ill-conditioning problems due to the internal resonances of the known subsystem with fixed interface. Sjövall and Abrahamsson [34] proposed a subsystem identification method that is based on reconstruction of the interface forces acting between the unknown subsystem and its neighbor. A general framework for dynamic substructuring is provided in [15] and [16] in which the so called dual domain decomposition technique that allows retaining the full set of global degrees of freedom (DOFs) by ensuring equilibrium at the interface between substructures is introduced. When performing substructuring by using the dual domain decomposition, the coupling problem can be directly formulated from [16], whereas a similar formulation for the decoupling problem is developed and discussed in [35] for collocated approach where DOFs used to enforce equilibrium are the same as DOFs used to enforce compatibility, and in [36] and [37] for non-collocated approach where DOFs used to enforce equilibrium are not the same as DOFs used to enforce compatibility. Batista and Maia [38] proposed three different formulations based on the classical decoupling procedure of Jetmundsen et al. [5] considering the effects of including different sets of DOFs on the coupled system. They concluded that the formulation that needs measurements at the connection point of substructures gives the best results. D'Ambrogio and Fregolent [39] also proposed the so-called hybrid assembly approach which gives similar results as dual assembly approach [35] in terms of the predicted FRFs of an unknown subsystem when applied to an experimental test bed. Dual assembly approach [35] was afterwards used to predict the subsystem dynamics in machine tools [40, 41], wind turbines [42] and flexible space payloads [43].

Although the dynamic decoupling problem of linear structures is well investigated in literature, the first study on dynamic decoupling problem of nonlinear structures was given quite recently by the authors of this paper [44]. The present study is based on a real-life application of this recently developed method, which is called FDM-NS (FRF Decoupling Method for Nonlinear Systems). The method can predict the FRFs of an unknown subsystem, whether linear or nonlinear, from the measured FRFs of the coupled nonlinear system and the measured or calculated FRFs of the remaining known subsystem. This method can be used for any type of nonlinearity provided that nonlinearity can be modeled as a single nonlinear element and its location is known. In this paper, a nonlinear experimental test rig is used in order to demonstrate the validity of FDM-NS in real life practice. Note that the experimental test system used in this paper differs mainly from the one given in [44] in terms of the location of the nonlinear element and availability of its parameters.

## 2 THEORY

In this section, the approaches used in FDM-NS are briefly summarized. The details of the theory of the method can be found in [44]. The decoupling problem can be studied in three different categories, based on the location of nonlinear element in the coupled system: The nonlinearity can be either in the unknown or in the known subsystem, or it can connect two subsystems.

### 2.1 Nonlinearity in the Unknown Subsystem

This is the case where the nonlinearity which can be modelled as a single nonlinear element is in the unknown subsystem and therefore its parameters are not available. The following approach is developed for this case after examining available nonlinear system identification techniques in literature, detailed reviews of which are presented by Kerschen et al. [45] and Noël et al. [46]. Firstly, the complete FRF matrix of the linear known subsystem for the coordinates of interest can be obtained either by using its available system parameters or experimentally. Also, sets of linear FRFs of the coupled system for the coordinates of interest can be measured via controlled response amplitude testing each set of which corresponds to a different displacement level of the nonlinear element. Then, sets of linear FRF curves for the unknown subsystem can be calculated by applying a decoupling method for linear systems (dual assembly approach [35] is used in this paper) to each set of coupled system FRFs measured. Finally, each FRF curve set can be identified through the modal identification technique developed by Richardson and Formenti [47]. Since each set of coupled system FRFs corresponds to a different displacement level of the nonlinear element, identified modal parameters of the unknown subsystem FRFs can be expressed as a function of the magnitude of the relative harmonic displacement between end coordinates of the nonlinear element [48]. As a result, unknown subsystem FRFs can be calculated for any level of excitation using the obtained modal parameter variations.

### 2.2 Nonlinearity in the Known Subsystem

This is the case where the nonlinearity which can be modelled as a single nonlinear element is in the known subsystem and therefore its parameters are available. Firstly, the point and transfer FRFs of the coupled system as well as of the known subsystem at coordinates that belong to the known subsystem should be obtained for a specific displacement level of the nonlinear element throughout the frequency range of interest [48]. This will ensure that the nonlinearity matrices [49], which are involved in the dynamic stiffness matrices of the coupled system and the known subsystem, will have the same values at each frequency point throughout the desired frequency range. While FRFs of the known subsystem can be calculated using its

available parameters, those of the coupled system have to be measured by performing controlled displacement amplitude testing. Note that including the same nonlinearity matrix into the dynamic stiffness matrices of the coupled system and the known subsystem mathematically corresponds to adding an additional stiffness matrix to the known parts of both systems. Thus, the problem can be reduced into decoupling of linear systems. So, FRFs of the unknown subsystem at its connection DOFs can be calculated via direct application of a linear decoupling approach.

### 2.3 Nonlinearity at the Connection of Two Subsystems

This is the case where a nonlinear element connects two subsystems. Based on the existence of the nonlinear element parameters, this problem can be transformed into one of those defined in section 2.1 or section 2.2. If the parameters of the nonlinear connection element are not available, the nonlinear element will be a part of the unknown subsystem. Then a massless node can be defined at the end coordinate of the nonlinear element which will be rigidly connected to the known subsystem when coupled. So, the problem transforms into the one considered in section 2.1. If the parameters of the nonlinear connection element are available, the problem can likewise be transformed into the one given in section 2.2.

## 3 EXPERIMENTAL APPLICATION

In this section, FDM-NS is applied to a nonlinear experimental test system in order to validate it through a real-life application. This experiment is a practical implementation of the case where nonlinearity is at the connection of two subsystems. Firstly, FRFs of the coupled system are measured at several different constant harmonic displacement levels of the nonlinear connection element. Then, FRFs of the known subsystem are also measured via modal testing and FDM-NS is applied. Thus, the modal parameters of the nonlinear unknown subsystem are calculated as a function of the magnitude of the relative harmonic displacement between end coordinates of the nonlinear element. Afterwards, in order to study the validity of the dynamic properties of the uncoupled nonlinear subsystem, the nonlinear subsystem is coupled to another beam which is longer than the previous one, and its FRFs are measured again through modal testing. Finally, measured FRFs of the new subsystem are coupled with those of the decoupled subsystem by using the modal parameter variations obtained. Calculated FRFs of the coupled new system are compared with those obtained performing controlled force amplitude testing on it.

### 3.1.1 Experimental Setup

The setup consists of a long cantilever beam and a shorter one connected tip to tip with each other by means of two thin identical beams which introduce nonlinear stiffness to the overall system. Both cantilever beams are of St37 steel alloy while the thin connection beams are of 6061-T3 aluminum alloy. Each cantilever beam is riveted to two thin identical beams in order to have fixed connections. A view of the experimental setup is given in Fig. 1. The dimensions and technical details of the test system are also illustrated in the same figure.

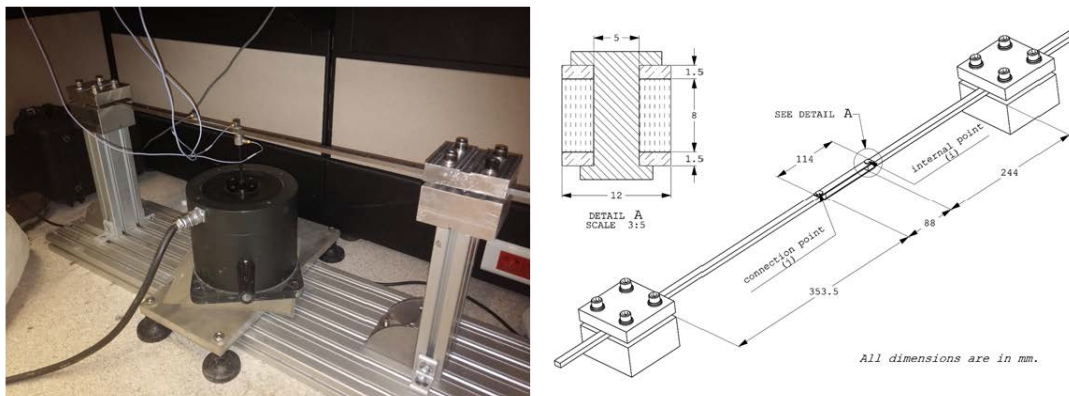


Fig. 1. View of the experimental setup (left) with its dimensions and technical details (right)

It is very difficult to achieve perfect fixed boundary conditions in physical applications. Therefore, both cantilever beams were manufactured longer than their effective lengths of 353.5 and 244 mm, respectively, so that the excess lengths could be squeezed between fixture blocks. A list of equipment used in the experiment is given in Table 1.

**Table 1.** List of modal test equipment

<b>Data Acquisition System</b>	Brüel&Kjaer Type 3560 C Frontend
<b>Shaker</b>	Brüel&Kjaer Type 4808
<b>Force Transducer</b>	Brüel&Kjaer Type 8230-002
<b>Power Amplifier</b>	Brüel&Kjaer Type 2712
<b>Accelerometer</b>	Brüel&Kjaer 4507B

### 3.1.2 The Preliminary Analyses

As explained in previous section, the experimental test system is mainly composed of two cantilever beams with different lengths. The longer one is taken as the linear known substructure. Two thin identical beams connect two cantilever beams to each other from their free ends and thus introduce nonlinearity into the coupled system. Due to unavailability of the type and parameter information regarding the nonlinear connection elements, short cantilever beam together with the two thin identical beams is considered as the unknown substructure. The aim in this application is to decouple this unknown substructure from the coupled cantilever beams. Preliminary modal analysis is performed in advance using a commercial FEA software to determine a proper frequency range for the FRF measurements, so that it includes the fundamental natural frequencies of the coupled structure and the known substructure. Modeling errors in the FEM of the analyzed structures are minimized by including the mass loading effects of the sensors in the analyses. The first natural frequency of the coupled cantilever beams is calculated as 72.2 Hz by performing modal analysis with ANSYS R15.0<sup>®</sup>. Results are illustrated in Fig. 2 along with the corresponding mode shape.

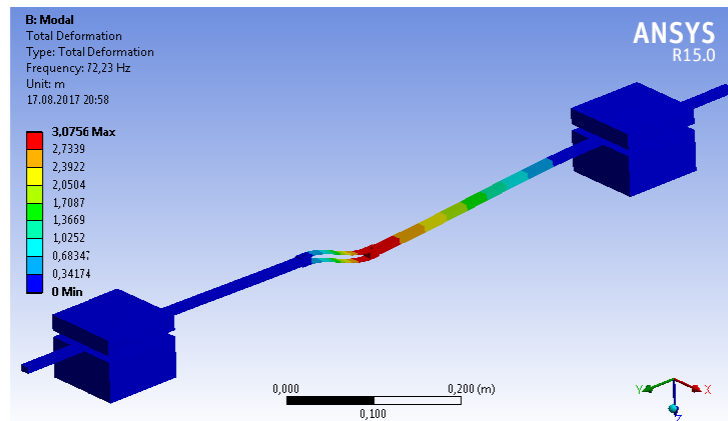


**Fig. 2.** Fundamental mode of the coupled cantilever beams

On the other hand, the fundamental natural frequency of the longer cantilever beam alone is obtained as 52.9 Hz by performing modal analysis with ANSYS R15.0<sup>®</sup>. The ANSYS result is presented in Fig. 3.

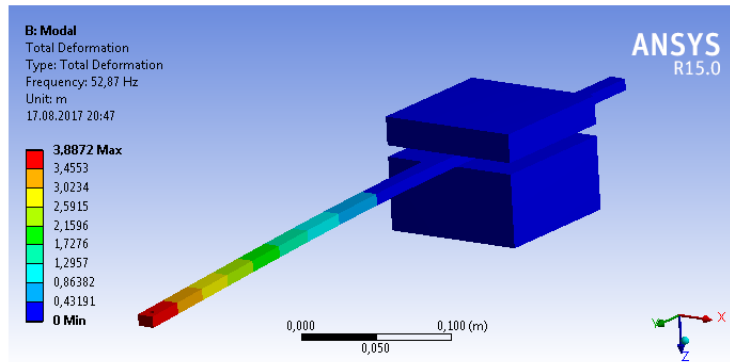


Fig. 3. Fundamental mode of the long cantilever beam alone

As a consequence, the frequency span to be used in the experiments is determined as 35 to 91 Hz which covers the wide neighborhood of pre-estimated fundamental resonances of the coupled cantilever beams and the long cantilever beam itself.

### 3.1.3 Experimental Work and Application of FDM-NS

As the initial step, point and transfer FRFs of the coupled cantilever beams in transverse direction ( $H_{jj}^{KU}$  and  $H_{ji}^{KU}$ , respectively) are experimentally obtained by employing constant displacement amplitude test procedure given in Fig. 4. An adaptive frequency resolution is employed during measurements so that the frequency resolution is further improved in the close neighborhood of the fundamental resonance.

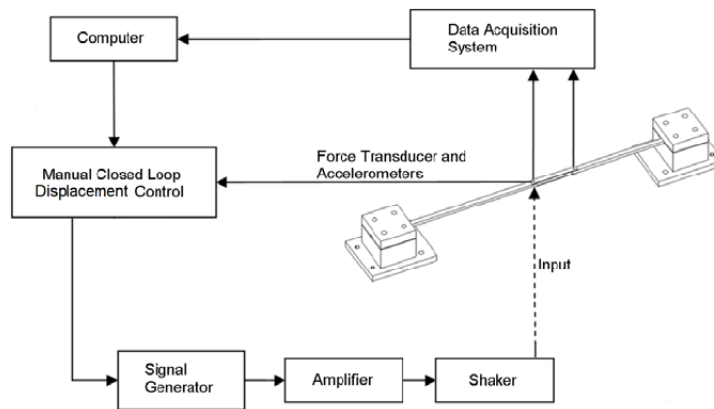
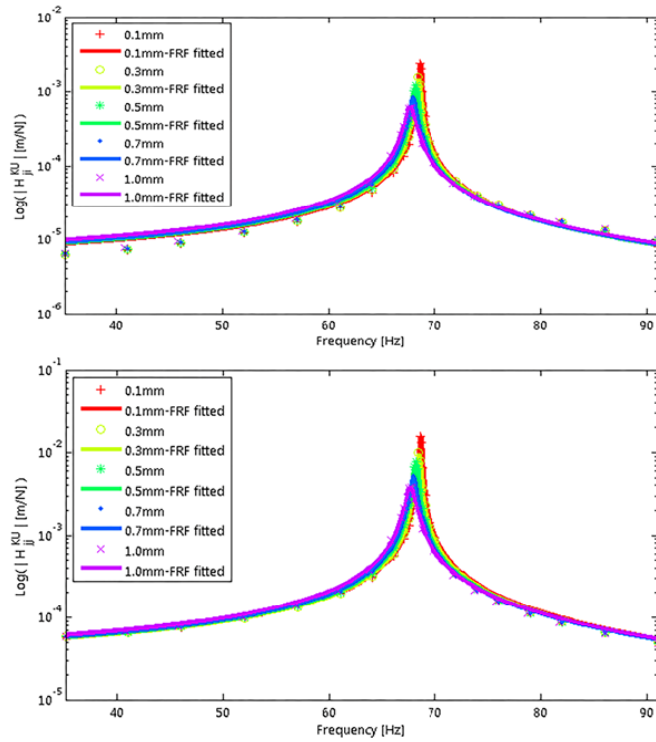


Fig. 4. Experimental procedure followed during constant displacement/force amplitude test

In order to obtain relative transverse displacement between two ends of the thin identical beams, an additional measurement is taken from the tip of the short cantilever beam. A number of modal tests are conducted for different amplitudes of the relative harmonic displacement (0.1, 0.3, 0.5, 0.7 and 1.0 mm) between two ends of the nonlinear element. Measured data points are given along with FRF curves fitted to them in Fig. 5.



**Fig. 5.** Measured transfer FRFs (symbols) and fitted FRF curves (lines) of the coupled system at internal point (i) and at connection point (j) in transverse direction for various response levels of the nonlinear element

As the next step, tip point FRFs of the long cantilever beam are measured by conducting a modal test under transverse excitation. Results are shown in Fig. 6 in the form of a fitted FRF curve to experimental data.

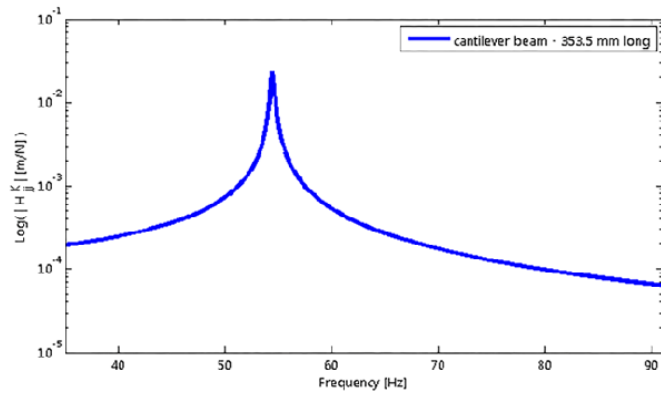


**Fig. 6.** FRF curve fitted to measured point FRFs of the known subsystem alone at its coupling DOF (j) in transverse direction

FRFs of the unknown substructure at its coupling DOF are obtained for various different harmonic displacement amplitudes of the nonlinear element by applying FDM-NS. Dual assembly approach [35] is used during decoupling calculations. Calculated unknown substructure FRFs are shown in Fig. 7 together with those of the coupled structure given in Fig. 5.

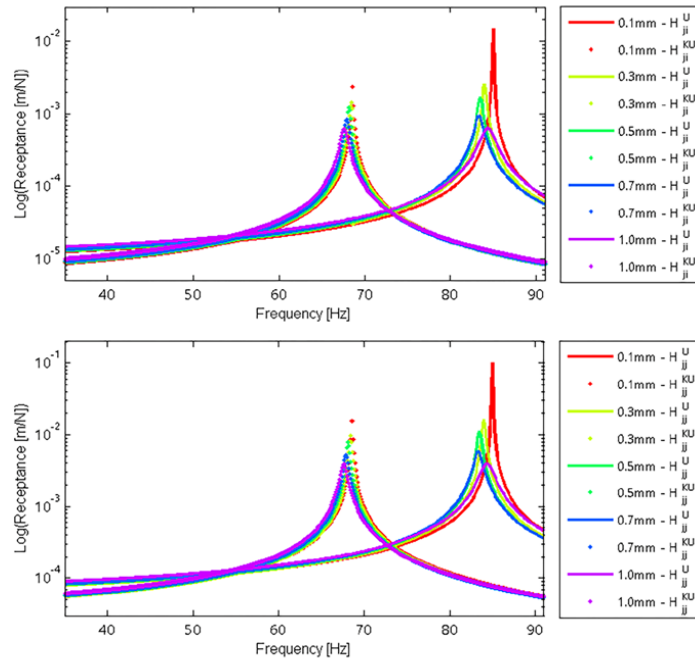


**Fig. 7.** Calculated point (above) and transfer (below) FRFs of the unknown subsystem (lines) and those of the coupled system (dots) under transverse excitation at connection point (j)

Not surprisingly, decoupling of the nonlinear subsystem from coupled nonlinear system by using a single linear FRF curve for long cantilever beam and several equivalent linear FRF curves for the coupled nonlinear structure, leads to several FRF curves each of which again corresponds to different displacement levels of the nonlinear connection element. It should be emphasized that FRF curves obtained for the unknown subsystem includes the nonlinear connection dynamics which could not be directly measured.

Each FRF curve obtained for the unknown subsystem is identified in order to construct the modal model of it as explained in section 2.1. Modal parameters corresponding to each FRF curve are extracted using a linear modal identification as they show linear behavior. Modal parameters in the form of natural frequencies, modal loss factors and modal constants of the unknown subsystem are identified by using the formulation suggested by Richardson and Formenti [47]. Since a modal constant is a complex quantity for a damped system, its magnitudes and phases are identified separately. Modal parameters related to the first mode of the unknown nonlinear subsystem are identified for point ( $H_{jj}^U$ ) and transfer ( $H_{ji}^U$ ) FRFs. Identified values for various values of the relative harmonic displacement amplitude of the nonlinear element are shown in Fig. 8 and Fig. 9.

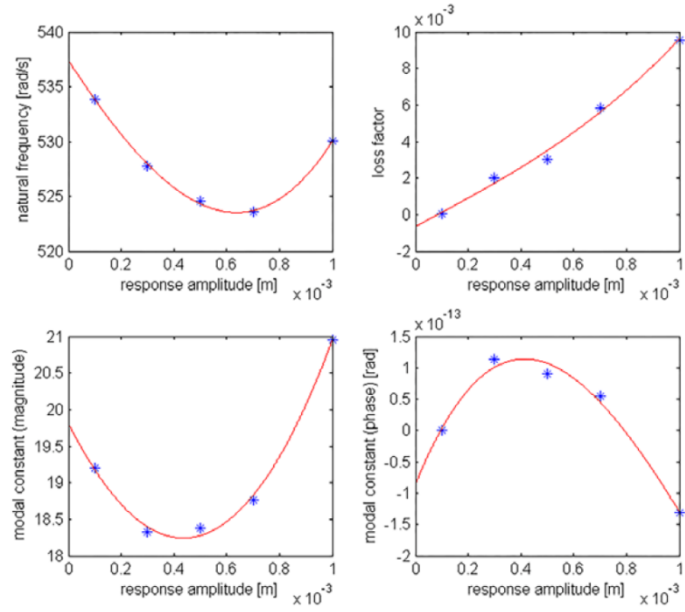


**Fig. 8.** Variation of the modal parameters of the unknown nonlinear subsystem at the first mode for  $\mathbf{H}_{jj}^U$  with the relative response amplitude,  $|\mathbf{X}_j - \mathbf{X}_i|$  (\*, identified parameters & —, fitted curves)

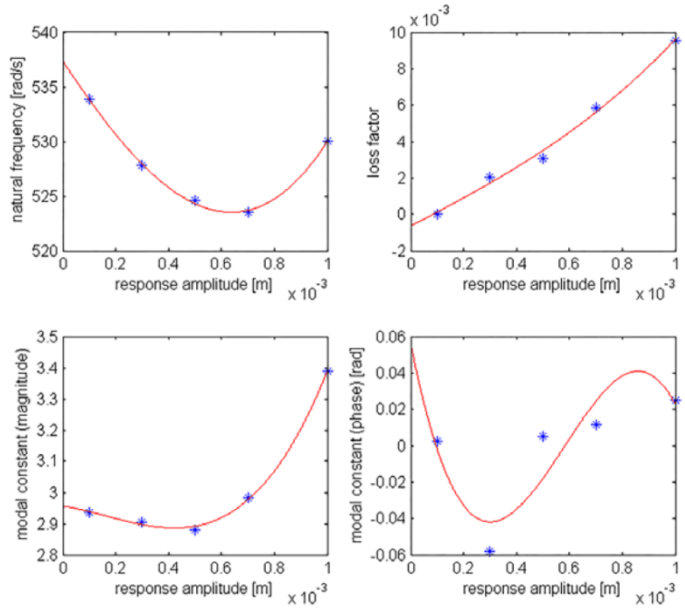


**Fig. 9.** Variation of the modal parameters of the unknown nonlinear subsystem at the first mode for  $\mathbf{H}_{ji}^U$  with the relative response amplitude,  $|\mathbf{X}_j - \mathbf{X}_i|$  (\*, identified parameters & —, fitted curves)

### 3.1.4 Verification of FDM-NS

In this section, it is aimed to verify the decoupling results obtained via FDM-NS in section 3.1.3. However, as the nonlinearity is due to the tension in thin beams, modal testing of the unknown subsystem itself will not give the correct dynamics of this subsystem. Therefore, the identified nonlinear subsystem is coupled to a longer cantilever beam and a coupled new system is obtained as shown in Fig. 10, and its dynamic response is predicted by using the decoupled subsystem dynamics, so that it can be compared with measured values for the verification of FDM-NS.

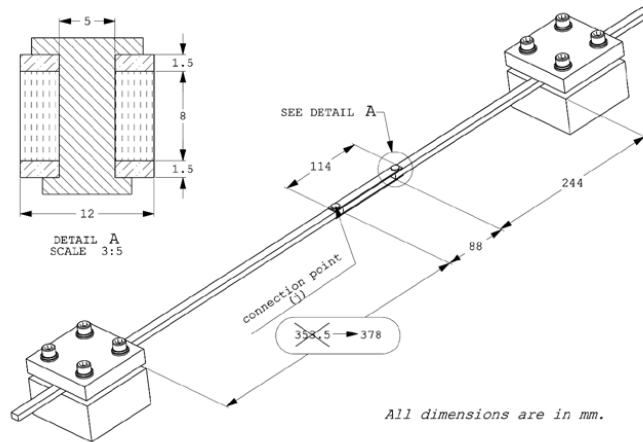


Fig. 10. Dimensions and technical details of the new test system

In this new test system, the decoupled subsystem is coupled to a longer cantilever beam of length 378 mm. Firstly, FRFs of 378 mm long cantilever beam alone are measured at its free tip by performing modal testing. The results obtained are given in Fig. 11 along with those obtained for 353.5 mm long cantilever beam used in section 3.1.3.

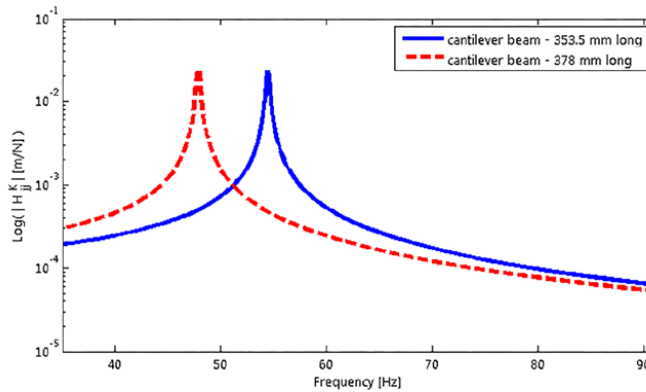


Fig. 11. FRF curves fitted to measured point FRFs of the known subsystems (both original and new) at their coupling DOF (j) in transverse direction

As the next step, FRFs of the decoupled subsystem and those of the 378 mm long cantilever beam are coupled in order to obtain the response of the coupled new system. It should be noted that an iterative solution is required for the computation, as the modal parameters of the decoupled subsystem obtained in section 3.1.3 are dependent on the displacement level of the nonlinear



element. Thus, the response of the coupled new system is numerically obtained for a harmonic excitation of magnitude 0.4 N, applied transversely to the connection point j.

Finally, point FRFs of the new test system are measured again for a harmonic excitation of amplitude 0.4 N applied to the connection point j in transverse direction. In this test, the same procedure given in Fig. 4 is followed where harmonic forcing level is controlled by manually regulating the voltage output of the power amplifier at each frequency step this time. Measured and numerically calculated point FRFs of the coupled new system at its coupling DOF are compared in Fig. 12. A zoomed comparison around resonance is given in Fig. 13.

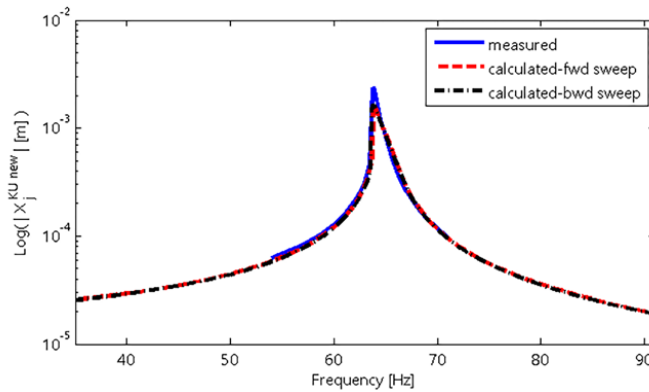


**Fig. 12.** Measured and calculated point FRFs of the coupled new system at its coupling DOF for harmonic forcing amplitude of 0.4 N in transverse direction

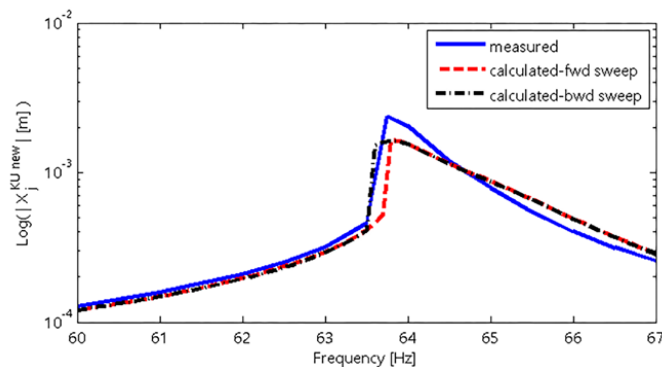


**Fig. 13.** Measured and calculated point FRFs of the coupled new system at its coupling DOF for harmonic forcing amplitude of 0.4 N in transverse direction – zoomed in the frequency range of 60-67 Hz

It can be observed from Fig. 12 and Fig. 13 that nonlinearity introduces softening stiffness, and measured response agrees quite well with those calculated through forward and backward frequency sweeping, particularly around frequency that jump occurs. Small discrepancy observed between the magnitudes of the resonances is believed to be due to the inaccuracies in extracting the loss factors from experimental FRFs. Because, unlike the case in linear systems, several controlled displacement amplitude tests are performed on the coupled nonlinear system, and therefore quite less number of frequency points had to be used in measuring FRFs, due to technical issues. Although frequency resolution is further increased in the immediate vicinity of the resonance, it may not be good enough to catch the frequency where the peak amplitude occurs. As a result, the unknown subsystem FRFs obtained through decoupling using these measured FRFs may involve some errors which may be due to the misidentified loss factor values.

#### 4 DISCUSSION AND CONCLUSIONS

In this work, the FRF Decoupling Method for Nonlinear Systems (FDM-NS) proposed recently [44] is applied to a test system in order to show its real-life applicability and validity. This method, which is believed to be the first method proposed for nonlinear decoupling, is capable of decoupling nonlinear systems having a nonlinearity of any type that can be modeled as a single element. Yet, the method allows the nonlinearity be either in the known or unknown subsystem, or connect both subsystems.

The proposed technique is applied to an experimental test system composed of two cantilever beams coupled with two thin identical beams. This study is an implementation of the case where two linear subsystems are coupled with an unknown nonlinear connection element. First, FRFs of the coupled system are measured through controlled displacement amplitude testing, while those of the known cantilever beam are obtained via classical modal testing. Then, modal parameter variations of the unknown subsystem are obtained as a function of the displacement level of the nonlinear element by applying FDM-NS. In order to verify these results, the experimental test system is modified such that the length of the known subsystem is increased whose FRFs are again obtained via classical modal testing. Then, the FRFs of the new system are calculated for a constant amplitude harmonic force by using the modal parameter variations of the unknown subsystem along with FRFs of the modified known subsystem. Finally, they are compared with those directly measured. Although the calculated results show slight deviations from the measured values around resonance, it is concluded that the agreement is quite well.

In this study, FDM-NS is verified for a practical case, where the nonlinear element couples two linear structures such that the unknown nonlinear subsystem cannot be tested alone. It can be concluded that FDM-NS proves itself as a promising tool in obtaining substructure dynamics of a nonlinear structure.

#### 5 REFERENCES

- [1] R. Craig, M. Bampton, Coupling of substructures for dynamic analysis, *American Institute of Aeronautics and Astronautics Journal*, 6 (7) (1968) 1313-1319.
- [2] J. Hallquist, V.W. Snyder, Synthesis of two discrete vibratory systems using eigenvalue modification, *AIAA Journal*, 11 (2) (1973) 247-249.
- [3] J.H. Crowley, G.T. Rocklin, A.L. Klosterman, H. Vold, Direct structural modification using frequency response functions, in: *Proceedings of the 2nd International Modal Analysis Conference*, Orlando, Florida, 1984, pp.58-65.
- [4] M. İmregün, D.A. Robb, D.J. Ewins, Structural modification and coupling dynamic analysis using FRF data, in: *Proceedings of the 5th International Modal Analysis Conference*, London, UK, 1987.
- [5] B. Jetmundsen, R.L. Bielawa, W.G. Flannelly, Generalized frequency domain substructure synthesis, *Journal of the American Helicopter Society*, 33 (1) (1988) 55-64.
- [6] A.P.V. Ugueira, *Dynamic analysis of coupled structures using experimental data* (Ph.D. thesis), Department of Mechanical Engineering, Imperial College London, London, England, 1989 (<http://www.imperial.ac.uk/dynamics/phd-theses/>).
- [7] A. Sestieri, W. D'Ambrogio, A modification method for vibration control of structures, *Mechanical Systems and Signal Processing*, 3 (3) (1989) 229-253.
- [8] H.N. Özgüven, Structural modifications using frequency response functions, *Mechanical Systems and Signal Processing*, 4 (1) (1990) 53-63.
- [9] Y. Ren, C.F. Beards, On substructure synthesis with FRF data, *Journal of Sound and Vibration*, 185 (5) (1995) 845-866.
- [10] Y.H. Park, Y.S. Park, Structural modification based on measured frequency response functions: An exact eigenproperties reallocation, *Journal of Sound and Vibration*, 237 (2000) 411-426.
- [11] J.E. Mottershead, C. Mares, M.I. Friswell, An inverse method for the assignment of vibration nodes, *Mechanical Systems and Signal Processing*, 15 (2001) 87-100.
- [12] W. Liu, D.J. Ewins, Substructure synthesis via elastic media, *Journal of Sound and Vibration*, 257 (2) (2002) 361-379.
- [13] W. D'Ambrogio, A. Sestieri, A unified approach to substructuring and structural modification problems, *Shock and Vibration*, 11 (3-4) (2004) 295-310.
- [14] A. Kyprianou, J.E. Mottershead, H. Ouyang, Assignment of natural frequencies by an added mass and one or more springs, *Mechanical Systems and Signal Processing*, 18 (2) (2004) 263-289.
- [15] D. De Klerk, D.J. Rixen, J. de Jong, Frequency based substructuring (FBS) method reformulated according to the dual domain decomposition method, in: *Proceedings of the 24th International Modal Analysis Conference*, 2006.
- [16] D. De Klerk, D.J. Rixen, S.N. Voormeeren, General framework for dynamic substructuring: history, review, and classification of techniques, *AIAA Journal*, 46 (5) (2008) 1169-1181.
- [17] H. Hang, K. Shankar, J.C.S. Lai, Prediction of the effects on dynamic response due to distributed structural modification with additional degrees of freedom, *Mechanical Systems and Signal Processing*, 22 (8) (2008) 1809-1825.

- [18] R.L. Mayes, Tutorial on experimental dynamic substructuring using the transmission simulator method, in: Proceedings of the 30th International Modal Analysis Conference, 2012.
- [19] B. Sayın, E. Cığeroğlu, A new structural modification method with additional degrees of freedom for dynamic analysis of large systems, in: Proceedings of the 31st International Modal Analysis Conference, 2013.
- [20] K. Watanabe, H. Sato, A modal analysis approach to nonlinear multi-degrees-of freedom system, *Journal of Vibration, Acoustics, Stress, and Reliability in Design*, 110 (1988) 410–411.
- [21] J.V. Ferreira, D.J. Ewins, Nonlinear receptance coupling approach based on describing functions, in: Proceedings of the 14th International Modal Analysis Conference, Dearborn, Michigan, USA, 1996, pp.1034–1040.
- [22] Y.H. Chong, M. İmregün, Coupling of non-linear substructures using variable modal parameters, *Mechanical Systems and Signal Processing*, 14 (2000) 731–746.
- [23] S. Huang, Dynamic analysis of assembled structures with nonlinearity (Ph.D. thesis), Department of Mechanical Engineering, Imperial College London, London, England, 2007 (<http://www.imperial.ac.uk/dynamics/phd-theses/>).
- [24] R.J. Kuether, M.S. Allen, Structural modification of nonlinear FEA subcomponents using nonlinear normal modes, in: Proceedings of the 31st International Modal Analysis Conference, Garden Grove, California, USA, 2013.
- [25] T. Kalaycıoğlu, H.N. Özgüven, Nonlinear structural modification and nonlinear coupling, *Mechanical Systems and Signal Processing*, 46 (2) (2014) 289–306.
- [26] F. Wenneker, P. Tiso, A substructuring method for geometrically nonlinear structures, in: Proceedings of the 32nd International Modal Analysis Conference, Orlando, Florida, USA, 2014.
- [27] C. Tepe, E. Cığeroğlu, Structural coupling of two-nonlinear structures, in: Proceedings of the 33rd International Modal Analysis Conference, Orlando, Florida, USA, 2015.
- [28] R.J. Kuether, M.S. Allen, Modal substructuring of geometrically nonlinear finite-element models, *AIAA Journal*, 54 (2) (2016) 691-702.
- [29] N. Okubo, M. Miyazaki, Development of uncoupling technique and its application, in: Proceedings of 4th International Modal Analysis Conference, 1986.
- [30] C. Gontier, M. Bensaïbi, Time domain identification of a substructure from in situ analysis of the whole structure, *Mechanical Systems and Signal Processing*, 9 (4) (1995) 379-396.
- [31] N.M.M. Maia, J.M.M. Silva, A.M.R. Ribeiro, P.L.C. Silva, On the dynamic characterization of joints using uncoupling techniques, in: Proceedings of the 16th International Modal Analysis Conference, 1998.
- [32] P. Kalling, T. Abrahamsson, T. McKelvey, Subsystem state-space model identification and its sensitivity to test variability, in: P. Sas, M. De Munck (Eds.), Proceedings of ISMA 2004 - International Conference on Noise and Vibration Engineering, Leuven, Belgium, 2004, pp. 2729-2744.
- [33] W. D'Ambrogio, A. Fregolent, Promises and pitfalls of decoupling procedures, in: Proceedings of the 26th International Modal Analysis Conference, 2008.
- [34] P. Sjövall, T. Abrahamsson, Substructure system identification from coupled system test data, *Mechanical Systems and Signal Processing*, 22 (1) (2008) 15-33.
- [35] W. D'Ambrogio, A. Fregolent, The role of interface DOFs in decoupling of substructures based on the dual domain decomposition, *Mechanical Systems and Signal Processing*, 24 (7) (2010) 2035-2048.
- [36] S.N. Voormeeren, D.J. Rixen, A dual approach to substructure decoupling techniques, in: Proceedings of the 28th International Modal Analysis Conference, 2010.
- [37] W. D'Ambrogio, A. Fregolent, Direct decoupling of substructures using primal and dual formulation, in: Proceedings of the 29th International Modal Analysis Conference, 2011.
- [38] F.C. Batista, N.M.M. Maia, Uncoupling techniques for the dynamic characterization of sub-structures, in: Proceedings of the 29th International Modal Analysis Conference, 2011.
- [39] W. D'Ambrogio, A. Fregolent, Inverse dynamic substructuring using direct hybrid assembly in the frequency domain, *Mechanical Systems and Signal Processing*, 45 (2) (2014) 360–377.
- [40] M. Law, H. Rentzsch, S. Ihlenfeldt, M. Putz, Application of substructure decoupling techniques to predict mobile machine tool dynamics: numerical investigations, *Procedia CIRP*, 46 (2016) 537–540.
- [41] M. Law, H. Rentzsch, S. Ihlenfeldt, Predicting mobile machine tool dynamics by experimental dynamic substructuring, *International Journal of Machine Tools and Manufacture*, 108 (2016) 127–134.
- [42] J. Brunetti, A. Culla, W. D'Ambrogio, A. Fregolent, Experimental dynamic substructuring of the Ampair wind turbine test bed, in: Proceedings of the 32nd International Modal Analysis Conference, 2014.
- [43] W. D'Ambrogio, A. Fregolent, Predicting the dynamics of flexible space payloads under different boundary conditions through substructure decoupling, in: Proceedings of the 35th International Modal Analysis Conference, 2017.
- [44] T. Kalaycıoğlu, H.N. Özgüven, FRF Decoupling of Nonlinear Systems, *Mechanical Systems and Signal Processing*, 102 (2018) 230-244 (<https://doi.org/10.1016/j.ymssp.2017.09.029>).
- [45] G. Kerschen, K. Worden, A.F. Vakakis, J.C. Golinval, Past, present and future of nonlinear system identification in structural dynamics, *Mechanical Systems and Signal Processing*, 20 (3) (2006) 505-592.

- [46] J.P. Noël, G. Kerschen, 10 years of advances in nonlinear system identification in structural dynamics: A review, in: Proceedings of ISMA 2016 - International Conference on Noise and Vibration Engineering, Leuven, Belgium, 2016.
- [47] M.N. Richardson, D.L. Formenti, Parameter Estimation from Frequency Response Measurements Using Rational Fraction Polynomials, Proceedings of the 1st International Modal Analysis Conference, 1982.
- [48] Ö. Arslan, M. Aykan, H.N. Özgüven, Parametric Identification of Structural Nonlinearities from Measured Frequency Response Data, *Mechanical Systems and Signal Processing*, 25 (4) (2011) 1112-1125.
- [49] Ö. Tanrikulu, B. Kuran, H.N. Özgüven, M. İmregün, Forced Harmonic Response Analysis of Non-linear Structures using Describing Functions, *AIAA Journal*, 31 (7) (1993) 1313-1320.

## CURRICULUM VITAE

### PERSONAL INFORMATION

Surname, Name: Kalaycıođlu, Taner

Nationality: Turkish (T.C.)

Date and Place of Birth: 3 November 1985, Zonguldak

Marital Status: Married

Phone: +90 544 643 32 39

Email: [kalayci.taner@gmail.com](mailto:kalayci.taner@gmail.com)

### EDUCATION

Degree	Institution	Year of Graduation
MS	METU Mechanical Engineering	2011
BS	METU Mechanical Engineering	2008
High School	Zonguldak High School of Science	2003

### WORK EXPERINCE

Year	Place	Enrollment
2008-Present	Aselsan	Mechanical Design Engineer
2007 July	Aselsan	Intern Engineering Student
2006 August	Erdemir	Intern Engineering Student

### FOREIGN LANGUAGES

Advanced English, Intermediate German

## PUBLICATIONS

1. T. Kalaycıođlu, H.N. Özgüven, Doğrusal Olmayan Deđişikliğe Uđrayan Büyük Mühendislik Yapılarının Harmonik Titreşim Analizi, in: Proceedings of the 15th National Symposium on Theory of Machines, Niğde, Turkey, 2011.
2. T. Kalaycıođlu, H.N. Özgüven, Harmonic Response of Large Engineering Structures with Nonlinear Modifications, in: Proceedings of the 8th International Conference on Structural Dynamics, EURO DYN 2011, Leuven, Belgium, 2011, pp. 3623-3629.
3. T. Kalaycıođlu, H.N. Özgüven, Nonlinear Structural Modification and Nonlinear Coupling, in: Topics in Nonlinear Dynamics, vol. 3, Proceedings of the 30th IMAC, A Conference on Structural Dynamics, Springer, New York, 2012, pp. 225-237, [https://doi.org/10.1007/978-1-4614-2416-1\\_18](https://doi.org/10.1007/978-1-4614-2416-1_18).
4. T. Kalaycıođlu, H.N. Özgüven, Nonlinear Structural Modification and Nonlinear Coupling, Mechanical Systems and Signal Processing, 46 (2) (2014) 289-306, <https://doi.org/10.1016/j.ymsp.2014.01.016>.
5. T. Kalaycıođlu, H.N. Özgüven, Nonlinear Structural Coupling – Experimental Application, in: Nonlinear Dynamics, vol. 2, Proceedings of the 32nd IMAC, A Conference on Structural Dynamics, Springer, New York, 2014, pp. 241-248, [https://doi.org/10.1007/978-3-319-04522-1\\_23](https://doi.org/10.1007/978-3-319-04522-1_23).
6. T. Kalaycıođlu, H.N. Özgüven, New FRF Based Methods for Substructure Decoupling, in: Dynamics of Coupled Structures, vol. 4, Proceedings of the 34th IMAC, A Conference on Structural Dynamics, Springer, New York, 2016, pp. 463-472, [https://doi.org/10.1007/978-3-319-29763-7\\_46](https://doi.org/10.1007/978-3-319-29763-7_46).

7. T. Kalaycıoğlu, H.N. Özgüven, Dynamic Decoupling of Nonlinear Systems, in: Dynamics of Coupled Structures, vol. 4, Proceedings of the 35th IMAC, A Conference on Structural Dynamics, Springer, New York, 2017, pp. 199-203, [https://doi.org/10.1007/978-3-319-54930-9\\_17](https://doi.org/10.1007/978-3-319-54930-9_17).
8. T. Kalaycıoğlu, H.N. Özgüven, FRF Decoupling of Nonlinear Systems, Mechanical Systems and Signal Processing, 102 (2018) 230-244, <https://doi.org/10.1016/j.ymssp.2017.09.029>.
9. T. Kalaycıoğlu, H.N. Özgüven, FRF Decoupling Method for Nonlinear Systems – An Experimental Application, in: Proceedings of the 36th IMAC, A Conference on Structural Dynamics, Orlando, Florida, USA, 2018.